



# Design and Simulation of Solar Desalination Systems

Thesis Submitted for the Ph.D. Degree in Energy Engineering

To

Faculty of Petroleum & Mining Engineering  
Suez Canal University  
Egypt

By

Mohamed Abdel Wahab Sharaf Eldean

B. Sc., Arab Academy for Science & Technology, 1999

M. Sc., Suez Canal University, 2007

Egypt



2011

Supervisory Committee

# Design and Simulation of Solar Desalination Systems

Thesis Submitted for the Ph.D. Degree in Energy Engineering

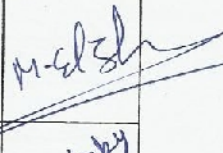
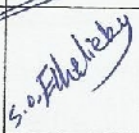
By

Mohamed Abdel Wahab Sharaf Eldean

B. Sc., Arab Academy for Science & Technology, 1999

M. Sc., Suez Canal University, 2007

Egypt

Supervision Committee:	Signature
<b>Prof. Dr. Mohamed Abd Elfatah Elzeky</b> Metallurgical And Material Dept, Faculty Of Petroleum & Mining Engineering, Suez Canal University, Suez, Egypt.	
<b>Dr. Sayed O. Elhelichy</b> Engineering Science Dept, Faculty Of Petroleum & Mining Engineering, Suez Canal University, Suez, Egypt.	
<b>Assco. Prof. Lourdes García Rodríguez</b> Energy Engineering Dept, Faculty of Engineering, University of Sevilla, Spain.	





Approval Sheet

## Design and Simulation of Solar Desalination Systems

Thesis Submitted for the Ph.D. Degree in Energy Engineering

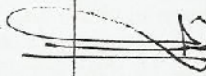

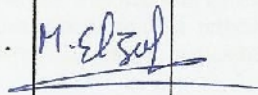
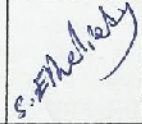
By

Mohamed Abdel Wahab Sharaf Eldean

B. Sc., Arab Academy for Science & Technology, 1999

M. Sc., Suez Canal University, 2007

Egypt

Examiners Committee:	Signature
<b>Prof. Dr. Mansour Awad Mohamed</b> Solar Energy Dept, National Research Center, Cairo, Egypt.	
<b>Prof. Dr. Mohamed Reda Abd Elkader</b> Mechanical Engineering Dept, Port Saied University.	
<b>Prof. Dr. Mohamed Abd Elfatah Elzeky</b> Metallurgical And Material Dept, Faculty Of Petroleum & Mining Engineering, Suez Canal University, Suez, Egypt.	
<b>Dr. Sayed O. Elhelieby</b> Engineering Science Dept, Faculty Of Petroleum & Mining Engineering, Suez Canal University, Suez, Egypt.	





# **Design and Simulation of Solar Desalination Systems**

Thesis Submitted for the Ph.D. Degree in Energy Engineering

To

Faculty of Petroleum & Mining Engineering  
Suez Canal University  
Egypt

By

**Mohamed Abdel Wahab Sharaf Eldean**

B. Sc., Arab Academy for Science & Technology, 1999  
M. Sc., Suez Canal University, 2007

**Egypt**

2011

Supervisory Committee

# Design and Simulation of Solar Desalination Systems

Thesis Submitted for the Ph.D. Degree in Energy Engineering

By

Mohamed Abdel Wahab Sharaf Eldean

B. Sc., Arab Academy for Science & Technology, 1999

M. Sc., Suez Canal University, 2007

**Egypt**

<b>Supervision Committee:</b>	<b>Signature</b>
<b>Prof. Dr. Mohamed Abd Elfatah Elzeky</b> Metallurgical And Material Dept, Faculty Of Petroleum & Mining Engineering, Suez Canal University, Suez, Egypt.	
<b>Dr. Sayed O. Elhelieby</b> Engineering Science Dept, Faculty Of Petroleum & Mining Engineering, Suez Canal University, Suez, Egypt.	
<b>Assco. Prof. Lourdes García Rodríguez</b> Energy Engineering Dept, Faculty of Engineering, University of Sevilla, Spain.	

## Approval Sheet

# Design and Simulation of Solar Desalination Systems

Thesis Submitted for the Ph.D. Degree in Energy Engineering

By

Mohamed Abdel Wahab Sharaf Eldean

B. Sc., Arab Academy for Science & Technology, 1999

M. Sc., Suez Canal University, 2007

**Egypt**

<b>Examiners Committee:</b>	<b>Signature</b>
<b>Prof. Dr. Mansour Awad Mohamed</b> Solar Energy Dept, National Research Center, Cairo, Egypt.	
<b>Prof. Dr. Mohamed Reda Abd Elkader</b> Mechanical Engineering Dept, Port Saied University.	
<b>Prof. Dr. Mohamed Abd Elfatah Elzeky</b> Metallurgical And Material Dept, Faculty Of Petroleum & Mining Engineering, Suez Canal University, Suez, Egypt.	
<b>Dr. Sayed O. Elhelieby</b> Engineering Science Dept, Faculty Of Petroleum & Mining Engineering, Suez Canal University, Suez, Egypt.	



## Abstract

Clean, fresh drinking water is essential to human and other life needs like agricultures needs, human needs and artificial needs. Access to safe drinking water has improved steadily and substantially over the last decades in almost every part of the world. However, some observers have estimated that by 2025 more than half of the world population will be facing water-based vulnerability, a situation which has been called a water crisis by the United Nations. Desalination provides such an alternative source, offering water for irrigational, industrial and municipal use.

Desalination technologies can be classified by their separation mechanism into thermal and membrane based desalination. Thermal desalination separates salt from water by evaporation and condensation, whereas in membrane desalination water diffuses through a membrane, while salts are almost completely retained. Thermal desalination includes multi-stage flash, multi-effect distillation, mechanical vapor compression, and thermal vapor compression while membrane desalination contains reverse osmosis, ion exchange, and electro-dialysis processes. Reverse osmosis and multi-stage flash are the techniques that are most widely used in the world.

Desalination uses a large amount of energy to remove a portion of pure water from a salt water source. Large commercial desalination plants using fossil fuel are in use in a number of oil-rich countries to supplement the traditional sources of water supply. However; people in many other areas of the world have neither the money nor the oil resources to allow them to develop on a similar manner. Furthermore; problems relevant to the use of fossil fuels, in part, could be resolved by considering possible utilization of renewable resources such as solar, biomass, wind, or geothermal energy. The coupling of renewable energy sources with desalination processes is seen by some researchers as having the potential to offer a sustainable route for increasing the supplies of potable water.

Solar energy can directly or indirectly be harnessed for desalination. Collection systems that use solar energy to produce distillate directly in the solar collector are called direct collection systems whereas systems that combine solar energy collection systems with conventional desalination systems are called indirect systems. In indirect systems, solar energy is used either to generate the heat required for desalination and/or to generate electricity that is used to provide the required electric power for conventional desalination plants such as multi-effect (ME), multi-stage flash (MSF) or reverse osmosis (RO) systems. For Middle East countries sun has a good presence beside a huge area of the desert. For example the number of sun shine hours over Egypt is about 3600h/year with an amount of 6-7kWh/m<sup>2</sup>/day as a global radiation.

Therefore utilization of solar energy as an alternative and renewable energy should be strongly taken into consideration, especially, when new communities are established in the desert and remote areas. For scientists, it is very important to decide or demonstrate the applicability of the solar desalination system based on energy, exergy, cost, and thermo-economic analysis. The decision should maintain different types, different configurations, and different techniques. To perform a reliable analysis for this wide range of solar desalination processes and different configurations, a flexible visualized computer program is required.

Therefore, the need to design and simulate solar desalination systems is very important and essential. The main objective of this work is to develop software in order to design and simulate different solar desalination systems such as Reverse Osmosis, Multi stage Flash, Multi Effect Evaporation, Mechanical and Thermal Vapor Compression. The developed software is performed for different calculations, different modifications, different comparisons, and different analysis. The developed software has some features such as validity, generality, flexibility, easy to handle, and executable. In this work, performing a survey about the importance of utilizing solar energy and

desalination is done. Designing & setting up the required software for the proposed processes are performed. Carrying out the validation results is accomplished based on different techniques. As a result, a developed software package (SDS) is constructed to design and simulate different types of solar desalination processes. Also, solar assisted organic Rankine cycle for reverse osmosis with pressure exchanger unit is considered attractive based on energy, exergy, and cost analysis. Multi effect distillation with thermal vapor compression comes next based on the same indicators. Also, a comparison for different techniques of combination between solar power cycle and desalination process is performed. The results reveal that solar desalination technique without power generation is remarkable while comparing with solar desalination technique with power generation.



## Acknowledgment

*First of all, I thank ALLAH the merciful, for helping me to complete this work, and I hope this work be useful to my country Egypt.*

*Thanks a lot to...*

***Prof. Dr. Mohamed Elzeky***, professor of metallurgical science, for his supreme supervising and his support to the fulfillment of this work.

***Prof. Dr. Sayed Othman ELhelieby***, the head of engineering science department, for offering all helps for the fulfillment this work.

***Prof. Dr. Ahmed Safwat Nafey***, thermal engineering in engineering science department, for giving me a great opportunity to learn from his experience along ten years of hard work.

***Prof. Dr. Lourdes Garcia-Rodríguez***, Universidad de Sevilla, Spain, for her encouragements, experience and honest guidance throughout this work.

# The Contents

<b>Abstract .....</b>	<b>4</b>
<b>Acknowledgment .....</b>	<b>6</b>
<b>The Contents .....</b>	<b>7</b>
<b>List of Figures.....</b>	<b>9</b>
<b>List of Tables .....</b>	<b>11</b>
<b>Nomenclature .....</b>	<b>13</b>
<b>Chapter 1: Introduction &amp; Review.....</b>	<b>17</b>
1.1 Water Shortage Problem.....	17
1.2 Solar Desalination Systems as a Choice .....	17
1.3 Solar Thermal Power Cycles: Technology Overview .....	19
1.4 Solar Powered-Rankine Cycles.....	21
1.5 The Review Considerations .....	23
<b>Chapter 2: A New Visual Library for Design and Simulation of Solar Desalination Systems (SDS)</b> <b>.....</b>	<b>24</b>
2.1 Types of Flow Sheeting Programs Used for Solar Systems .....	24
2.2 MatLab/SimuLink Software Tool .....	26
2.3 Simulation of Different Solar Desalination Units .....	27
2.4 Solar Power Cycle for Desalination Processes: Case Study .....	34
<b>Chapter 3: Exergy &amp; Thermo-economic Analyses of Solar Organic Cycles Assisted Desalination Processes .....</b>	<b>36</b>
3.1 Working Fluids Selection for Solar ORC .....	36
3.2 Solar ORC Assisted RO Desalination Process .....	41
3.3 Solar Thermal Organic Cycles Assisted Multi Effect Distillation (MED) Desalination Process.....	60
3.4 Solar Thermal Organic Cycles Assisted Multi Effect Distillation-Vapor Compression (MED-VC) Desalination Processes .....	74
3.5 Solar Thermal Organic Cycles Assisted Multi Stage Flash (MSF) Desalination Process .....	86
<b>Chapter 4: Comparison of Different Types of Solar Desalination Processes: Results &amp; Discussions</b> <b>.....</b>	<b>93</b>
4.1 Process Configurations .....	93
4.2 Comparison Methodology .....	95
4.3 Results and Discussions.....	99
<b>Chapter 5: Conclusion, Recommendations and Future Work .....</b>	<b>105</b>
5.1 Conclusion .....	105

5.2 Recommendations .....	107
5.3 The Future Work .....	107
<b>The Appendix .....</b>	<b>108</b>
Appendix-A .....	108
Appendix-B .....	112
Appendix-C .....	133
Appendix-D .....	137
<b>References.....</b>	<b>143</b>

## List of Figures

Figure		Page
(1.1)	World solar radiation.	18
(1.2)	Flow chart of renewable energies powered desalination processes.	18
(1.3)	Photographs of PTC type for solar power generation.	20
(1.4)	Desalinated water costs for various combinations of desalination processes powered by renewable energy sources.	21
(1.5)	POWERSOL concept: A solar-heated Rankine cycle drives either, a generator or the high pressure pump of a reverse osmosis.	22
(2.1)	Performance and design characteristics for common flow sheeting programs.	25
(2.2)	Types of simulation programs used for solar desalination processes.	26
(2.3)	SDS software library browser under MatLab/SimuLink interface.	27
(2.4)	Schematic display of Single Effect Evaporation (SEE) under MatLab-SimuLink software environment.	31
(2.5)	MED model environment designed using SDS package.	33
(3.1)	The selected fluids behavior on T-S diagram for different solar collectors (FPC, CPC, and PTC)	39
(3.2)	Saturation pressures for different collectors with different working fluids at the saturation temperature at the range of 35-100°C	40
(3.3)	Schematic diagram of DVG solar ORC powered RO (basic cycle).	42
(3.4)	Total Water Price (TWP, \$/m <sup>3</sup> ) for cycles different working fluids & different steam operating conditions with different collector types.	45
(3.5)	A schematic diagram of solar Rankine cycle components for saturation and/or superheat with recuperator unit.	47
(3.6)	A schematic diagram of solar Rankine cycle components for saturation and/or superheat with OFH unit.	47
(3.7)	A schematic diagram of solar Rankine cycle components for saturation and/or superheat with OFH and recuperator units.	48
(3.8)	A schematic diagram of the RO process with different energy recovery units.	53
(3.9)	Variation of thermo-economic product cost against the variation in productivity.	58
(3.10)	Variation of product stream exergy rate (MW) and power consumed (MW) by the RO-PEX against the variation in fresh water production rate (m <sup>3</sup> /h).	58
(3.11)	Data streams for solar ORC with RO-PEX configuration (145m <sup>3</sup> /h).	59
(3.12)	A schematic diagram of solar MED units for desalination: Solar field, Boiler heat exchanger, Pump, MED.	63
(3.13)	Solar radiation data results based on hourly, daily average (11 hrs), and daily average (24 hrs) variations.	64
(3.14)	A schematic diagram of solar MED components for desalination and power generation: Solar field, Boiler heat exchanger, Pump, Turbine, Recuperator, MED.	65
(3.15)	The GR variations for different MED configurations due to the variations of effect numbers at 100m <sup>3</sup> /day based on SDMED technique.	68
(3.16)	Effect of evaporators' number and steam temperature on based on both techniques.	72
(3.17)	Effect of daily productivity (m <sup>3</sup> /d) on thermo-economic product cost (\$/GJ) for SDMED-PF case study.	73
(3.18)	Effect of daily productivity (m <sup>3</sup> /d) on the developed power by the turbine unit based on PSDMED-PF technique.	73
(3.19)	A schematic diagram of solar MED-PF-TVC components: (1) Solar field, (2) Boiler heat exchanger, (3) HTO pump, (4) MED-PF-TVC, (5) Water pump.	75

(2.20)	A schematic diagram of solar MED-PF-MVC components: (1) Solar field, (2) Boiler heat exchanger, (3) HTO Pump, (4) Turbine, (5) Recuperator, (6) Condenser, (7) Pump (8) MED-PF, (9) MVC.	76
(3.21)	Effect of CR and number of evaporators on both: (a) SPC, kWh/m <sup>3</sup> , and (b) Thermo-economic product cost, \$/GJ.	78
(3.22)	Effect of CR and number of evaporators on both: (a) Solar field area, m <sup>2</sup> , and (b) Total exergy destruction rate, kW.	78
(3.23)	Effect of Neff and steam temperature on both: (a) SPC, kWh/m <sup>3</sup> , and (b) Thermo-economic product cost, \$/GJ.	81
(3.24)	Effect of Neff and steam temperature on both: (a) Solar field area, m <sup>2</sup> , and (b) Total exergy destruction rate, kW.	81
(3.25)	Effect of Neff and steam temperature on both: (a) CR, and (b) GR.	82
(3.26)	The effect of daily productivity (m <sup>3</sup> /d) on thermo-economic product cost for both techniques (MED-MVC & MED-TVC).	85
(3.27)	Effect of daily productivity (m <sup>3</sup> /d) on the developed power for both techniques (MED-MVC & MED-TVC).	85
(3.28)	A schematic diagram of solar MSF-BR components: (1) Solar field, (2) Boiler heat exchanger, (3) Pump, (4) Brine heater, (5) MSF-BR.	88
(3.29)	A schematic diagram of solar MED-PF-MVC components: (1) Solar field, (2) Boiler heat exchanger, (3) HTO Pump, (4) Turbine, (5) Recuperator, (6) Condenser, (7) Pump (8) MSF-BR.	88
(3.30)	Effect of TBT and Nstg on: (a) SPC, kWh/m <sup>3</sup> , (b) cp, \$/GJ, (c) $A_{col}$ , m <sup>2</sup> , (d) GR.	90
(3.31)	The daily productivity effect on the thermo-economic product cost for both techniques (SDMSF & PSDMSF).	92
(3.32)	The effect of productivity on the developed power for both techniques (SDMSF & PSDMSF).	92
(4.1)	A schematic diagram of SORC assisted RO-PEX and MED-PF-MVC desalination processes.	94
(4.2)	A schematic diagram of solar thermal power cycle assisted thermal desalination processes (MSF-BR, MED-PF, MED-PF-TVC).	95
(4.3)	A schematic diagram of solar PV powered RO system for 100m <sup>3</sup> /day.	104

## List of Tables

Table	Page
(1.1) Fresh water demand and desalination capacity in the Red Sea and south Sinai regions.	17
(1.2) Some of indirect solar desalination pilot plants implemented at different locations.	19
(1.3) CSP vs PV solar power generation.	21
(2.1) Data results for solar radiation model based on the specified location of operation.	28
(2.2) A comparison between the SDS and reference results for Solar Rankine power cycle (direct vapor generation operation).	29
(2.3) Specified design parameters of Sharm El-Shiekh RO desalination plant.	30
(2.4) SDS results of Sharm El-Shiekh desalination plant vs. ROSA6.1.	30
(2.5) Comparison results of SDS Eoun Mousa MSF-BR plant.	31
(2.6) The SDS and ref [43] results comparison for SEE model.	32
(2.7) Data validation between SDS and ref [52] for MED model.	33
(2.8) Energy and thermo-economic results for solar powered RO-PEX technique.	34
(3.1) Properties list of the selected working fluids.	31
(3.2) Specified design parameters of Sharm El-Shiekh RO desalination plant.	41
(3.3) Results of ORC/RO process with different working fluids and different types of solar collectors.	43
(3.4) <i>ICC</i> and <i>O&amp;M</i> costs for solar organic Rankine cycle components.	44
(3.5) <i>ICC</i> and <i>O&amp;M</i> costs for RO desalination plant.	44
(3.6) Data results of Toluene (PTC) for different configurations under saturation operation.	50
(3.7) Data results of Toluene (PTC) for different configurations under superheat operation.	50
(3.8) Data results of Water (PTC) for basic configuration under superheat operation.	51
(3.9) Data comparisons between different working fluids for recuperator configuration under saturation and superheat operations.	51
(3.10) Specifications and design parameters of the considered processes.	54
(3.11) Energy and thermo-economic results for different configurations.	56
(3.12) The comparison percentages for different configurations based on thermo-economic results.	57
(3.13) Specifications of MED desalination plant (all configurations) under winter operating conditions for 100m <sup>3</sup> /day capacity.	61
(3.14) Data results for solar radiation model based on the specified location of operation.	64
(3.15) Design points considered for MED according to the 1 <sup>st</sup> and the 2 <sup>nd</sup> techniques.	66
(3.16) Data results for <u>1<sup>st</sup> technique</u> operated by Water and HTO fluids.	67
(3.17) Data results for <u>2<sup>nd</sup> technique</u> operated by Toluene and HTO fluids.	69
(3.18) Data results for both techniques based on 5000m <sup>3</sup> /d.	71
(3.19) Design points for <u>SMED-PF-VC</u> according to the 1 <sup>st</sup> and the 2 <sup>nd</sup> techniques.	76
(3.20) Data results for <u>SMED-PF-TVC</u> operated by Water and HTO fluids.	79
(3.21) Data results for <u>SMED-PF-MVC</u> operated by Toluene and HTO fluids.	82
(3.22) Data results for both techniques based on 4545m <sup>3</sup> /d.	84
(3.23) Specifications of Eoun Mousa MSF desalination plant (5000m <sup>3</sup> /day).	86
(3.24) Design points for MSF-BR according to the 1 <sup>st</sup> and the 2 <sup>nd</sup> techniques.	87
(3.25) Data results for <u>1<sup>st</sup> and 2<sup>nd</sup> techniques</u> operated by Water and Toluene fluids.	91
(4.1) Specifications and design input data based on S-RO-PEX (1 <sup>st</sup> method).	96
(4.2) Specifications and design input data based on S-MED-MVC (1 <sup>st</sup> method).	96
(4.3) Specifications and design input data based on S-MED (1 <sup>st</sup> method).	97
(4.4) Specifications and design input data based on S-MED-TVC (1 <sup>st</sup> method).	97
(4.5) Specifications and design input data based on S-MSF-BR (1 <sup>st</sup> method).	98
(4.6) Specifications of solar assisted thermal and mechanical desalination processes (2 <sup>nd</sup> method).	98
(4.7) Data results for all solar desalination processes based on different operating conditions	100



	method.	
(4.8)	Data results for solar desalination processes based on the same productivity.	101
(4.9)	Data results for solar desalination processes based on same solar field area.	101
(4.10)	Data results for solar desalination processes based on the same TWP.	102
(4.11)	Specifications and input data for PV-RO and CSP-RO systems (100m <sup>3</sup> /day).	103
(4.12)	Data results for both systems (CSP Vs PV) combined with RO desalination unit.	104

## Nomenclature

$A$	Area, $m^2$ , Availability
$A_e$	Effect heat transfer area, $m^2$
$A_f$	Amortization factor, $y^{-1}$
$ACC$	Annualized capital cost, \$/year
$BHX$	Boiler heat exchanger
$BPE$	Boiling point elevation, $^{\circ}C$
$BPR$	Boiling point ratio, $^{\circ}C$
$Bp$	Booster pump
$C$	Cost, \$
$CC$	Capital costs, \$
$CPC$	Compound parabolic concentrator
$CSP$	Concentrated solar power
$C_p$	Specific heat capacity at constant pressure, $kJ/kgK$
$cp$	Thermo-economic product cost, \$/GJ
$CSP$	Concentrated solar power
$CR$	Compression ratio
$D$	Distillate, $kg/s$
$DCC$	Direct capital cost, \$
$DVG$	Direct vapor generation
$dT$	Temperature drop between effects or stages, $^{\circ}C$
$E_{xin}$	Exergy in, $kW$
$E_{xout}$	Exergy out, $kW$
$FPC$	Flat plate collector
$GR$	Gain ratio, $M_d/M_s$
$HPP$	High pressure pump
$HTO$	Heat transfer oil
$h$	Specific enthalpy, $kJ/kg$
$I$	Exergy destruction rate, $kW$
$ICC$	Investment capital costs, \$
$IDCC$	Indirect capital cost, \$
$IDVG$	Indirect vapor generation
$i$	Interest rate, %
$L$	Latent heat of vaporization, $kJ/kg$
$LF$	Load factor
$LT$	Life time, year
$MED-PF$	Multi effect distillation parallel cross feed arrangement
$MED-PF-MVC$	Multi effect distillation parallel cross feed mechanical vapor compression
$MED-PF-TVC$	Multi effect distillation parallel cross feed thermal vapor compression
$MSF-BR$	Multi stage flash brine recycle
$M_d$	Distillate mass flow rate, $kg/s$
$NEA$	Non equilibrium allowance, $^{\circ}C$
$N_{eff}$	Number of effects for MED process
$N_{stg}$	Number of stages for MSF process
$n_v$	Number of pressure vessels
$ne$	Number of elements

<i>P</i>	Pressure, bar
<i>PCF</i>	Pressure correction factor, kPa
<i>PEX</i>	Pressure exchanger
<i>PR</i>	Performance ratio
<i>PTC</i>	Parabolic trough collector
<i>PV</i>	photovoltaic
<i>PWT</i>	Pilton wheel turbine
<i>Q</i>	Thermal power, kW
<i>RO</i>	Reverse osmosis process
<i>RR</i>	Recovery ratio, %
<i>SDS</i>	Solar desalination systems
<i>SSA</i>	Specific solar field area, m <sup>2</sup> /(m <sup>3</sup> /day)
<i>M</i>	Mass flow rate, kg/s
<i>MED</i>	Multi-effect distillation
<i>MSF</i>	Multi-stage flash
<i>MVC</i>	Mechanical vapor compression
<i>N, n</i>	Number
<i>N<sub>eff</sub></i>	Number of effects
<i>OC</i>	Operating cost, \$
<i>O&amp;M</i>	Operating and maintenance costs
<i>S</i>	Salinity ratio, g/kg (ppm)
<i>SDS</i>	Solar desalination systems
<i>SEMVC</i>	Single effect mechanical vapor compression
<i>SETVC</i>	Single effect thermal vapor compression
<i>S-ORC</i>	Solar organic Rankine cycle
<i>SCC</i>	Specific chemical cost, \$/m <sup>3</sup>
<i>SEC</i>	Specific electrical cost, \$/kWh
<i>SHC</i>	Specific heating steam cost, \$/MkJ
<i>SLC</i>	Specific labor cost, \$/m <sup>3</sup>
<i>SPC</i>	Specific Power Consumption, kWh/m <sup>3</sup>
<i>S-RO</i>	Solar reverse osmosis
<i>S-MED</i>	Solar multi effect distillation
<i>s</i>	Specific entropy, kJ/kg°C
<i>T</i>	Temperature, °C
<i>T<sub>ci</sub></i>	Inlet collector temperature, °C
<i>T<sub>co</sub></i>	Outlet collector temperature, °C
<i>T<sub>n</sub></i>	Last stage temperature at stage n, °C
<i>T<sub>stg</sub></i>	Stage temperature drop, °C
<i>TAC</i>	Total annual cost, \$/y
<i>TCC</i>	Total capital costs, \$
<i>TBT</i>	Top brine temperature, °C
<i>TDI</i>	Top distillate temperature, °C
<i>TCF</i>	Temperature correction factor, °C
<i>TPC</i>	Total plant costs, \$
<i>TST</i>	Top steam temperature, °C
<i>T<sub>sun</sub></i>	Sun temperature, 6000K

$TCC$	Total capital cost, \$
$TVC$	Thermal vapor compression
$TWP$	Total water price, \$/m <sup>3</sup>
$U$	Overall heat transfer coefficient, W/m <sup>2</sup> °C
$UPC$	Unit product cost, \$/m <sup>3</sup>
$V$	Volume, m <sup>3</sup>
$W_t$	Turbine work, kW
$W_p$	Pump work, kW
$X$	Steam quality
$Y$	Extraction percentage, %
$Z$	Hourly costs, \$/h
$Z^{IC\&OM}$	Total investment and operating and maintenance cost, \$/h

### **Subscripts**

$amb$	Ambient
$av$	Average
$b$	Brine
$chm$	Chemical
$col$	Collector
$cond$	Condenser
$comp$	Compressor
$cw$	Cooling water
$d$	Distillate product
$ext$	Extraction
$f$	Feed
$i$	In
$MED$	Multi effect distillation
$o$	Out
$orc$	Organic Rankine cycle
$p$	Pump
$rec$	Recuperator
$reg$	Regeneration
$ro$	Reverse osmosis
$s$	Salt, steam
$st$	Steam turbine
$sat$	Saturation
$sup$	Supper heat
$t$	Turbine
$v$	Vapor
$w$	Water

### **Greek**

$\varepsilon$	Effectiveness
$\eta$	Thermal efficiency, %
$\eta_o$	Optical efficiency, %
$\eta_g$	Generator efficiency, %
$\eta_t$	Turbine efficiency, %
$\rho$	Density, kg/m <sup>3</sup>

$\mu$	Dynamic viscosity, Pa.s
$\Pi$	Osmotic pressure, kPa

# Chapter 1: Introduction & Review

## 1.1 Water Shortage Problem

Water and its natural resources are considered very important part for living on the earth. Water is very important for the proceeding of the all life needs and in all life fields like agricultures needs, human needs and artificial needs. But at the last few decades water shortage problems appeared at many countries especially developing countries. Many remote areas of the world such as coastal desert areas in the Middle East or some Mediterranean and Caribbean islands are suffering from acute shortage of drinking water [1]. By the year of 2025, about 60% of the world population will be suffering from serious water shortages. Moreover; common use of unhealthy water in developing countries causes 80-90% of all diseases and 30% of all deaths [2].

For the North African countries, Egypt lays in a semi-arid to arid region where most of its renewable fresh water is transported by the Nile River from the Ethiopian and Equatorial plateau. It is anticipated that by the year 2025 water per capita will drop to about  $600\text{m}^3/\text{y}$ , thus approaching the water poverty limit. The immediate answer is to turn towards non-conventional sources such as water recycling, reuse of drainage water, treated industrial and sewage effluents, rainfall harvesting and desalination [3]. As an example, the geographical locations of the Red Sea natural scenarios controlled the distribution of the hotels, villages and resorts in a sporadic pattern over the long coastline, which spreads along about 1500 km. A severe shortage of fresh water in the Red Sea region and south Sinai in the year 2020 is depicted as shown in Table 1.1 [4]. Table 1.1 shows that the great gab between the demand and the available fresh water is widening and the estimated water will be around  $10^6\text{m}^3/\text{day}$ . As a result, the desalination of the Red Sea water is the only option under the expected shortage of the Nile water resources.

Table 1.1: Fresh water demand and desalination capacity in the Red Sea and south Sinai regions [4].

Year	2001		2020	
Fresh water source	Red Sea coast $\text{m}^3/\text{day}$	South Sinai coast $\text{m}^3/\text{day}$	Red Sea coast $\text{m}^3/\text{day}$	South Sinai coast $\text{m}^3/\text{day}$
Nile water pipe-line	80,000	0	140,000	30,000
Fresh ground water	0	10,000	0	25,000
Seawater desalination	97,000	40,000	250,000	150,000
Estimated demand	500,000	125,000	1,000,000	600,000
<b>Water shortage</b>	<b>323,000</b>	<b>75,000</b>	<b>610,000</b>	<b>395,000</b>

## 1.2 Solar Desalination Systems as a Choice

Desalination of sea water considered the most important method to free water from salt and simply makes it ready to be used in the human needs. However; desalination process consumes a huge thermal energy based on the amount of productivity produced. The use of solar energy in thermal desalination processes is one of the most promising applications of the renewable energies. Countries in south Mediterranean basin (Egypt) usually have abundant seawater resources and a good level of solar radiation, which could be used to produce drinking water from seawater. Figure (1.1) shows the good presence of the solar radiation in Egypt. It is pinpointed on the figure that an amount of  $6\text{-}6.9\text{kWh}/\text{m}^2/\text{day}$  of global radiation is in the Middle East countries [5]. Solar desalination can either be direct; use solar energy to produce distillate directly in the solar collector, or indirect; combining



conventional desalination techniques, such as multistage flash desalination (MSF), vapor compression (VC), reverse osmosis (RO), membrane distillation (MD) and electro-dialysis (ED), with solar collectors for heat generation. Solar thermal energy coupled to a power cycle by using direct mechanical power can also be employed [6]. Figure (1.2) shows a flow chart of renewable energies powered different types of desalination processes [7]. It clear from the figure that solar energy can power thermal and electrical desalination systems. Solar desalination is particularly important for locations where solar intensity is high and there is a scarcity of fresh water.

Techniques of solar desalination are many and varying according to the size of the demanding of fresh water and the size of solar energy presence. In this section; a review of using solar energy with desalination techniques are investigated. Table 1.2 illustrates some of desalination processes combined with solar energy. It is clear from literature that the possibility of utilizing reliable solar thermal power with different types of distillation processes such as MED already exists. However, the technique of such utilization with different working fluids needs more investigations. Moreover; the techniques that are presented in literature are significantly at low capacities of operation. Therefore; it very important to evaluate large capacities based on energy, exergy, cost and thermo-economic.

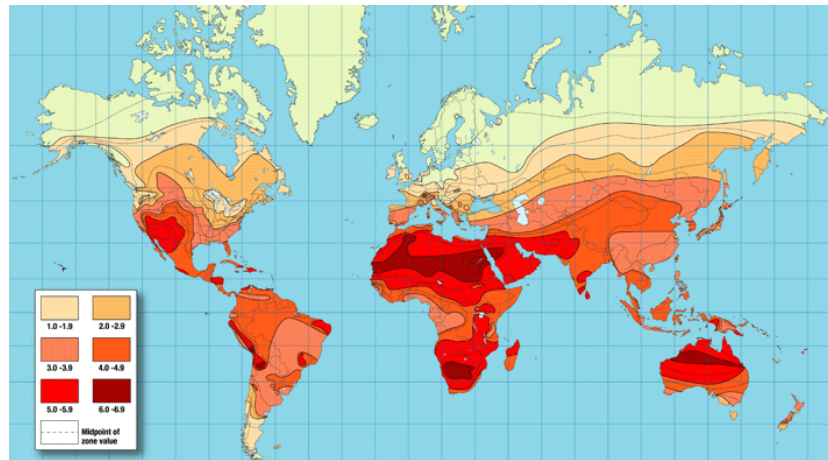


Figure (1.1) World solar radiation [5].

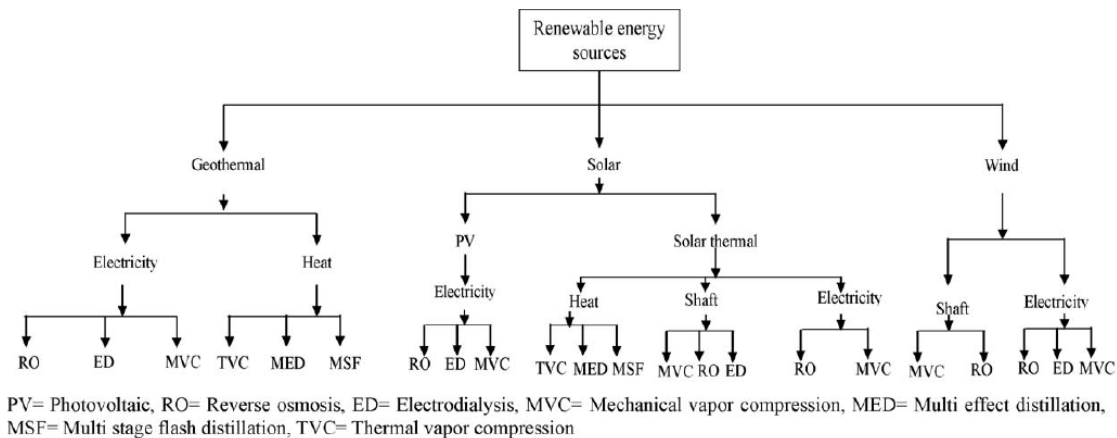


Figure (1.2) Flow chart of renewable energies powered desalination processes [7].

Table 1.2: Some of indirect solar desalination pilot plants implemented at different locations.

Desalination process type	Location	Capacity	Type of power	Reference
MSF	Safat, Kuwait	10m <sup>3</sup> /day	Solar collectors	[8]
MSF	Al Azhar University in Gaza	0.2m <sup>3</sup> /day	Solar thermal collectors and PV cells	[9]
MSF	Berken, Germany	10m <sup>3</sup> /day	--	[10]
MSF	Gran Canaria, Spain	10m <sup>3</sup> /day	Low concentration solar collectors	[11]
MSF	Lampedusa Island, Italy	0.3m <sup>3</sup> /day	Low concentration solar collectors	[12]
MSF	La Paz, Mexico	10m <sup>3</sup> /day	Flat plate and Parabolic trough collectors	[13]
MSF	Kuwait	100m <sup>3</sup> /day	Parabolic trough collectors	[14]
MSF+MED	Al-Ain, UAE	500m <sup>3</sup> /day	Parabolic trough collectors	[15]
PV+RO		1m <sup>3</sup> /day	PV	[16]

### 1.3 Solar Thermal Power Cycles: Technology Overview

Solar thermal power plants, often also called Concentrating Solar Power (CSP) plants, produce electricity in much the same way as conventional power stations. The difference is that they obtain their energy input by concentrating solar radiation and converting it to high-temperature steam or gas to drive a turbine or motor engine. Solar troughs as a concentrated solar power (CSP) (see figure (1.3)) can concentrate the sunlight by about **70–100 times**. Typical operating temperatures are in the range of **200–400°C**. Plants of 200 MW rated power and more can be built by this technology [18]. This technology can provide a suitable and sufficient power to drive on membrane and thermal desalination technologies. The CSP plants have some features:

- Concentrating solar power plants can generate electricity which can be used for membrane desalination.
- Each square meter of the CSP's reflector surface in a solar field is enough to avoid the annual production of 150 to 250 kilograms (kg) of carbon dioxide (CO<sub>2</sub>).
- CSP plants can be used for combined heat and power.
- Thermal desalination methods like MED or MSF can be directly/indirectly powered by CSP, either directly or in co-generation with electricity.
- CSP (Concentrated Solar Power) reduces emissions of local pollutants and considerably contribute to global climate protection.
- A major benefit of CSP is that it has little adverse environmental impact, with none of the polluting emissions or safety concerns associated with conventional generation technologies.

CSP is a domestic energy source of all MENA countries. The present increase of electricity costs can be stopped and reversed in the medium term by introducing concentrating solar power for electricity and seawater desalination at a large scale. CSP can be made available today at a cost of about **0.18 \$/kWh** for a first, small CSP plant with about **5–10 MW** capacity operating in solar only mode. In the time span until 2010, the solar electricity cost of newly installed plants will drop to less than **0.100 \$/kWh**, in 2020 to **0.056 \$/kWh** and in 2030 it would be close to **0.050 \$/kWh** [18].

A parabolic dish-shaped reflector is used to concentrate sunlight on to a receiver located at the focal point of the dish. The concentrated beam radiation is absorbed into the receiver to heat a fluid or gas (air) to approximately 750°C. This fluid or gas is then used to generate electricity in a small piston or Stirling engine or a micro turbine, attached to the receiver. Parabolic trough systems represent the most mature solar thermal power technology, with **354MWe** connected to the Southern California grid since the 1980s and over 2 million square meters of parabolic trough collectors operating with a long term availability of over 99%. Supplying an annual 924 million kWh at a generation cost of about 12 to 15 US cents/kWh, these plants have demonstrated a maximum summer peak efficiency of 21% in terms of conversion of direct solar radiation into grid electricity.

It is important to understand that solar thermal technology is not the same as solar panel, or photovoltaic, technology. Solar thermal electric energy generation (CSP) concentrates the light from the sun to create heat, and that heat is used to run a heat engine, which turns a generator to make electricity. The working fluid that is heated by the concentrated sunlight can be a liquid or a gas. Different working fluids include water, oil, salts, air, nitrogen, helium, etc. Different engine types include steam engines, gas turbines, Stirling engines, etc. Heat engines can be quite efficient, often between 30% and 40%, and are capable of producing about 10's up to 100's of megawatts of sufficient thermal power. However; Photovoltaic, or PV energy conversion, directly converts the sun's light into electricity.

This means that solar panels are only effective during daylight hours because storing electricity is not a particularly efficient process. Heat storage is a far easier and efficient method, which is what makes solar thermal so attractive for large-scale energy production. Heat can be stored during the day and then converted into electricity at night. Solar thermal plants that have storage capacities can drastically improve both the economics and the dispatch ability of solar electricity. Table 1.3 shows a comparison between CSP and PV solar power plants. Based on the comparison terms, CSP considered more effective while coupling with wider types of desalination processes. Also, Figure (1.4) shows that the specific cost for CSP with thermal desalination systems achieves lower results against the PV operation. According to the available data in Table 1.3 and Figure (1.4), CSP operated by PTC technique is considered in this study. The following table gives a brief comparison between solar thermal power cycles against the Photovoltaic's power cycles.



Figure (1.3) Photographs of PTC type for solar power generation.

Table 1.3: CSP vs PV solar power generation [19].

Parameter:	CSP (thermal)	PV (electric)
Resource quality	2400 kWh/m <sup>2</sup> /yr	2445 kWh/m <sup>2</sup> /yr
Power type	Thermal (indirect)	Electrical (direct)
Desalination system to combined with	All types (MSF, MED, MED-TVC, MED-MVC, RO, ED)	RO, MED-MVC and ED
Levelised cost of energy \$/MWh	60-350 (214\$ in 2030)	100-450 (303\$ in 2030)
Construction period/life time	2/30 years	1/30 years
Capacity factor	23-50%	20%
Heat engines	Stirling, Rankine, gas turbines, steam turbines	N/A

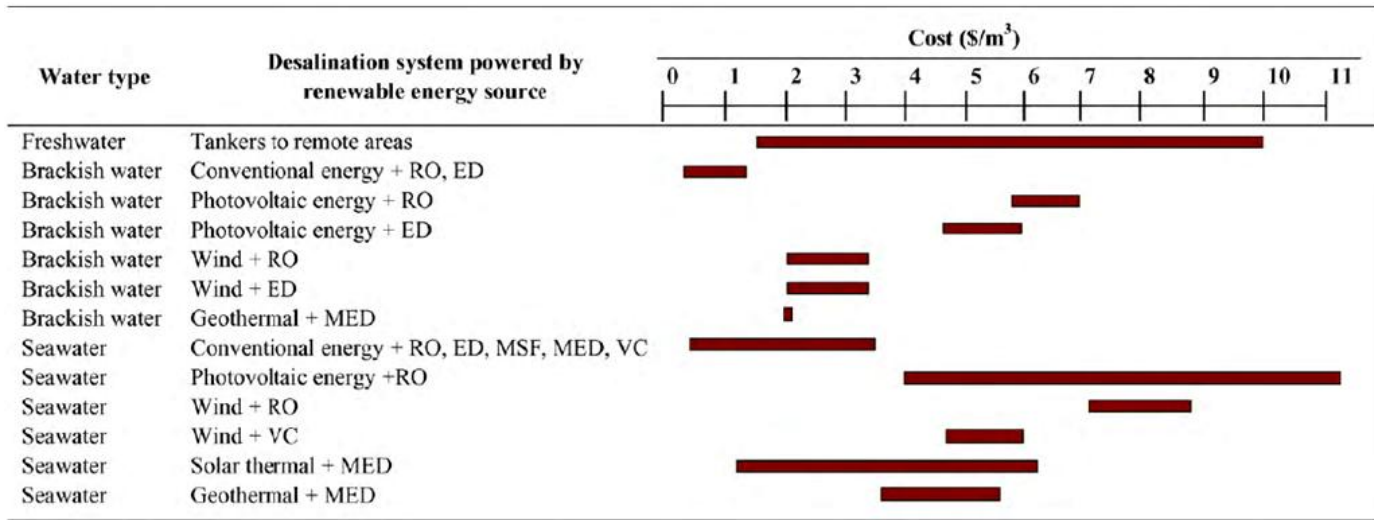


Figure (1.4) Desalinated water costs for various combinations of desalination processes powered by renewable energy sources [20].

## 1.4 Solar Powered-Rankine Cycles

Power generation based on solar thermal medium temperature collectors are mature enough to cover power demand around tens of MW based on Rankine cycle. In addition, a considerable additional advantage is that a solar-heated thermodynamic cycle is able to provide low-grade thermal energy to drive other applications as water or space heating as well as thermal energy at higher temperature for driving an absorption chiller, a seawater distiller, etc. Furthermore; solar thermal systems have the following additional advantages:

- Potential overall efficiency of solar thermal systems is higher than photovoltaic systems.
- Solar thermal systems permit thermal storage instead of batteries. That avoids costly operational maintenance, toxic wastes and replacement problems.
- Many applications do not require electricity but mechanical power as pumping or reverse osmosis desalination.
- The system is able to operate continuously with thermal energy backup.

Solar thermal collectors are able to generate shaft power by means of a Rankine, Brayton or Stirling cycle or by other specially designed expansion system. Therefore; Rankine cycle is used in conventional solar electricity a generation system which uses medium temperature solar collectors-parabolic trough collectors. The use of solar-powered heat engines offers interesting potentials for small to medium size communities in developing and isolated areas. Direct applications are: electricity production, water pumping, reverse osmosis (RO) desalination, vapor compression chillers, etc. Except very small systems for water irrigation pumping, none of above applications has been thoroughly analyzed or developed and very few pilot systems exist. With regard to seawater desalination, only three designs of solar heat engine-driven RO have been published and only one of them has been implemented [21]. The primary advantages of an ORC power cycle for applications with troughs are [22]:

Organic Rankine Cycles are not new technology. A recent resurgence of interest in ORCs as a viable option for small-scale solar electricity generation has been spurred by the construction of the 1 MW Saguaro parabolic trough ORC power plant [23]. A project entitled POWERSOL [24] (Mechanical Power Generation Based on Solar Heat Engines), partially supported by the European Commission. The project focuses on the technological development of a solar powered ORC for RO desalination process. Figure (1.5) shows a schematic diagram of the process configuration implemented by [24].

Figure (1.5) POWERSOL concept: A solar-heated Rankine cycle drives either, a generator or the high pressure pump of a reverse osmosis [24].



D. Manolakos [25] presented an experimental evaluation of the performance under laboratory conditions, of a low-temperature solar organic Rankine cycle system for reverse osmosis (RO) desalination. The operation principle of the system is given briefly below. Thermal energy produced by a solar collectors' array evaporates the refrigerant (R134a) in the evaporator surface of Rankine engine. The super-heated vapor is driven to the expander where the generated mechanical work produced from expansion drives the RO unit high-pressure pump.

Zhang [26] presented an experimental study in order to investigate feasibility of CO<sub>2</sub>-based Rankine cycle powered by solar energy. The proposed cycle is to achieve a cogeneration of heat and power, which consists of evacuated solar tube collectors, power generating turbine, heat recovery system, and feed pump. The cycle recovers thermal energy, which can be used for absorption refrigerator, air conditioning, hot water supply so on for a building. It is clear that solar ORC exhibits a reasonable efficiency to be utilized power generation with different organic working fluids.

## 1.5 The Review Considerations

It is clear from literature that solar powered desalination technologies are varied. PV and CSP are considered to power on different types of desalination systems. However; CSP is considered in this study according to many features such as cost and the combination with all types of desalination technologies. Rankine cycle is widely used. However, it needs more investigations besides considering different techniques. Parabolic trough solar-thermal power generation is a proven technology. Organic Rankine cycle (ORC) power plants are more compact and less costly than traditional steam cycle power plants and are able to better exploit lower temperature thermal resources. Utilizing organic Rankine cycles allows solar-thermal power generation to become a more modular and versatile means of supplanting traditional fuels.

It is shown that solar desalination techniques are characterized as a complex processes. This is because there are different techniques that are either thermal or membrane. Each of these configurations consists of collective units which are connected by interactive streams. These streams differ according to the working fluid. Therefore; to perform reliable analysis for this wide range of solar desalination techniques and different configurations under different operating conditions, a flexible visualized computer package has been constructed and developed in this work. This package is built up for design and simulation of solar desalination systems (SDS). The package aids design and operation engineers to perform different types of calculations such as energy, exergy, and thermo-economic. Additionally, the package enables the designers to perform different modifications for any imaginary or existing system. The aims of this work are pinpointed as follows:

- ✓ Developing a new flexible visualized computer package for design and simulation of different types and different configurations of thermal and membrane solar desalination processes.
- ✓ Developing a reliable tool of analysis based on the first and second laws of thermodynamics (energy, exergy and thermo-economics).
- ✓ Examining the reliability, flexibility, wide capability, and the validity of the developed package.
- ✓ Comparing thermo-economically between the studied solar desalination processes in order to elect the most reliable process and technique.



# Chapter 2: A New Visual Library for Design and Simulation of Solar Desalination Systems (SDS)

## 2.1 Types of Flow Sheeting Programs Used for Solar Systems

Solar desalination processes consist of a number of interactive units. Using these units a wide range of process configurations and types can be obtained. Generally, to understand the behavior of these processes under different operating conditions, a flexible computer program is really needed. Using such program, large number of flow sheeting problems can be manipulated. These problems can be generally divided into three classes: (i) **performance problems**, (ii) **design problems**, and (iii) **optimization problems** [27]. In the performance problem (Figure 2.1-a), the variables associated with the feed streams to a process unit and all design parameters (such as solar collector area, heat exchanger area, etc.) are assumed to be known. The variables associated the internal and output streams are the unknowns. However, in the design problem, some design parameters (Figure (2.1-b)) and/or feed variables are left unspecified and become unknown. A corresponding number of additional equations (equality constraints) relating some of these variables are added, such that the total number of unknowns equates the number of equations. A number of computer programs have been developed for solar and desalination processes simulation, design and optimization. These computer programs were developed through three stages. In the first stage, a special purpose programs (one-off program) are used to solve problems related to a particular process (or unit) with a fixed configuration. The structure of these programs is rigid, simple, and straightforward. All that the user has to supply is the data and the executive handles the program in the same way, irrespective of the nature of the process simulated. The disadvantage of such programs is that a model exists for only one process and any changes made to that process might require extensive re-programming. However, the specialized program makes it much easier to produce mathematical models of sufficient realism. A large number of the published programs for design and simulation of distillation processes are of this type, e.g., these programs are developed by [28] and [29]. In the second generation, the developed computer programs are nominated either general purpose programs or modular programs (flow sheeting approach). These programs are developed to overcome the problems and limitations of the first generation. In these programs, the mathematical model is usually formulated in terms of a set of equations representing the unit processes. Each of these sets of equations is regarded as an independent and self-standing module. In the field of power generation plants, a modular computer program was developed by [30]. This program takes into account the varying in power demands and in operating conditions, as well as varying cycle configurations. A flexible computer program for thermodynamic power cycle calculations was also developed and described by [31]. With this program, the designer can model different cycle schemes by selecting components from an unseen library (under DOS) and connecting them appropriately. A developed FORTRAN program to tackle steady-state simulation and data validation for multi stage flash desalination process is developed by [32]. The process is carried out using an equation-oriented approach in which the decomposition of the system leads to a sensitivity matrix. This type of programs needs expert users to describe the process topology and to enter the required data. The third generation of computer programming for desalination processes is the visual modular program approach. This approach aids operators and designers to build up the process configuration and enter the required data and parameters easily. A visualized program was developed for power station plants by [33]. This program was based on a strong library of thermal units. Different configurations of power plants can be considered by this program. Also, a commercial process simulation tool, ISPEpro, was developed by

Schausberger et al. [34] for studying the performance of a combined power and MSF desalination process. The user defines process flow sheets graphically by icons. Uche et al. [35] developed an object-oriented program for the analysis of power and desalination plants. This software was developed in the form of building blocks for water and energy systems by using a multi-platform (Java language). VDS program [36] is developed for design and simulation of different types and configurations of conventional desalination processes. Object-oriented programming with Visual Basic was implemented to offer a flexible reliable and friendly user-interface. A visual library was built by Mabrouk et al. enables the user to construct different configurations by just clicking the mouse over the required units (icons). The interface aids plant designers, operators and other users to perform different calculations such as energy, exergy, and thermo-economics. In addition, the package enables designers to perform different modifications of an existing plant or to develop a conceptual design for new configurations. A matrix generation technique was used in this program. Large matrix representing the process mathematical model was solved by a developed decomposition technique. This technique is called “Variable Type by Variable Type (VTBVT) technique. In fact, this decomposition technique imposes some limitations on the program generality and flexibility. So, the visual programming techniques of the second generation provide a good solution for some problems related to the first generation programs. These problems include interface, and data & configuration entry. However, nested recycle streams, and the large size of the matrix representing the considered process are still imposing some limitations on this program generation of solar heating and desalination systems. Now, with the rapid uprising of the personal computer hardware and computational & graphics mathematical software, the third generation of modeling and simulation programs for desalination processes is established. These programs are based on the mathematical computations and modeling capabilities of some available commercial programs. MatLab/SimuLink browser is one of the best powerful tool software introduced in the last decades. Gambier [37] introduced the ability of MatLab/SimuLink to design library for multi stage flash components. In Gambier demonstration, the physical properties, and heat transfer correlations, were simulated individually in embedded MatLab/SimuLink blocks. The main objective of this chapter is to demonstrate the developed modular computer program using MatLab/SimuLink environments for different types and configurations of solar desalination units and processes. This modular program has great capabilities to overcome previous programming problems and limitations such as the recycle streams. Some units are modeled to present a good example of the proposed modular program.

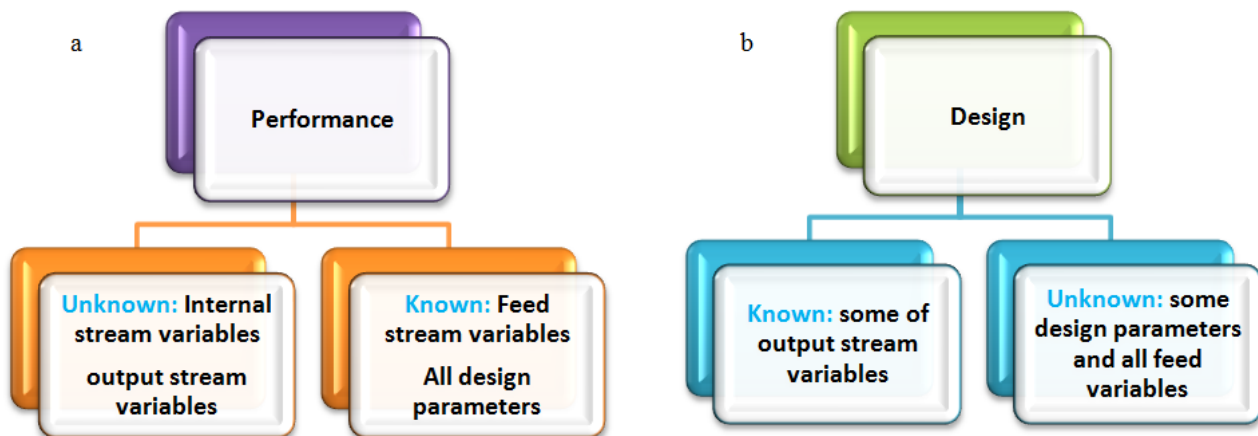


Figure (2.1-a, b) Performance and design characteristics for common flow sheeting programs.

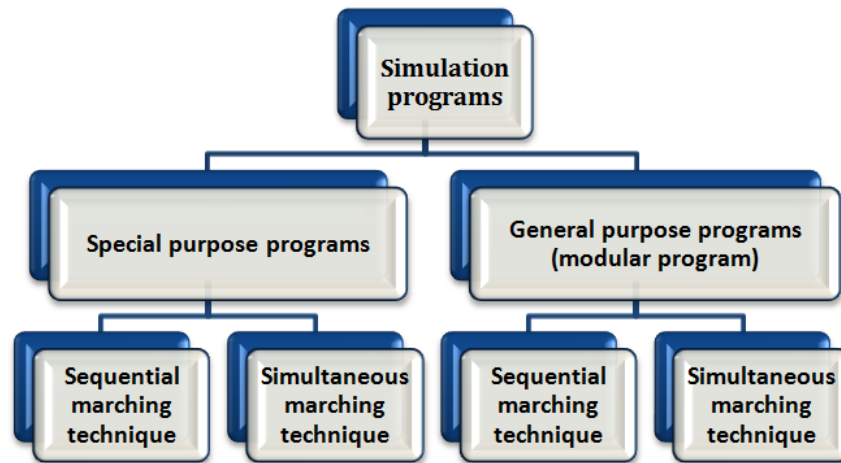


Figure (2.2) Types of simulation programs used for solar desalination processes.

## 2.2 MatLab/SimuLink Software Tool

SimuLink [38] is a general-purpose software program for dynamic systems. This program has been selected to carry out the task of solar desalination modeling and simulation because it offers excellent performance qualities for designing regulation algorithms. SimuLink encourages users to try things out. User can easily build models from scratch, or modifying an existing model. For modeling, SimuLink provides a graphical user interface (GUI) for building models as block diagrams, using click-and-drag mouse operations.

With this interface, user can draw the models just as it would with pencil and paper (or as most textbooks depict them). SimuLink includes a comprehensive block library of sinks, sources, linear and nonlinear components, and connectors. User can also customize and create his own blocks. SimuLink can also utilize many MatLab features. The Library Browser displays the SimuLink block libraries installed on the user system. User builds models by copying blocks from a library into a model window.

SimuLink can also utilize many MatLab features. MatLab is a high-performance language for technical computing. It integrates computation, visualization, and programming in an easy-to-use environment where problems and solutions are expressed in familiar mathematical notation. Typical uses include Math and computation Algorithm development Data acquisition Modeling, simulation, and prototyping data analysis, exploration, and visualization scientific and engineering graphics application development, including graphical user interface building.

MatLab is an interactive system whose basic data element is an array that does not require dimensioning. In industry, MatLab is the tool of choice for high-productivity research, development, and analysis. It supports linear and nonlinear systems, modeled in continuous time, sampled time, or a hybrid of the two. Systems can also be multi-rate, i.e., have different parts that are sampled or updated at different rates.

## 2.3 Simulation of Different Solar Desalination Units

Solar desalination flow sheets often contain the followings:

**1. Solar power cycle (Rankine example) and contains:**

- ✓ Solar radiation model to quantify the amount of thermal power.
- ✓ Solar field (solar collectors) to collect and transfer the amount of thermal power.
- ✓ Boiler heat exchanger to transfer thermal power (in case of indirect vapor generation).
- ✓ Turbine expander unit for electricity generation.
- ✓ Condenser/Brine heater unit for preheating and heating processes.
- ✓ Pump to overcome the pressure losses in the cycle and to close the cycle.

**2. Desalination plants which include:**

- ✓ Membrane desalination technique (reverse osmosis, forward osmosis, ion exchange, and electro-dialysis).
- ✓ Thermal desalination technique (multi stage flash, multi effect distillation, and thermal vapor compression).

In general, solar desalination plants contain a lot of feedback streams, forward streams, different units, and different types with different configurations for each type. Therefore, simulation and programming for a solar desalination plant are tedious problems. Figure (2.3) shows the interface panel of the SDS [39] library under MatLab/SimuLink tool box.

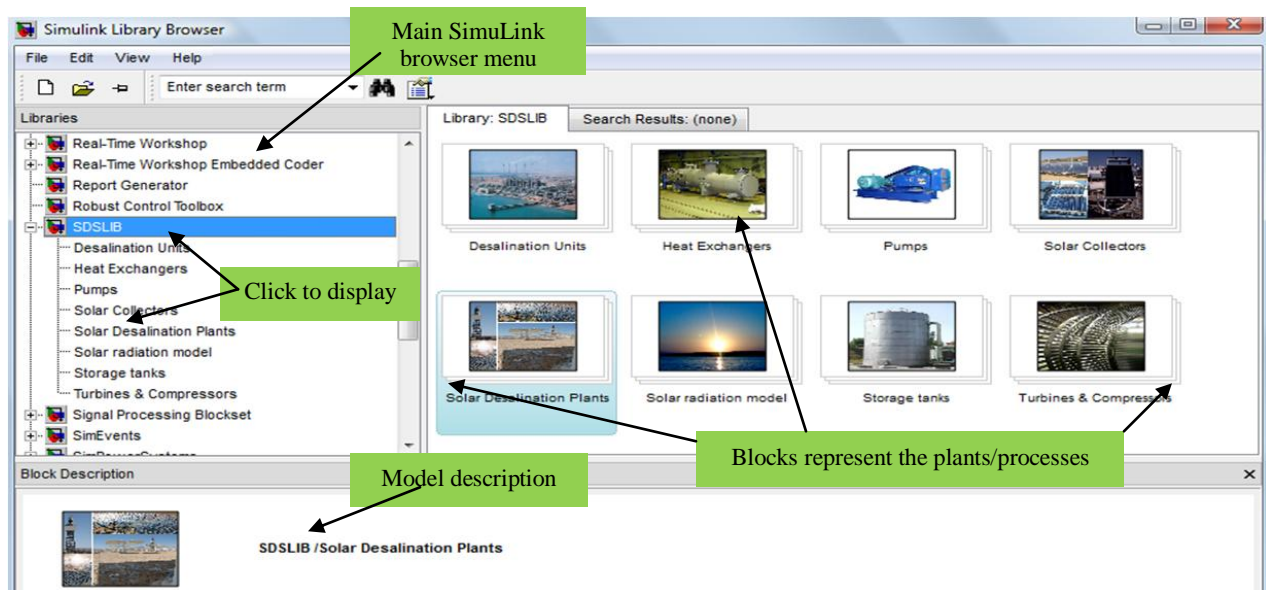


Figure (2.3) SDS software library browser under MatLab/SimuLink interface [39].

### 2.3.1 Validity and reliability of the developed SDS program under SimuLink environment

Different solar desalination processes are considered in this section to show the reliability and flexibility of the developed SDS package. Solar radiation model, organic Rankine cycle (ORC), reverse osmosis (RO), multi stage flash (MSF), thermal and mechanical vapor compressions (TVC & MVC), MED processes are considered as examples to show the scope of the package.

### *a. Solar radiation model*

Solar radiation models are highly useful to estimate the flux over solar plant location. Therefore, it is very important to decide maximum and minimum flux over a specified period for the place of operation. It would not be enough for the scientists or engineers in this location to depend on the measured data only, but it would be important to use a useful theoretical model which could correctly estimate and predict the solar radiation. In the absence of measured data, theoretical models are the only available tool for solar radiation estimation. The correlations for daily global radiation ( $\text{MJ/m}^2$ ), monthly global radiation ( $\text{MJ/m}^2$ ), and instant radiation in  $\text{W/m}^2$  for horizontal surfaces are obtained from El-Sayed [40]. For solar radiation correlation model, input parameters include current hours, Julian day, latitude angle, longitude, and altitude.

The model can estimate different solar angles for a specified location. (zenith, incidence, azimuth, declination), sun set, sun rise times, day hours during the day light, solar time, equation of time, and global radiation (monthly, daily, hourly, and instantaneously). Data results for the location of operation are presented in Table 2.1. Solar radiation correlations are presented in the Appendix. The results of Table 2.1 were obtained using the following parameters for Suez Gulf site: latitude angle  $=30^\circ$  N, and longitude  $=32.55^\circ$  E. Correlations of the solar radiation model are presented in Appendix D.2.

Table 2.1: Data results for solar radiation model based on the specified location of operation.

<b>Parameter:</b>	<b>Data results</b>
Location	Suez Gulf region
longitude	longitude: $32.55^\circ$ E
latitude	latitude: $30^\circ$ N
Equation of time, min	-11.25
Day hours	10.37
Declination-angle	-20.138
Daily average solar radiation, $\text{MJ/m}^2$	21.76
Monthly average of daily total radiation, $\text{MJ/m}^2$	15.623
Extraterrestrial intensity, $\text{W/m}^2$	1409.19
Sun temperature, K	5833.11
Sun rise time	6.814
Sun set time	17.19
Julian day	21 of January

### *b. Solar field model validity*

In this section, the validity of the solar field results under the SimuLink environment is illustrated. Different types of thermal solar collectors are designed and modeled in the SDS library, such as; flat plate collector (FPC), compound parabolic concentrator (CPC), and parabolic trough collector (PTC). The PTC collector is illustrated in this chapter to examine the model validity. Specified input and output parameters and variables are ; ambient temperature  $^\circ\text{C}$ , solar radiation  $\text{W/m}^2$ , collector width m, collector length m, glass cover envelope m, and inner tube diameter m.

Variables such as mass flow rate  $\text{kg/s}$ , inlet collector temperature  $^\circ\text{C}$ , enthalpy  $\text{kJ/kg}$ , and thermo-economic streams are obtained. Also, the results include thermo-physical properties (pressure, temperature, enthalpy, entropy), performance analysis (stream exergy, exergy destruction, thermal power, thermal efficiency, and collector exergetic efficiency), and field design variables (total field area, total field length, number of loops, area per each loop, and total number of solar collectors). Table 2.2 shows the results of the solar PTC block. The validity of these results is examined by comparing it with that obtained by Torres [41].

Table 2.2: A comparison between the SDS [39] and reference [41] results for Solar Rankine power cycle (direct vapor generation operation).

Parameter:	SDS [48]: $\varepsilon=0$	Ref [29] $\varepsilon=0$	SDS [29]: $\varepsilon=0.8$	Ref [29] $\varepsilon=0.8$
<b>Working fluid</b>	<b>Toluene</b>			
<b>Evaporation temp, °C</b>	<b>300</b>	<b>300</b>	<b>300</b>	<b>300</b>
<b>Evaporation pressure, bar</b>	32.75	32.757	32.75	33.737
<b>Superheating temp, °C</b>	300	300	<b>380</b>	<b>380</b>
<b>Condenser pressure, bar</b>	0.06215	0.0624	0.06215	0.0624
<b>Working fluid flow rate, kg/s</b>	0.5744	0.563	0.4511	0.442
<b>Rejected power, kW</b>	323.2	318.4	208.9	209.8
<b>Rankine efficiency, %</b>	22.82	23.37	31.33	31.78
<b>PTC area, m<sup>2</sup></b>	681.3	672	500	514.3

$\varepsilon$ : The effectiveness

### c. Turbine model

Turbine model is developed by specifying the input parameters such as the power needed by the load, turbine thermal, and generator efficiencies. The output variables are thermo-physical properties (pressure, temperature, entropy, enthalpy...), thermo-economic streams, and mass flow rate. The mass flow rate would replace the old value from the memory block after some iteration.

### d. Recuperator & feed heater models

Recuperators are widely used for organic cycle's operations. The presence of the recuperator unit utilizes available energy in the turbine exhaust to preheat the working fluid stream entering the solar field. Open feed heater is basically a mixing chamber, where the steam extracted from the turbine mixes with the feed fluid exiting the pump. The mixture leaves the heater as a saturated liquid at the heater pressure. This kind of regeneration not only improves the cycle efficiency, but also provides a convenient means of de-aerating the feed fluid. The extracted pressure values are assigned based on each working fluid property.

### e. Condenser/Brine-heater model

Condenser/brine-heater model is simulated and designed to find out the total area, number of tubes, overall heat transfer coefficient, heat rejection, and effectiveness. The block also calculates thermo-economic and exergetic values in the output streams. Some data results for the condenser block are illustrated in Table 2.2.

### f. Pump model

Pump unit is modeled to calculate the power required across inlet and outlet streams and by the pressure loss through the solar field and condenser unit. The output stream from the pump unit will enter the recuperator unit in case of regeneration, or the directly to the solar field in case without regeneration.

## 2.3.2 Validity evaluation of some desalination processes under SimuLink environment

### a. Reverse Osmosis (RO) model

The mathematical model validity of RO is examined in this section. The real data for Sharm El-Shiekh desalination plant [36] is used for this purpose. The model results are compared with the ROSA6.1. [42] software program and Sharm El-Shiekh desalination plant [36]. The plant design parameters are presented in Table 2.3.



Table 2.3: Specified design parameters of Sharm El-Shiekh RO desalination plant [36].

Variable	Value
Feed flow rate, m <sup>3</sup> /h	468
Feed salinity, TDS, ppm	45000
Recovery ratio	0.30
# of stages	1
# of pressure vessels/elements	42/7
Feed temperature, °C	24-40
Fouling factor	0.85
Feed pressure, bar	67

Fresh water product  $M_p$  and the plant recover ratio are specified for design calculations of RO desalination process. The fresh water product will decide the plant power, specific power consumption  $SPC$ , the needed feed  $M_f$ , the required feed pressure  $\Delta P$ , the product salinity  $X_d$ , the rejected brine  $M_b$ , salt rejection percentage  $SR$ , and the pump horse power needed  $HP$ . The RO pump efficiency is about 80% and the feed flow rate salinity is specified as 45,000 ppm.

The input feed sea water temperature is fixed as 25°C. The plant recovery ratio is specified as 30%. The results of the developed program show a good agreement with the other software results (ROSA6.1, and [36]) as presented in Table 2.4. This indicates the validity of both the proposed RO mathematical model and the SDS program. RO block is built as one block contains all equations needed for the simulation process. It can then be copied and dragged with solar cycle or with any thermal desalination process such as MSF plant as hybrid processes.

Table 2.4: SDS results of Sharm El-Shiekh desalination plant vs. ROSA6.1 and [36].

Variable	SDS [39]	ROSA6.1 [42]	Sharm El-Shiekh [36]	Units
$SPC$	7.75	7.76	7.76	$kWh/m^3$
$HP$	1131	1131.42	1130	$kW$
$M_f$	485.9	485.9	486	$m^3/h$
$M_b$	340.4	340.36	340.23	$m^3/h$
$X_b$	64180	62150	66670	$ppm$
$X_d$	250	283.83	200	$ppm$
$SR$	0.9944	--	0.9927	--
$\Delta P$	6850	6670	6700	$kPa$

#### *b. Multi Stage Flash (MSF) model*

Different configurations of MSF desalination processes (brine recycles MSF-BR, once through MSF-OT, and brine mixing MSF-MX) can be manipulated by the developed SDS program under SimuLink environment. For design mode, distillate product, blow down temperature, inlet sea water temperature, top brine temperature, and number of stages are specified.

The process validity of MSF-BR (Eoun Mousa, Egypt with capacity of 5000m<sup>3</sup>/day [36]) is examined by comparing the results the present SDS program. Both results are illustrated in Table 2.5. A good agreement is obtained for both programs.

Table 2.5: Comparison results of SDS Eoun Mousa MSF-BR plant [36].

Variables:	Eoun Mousa MSF-BR [36]	SDS
Total feed, kg/s	436.11	438.2
Capacity, kg/s	57.87	57.87
Make up, kg/s	183.33	184.2
Recycle flow rate, kg/s	510	507.8
Cooling water splitter ratio	0.42	0.42
Brine recycle splitter ratio	0.724	0.719
Top brine temperature, °C	110	110
Recycle blow down temperature, °C	48.05	49.7
Vapor temperature at last stage, °C	41	41.47
Sea water salinity, ppm	48620	48620
Area/Heat recovery stages, m <sup>2</sup> /#	488/17	440/17
Area/Heat rejection stages, m <sup>2</sup> /#	357/3	321/3

### c. Single Effect Thermal and Mechanical Vapor Compression models

Single effect evaporation (SEE) has limited industrial applications. The system is used in marine vessels and this because the system has a thermal performance ratio less than one, i.e.; the amount of water produced is less than the amount of heating steam used to operate the system. However, it is considered here just to examine the program validity for effect evaporation process. Figure (2.4) shows a schematic diagram for the SEE system.

The main components of the process are the evaporator and the feed pre-heater condenser. The evaporator consist of an evaporator\condenser heat exchanger tubes, a vapor space, un-evacuated water pool, a line for removal of non condensable gases, a water distribution system, and a mist eliminator. Table 2.6 demonstrates the obtained results by the present SDS program and by Dessouky [43]. Also, results for a single effect thermal and mechanical vapor compression are illustrated in Table 2.6. Results from the developed SDS program compared with the experimental results of Dessouky [43] and [36] shows a good agreement under the same range of operating conditions.

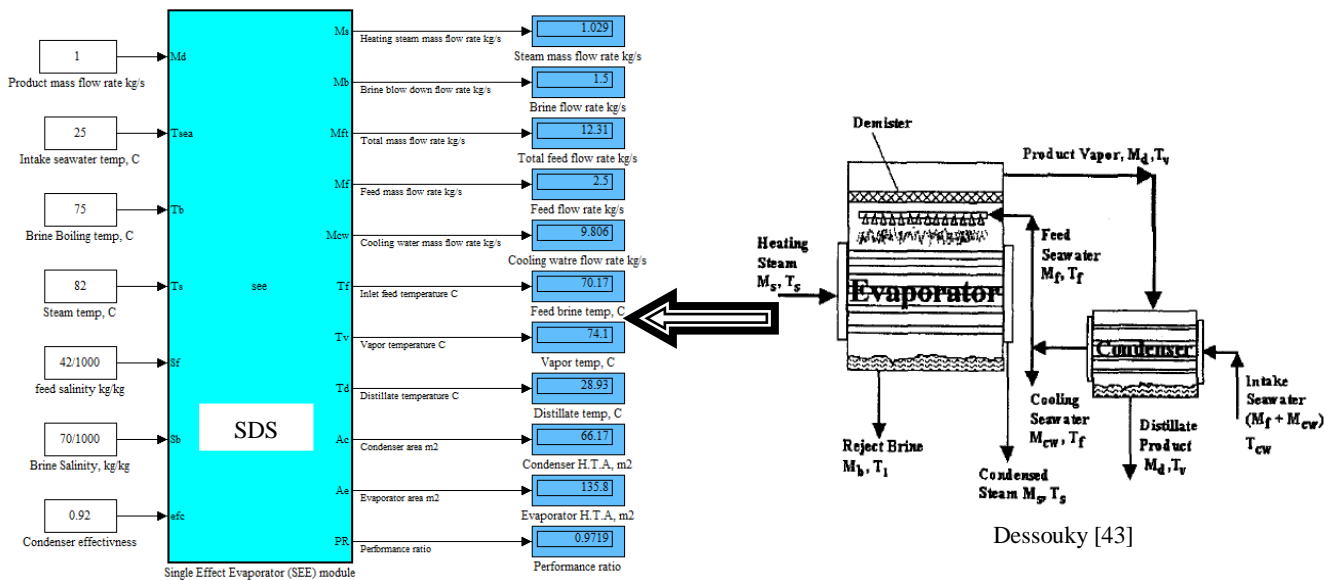


Figure (2.4) Schematic display of Single Effect Evaporation (SEE) under MatLab-SimuLink software environment.

Table 2.6: The SDS and Dessouky [43] results comparison for SEE model.

Single effect evaporation (SEE)		
Variables:	Dessouky [43]	SDS
Steam mass flow rate kg/s	1.03	1.029
Brine mass flow rate kg/s	1.5	1.5
Total feed mass flow rate kg/s	12.3	12.31
Feed mass flow rate kg/s	2.5	2.5
Cooling water mass flow rate kg/s	9.8	9.806
Feed temperature °C	70	70.17
Vapor temperature °C	74.097	74.1
Distillate temperature °C	28	28.93
Condenser area m <sup>2</sup>	65.5	66.17
Evaporator area m <sup>2</sup>	135.9	135.8
Performance ratio	0.97	0.9719
*Product mass flow rate kg/s	1	1
*Seawater temperature	25	25
*Condenser effectiveness	--	0.92
*Feed salinity ppm	42000	42000
*Steam temperature °C	82	82
*Brine temperature °C	75	75
*Brine salinity ppm	70000	70000
Single effect thermal vapor compression (SETVC)		
Variables:	Dessouky [43]	SDS
Steam mass flow rate kg/s	1.03	1.029
Brine mass flow rate kg/s	1.5	1.5
Total feed mass flow rate kg/s	12.3	12.31
Feed mass flow rate kg/s	2.5	2.5
Cooling water mass flow rate kg/s	9.8	9.806
Preheated feed temperature °C	70	69.2
Vapor temperature °C	74.097	74.1
Entrained vapor mass flow rate kg/s	0.37	0.373
Motive steam flow rate kg/s	0.678	0.68
*Product mass flow rate kg/s	1	1
*Seawater temperature	25	25
*Condenser effectiveness	0.9	0.9
*Steam temperature °C	82	82
*Brine temperature °C	75	75
*Brine salinity ppm	70000	70000
*Feed salinity ppm	42000	42000
*Motive steam pressure kPa	750	750
*Compression ratio	2.5	2.5
Evaporator area m <sup>2</sup>	39.8	41
Single effect mechanical vapor compression (SEMVC)		
Variables:	Mabrouk [36]	SDS
*Product mass flow rate kg/s	17.36	17.36
Steam mass flow rate kg/s	17.36	17.36
Brine mass flow rate kg/s	31.25	31.25
Total feed mass flow rate kg/s	48.61	48.61
*Brine salinity ppm	70000	70000
*Feed salinity ppm	45000	45000
*Seawater temperature	27	27
Vapor temperature °C	60	60
Feed temperature °C	57.93	57.04
Steam temperature °C	96.2	96.17
Distillate blow down temperature °C	32.51	32.93
Brine blow down temperature °C	37.72	37.7
Inlet compressor pressure kPa	20.03	19.84
Outlet compressor pressure kPa	27.047	26.8
Compressor power kW	1081	1076
Specific power consumption kWh/m <sup>3</sup>	17.291	17.2
*: Specified variables		

#### d. Multi Effect Distillation models

A multi-effect distillation (MED) desalting system with unit capacity up to 5 MIGD is a strong competitor to the multi-stage flash (MSF) desalting system due to its low specific energy consumption and the low temperature steam required to operate the system [44]. The process of adding more evaporators can be continued to a final (n) evaporator.

The vapor generated in the last evaporator (n) is directed to a bottom condenser where it is condensed. The heating steam (heat source) is condensed in the first effect at the highest temperature. This is called the n-effect distillation system. The temperature and pressure in each effect are decreased by the increase of the effect number.

Different MED configurations and types are simulated and designed using SDS package. The results show a very good agreement with some existing plants. Figure (2.5) shows a display of the MED under SDS package. Also Table 2.7 shows the data results comparisons between SDS and Darwish [45].

Data comparison with reference [45] is implemented according to Sidem 12-effect units and 11 feed heaters. The unit given data are: n (number of effects) =12, output  $D=500$  ton/h (139 kg/s), TBT=65°C,  $T_b=38^\circ\text{C}$ ,  $T_f=28^\circ\text{C}$ , feed temperature at condenser exit=35°C, feed salinity  $S_f=46$  g/kg, and maximum salinity  $S_b=72$  g/kg where  $f$  and  $b$  related to feed and brine respectively.

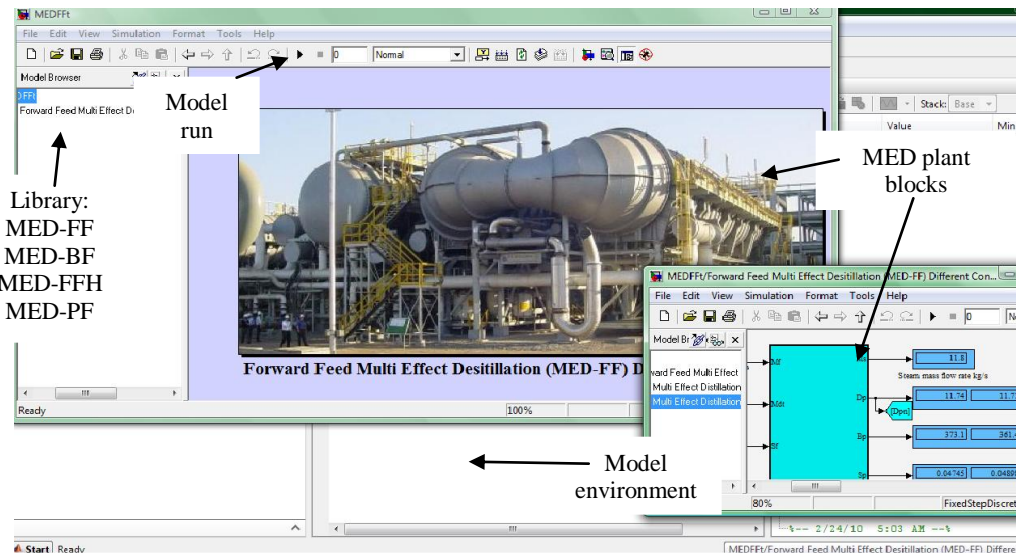


Figure (2.5) MED model environment designed using SDS package.

Table 2.7: Data validation between SDS and Darwish [52] for MED model.

Effect #	T brine °C		T feed °C		M brine kg/s		M distillate kg/s		S brine g/kg	
	SDS	Ref [45]	SDS	Ref [45]	SDS	Ref [45]	SDS	Ref [45]	SDS	Ref [45]
1	65	65	62	62	373.09	373.18	11.74	11.85	47.44	47.46
2	62.54	62.55	59.54	59.55	361.41	361.37	11.71	11.8	48.98	49.01
3	60.09	60.09	57.09	57.09	349.79	349.62	11.68	11.75	50.6	50.66
4	57.63	57.64	54.63	54.64	338.22	337.91	11.65	11.71	52.33	52.41
5	55.18	55.18	52.18	52.18	326.72	326.26	11.62	11.66	54.18	54.29
6	52.72	52.37	49.73	49.73	315.27	314.65	11.59	11.61	56.14	56.29
7	50.27	50.27	47.27	47.27	303.88	303.09	11.56	11.56	58.25	58.44
8	47.81	47.82	44.82	44.82	292.55	291.58	11.53	11.51	60.51	60.74
9	45.36	45.36	42.36	42.36	281.27	280.12	11.5	11.46	62.93	63.23
10	42.9	42.91	39.91	39.91	270	268.71	11.47	11.41	65.55	65.91
11	40.45	40.45	37.45	37.45	258.87	257.34	11.45	11.36	68.38	68.82
12	38	38	35	35	247.76	246.03	11.42	11.32	71.45	71.99

## 2.4 Solar Power Cycle for Desalination Processes: Case Study

In this section, a solar organic Rankine cycle for electricity and power generation is combined with reverse osmosis desalination plant. The plant contains different units such as; solar PTC field, turbine unit, condenser, and recuperator, pump, and RO block. RO desalination plant is operated with pressure exchanger (RO-PEX) unit. A higher efficiency positive displacement power recovery devices (pressure exchangers), that in the past were only used in small RO seawater units, are also slowly gaining acceptance in large desalination plants.

Hydraulic efficiency of this type of equipment is in the range of 94-96% [46]. In this work, the values of 80% and 96% are considered for booster pump and PEX unit respectively. Some of these devices utilize pistons; another transfer energy through a direct contact between concentrate and the feed stream. The process is modeled and designed under SimuLink environment. By specifying the fresh water demand, the cycle design calculations are performed.

Table 2.8: Energy and thermo-economic results for solar powered RO-PEX technique.

Variables:	SDS results:
<b>RO-PEX section:</b>	
RO Mass flow rate, m <sup>3</sup> /h	486
RO brine loss flow rate, m <sup>3</sup> /h	340.2
Brine loss salinity, g/m <sup>3</sup>	63.56
Product salinity, g/m <sup>3</sup>	0.2682
PEX hydraulic power, kW	607.8
Booster pump power, kW	62.08
High pressure pump power, kW	332.1
High pressure pump pressure, bar	68.74
RO Specific Total cost, \$/m <sup>3</sup>	0.68
<b>Organic power cycle (ORC) section:</b>	
Site	latitude angle =30° N, and longitude =32.55° E.
Working fluid	Toluene
Solar field area, m <sup>2</sup>	1887
Solar field efficiency, %	73.61
Solar field thermal power, kW	1181
Developed turbine power, kW	394.18
Organic cycle flow rate, m <sup>3</sup> /h	6.235
Rankine efficiency, %	32.64
Specific power consumption, kWh/m <sup>3</sup>	2.704
Organic pump power, kW	8.89
Condenser power rejection, kW	774.6
Total cycle exergy destruction, kW	2538
Overall exergy efficiency, %	11.61
Total cycle exergy inlet, kW	2871
Total operating & maintenance cost, \$/h	99.26
Thermo-economic product cost, \$/GJ	66
Total water price, \$/m <sup>3</sup>	0.71

The RO plant productivity is set as 3500m<sup>3</sup>/day. Salinity gradient is 45g/kg. Recovery ratio is 30%, number of elements per pressure vessels is 7/48, element area is 35.3m<sup>2</sup>, high pressure pump (HPP) efficiency is 80%, and the fouling factor (FF) is set as 85%. The results are obtained. A typical summer operating conditions are considered with global radiation of 850W/m<sup>2</sup>. The outlet collector temperature is 340°C with Toluene as a working fluid. The turbine, pump, generator efficiencies are

85%, 75%, and 95% respectively. RO plant life time normally set as 20years with 5years for element per vessel, and load factor is set as 90%. The developed model can perform energy, exergy, and cost and thermo-economic analysis for the considered process. Some results are illustrated above in Table 2.8. The RO section with PEX device exhibits a total area of parabolic trough collector (PTC efficiency=73%) equal to 1887m<sup>2</sup> with Toluene as a working fluid. This area would generate a thermal power about 1887kW with outlet temperature 340°C. PEX operation reduces the required electric power from the generator to reach 394kW instead of 1131kW in basic configuration. Lowering the required power by the existence of PEX would lower all the dependent parameters (solar field area, pump power, mass flow rate, condenser area, exergy destruction, and operational costs).

Based on the above comparisons, SDS program is developed for design and simulation of different types and configurations of conventional and solar desalination processes. Embedded block programming with SimuLink environment are used to develop a flexible reliable and friendly user-interface. The desalination plant components such as heat exchangers, flash chambers, evaporators, pumps, steam ejectors, compressors, reverse osmosis membranes, pipes, etc., are modeled and stored as blocks in SimuLink visual library.

The library enables the user to construct different desalination techniques and configurations by just clicking the mouse over the required units (blocks). The interface aids plant designers, operators and other users to perform different calculations such as energy, exergy, and thermo-economics. In addition, the package enables the designers to perform different modifications of an existing plant or to develop the conceptual design of new configurations. Some operating desalination plants are simulated by the present package to show its reliability and flexibility. The developed SDS package has some features concluded in:

- Easy model construction.
- Easy to convert the designed code to be self executable and work under different computer languages (Visual basic, Visual C, Visual C++, and Visual Fortran).
- The model allows users easily change to the plant variables and different operating conditions with ultimate stream allowance.
- The developed program overcomes the problem appears in other techniques of simulation such as sequential approach, matrix manipulation technique.

Based on the developed SDS, the upcoming chapters study the thermo-economic results of solar powered different types of desalination systems. It became very easy to analyze and optimize the solar desalination systems based on the developed package. Further information about the methodologies, analysis, equations, working fluids thermo physical properties, desalination configurations and the processes description are available in the Appendices.

## Chapter 3: Exergy & Thermo-economic Analyses of Solar Organic Cycles Assisted Desalination Processes

### 3.1 Working Fluids Selection for Solar ORC

The use of solar energy to generate mechanical power, one can in principle employ the thermodynamic power cycles commonly used for the generation of mechanical power from a heat source. The general method of converting thermal energy into mechanical energy in this case is to apply several processes on the *working fluid* of the power cycle. The selection of the more reasonable working fluid that can be used with the solar operated Rankine cycle depends on many criteria the most important of which is the maximum temperature of the cycle. Other criteria include the following [47];

- High molecular weight to reduce the turbine nozzle velocity.
- Reasonable pressure corresponding to boiling temperature of the fluid (high pressure requires careful sealing to avoid leakage).
- Dry expansion, i.e., positive slope of the vapor saturation curve on T-S diagram, to assure that all expansion states in the turbine exist on the superheat region.
- A critical temperature well above the maximum operating temperature of the cycle.
- Inexpensive, non-corrosive, non-flammable, and non-toxic fluid.
- Reasonable pressure at condensing temperature (usually about 30-40°C).

In many solar operated Rankine systems the maximum temperature does not exceed 400°C and thus water loses its advantages as a working fluid. Many organic fluids were found to satisfy the criteria stated above. Literature [47] shows that the selection of organic fluids is variable, wide and based on different criteria.

Some literatures built their choices based on molecular weight and P-T behavior [47]. Others selected the organic fluid based on boiling point and melting point; while others made their selection based on the thermal efficiency [48, 49].

For thermal efficiency; it is not recommended as the only reference for comparison and selection of the organic fluids because the systems with high thermal efficiency may also have high irreversibility and economically not favorable.

In this part; the selection of the organic fluids is based on the combination of all the above criteria. Based on critical temperature which should be well above the collector operating temperature; Butane, Isobutane, Propane, R134a, R152a, R245ca, and R245fa are selected to operate ORC with FPC. Fluids like R113, R123, Hexane, and Pentane; are chosen for CPC type.

For PTC type; Dodecane, Nonane, Octane, and Toluene are suitable for this kind of collectors. Table 3.1 shows a list of the considered working fluids grouped according to collector's operating temperature.

Table 3.1: Properties list of the selected working fluids.

<i>Working fluid (WF)</i>	<i>Formula</i>	<i>Molecular weight, kg/mol</i>	<i>T<sub>critical</sub> °C</i>	<i>P<sub>critical</sub> bar</i>	<i>Collector type</i>
<b>Butane</b>	$C_4H_{10}$	58.122	151.9	37.96	FPC
<b>Isobutane</b>	$C_4H_{10}$	58.122	134.66	36.23	FPC
<b>Propane</b>	$C_3H_8$	44.1	95	39.75	FPC
<b>R134a</b>	$C_2H_2F_4$	102.03	101	40.54	FPC
<b>R152a</b>	$C_2H_4F_2$	66.05	113.261	45.1675	FPC
<b>R245ca</b>	$C_3H_3F_5$	134.04	170	36.36	FPC
<b>R245fa</b>	$C_3H_3F_5$	134.048	153	35.7	FPC
<b>Pentane</b>	$C_5H_{12}$	72.1488	196.6	33.7	CPC
<b>R113</b>	$C_2Cl_3F_3$	187.37	213	32.42	CPC
<b>R123</b>	$C_2HCl_2F_3$	152.93	182	35.63	CPC
<b>Hexane</b>	$C_6H_{14}$	86.175	231	29.71	CPC
<b>Dodecane</b>	$C_{12}H_{26}$	170.334	382	17.94	PTC
<b>Nonane</b>	$C_9H_{20}$	128.25	321	22.7	PTC
<b>Octane</b>	$C_8H_{18}$	114.22	296	24.92	PTC
<b>Toluene</b>	$C_7H_8$	92.1384	318	41.26	PTC

The fluids selected for FPC (Table 3.1) are regrouped again based on the operating temperature of the used collector. For R152a, R134a and Propane are not recommended to be in use with FPC because these two fluids have a critical temperature not well above the collector design temperature (80~100°C). At the same time, these fluids present an isentropic action (not dry and/or positive slope) on the T-S diagram. However; the remaining fluids (Butane, Isobutane, R245ca, and R245fa) considered suitable for FPC according to the critical temperature range (130-170°C) and the positive slope on T-S.

However; according to the molecular weight, R245ca presents the highest value about (134 kg/mol) followed by Butane and Isobutane. For condenser pressure, lowering it will increase the cycle efficiency and also the cycle net work. To take advantage of the increased efficiencies at low pressure, the condensers usually operate well below or near the atmospheric pressure. However, there is a lower limit on the condenser pressure that can be used. It can't be lower than the saturation pressure of cooling water temperature (range of 30-35~40 °C *i.e.*,  $P_{cond}=0.032\sim0.06$  bar).

However; lowering the condenser pressure is not without any side effects; it creates the possibility of air leakage into the condenser and will increase the moisture content at the final stages of the turbine. Therefore, R245ca recorded suitable condenser pressure (about 1.51 bar) at temperature about 35°C while Isobutane achieves condenser pressure about 4.72 bar at the same condenser temperature. Also, R245ca, its lower saturation pressure at 100°C (about 7.8 bar) may be considered an advantage when used in DVG process inside the absorber tubes of a FPC.

Therefore, R245ca is suitable for FPC from the molecular weight, critical temperature, and condenser pressure. But R245ca shows an isentropic behavior on T-S diagram. On the other hand, Butane shows dry (sharp positive slope than R245ca) behavior on T-S diagram. At the same time R245ca considered more toxic than Butane. For these reasons Butane is considered for FPC. Figure (3.1-a) shows a schematic diagram of the considered working fluids on T-S.

Figure (3.2-a) shows the saturation pressures for different collector types with different working fluids at the saturation temperature at the range of 35-100°C. For CPC unit, Pentane, Hexane, R113, and R123 are examined as working fluids. R113 has a highest molecular weight against the remaining (187.3 kg/mol) followed by R123, Hexane, Pentane respectively. However, regarding the condenser pressure, Hexane recorded the minimum value (0.3064 bar) at saturation temperature equal 35°C, followed by R113 with 0.654 bar. Pentane gives higher values little bit more than R113 and Hexane with a value of 1.011 bar. However; R123 gives the highest value for condenser pressure as 1.34 bar. Therefore, Hexane



is recommended for the operation of CPC with ORC. Also it is highly recommended to choose an organic fluid with high critical temperature to achieve highest cycle efficiency and that's another advantage for Hexane against the remaining fluids for CPC operation. Figure (3.1-b) shows a schematic diagram of the selected working fluids on T-S related to CPC collector. Figure (3.2-b) shows the saturation pressures for CPC collector with different working fluids at the saturation temperature of the range of 35-100°C.

Dodecane, Toluene, Nonane, and Octane are evaluated for PTC operation. They have high critical temperature with accepted range for PTC to operate ORC. Dodecane gives the highest molecular weight against the others with a value equal to 170.3 kg/mol, followed by Nonane, Octane, and Toluene respectively. However, Dodecane gives very low value for condenser pressure at 35°C (about 0.00043 bar). At this pressure value many aspects for safety are required and large condensers are needed. Nonane comes next with respect to the condenser pressure by 0.0106 bar.

Octane achieves a suitable value for condenser pressure about 0.0336 bar but with lowest critical temperature (about 296°C) value. Dodecane and Octane are not suitable for solar ORC due to very low condenser pressure and low critical temperature respectively. Toluene gives a condenser pressure value about 0.0648 bar. And that's mean it is suitable for this selection. Although Nonane is recommended by its molecular weight and critical temperature (little bit higher than Toluene), Toluene achieves the recommended condenser pressure value at the same saturation temperature.

Also, Toluene achieves lower values of specific vapor volume ( $0.00117 \text{ m}^3/\text{kg}$  Vs  $18.75 \text{ m}^3/\text{kg}$ ), this leading to a low condenser area followed by achieving low in economic evaluation. Figure (3.2-c) shows the saturation pressures for PTC collectors with different working fluids at the saturation temperature at the range of 35-100°C.

From the working fluid analysis, it is clear to elect Butane, Hexane, and Toluene to be work with FPC, CPC, and PTC respectively in case of direct vapor generation (DVG). Pentane considered valuable however; its effect on the condenser unit is not remarkable. Also, Nonane is not recommended for Rankine condensation stage due to lower density meaning high specific vapor volume.

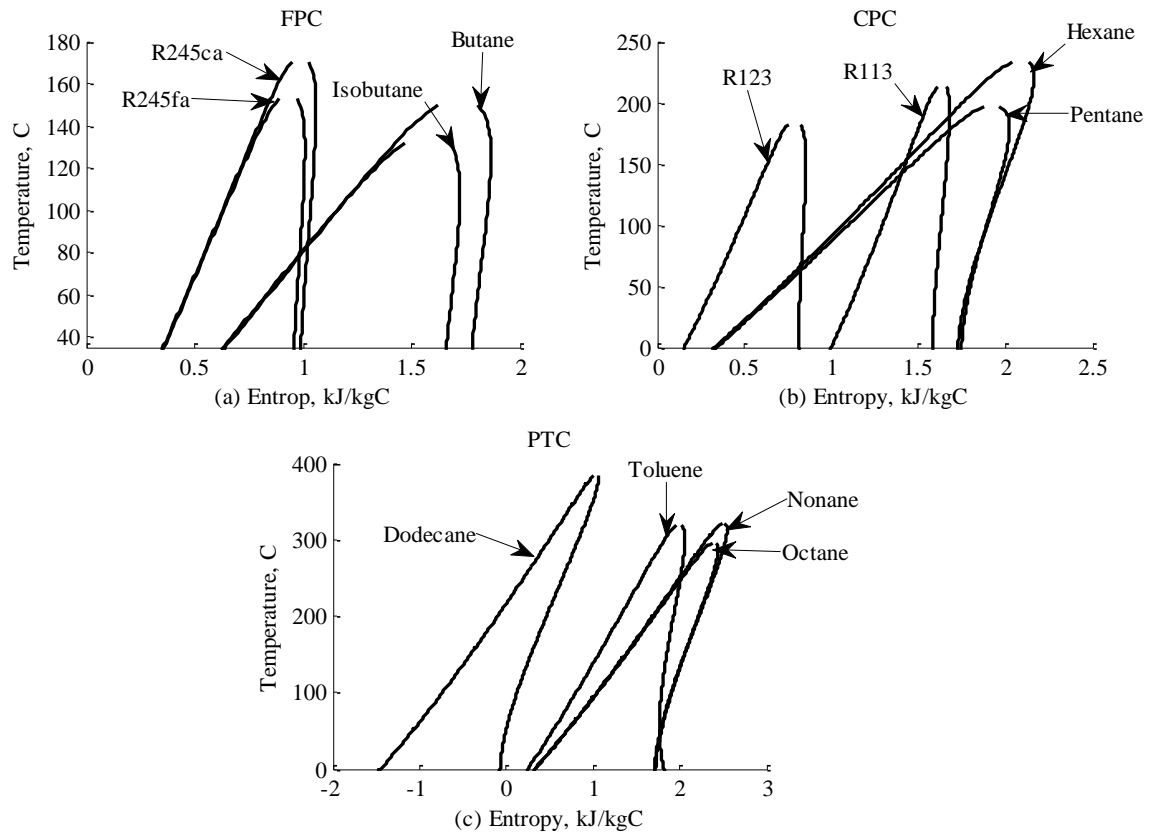


Figure (3.1) The selected fluids behavior on T-S diagram for different solar collectors (FPC, CPC, and PTC).

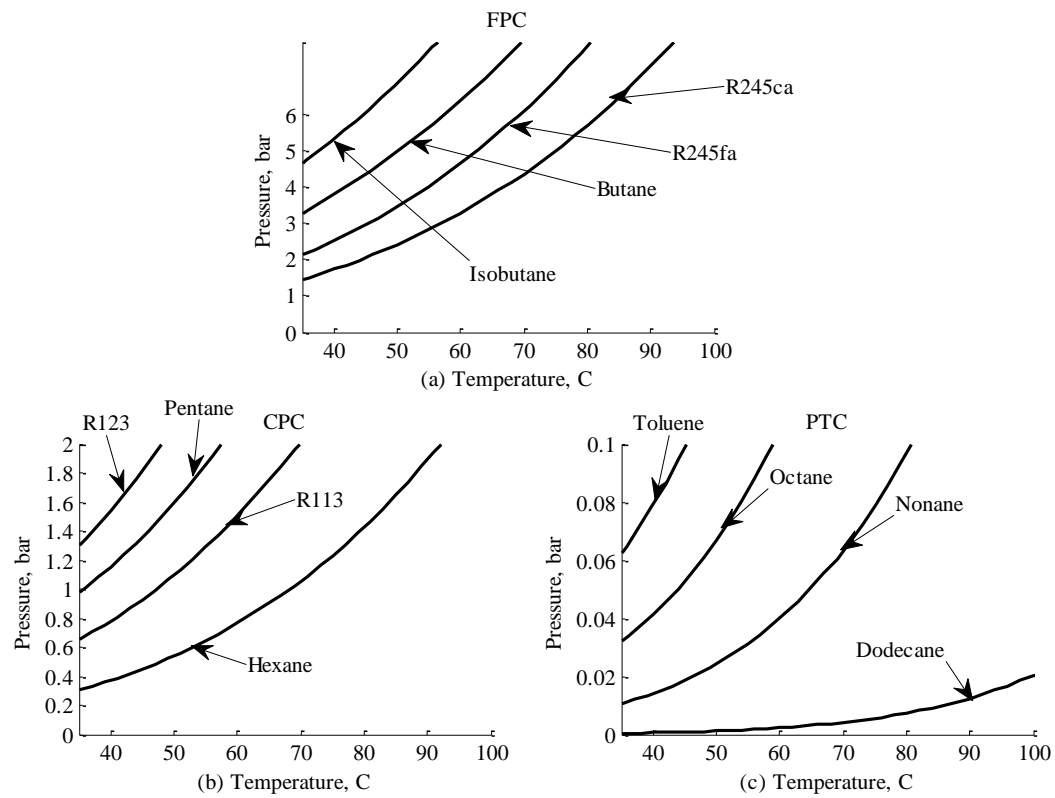


Figure (3.2) Saturation pressures for different collectors with different working fluids at the saturation temperature at the range of 35-100°C.

## 3.2 Solar ORC Assisted RO Desalination Process

### 3.2.1 Solar ORC/RO process: Basic Cycle

Although a small ORC is characterized by rather low efficiencies (8–12%), it is particularly easy to manufacture. Another important advantage of ORC's is that it can utilize waste heat from low-quality exhausts or steam, which makes it suitable for a very large range of applications which include those with low temperature waste heat sources [47]. Donghong Wei [50] presented a system performance analysis and optimization of an organic Rankine cycle (ORC) system using HFC-245fa (1,1,1,3,3-pentafluoropropane) as working fluid driven by exhaust heat.

The thermodynamic performances of an ORC system under disturbances have been analyzed. Pedro J. Mago [51] presented an analysis of regenerative organic Rankine cycles using dry organic fluids, to convert waste energy to power from low-grade heat sources. The dry organic working fluids that selected for that investigation were R113, R245ca, R123, and Isobutane, with boiling points ranging from -12°C to 48°C. The evaluation was performed using a combined first and second law analysis by varying certain system operating parameters at various reference temperatures and pressures.

Delgado-Torres et al [52, 53, 54] gave a detailed analysis of low power (100kW) solar driven Rankine cycles for medium range of operating temperatures. Toluene, Octamethylcyclotetrasiloxane (D4) and Hexamethyldisiloxane (MM) were considered working fluids for ORC. The direct solar vapor generation (DVG) configuration of solar with ORC was analyzed and characterized with LS-3 and IND300 parabolic trough collector (PTC) models. According to Torres results, PTC LS-3 type is implemented for this study. The proposed configuration consists of the vapor generation within the absorber tube of the parabolic trough. The power output from the turbine is used to drive the (RO) unit. It is clear from literature that solar powered organic Rankine cycle is implemented however; such systems should be evaluated based on exergy and thermo-economic analyses.

In this part, exergy and thermo-economic approaches are used to evaluate the operation of solar ORC combined with RO desalination system. For more details, all the specific relations and the mathematical models are illustrated in the appendix. The validity of the mathematical model is examined in the past chapter. The real data for Sharm El-Shiekh desalination plant [36] is used for this purpose based on Suez Gulf region (latitude angle =30° N, and longitude =32.55° E). The plant design parameters are presented in Table 3.2. Figure (3.3) shows a schematic diagram of the basic solar-ORC powered RO process.

Table 3.2: Specified design parameters of Sharm El-Shiekh RO desalination plant [36].

Variable	Value
Feed flow rate, m <sup>3</sup> /h	468
Feed salinity, TDS, ppm	45000
Recovery ratio	0.30
# of stages	1
# of pressure vessels	42
Feed temperature, °C	24-40
Fouling factor	0.85
Feed pressure, bar	67
# of elements	7
Element type	FTSW30HR-380

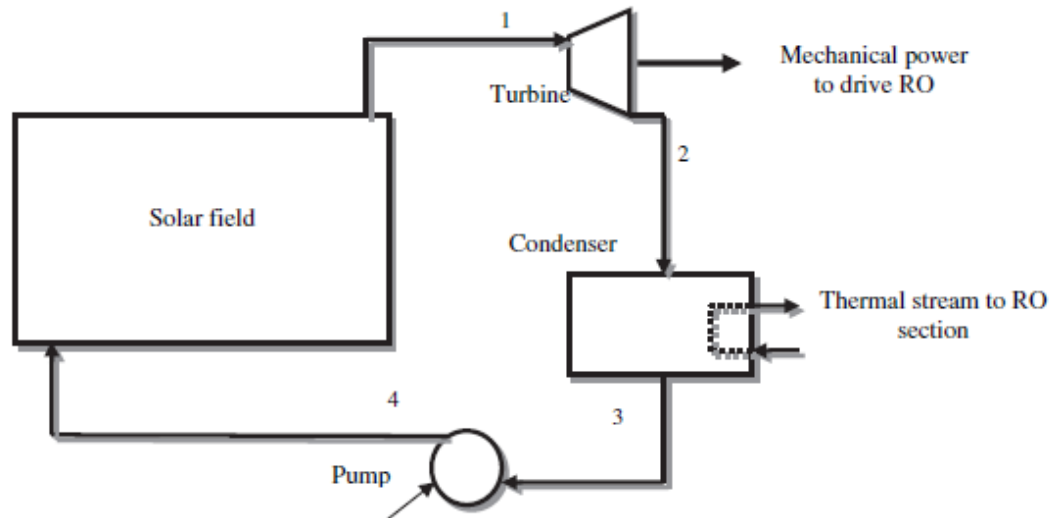


Figure (3.3) Schematic diagram of DVG solar ORC powered RO (basic cycle).

For design calculation based on the RO mathematical model; it should be noted that the distillate product  $M_d$  should be specified with plant recovery ratio. The distillate product will decide the plant power capacity, specific power consumption  $SPC$ , the demanded feed, the required feed pressure, the product salinity, the rejected brine, salt rejection percentage, and the pump horse power needed. The proposed RO section has an element area fixed as  $35.4 \text{ m}^2$  while using FTSW30HR-380. The RO pump efficiency is about 80% and the feed flow rate salinity is specified as 45,000ppm. The input feed sea water temperature is fixed as  $25^\circ\text{C}$ . The plant recovery ratio is specified as 30%. The assumptions and specified parameters for the proposed cycle may be listed as follows:

- The isentropic efficiencies of the turbine, and the pump would be fixed as 85% and 75% respectively.
- The value of 95% is assigned for generator unit.
- Condensation and inlet cooling water temperatures would be fixed at  $35^\circ\text{C}$  and  $20^\circ\text{C}$  respectively.
- For climate conditions, solar radiation is maintained based on Suez Gulf region (latitude angle  $=30^\circ \text{ N}$ , and longitude  $=32.55^\circ \text{ E}$ ), and ambient temperature is maintained at  $25.4^\circ\text{C}$ .
- Feed water salinity is about 45,000ppm.
- Inlet seawater temperature to the RO module is depending on the outlet temperature value from condenser/pre-heater unit.
- RO product will be set as  $145.8 \text{ m}^3/\text{h}$ .
- Other specifications of Sharm El-Shiekh RO desalination plant like fouling factor, recovery ratio, and high pressure pump are presented in Table 3.2.

For DVG saturation operation; maximum operating temperature for FPC is set as  $80^\circ\text{C}$ , and  $130^\circ\text{C}$  for CPC and  $300^\circ\text{C}$  for PTC. However, for DVG superheat operation; the deference temperature between saturation and superheat degrees is set as  $20^\circ\text{C}$  for all collector types. The obtained results are illustrated in Table 3.3.

Table 3.3: Results of ORC/RO process with different working fluids and different types of solar collectors.

Parameter	Saturation			Superheat		
	Butane, FPC $T_{co}=80^{\circ}C$	Hexane, CPC $T_{co}=130^{\circ}C$	Toluene, PTC $T_{co}=300^{\circ}C$	Butane, FPC $T_{co}=100^{\circ}C$	Hexane, CPC $T_{co}=150^{\circ}C$	Toluene, PTC $T_{co}=320^{\circ}C$
$P_{ev}$ , bar	10.14	4.992	32.78	10.14	4.992	32.78
$A_{cob}$ , $m^2$	2.111E+04	1.506E+04	6747	2.14E+04	1.696E+04	6734
$W_b$ , kW	999.4	1065	1119	997.8	1054	1120
$\eta_R$ , %	8.15	14.46	25.81	8.07	13.89	26
$\dot{m}$ , kg/s	28.31	13.94	5.75	26.16	13.8	5.24
$I_{total}$ , MW	16.48	11.65	4.951	16.7	13.18	4.94
$\eta_{ex}$ , %	5.22	6.5	14.04	5.2	5.85	14.06
SPC, kWh/m <sup>3</sup>	6.855	7.302	7.677	6.84	7.231	7.679

Parameter	Water					
	FPC $T_{co}=80^{\circ}C$	Saturation CPC $T_{co}=130^{\circ}C$	PTC $T_{co}=300^{\circ}C$	FPC $T_{co}=100^{\circ}C$	Superheat CPC $T_{co}=150^{\circ}C$	PTC $T_{co}=320^{\circ}C$
$P_{ev}$ , bar	0.576	2.755	85.9	0.576	2.755	85.9
$A_{cob}$ , $m^2$	1.864E+04	1.27E+04	5949	1.82E+04	1.626E+04	5851
$X$ , quality	0.92	0.86	0.74	0.93	0.93	0.76
$W_b$ , kW	1019	1084	1130	1022	1055	1131
$\eta_R$ , %	8.89	17.68	29.93	10.17	13.34	30.47
$\dot{m}$ , kg/s	4.12	2.38	1.407	3.97	3	1.335
$I_{total}$ , MW	14.48	9.731	4.28	14.13	12.6	4.2
$\eta_{ex}$ , %	5.64	7.64	16	6.82	7.86	22.52
SPC, kWh/m <sup>3</sup>	6.988	7.437	7.748	7.01	7.24	7.756

Note:  $T_{co}$ : Outlet collector top temperature to the sink (turbine).

It is clear from the result table that saturation operation for Butane with (FPC) collector gives lower values of collector area, and total exergy destruction than superheat operation. Therefore; saturation operation for Butane (FPC) would give higher values of power output, Rankine efficiency, mass flow rate, overall exergy efficiency, and specific power consumption than the superheat operation. While comparing with the conventional working fluid (Water); Water (FPC) gives lower values against Butane (FPC) with respect to evaporation pressure, collector area, mass flow rate, and total exergy destruction.

Also; Water with (FPC) gives higher values with respect to power output, Rankine efficiency, overall exergy efficiency, and specific power consumption. However, Water with (FPC) needs an expansion wet turbine for dryness fraction of about 0.92 otherwise the superheat operation should be implemented with the expense of reducing in overall exergy efficiency and increasing in collector area. Saturation operation of Hexane (CPC) would give the same behavior as Butane results. That's mean, lower values in collector area, and total exergy destruction than superheat operation. And that would be followed by an increase in power output, Rankine efficiency, mass flow rate, overall exergy destruction, and the specific power consumption. Water with (CPC) gives lower results in collector area, and total exergy destruction than that of Hexane (CPC).

However; the steam quality 0.86 is lower than that of the FPC. But; Hexane (CPC) achieved lower results than Butane (FPC) with respect to evaporation pressure, collector area, mass flow rate, and total exergy destruction. At the same time Hexane (CPC) gives higher results than Butane (FPC) with respect to power output, Rankine efficiency, overall exergy efficiency, and specific power consumption. The same behavior exists for Water (CPC) results Vs Water (FPC) results regardless the quality of steam produced at the turbine last stage. PTC operation is quite different against the other two types. Saturation operation for Toluene (PTC) gives lower values than superheat ones with respect to Rankine efficiency, overall exergy efficiency, and specific power consumption. At the same time saturation operation gives

higher results than superheat operation for Toluene (PTC) with respect to collector area, mass flow rate, and total exergy destruction. Water with (PTC) produces more attractive results than Toluene with (PTC) collector regardless the steam quality produced at the turbine last stage and the higher values of evaporation pressure (higher values of evaporation pressure may cause problems to the collector sealing and joints). From the above analysis it could be concluded that, Toluene (PTC-superheat) and Water (PTC-superheat) considered valuable for the operation of Sharm El-Shiekh RO desalination plant. Moreover; saturation operating condition for Toluene operation is quite remarkable with no need for superheat.

Cost analysis is introduced based on two major parts. First of them is the solar organic Rankine cycle, and the second is the RO desalination plant. There is no much precise information about the current capital cost of ORC. By information obtained from literatures; solar collectors costs may be evaluated as 150~200\$/m<sup>2</sup>. The operation and maintenance costs for the case of these solar collectors have been estimated to be 15% of the investment cost. Table 3.4 shows the investment capital costs (*ICC*) and operation and maintenance costs (*O&M*) of solar Rankine cycle. For the RO, the operation and maintenance costs have been considered as shown in Table 3.5 [55]. The investment and operating & maintenance costs analyses are performed for each component, solar field, steam turbine, condenser, and pump unit. For that purpose; the amortization factor is estimated based on the following relation [56];

$$A_f = \frac{i \cdot (1 + i)^{LT_p}}{(1 + i)^{LT_p} - 1} \dots (1)$$

Where *i* is the interest rate and set as 5%, *LT<sub>p</sub>* is the plant lifetime and set as 20 years. For RO section, cost analyses are estimated based on direct capital costs (*DCC*), indirect capital costs (*ICC*), and the total capital costs (*TCC*). Table 3.5 [63] illustrates the costs for RO desalination section. Cost analysis are performed based on USD (\$) currency. The total water price (TWP, \$/m<sup>3</sup>) for the ORC-RO plant may be estimated based on the following relation:

$$TWP = \frac{Cost_{ORC} + Cost_{RO}}{M_d} \dots (2)$$

Table 3.4: *ICC* and *O&M* costs for solar organic Rankine cycle components.

Parameter	<i>ICC</i> , \$	<i>O&amp;M</i> , \$	<i>TCC</i> , \$/year	<i>Z<sup>IC&amp;OM</sup></i> , \$/h	Ref
Solar field	$639.5 \times (A_{col})^{0.95}$	$15\% \times ICC_{col}$	$A_f \times (ICC + O\&M)_{col}$	$TCC_{col}/8760$	[55]
Steam turbine	$4750 \times (W_t)^{0.75}$	$25\% \times ICC_{st}$	$A_f \times (ICC + O\&M)_{st}$	$TCC_{st}/8760$	
*Recuperator	$150 \times (A_{rec})^{0.8}$	$25\% \times ICC_{rec}$	$A_f \times (ICC + O\&M)_{rec}$	$TCC_{rec}/8760$	
Condenser	$150 \times (A_{cond})^{0.8}$	$25\% \times ICC_{cond}$	$A_f \times (ICC + O\&M)_{cond}$	$TCC_{cond}/8760$	
Pump	$3500 \times (W_p)^{0.47}$	$25\% \times ICC_{pump}$	$A_f \times (ICC + O\&M)_{pump}$	$TCC_{pump}/8760$	

Note: All parameters in Table 3.4 are identified in the Appendix.

Table 3.5: *ICC* and *O&M* costs for RO desalination plant [56].

<i>DCC</i> , \$	<i>ICC</i> , \$	<i>TCC</i> , \$	<i>ACC</i> , \$/year	<i>O&amp;M</i> , \$/year	<i>Z<sup>IC&amp;OM</sup></i> , \$/h
$CC_{swip} = 996 \times M_f^{0.8}$	$ICC = 27\% \times DCC$	$TCC = ICC + DCC$	$ACC = TCC \times A_f$	$OC_{power} = LF \times 0.06 \times SPC \times M_d$	$Z^{IC\&OM} = (ACC + OC_m) / 8760$
$CC_{hpp} = 393000 + 10710 \times \Delta P_f$				$OC_{labor} = LF \times 0.01 \times M_d$	
$CC_e = Fe \times P_p \times N_p + Fe \times PV_p \times n_v$				$OC_{chm} = LF \times 0.04 \times M_d$	
$CC_{equip} = CC_{swip} + CC_{hpp} + CC_e$				$OC_{insur} = 0.005 \times TCC \times A_f$	
$CC_{site} = 10\% \times CC_{equip}$				$OC_{memb} = P_p \times N_p / LT_m$	
$DCC = CC_{equip} + CC_{site}$				$OC_{ro} = OC_{power} + OC_{labor} + OC_{chm} + OC_{insur} + OC_{memb}$	

Note: All parameters in Table 3.5 are identified in the Appendix.

The results for DVG process for both steam operating conditions (saturation and superheat) are shown in Figure (3.4). The figure shows that total water price (TWP,  $\$/\text{m}^3$ ) for superheated steam under FPC and CPC is higher than saturation operating conditions. This may due to the area added on the T-S curve for each working fluid based on mass flow rate, power produced, and condenser area. Butane (FPC)<sub>sat-sup</sub> gives the highest values among the other fluids followed by Water (FPC)<sub>sat-sup</sub>. And that is referring to the massive effect of solar field costs (larger area means higher costs) compared with the other unit's costs. Hexane (FPC)<sub>sat-sup</sub> followed by Water (FPC)<sub>sat-sup</sub> comes next with an advantage for Water (CPC)<sub>sat-sup</sub>. Toluene (PTC)<sub>sat-sup</sub> followed by Water (PTC)<sub>sat-sup</sub> give lowest values of total water price (TWP,  $\$/\text{m}^3$ ) with an advantage to Water (PTC)<sub>sat-sup</sub> operation. From the techno-economic analysis of the considered cycles, it can be deduced that PTC is the best option in both steam operating conditions.

It is quite clear that Water and Toluene are suitable for both operations. However, Water needs expansion wet turbine for dryness fraction ranged between 0.7 and 0.95 for both operations. Moreover, the evaporation high pressure (85.9 bar) considered not safe for the collector design requirements. Between all units, solar collector field (based on area as a cost function) exhibits the largest effect on the cycle specific cost, minimum exergy destruction, and overall exergy efficiency. Generally and for both operations; increasing the collector evaporation temperature will cause an increase in turbine power, Rankine efficiency, pump work, *SPC*, and reverse osmosis operating pressure; with decrease in collector area, working fluid flow rate, condenser area, condenser heat load. Thus, according to the current techno-economic framework, the PTC system is the best choice.

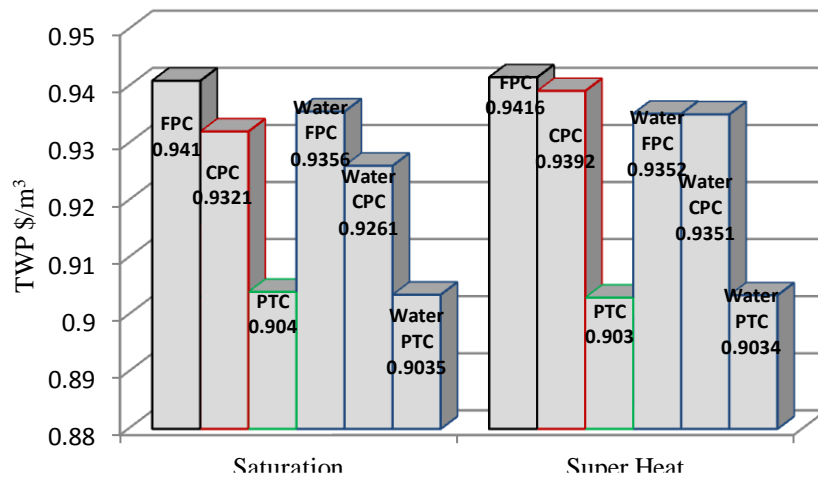


Figure (3.4) Total Water Price (TWP,  $\$/\text{m}^3$ ) for cycles different working fluids & different steam operating conditions with different collector types.

### 3.2.2 Solar ORC/RO process: Regenerative Cycles

There are many possible organic Rankine cycle configurations, several of which will be considered. However, a particular design that is by far the most commonly observed in commercial applications. Also, reverse osmosis (RO) is quite suitable for small to medium capacity systems and also has good perspectives for cost reduction and improvement in efficiency in the near future. In this part, the considered process power plant cycle consists of solar organic Rankine cycle (solar collector, turbine, condenser, and pump). It is revealed from the previous part that Toluene is recommended and



considered to drive the solar ORC part as a DVG technique. The aim of this section may be concluded into these points:

- Investigating and analyzing the design of solar Rankine cycle under different configurations, and different types of operations.
- Saturation and superheat operations are used to examine the cycle configurations performance with different working fluids (Water and Toluene for parabolic trough collector-PTC).
- Adding open feed heater (OFH) and recuperator units under saturation and superheat operation is investigated. Also adding OFH with recuperator together is established for both operations (saturation and superheat).
- Examining and comparing the results with the basic cycle (cycle without OFH or/and recuperator) is evaluated.

Different schematic diagrams of the proposed cycles (Regenerative ORC+RO) are presented below. The assumptions and specified parameters for the proposed cycle model may be listed as following:

- Rankine cycle gross work will be assigned by RO unit.
- Turbine, generator, and all Rankine pumps efficiencies would be fixed as 85%, 95%, and 75% respectively.
- Condensation and inlet seawater temperatures would be fixed at 35°C and 20°C respectively.
- Recuperator effectiveness will set at 0 for basic ORC, and 0.8 for regeneration case.
- For saturation operation; maximum operating temperature is set as 300°C for PTC. For superheat operation the degree temperature of superheat is set to be higher than the saturation temperature by 20°C for all collectors (PTC=300+20°C).
- Based on the unremarkable results in the previous section, Butane (FPC) and Hexane (CPC) are eliminated from this comparison.

#### *a. ORC/RO with recuperator unit*

Figure (3.5) shows a schematic diagram of regenerative Rankine cycle (R-ORC). The recuperator unit is added to the basic cycle components to preheat the inlet fluid stream entering the collectors field. The only departure from the basic Rankine cycle in the system shown in Figure (3.2) is the presence of the recuperator unit which utilizes available energy in the turbine exhaust to preheat the working fluid stream entering the solar field.

#### *b. ORC/RO with OFH unit*

Figure (3.6) shows a schematic diagram of organic Rankine cycle with Open Feed Heater (OFH) unit (OFH-ORC). Open feed heater is basically a mixing chamber, where the steam extracted from the turbine mixes with the feed fluid exiting from the pump. The mixture leaves the heater as a saturated liquid at the heater pressure. Such kind of regeneration not only improves the cycle efficiency, but also provides a convenient means of deaerating the feed fluid. The extracted pressure values are assigned based as 0.8bar Toluene.

#### *c. ORC/RO with OFH and recuperator*

Figure (3.7) shows a schematic diagram of the 3<sup>rd</sup> configuration. This configuration is considered the same as the basic one. Otherwise, adding open feed heater and recuperator unit together is the difference. Before entering the solar field, the working fluid passes first through the recuperator then the OFH. A portion of extracted steam is mixed with the preheated fluid from the recuperator unit. For each working fluid, the value of extraction pressure is considered with value of recuperator effectiveness. For Toluene, 0.8bar of extraction is operated with 0.8 of recuperator effectiveness.

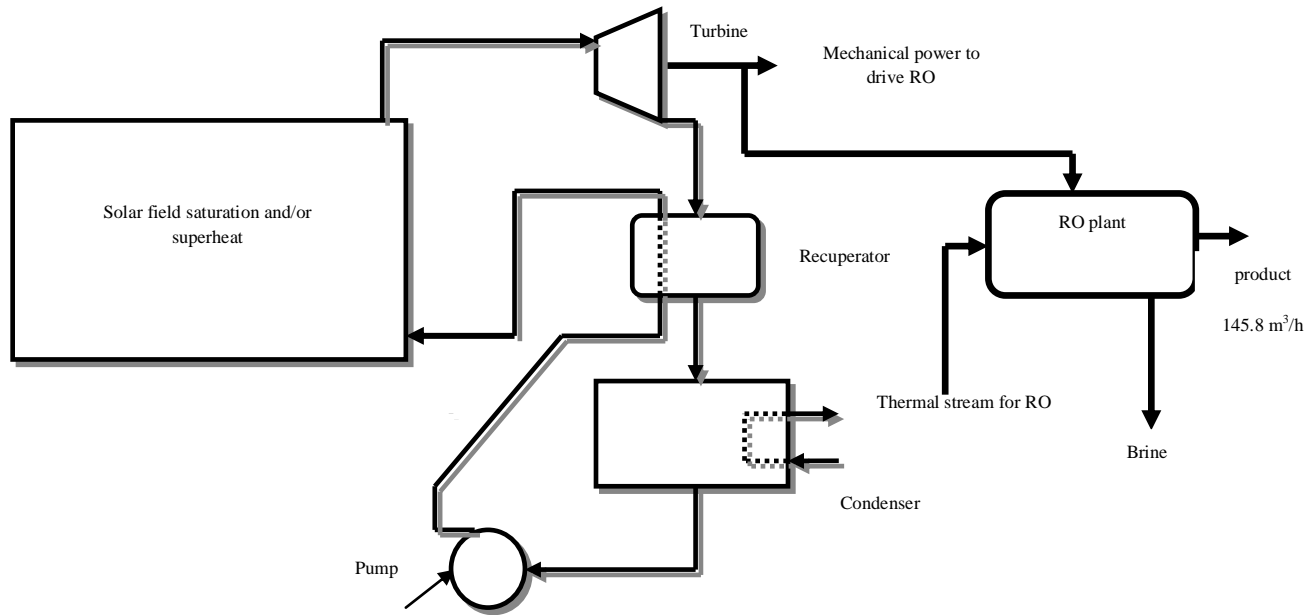


Figure (3.5) A schematic diagram of solar Rankine cycle components for saturation and/or superheat with recuperator unit.

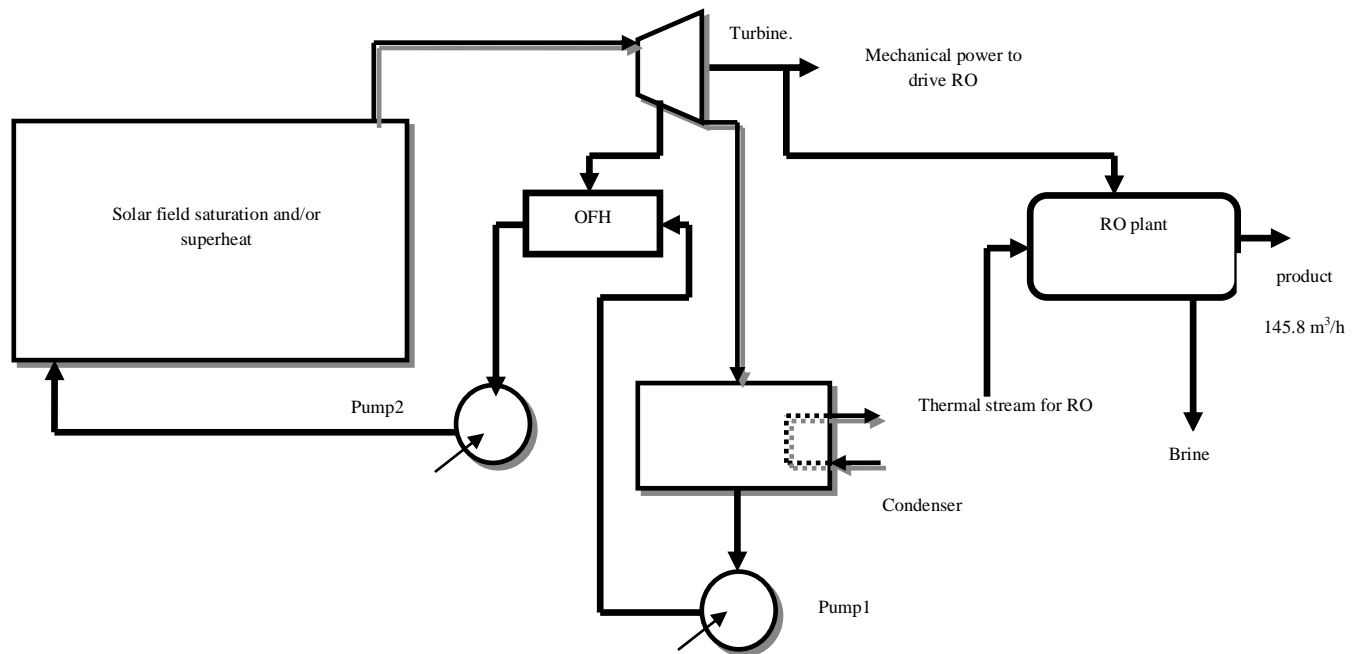


Figure (3.6) A schematic diagram of solar Rankine cycle components for saturation and/or superheat with OFH unit.

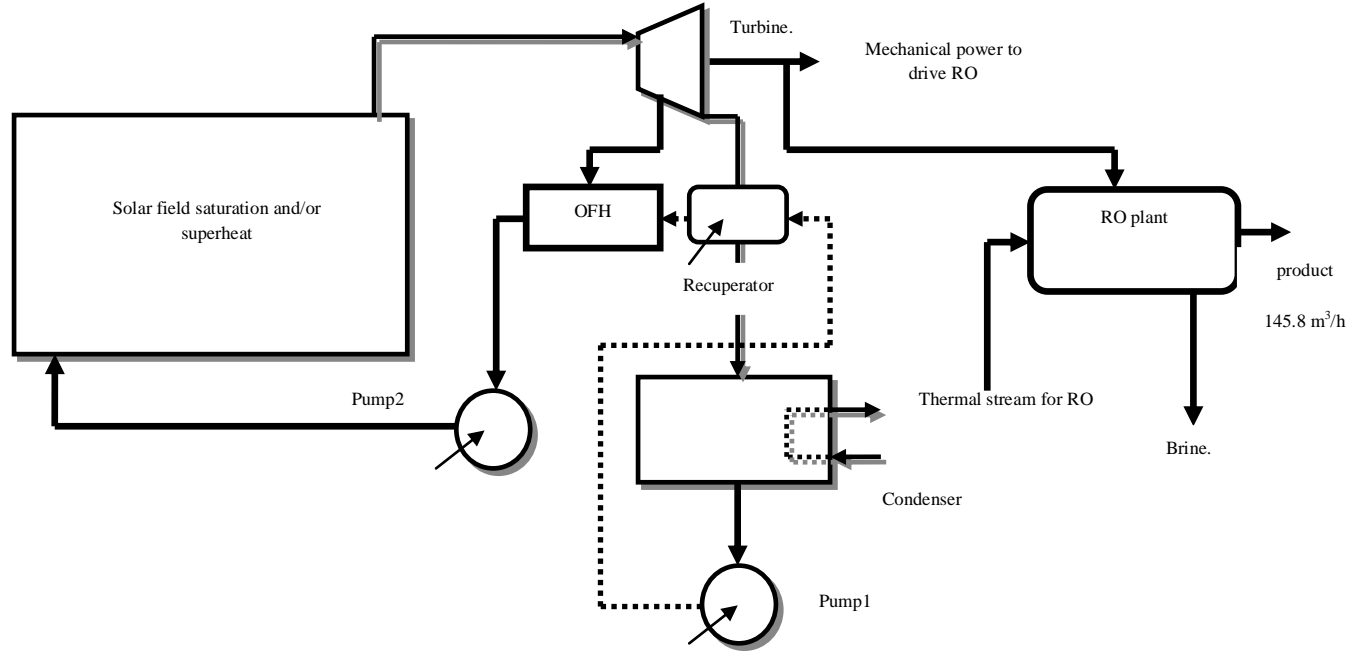


Figure (3.7) A schematic diagram of solar Rankine cycle components for saturation and/or superheat with OFH and recuperator units.

A methodology of energy, exergy and cost analysis for performance of different configurations of solar organic Rankine cycle is presented in this part (more analyses are mentioned in the appendix). The performance analysis of the energy part is concluded in Rankine efficiency, collector area, power generation, and specific power consumption (*SPC*). The first law Rankine efficiency is calculated from the following relation;

$$\eta_{ORC} = \left( \frac{W_t - W_p}{m \cdot (h_{co} - h_{ci})} \right)_{Basic} = \left( \frac{W_t - W_{p1} - W_{p2}}{m \cdot (h_{co} - h_{ci})} \right)_{Reg} \dots (3)$$

Collector area is a very effective parameter to judge the system performance causing an increasing or decreasing in the plant total cost. The collector total area is estimated based on the collector energy balance equation as a function of collector efficiency as following;

$$A_{col} = Q_u / \eta_{col} G_b \dots (4)$$

Where  $Q_u$  is the collector thermal power and ( $G_b$ ) is the direct global beam over the collector area, and  $A_{col}$  is the collector total area. The characteristics efficiency curve of the collector is presented in the **Appendix B.1.1**. The collector energy equation may exist according to the following relation;

$$Q_u = m_{col} \times (h_{co} - h_{ci}) \dots (5)$$

The required power input in kW to the RO high pressure pump (HPP) is estimated as;

$$HPP_{power} = \frac{1000 \times M_f \times \Delta P}{3600 \times \rho_f \times \eta_p} \dots (6)$$

Where  $\rho_f$  is the feed flow rate density, and  $\eta_p$  is the driving pump mechanical efficiency and  $\Delta P$  is the pressure difference across the RO module. The specific power consumption in kWh/m<sup>3</sup> is estimated as;

$$SPC = \frac{HPP_{power}}{M_d} \dots (7)$$

The cycle flow rate in kg/s is presented as following;

$$m = \left( \frac{W_t}{\eta_t \times \eta_{g \times} (h_{ti} - h_{tos})} \right)_{Basic} = \left( \frac{W_t}{\eta_t \times \eta_{g \times} ((h_{ti} - Y \times h_{to_b}) - ((1 - Y) \times h_{to}))} \right)_{Reg} \dots (8)$$

Where  $h$  is the specific enthalpy across the turbine,  $Y$  is the extraction percentage, and  $\eta_g$  is the generator efficiency. The subscript  $b$  is referring to the bled steam from the turbine. Where,  $t_{i,o}$  is referring to inlet and outlet turbine conditions. Exergy and cost analyses are presented based on the previous indicators that are presented in the Appendix. For Toluene (PTC), Tables 3.6, 3.7 summarize the results obtained for saturation and superheat operations at different configuration. Toluene results give a superior data related to Rankine efficiency, solar collector aperture area, exergy efficiency, and total water price.

In Toluene case, the cycle mass flow rate is decreased causing an increasing in seawater temperature stream to the RO leading to a significant increase in power generated. Saturation operating conditions for the basic configuration considered competitive only against OFH and OFH+REC configurations. Basic configuration gives lowest solar field area against the regeneration techniques except recuperator configuration.

Recuperator configuration results a minimum solar field area ranged as 5866m<sup>2</sup>. However, recuperator configuration generates more power due to the decreasing of seawater stream temperature to the RO module. The generated power would affect the plant  $SPC$ ,  $TPC_{cost}$ , and mass flow rate. Due to this effect,  $TPC_{cost}$  for recuperator configuration considered the lowest among the other configurations causing a decrease in  $TWP$  \$/m<sup>3</sup> (from 1\$/m<sup>3</sup> in basic technique to 0.903\$/m<sup>3</sup> in recuperator technique).

Saturation results based on Rankine efficiency drive to assure that recuperator configuration gives the highest value (30%) followed by the configurations of OFH+REC (25.92%), basic (25.81%), and OFH (24.06%) respectively. The total exergy destruction rate explains the massive effect of total solar field area. As a result of increasing or decreasing the solar field area, the exergy destruction rate is followed. Due to this, recuperator gives the lowest values of exergy destruction rate through the process units followed by OFH+REC, basic, and OFH respectively.

Moreover, recuperator configuration achieves maximum exergy efficiency among the other configurations (16.99% Vs 14% in basic, 15.3% in OFH, and 16.8% in OFH+REC). Recuperator configuration gives lowest values while comparing to  $TPC_{cost}$ ,  $SPC$ , and  $TWP$ . That is referring to the effect of solar field area. Moreover, the total water price ( $TWP$ , \$/m<sup>3</sup>) is considered the final judge on process cycle from the side of techno-economic evaluation.

Superheat operation almost gives the same behavior but a significant changes are noticed. Solar field area decreased against saturation operation and that affects on the cycle exergy destruction rate, inlet exergy to the process cycle, exergy efficiency, and specific total plant cost. Recuperator configuration gives the highest results in Rankine efficiency followed by the OFH+REC cycle, basic, and OFH respectively. Also recuperator configuration achieves minimum inlet exergy and exergy destruction rate among the other configurations (4.2MW Vs 5MW in basic technique). It is obvious that Toluene (PTC) under superheat operation gives remarkable results with only recuperator configuration against the other configurations.

Unlike organic fluids, Water is the working fluid of choice for the vast majority of large scale fossil-fired Rankine cycle power plants. Water is well-suited for those high-temperature applications, but it has its limitations that become more significant during lower temperature operation. It is the unique properties of organic fluids that allow them to excel where water falters. The principle difference between organic fluids and water is their behavior when expanding from a saturated or superheated state through a turbine at low to moderate temperature (200-400°C). The analysis shows that recuperator configuration is not suitable for Water operation (saturated and superheat). Because the turbine outlet

conditions considered wet with quality ranged from 70% to 85%. At the same time, under the case of PTC ( $T_{evp}=200^{\circ}\text{C}$  &  $300^{\circ}\text{C}$ ) steam superheat temperature should reach  $465^{\circ}\text{C}$  &  $620^{\circ}\text{C}$  to achieve quality about 100% and that can't meet the PTC operation and its safety requirements. Moreover, evaporation and superheated steam pressures give higher values in case of Water (at  $T_{evp}=300^{\circ}\text{C}$   $P=85.9\text{bar}$ ) against Toluene case. These terms are considered not safe for the collector absorber tubes. For these mentioned reasons, recuperator, OFH and OFH+REC configurations wouldn't be used in Water analysis, only the basic configuration (see figure (3.2)) is performed. Results for basic configuration are carried out for superheat operation only. Also, Water results are established only for PTC technology. Parabolic dish is suitable for water operation however; it needs a complicated tracking system. Also, holding a massive tanks (filled with water) is not favorable and needs a special structure. Therefore; parabolic dish is not considered in this work.

Basic configuration gives higher results based on Rankine 1<sup>st</sup> and 2<sup>nd</sup> efficiencies. Based on power generated by the HPP unit, basic configuration gives a little bit more power compared with the other working fluids resulting an increasing in  $TPC_{costs}$ ,  $SPC$ , and  $TWP$ . This is due to that the solar field area has a massive effect against the effect of generated power by the HPP unit. Water with PTC gives attractive results (see Table 3.9) against the remaining fluids but the steam quality considered low about 77% and needs a large turbines. For that, Toluene for PTC with recuperator configuration gives superior results regardless Water operation with steam quality less than 100%. Table 3.9 shows and summarizes the results obtained only for recuperator configuration for Toluene and Water working fluids.

Table 3.6: Data results of Toluene (PTC) for different configurations under saturation operation.

<b>Toluene (PTC, Saturation)</b>							
<b>Parameter:</b>	<b><math>A_{cob} \text{ m}^2</math></b>	<b><math>W_b \text{ kW}</math></b>	<b><math>m_{ORC} \text{ kg/s}</math></b>	<b><math>\eta_R \%</math></b>	<b><math>P_{exb} \text{ bar}</math></b>	<b><math>\epsilon_{rec}</math></b>	<b><math>Y</math></b>
<b>Basic</b>	6747	1119	5.75	25.81	--	--	--
<b>OFH</b>	7136	1115	7.38	24.06	0.8	--	0.208
<b>REC</b>	5866	1130	5.8	30	--	0.8	--
<b>OFH+REC</b>	6677	1121	6.9	25.92	0.8	0.8	0.04
<b>Exergy and Cost</b>							
<b>Parameter:</b>	<b><math>I_{cycles} \text{ MW}</math></b>	<b><math>\eta_{ex} \%</math></b>	<b><math>E_{xin} \text{ MW}</math></b>	<b><math>TWP, \\$/\text{m}^3</math></b>	<b><math>TPC_{costs} \\$</math></b>	<b><math>SPC, \text{kWh}/\text{m}^3</math></b>	
<b>Basic</b>	4.952	14.02	5.76	0.904	$2.277 \times 10^7$	7.677	
<b>OFH</b>	5.153	15.32	6.08	0.9047	$2.279 \times 10^7$	7.648	
<b>REC</b>	4.2	16.99	5.04	0.9035	$2.276 \times 10^7$	7.753	
<b>OFH+REC</b>	4.74	16.85	5.71	0.9048	$2.28 \times 10^7$	7.689	

Table 3.7: Data results of Toluene (PTC) for different configurations under superheat operation.

<b>Toluene (PTC, Superheat)</b>							
<b>Parameter:</b>	<b><math>A_{cob} \text{ m}^2</math></b>	<b><math>W_b \text{ kW}</math></b>	<b><math>m_{ORC} \text{ kg/s}</math></b>	<b><math>\eta_R \%</math></b>	<b><math>P_{exb} \text{ bar}</math></b>	<b><math>\epsilon_{rec}</math></b>	<b><math>Y</math></b>
<b>Basic</b>	6734	1120	5.24	26	--	--	--
<b>OFH</b>	7180	1115	6.66	24	0.8	--	0.1913
<b>REC</b>	5600	1134	5.31	31.57	--	0.8	--
<b>OFH+REC</b>	6573	1123	6.1	26.47	0.8	0.8	0.005
<b>Exergy and Cost</b>							
<b>Parameter:</b>	<b><math>I_{cycles} \text{ MW}</math></b>	<b><math>\eta_{ex} \%</math></b>	<b><math>E_{xin} \text{ MW}</math></b>	<b><math>TWP, \\$/\text{m}^3</math></b>	<b><math>TPC_{costs} \\$</math></b>	<b><math>SPC, \text{kWh}/\text{m}^3</math></b>	
<b>Basic</b>	4.94	14.06	5.74	0.9039	$2.277 \times 10^7$	7.679	
<b>OFH</b>	5.18	15.25	6.11	0.9047	$2.279 \times 10^7$	7.645	
<b>REC</b>	3.96	18	4.83	0.9033	$2.276 \times 10^7$	7.776	
<b>OFH+REC</b>	4.7	17.5	5.7	0.9046	$2.279 \times 10^7$	7.691	

Table 3.8: Data results of Water (PTC) for basic configuration under superheat operation.

<i>Water (PTC, Superheat)</i>							
<i>Parameter:</i>	$A_{coh}, m^2$	$W_b, kW$	$\dot{m}_{ORC}, kg/s$	$\eta_R, \%$	$P_{ext}, bar$	$\varepsilon_{rec}$	$Y$
<i>Basic</i>	5851	1131	1.335	30.47	--	--	--
<i>Exergy and Cost</i>							
<i>Parameter:</i>	$I_{cycles}, MW$	$\eta_{ex}, \%$	$E_{xin}, MW$	$TWP, \$/m^3$	$TPC_{cost}, \$$	$SPC, kWh/m^3$	
<i>Basic</i>	4.2	22.52	5.42	0.9034	$2.276 \times 10^7$	7.756	

Table 3.9: Data comparisons between different working fluids for recuperator configuration under saturation and superheat operations.

<i>Parameter:</i>	<i>Collector</i>	$\eta_R, \%$	$I_{cycles}, MW$	$TWP, \$/m^3$	<i>Quality, %</i>
<i>Toluene<sub>sat</sub> (<math>\varepsilon_{rec}=0.8</math>)</i>	PTC	30	4.2	0.9035	--
<i>Toluene<sub>sup</sub> (<math>\varepsilon_{rec}=0.8</math>)</i>	PTC	31.5	3.96	0.9033	--
<i>Water<sub>sup</sub> (Basic)</i>	PTC	30.47	4.2	0.9034	77

### 3.2.3 Solar ORC/RO process: RO-Energy Recovery Units

Toluene is the working fluid used in most of the solar pilot facilities [54]. Also, Toluene gives superior results as presented in the previous sections. Therefore, it is selected to perform the analysis presented in this section. Direct solar vapor generation (DVG) within the absorber tube configuration of solar collector with ORC is analyzed and characterized with LS-3 parabolic trough collector (PTC) models. The power output from the turbine is used to drive a (RO) unit with Pressure Exchanger (PEX) configuration. In Delgado-Torres's work, the organic Rankine cycle and the RO systems were not modeled by the same simulation platform and the cost analysis wasn't considered in Torres [54] work.

Voros [55] investigated the solar energy exploitation for assisting the operation of reverse osmosis seawater desalination plants. A hybrid solar-assisted steam cycle was designed in order to provide the required shaft work to drive the RO high pressure pump. In Voros work, solar energy was in share with conventional cycle and not stands alone. Moreover, Voros [55] work established for RO unit with only Pelton Wheel Turbine (PWT) device. Sharaf et al [47] investigated the operation of RO system with different operating conditions and different configurations of solar Rankine cycle. In Sharaf's work, energy, exergy, and cost analysis was performed only for RO basic configuration (PWT and Pressure Exchanger (PEX) were not considered).

Mark Wilf [46] considered the configuration and operating parameters of RO desalination systems. In this section, a combined solar ORC (solar collector, turbine, recuperator, condenser, and pump), with a RO unit and different RO energy recovery configurations are considered. Using a thermo-economic approach, a comparison for the considered configurations of energy recovery units (PWT, and PEX) with RO desalination system is executed. The analysis and investigations are performed using the developed Solar Desalination Systems (SDS) package [39] under same platform of MatLab/SimuLink computational environments.

It is required to desalinate and produce a total capacity of  $145.8 m^3/h$  from RO module (Sharm El-Shiekh desalination plant-case study). The site data are specified as latitude angle  $=30^\circ$  N, and longitude  $=32.55^\circ$  E. The developed SDS program is used to assemble and design the required solar ORC-RO units. The RO high pressure pump (HPP), and PWT efficiencies were fixed at 80% and 96% value was fixed for PEX. The input feed seawater temperature is assigned by the output preheated stream from the ORC condenser unit.

*a. ORC-RO (RO-Basic configuration)*

Figure (3.8-a) shows the process schematic diagram of the solar ORC with the basic configuration of RO desalination system. The process consists of solar field, expansion turbine for power generation, recuperator unit for regeneration, condenser unit for heat rejection and preheating processes, and circulation pump unit. The condenser outlet stream (preheated seawater) is pumped into the RO module for desalination process by a high pressure pump.

*b. ORC-RO (RO-PWT configuration)*

Figure (3.8) shows a schematic diagram of a combined RO desalination process with different energy recovery units. Figure (3.8-b) illustrates the combined RO process with a Pelton Wheel Turbine (PWT) unit. The rejected brine from RO unit with its high pressure will drive the PWT and that can provide sufficient operational flexibility as a power recovery device. The value of 80% for PWT efficiency is considered in this work. The advantage of the Pelton wheel is that the flat efficiency curve in a wide range of concentrate flows, and concentrate exits the Pelton wheel at atmospheric pressure.

*c. ORC-RO (RO-PEX configuration)*

Figure (3.8-c) shows the process schematic diagram of the RO process with a pressure exchanger unit (RO-PEX). A higher efficiency positive displacement power recovery devices (pressure exchangers), that in the past were only used in small RO seawater units, are also slowly gaining acceptance in large desalination plants. Hydraulic efficiency of such types of equipment is in the range of 94-96% [36]. In this study, the values of 80% and 96% are considered for booster pump and PEX unit respectively.

Some of these devices utilize pistons; other transfer energy through a direct contact between concentrate and the feed stream. According to the Figure (3.8-c), feed (F) is split into two streams. One stream (F1), which has a flow rate equivalent to the permeate flow (P), is pumped to the feed pressure by the main high pressure pump (HPP). The second stream (F2), which flow rate is equivalent to the concentrate flow, flows through pressure exchanger and exchanges pressure with the concentrate stream (C).

The pressure of stream F2 at the exit from the pressure exchanger is a function of concentrate pressure and efficiency of the pressure exchanger device. The pressure of stream F2 is lower by 3-5 bars than the pressure of stream F1 at the discharge of the HPP [36]. The pressure of stream F2 is increased to the pressure of stream F1 by a Booster Pump (BP). Both streams (F1+F2) are combined at the entrance to the membrane feed manifold. The pressure exchangers are positive displacement devices and therefore have high transfer efficiency.

Splitting the feed stream, as in the case of operating a PEX, leads to a significant reduction of the energy demand for the far smaller high pressure pump. Additionally, due to the high efficiency of the PEX, an amount of about 36.8% of the input energy can be recovered from the energy contained in the concentrate that leaves the modules with 37.4% of the initial value [57]. Nowadays PEX configuration has been used in over 400 seawater reverse osmosis plants worldwide [58]. The general specifications and the specified design parameters of the combined processes for two energy recovery configurations for a RO desalination process are illustrated in Table 3.10.

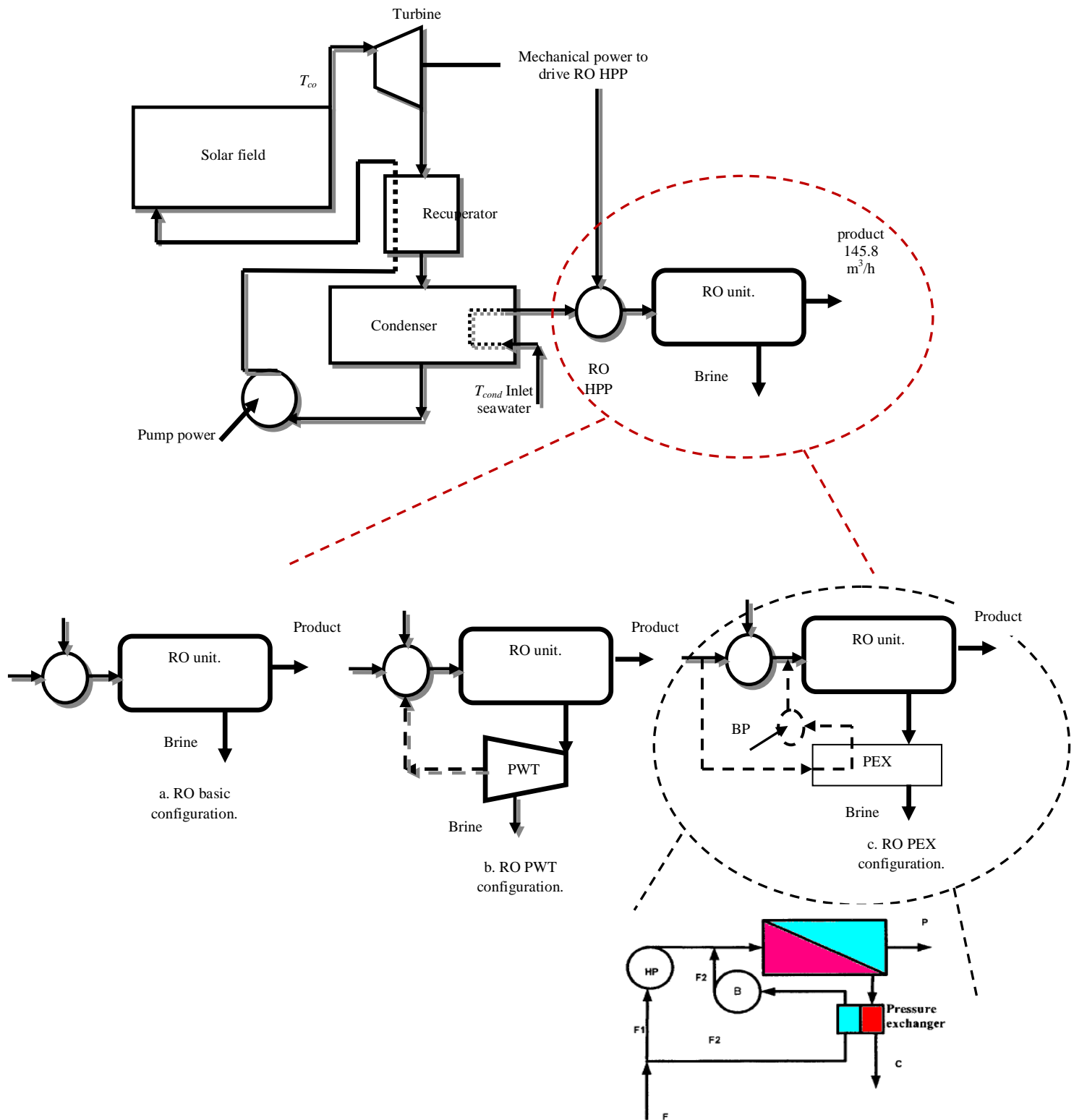


Figure (3.8) A schematic diagram of the RO process with different energy recovery units.



Table 3.10: Specifications and design parameters of the considered processes.

Parameter:		ORC/RO-Basic	ORC/RO-PWT	ORC/RO-PEX
Design point	$G_b, W/m^2$	850	850	850
	$T_{amb}, ^\circ C$	25	25	25
	$T_{co}/T_{sup}$	300/340	300/340	300/340
	$T_{cond}, ^\circ C$	35	35	35
ORC	$\eta_t$ %	85	85	85
	$\eta_p$ %	75	75	75
	$\eta_g$ %	95	95	95
	$\varepsilon_{rec}$ %	80	80	80
	$m_p, kg/s$	40.5	40.5	40.5
	$X_f, ppm$	45000	45000	45000
	$RR$	0.3	0.3	0.3
RO plant	$n_d/n_v$	7/43	7/44	7/48
	$A_s, m^2$	35.3	35.3	35.3
	$\eta_{HPP}$ %	80	80	80
	$\eta_{PWT}$ %	--	80	--
	$\eta_{PEX}$ %	--	--	96
	$FF$ %	85	85	85
	$LT_p, year$	20	20	20
	$LT_m, year$	5	5	5
Cost	$LF$ %	90	90	90
	$i$ %	5	5	5

Based on the mathematical model for the considered process (see the Appendix for more details) and the energy, cost, and thermo-economic analysis presented in Part I, the developed SDS program [39] give the results illustrated in Tables 3.11 and 3.12. Table 3.11 shows that the required power for the HPP of the RO process is 1.123MW. This power is obtained by a 5377m<sup>2</sup> (site: latitude angle =30° N, and longitude =32.55° E) of solar collector area and a mass flow rate of 4.934kg/s.

Also, Table 3.11 shows that the irreversibility of the basic configuration is 6MW. This amount is distributed on the process components as shown in Table 3.12. The solar collector field irreversibility rate considered the highest among the other units with percentage about 48.3% of the total irreversibilities, followed by the RO plant with 45.4%, steam turbine with 2.8%; condenser and recuperator units both give 1.2%, and the pump unit with a sharing percentage of about 0.4%.

The overall exergy efficiency is 9.38% due to the outlet exergy streams (product stream) over inlet exergy streams (feed, pump power, and solar power to the system). The specific annual total costs ( $C_t$ , \$/m<sup>3</sup>) for this configuration is about 0.898\$/m<sup>3</sup>, with total investment and operation & maintenance costs ( $Z^{IC+O\&M}$ ) about 131\$/h. RO sector exhibits the largest percentage of ( $Z^{IC+O\&M}$ =131\$/h) by 89.16% followed by steam turbine unit with 8.44\$/h and a percentage of 6.44%.

Solar field gives a percentage of 4.22%, recuperator unit with 0.018%, and condenser unit with 0.022%, and the pumping unit with a percentage of 0.111%. Thermo-economic unit product exergy cost is about 58.7\$/GJ with a total water price (TWP) about 0.89\$/m<sup>3</sup>. The specific power consumption (SPC) is about 7.7kWh/m<sup>3</sup> and this considered high regarding to the other configurations. The PWT efficiency is set as 80% the same as the efficiency of HPP unit. The consumed power ( $W_{HPP}-W_{PWT}$ ) would require about 3038m<sup>2</sup> of solar collector field area with a percentage of decrease about 43.5% against the basic configuration. The consumed power of this configuration is decreased by 43.5% producing specific power consumption (SPC) about 4.35kWh/m<sup>3</sup>. To maintain the same operating

conditions for RO section (HPP pressure load should be=68 bar for all configurations) the number of pressure vessels is then increased to become 44 instead of 42 as in basic plant.

According to the less in total solar field area comparing with the basic one, the total irreversibility (3.763MW) would decrease against the basic configuration (6MW) with a percentage of 37.2%. RO section gives the highest exergy destruction of about 1.91MW with a percentage of 50.7% followed by solar collector field with a percentage of 43.45%, steam turbine gives a percentage about 2.6%, recuperator and condenser units result together 2.84%, and the organic cycle pump unit gives 0.34%. This configuration exhibits larger exergy efficiency than of the basic one (11% against 9.3%) with a percentage of increases about 15%.

The specific annual total costs for this configuration is about 0.683\$/m<sup>3</sup>, with total investment and operation & maintenance costs ( $Z^{IC+O\&M}$ ) about 99.58\$/h meaning by this a percentage of decreasing equal to 24% against the basic configuration. RO sector costs about 91.2% of all the total  $Z^{IC+O\&M}=99.58$ \$/h, and this due to the additional costs of PWT drive, and the exceeding of permeators numbers. Steam turbine is followed by a cost of 5.5\$/h with a sharing percentage about 5.5%. Solar collector field consumes about 3.215\$/h with a percentage of 3.22%, followed by both recuperator and condenser units with a percentage 0.035%, and the organic Rankine cycle pump unit with a percentage of 0.11%. The plant total water price is about 0.69\$/m<sup>3</sup>, and the unit product cost becomes 59.2\$/GJ. This configuration is favorable against the basic configuration due to many aspects such as total exergy efficiency, total irreversibility, total solar collector area, specific power consumption (SPC) and total water price (TWP).

Table 3.11 shows that the PEX configuration consumes very low power compared against the past two configurations. The developed power by the Rankine cycle steam turbine is about 0.394MW with a power decreasing percentage of about 65% against the basic configuration. This leads to specific power consumption of about 2.7kWh/m<sup>3</sup> with mass flow rate and total solar field area of about 1.732kg/s and 1887m<sup>2</sup> respectively. To maintain the operating pressure over the HPP in RO section; the number of pressure vessels become 48 instead of 42 as in the basic and 44 as in PWT configurations. The reduction in the power is caused by splitting the sea water feed stream which in turn decreases the total solar collector field area.

Therefore; the total irreversibility rates for this configuration is about 2.538MW which representing a percentage of decrease of about 57.7% against the basic configuration. RO section irreversibility has a large sharing with a percentage of about 54.5%, and the steam turbine gives about 2.36%, recuperator and condenser units together give about 2.5%, and the Rankine cycle pump unit gives about 0.33%, and the solar field gives about 41.8%. The overall exergy efficiency is increased from 9.3% for the basic to become 11.6% for this configuration. Also the total inlet exergy rate is reduced from 6.59MW in the basic to become 2.87MW.

This is due to the reduction of the solar collector area against the basic configuration. The specific annual total cost ( $C_t$ , \$/m<sup>3</sup>) for this configuration is about 0.68\$/m<sup>3</sup>, with total investment and operation & maintenance costs ( $Z^{IC+O\&M}$ ) of about 99.26\$/h which leads to 24.2% less than the basic configuration. The major costs belong to RO section which consumes about 93.94% followed by solar collector field with 2.06%, steam turbine gives about 3.8%, and recuperator, condenser, and pump units give about 0.023%. The expenditures of RO section exceeded due to the high prices of recovery units however the total plant expenditures for this configuration considered the lowest against the other configurations due to the high effect of solar collector cost. It is clear from tables (3.11, 3.12) that PEX configuration appears lowest against the remaining configurations regarding to the solar collector area cost, collector area irreversibility, total power, specific power consumption, cycle flow rate, total water price, total capital costs, total investment and operating & maintenance costs. It is clear that solar

collector field produces larger irreversibility only in case of the basic RO; however; RO<sub>section</sub>/PWT-PEX produces larger exergy destruction due to the less in exergy inlet to the cycle. Moreover, larger costs are belonging to RO section followed by steam turbine, and solar field respectively. ORC pump produces the lowest cycle irreversibility rate in the range of 9-28kW for the considered configurations followed by the recuperator and the condenser units respectively.

From Table 3.12, it is obvious that and regardless the final thermo-economic product cost  $c_p$ , the unit cost stream from pump unit to recuperator unit  $c_{p-rec}$  is particularly high (about 2.07, 2.32, and 2.57\$/GJ for basic, PWT, and PEX configurations respectively). The recuperator to solar collector stream cost  $c_{rec-col}$  comes next and it decreases from the basic configuration down to PEX. Cooling sea water cost stream is decreased from the basic down to PEX. The most important parameter is thermo-economic unit product cost which is obviously less in basic followed by PWT, then the PEX configuration. That's because the increase of power cost stream and at the same time the decreasing of exergy of product stream as presented in exergy equations.

This effect is indirectly proportional of preheated inlet seawater stream from the condenser unit. The exergy of the inlet seawater stream for the basic configuration considered the highest comparing against PWT and PEX respectively. And that would follow a decreasing in product exergy stream, moreover; that would increase the unit product cost of PEX followed by PWT then the basic one. Although the operation & maintenance costs ( $Z^{C+O\&M}$ ) is notable less in PEX configuration but the effect of unit power cost  $c_w$  and product exergy  $E_p$  is highly effective. It is clear that the energy conservation related to the RO section has a priority against the solar energy utilization. Because the conservation in the RO section would reduce the total solar field area thence the capital costs.

Table 3.11: Energy and thermo-economic results for different configurations.

<b>Energy</b>							
<b>Parameter:</b>	<b><math>A_{col}, m^2</math></b>	<b><math>W_b, MW</math></b>	<b><math>m_{ORC}, kg/s</math></b>	<b><math>\eta_R, \%</math></b>	<b><math>P_{ev}, bar</math></b>	<b><math>SPC, kWh/m^3</math></b>	<b><math>RO \Delta P, bar</math></b>
<b>Basic</b>	5377	1.123	4.934	32.64	32.78	7.704	68.66
<b>PWT</b>	3038	0.634	2.788	32.64	32.78	4.35	68.74
<b>PEX</b>	1887	0.394	1.732	32.64	32.78	2.704	68.74
<b>Thermo-economic (Exergy &amp; Cost)</b>							
<b>Parameter:</b>	<b><math>I_{cycle}, MW</math></b>	<b><math>\eta_{ex}, \%</math></b>	<b><math>E_{xim}, MW</math></b>	<b><math>TWP, \\$/m^3</math></b>	<b><math>Z^{C+O\&amp;M}, \\$/h</math></b>	<b><math>c_p, \\$/GJ</math></b>	
<b>Basic</b>	6	9.38	6.593	0.898	131	58.7	
<b>PWT</b>	3.763	11.06	4.231	0.683	99.37	59.2	
<b>PEX</b>	2.538	11.61	2.871	0.572	83.45	66.6	

Table 3.12: The comparison percentages for different configurations based on thermo-economic results.

<i>Parameter:</i>		<i>RO-Basic</i>		<i>RO-PWT</i>		<i>RO-PEX</i>	
<b>Irreversibility, MW</b>	<i>I<sub>col</sub></i>	2.89	(48.3%)	1.635	(43.45%)	1.061	(41.8%)
	<i>I<sub>st</sub></i>	0.173	(2.8%)	0.098	(2.6%)	0.06	(2.36%)
	<i>I<sub>rec</sub></i>	0.072	(1.2%)	0.04	(1.063%)	0.025	(0.985%)
	<i>I<sub>cond</sub></i>	0.111	(1.85%)	0.067	(1.78%)	0.043	(1.6%)
	<i>I<sub>pump</sub></i>	0.024	(0.4%)	0.013	(0.34%)	0.008	(0.335%)
	<i>I<sub>ro</sub></i>	2.725	(45.4%)	1.91	(50.7%)	1.384	(54.53%)
<b>Z<sup>IC+O&amp;M</sup>, \$/h</b>	<i>Z<sub>col</sub></i>	5.53	(4.22%)	3.215	(3.22%)	2.045	(2.06%)
	<i>Z<sub>st</sub></i>	8.442	(6.44%)	5.5	(5.5%)	3.85	(3.8%)
	<i>Z<sub>rec</sub></i>	0.024	(0.018%)	0.015	(0.015%)	0.01	(0.01%)
	<i>Z<sub>cond</sub></i>	0.03	(0.022%)	0.02	(0.02%)	0.013	(0.013%)
	<i>Z<sub>pump</sub></i>	0.146	(0.111%)	0.112	(0.11%)	0.09	(0.09%)
	<i>Z<sub>ro</sub></i>	116.8	(89.16%)	90.77	(91.2%)	77.48	(93.94%)
<b>Thermo-economic streams, \$/GJ</b>	<i>C<sub>col-st</sub></i>	1.073		1.095		1.112	
	<i>C<sub>st-rec</sub></i>	1.073		1.095		1.112	
	<i>C<sub>rec-col</sub></i>	1.295		1.171		1.03	
	<i>C<sub>rec-cond</sub></i>	1.073		1.095		1.112	
	<i>C<sub>cond-p</sub></i>	1.073		1.095		1.112	
	<i>C<sub>p-rec</sub></i>	2.07		2.32		2.573	
	<i>C<sub>cw</sub></i>	0.043		0.032		0.027	
	<i>C<sub>p</sub></i>	54.7		56.1		66.6	
	<i>C<sub>w</sub></i>	3.326		3.672		3.996	

Based on the overall thermo-economic equation ( $c_p = \frac{C_{cw} + C_{w-pump} + Z_{total}^{IC\&OM}}{E_p}$  \$/GJ), it is obvious that the unit product cost is highly dependent on product exergy which is also depending on the product mass flow rate. By increasing of water demand, the product exergy would increase related to the increase of mass flow rate. Also the upper side in the overall thermo-economic equation ( $C_{cw} + C_{w-pump} + Z_{total}^{IC\&OM}$ ) will increase but the effect of product exergy is massive and leads to a decrease in the overall thermo-economic product cost.

The unit product cost for basic configuration is noticed less than PWT and PEX configurations respectively. Although the basic configuration considered not recommended based on the consumed power, total solar collector area, total water price, but the product exergy is the highest due to the effect of the temperature of the preheated seawater from condenser unit. The preheated seawater leads to an increase in product exergy which will decrease the thermo-economic unit product cost.

Figure (3.9) shows the effect of fresh water production rate (m<sup>3</sup>/h) on thermo-economic product cost (\$/GJ). Increasing the productivity would decrease thermo-economic unit product cost but also would harvest much larger solar collector area and power from turbine unit. Figure (3.10) shows the behavior of increasing the power consumption related to the productivity demand. Figure (3.11) represents data results for each stream in solar ORC/RO-PEX configuration.

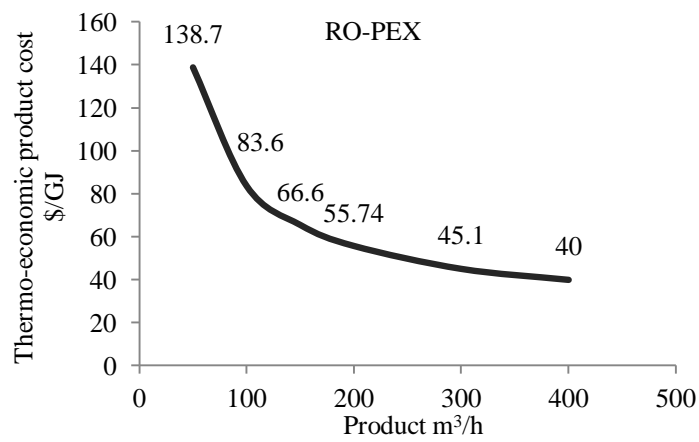


Figure (3.9) Variation of thermo-economic product cost against the variation in productivity.

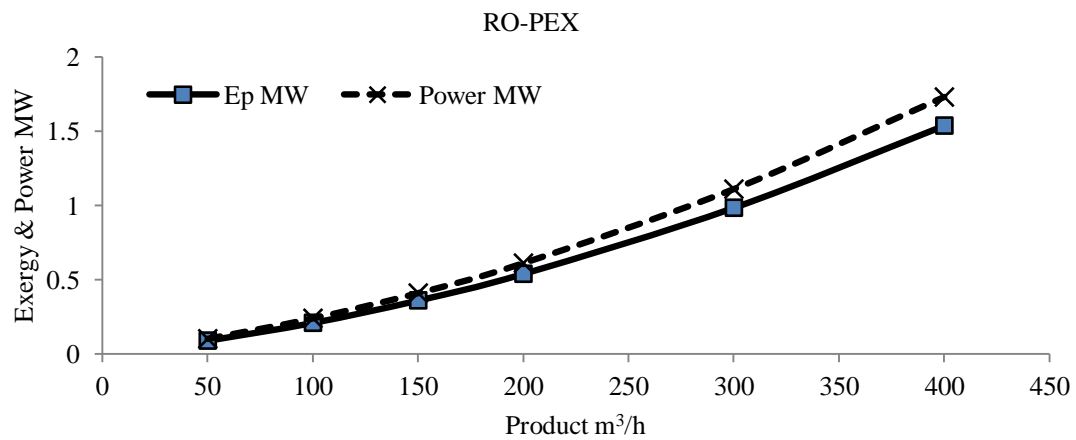
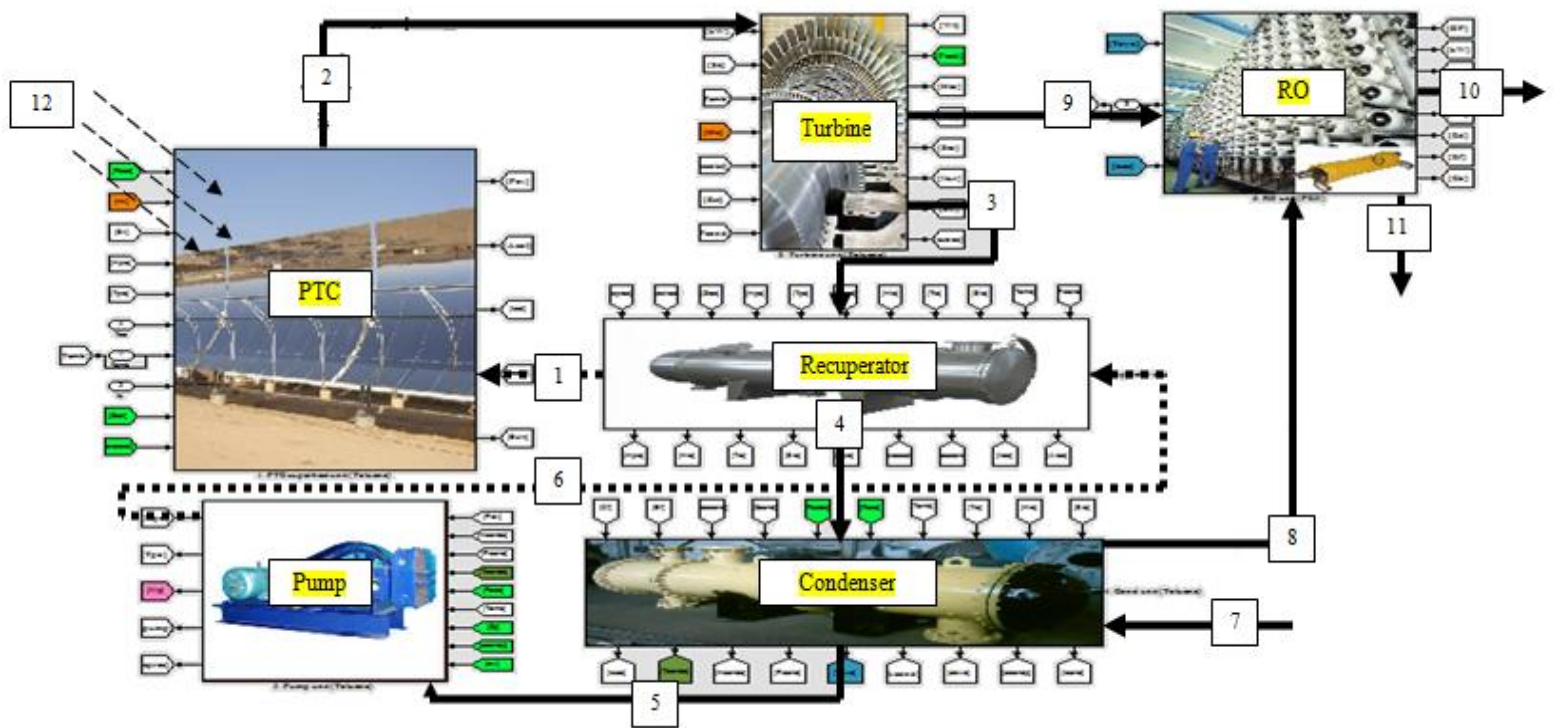


Figure (3.10) Variation of product stream exergy rate (MW) and power consumed (MW) by the RO-PEX against the variation in fresh water production rate (m<sup>3</sup>/h).



streams		1	2	3	4	5	6	7	8	9	10	11	12
$p$	bar	32.78	32.78	0.062	0.062	0.062	32.78	1	68	--	1	1	--
$t$	$^{\circ}\text{C}$	143.1	340	198.4	70	35	38	20	22	--	22	22.2	5727
$h$	$\text{kJ/kg}$	330	987.6	774	571	121.6	126.8	84	91	--	91	91	--
$\dot{m}$	$\text{kg/s}$	1.732	1.732	1.732	1.732	1.732	1.732	135	135	--	40.5	94.55	--
$Ex$	$\text{kW}$	43.75	573.6	125.5	7	3	37.2	0	1367	394	346.1	0	1568
$c$	$\$/\text{GJ}$	1.03	1.112	1.112	1.112	1.112	2.573	0	0.027	3.99	66.6	0	0

- Solar field area= $1887\text{m}^2$
- Recuperator area= $3\text{m}^2$
- Condenser area= $18\text{m}^2$

Figure (3.11) Data streams for solar ORC with RO-PEX configuration ( $145\text{m}^3/\text{h}$ ).

### 3.3 Solar Thermal Organic Cycles Assisted Multi Effect Distillation (MED) Desalination Process

Solar desalination systems are classified into two categories: direct and indirect collection systems. As their name implies, direct collection systems use solar energy to produce distillate directly in the solar collector, whereas in indirect collection systems, two sub-systems are employed (one for solar energy collection and the other one for desalination). Among the several options to connect a seawater desalination system with a solar power plant the combination of a thermal desalination system such as a Multi Effect Distillation (MED) and a solar trough field as the heat source is one of the most promising [59]. The race for the second generation of the seawater desalination systems has been settled with Reverse Osmosis (RO) and low temperature MED of horizontal tube evaporators. Both systems are characterized by their low energy consumption as compared to the Multi Stage Flash (MSF) system, [60]. Conventional MED desalting system uses about half of the MSF pumping energy, and almost the same amount of thermal energy used by the MSF, if both have the same gain ratio [61]. However, a recent trend of using low-temperature MED allows the use of low temperature (in the range of 70°C) steam as heat source, and consequently of low exergy and low equivalent work. This can bring the MED consumed equivalent mechanical energy close to that consumed by the efficient RO system. Recent construction in Abu Dhabi of an MED plant with a 240,000 m<sup>3</sup>/day capacity shows a breakthrough in large-scale MED plants [59]. In this part, investigation analyses are performed for different configurations of MED with low capacity range (100m<sup>3</sup>/day) by using solar energy. Two different techniques are studied in this part: The first technique utilizes the solar energy by using the concentrator (PTC) to deliver thermal power via heat exchanger boiler to drive MED directly. And the second technique utilizes the rest of the exhaust energy from solar Rankine cycle turbine unit to drive the MED process. First effect for both techniques works as a brine heater for MED plant. Both techniques use Therminol-VP1 [62] heat transfer oil (HTO) for indirect vapor generation via heat exchanger boiler. The MED introduced in this work has a capacity about 100m<sup>3</sup>/day. The analyses are introduced based on thermo-economic mathematical approaches. The comparison is made to evaluate the most economical and reliable MED-configuration to be implemented with solar energy. The aim of this work may be concluded into these points:

- Investigating and analyzing the design limitations of utilizing solar energy with different configurations of MED process.
- Electing the most reliable MED configuration based on energy, exergy, cost and thermo-economic analysis putting in mind the number of MED effects.
- Comparisons are introduced versus conventional operation (Water working fluid). The design points are summarized according to typical winter operating conditions due to the high demanded thermal load for such types of desalination processes (MED or MSF).

#### 3.3.1 MED Process Configurations

MED plants utilize horizontal tube, falling-film evaporative condensers in a serial arrangement, to produce through repetitive steps of evaporation and condensation, each at a lower temperature and pressure, a multiple quantity of distillate from a given quantity of low grade input steam. Technically the number of effects is limited only by the temperature difference between the steam and seawater inlet temperatures (defining the hot and cold ends of the unit) and the minimum temperature differential allowed on each effect [61].

The low temperature operation aided by a comprehensive multi-disciplinary development and design approach has made possible the utilization of economical and durable materials of construction such as aluminum alloy for heat transfer tubes, plastic process piping and epoxy-painted carbon steel shells which show a better resistance against corrosion when matched with aluminum alloy or titanium. Also, the significant increase in heat transfer area, in addition to the thermodynamic superiority of MED over the MSF process, results in a very low temperature drop per effect (1.5–2.5°C), enabling the incorporation of a large number of effects (10–16) even with a maximum brine temperature as low as 70°C, consequently resulting in very high economy ratios (product to steam).

There are different schemes for supplying the feed seawater water to the evaporators, mainly forward, backward, parallel, and mixed feed systems [44]. In the forward feed (MED-FF) arrangement, the feed water (after leaving the bottom condenser) is supplied to the first effect of the highest temperature. In the backward feed (MED-BF) arrangement, the feed water is directed from the end condenser to the last effect, (of the lowest temperature) and the brine leaving the first effect is blown down to the sea. Thus, the feed and vapor entering the effects have opposite flow directions. In the parallel feed (MED-PF) arrangement, the feed leaving the condenser is divided and distributed almost equally to each effect.

The choice of any of these feed arrangements affects the design and performance of the MED desalting system, e.g. the evaporator arrangements, the required heat transfer areas of the effects, the amount of vapor generated in each effect (evaporator), the amounts of vapor generated by boiling and by flashing, the pumping energy, the gain ratio (distillate to heating steam ratio), and the cooling water to distillate ratio. For forward feed with feed heaters (MED-FFH), cooling water enters an end condenser to condense (last effect vapor output) and part of the leaving cooling water is pre-treated and becomes feed water, and is heated successively as it flows in the feed heaters before entering the first effect (for more details, see ref [44]).

In this work, all the above mentioned feed arrangements (see MED section in the Appendix) are considered and compared to pin point the most reliable configuration. Moreover, the number of 16 effects is offered to ensure minimum temperature drop between effects. Top steam temperature is maintained based on the type of technique presented (solar desalination and/or power and solar desalination). The design limits for MED is maintained under winter operating conditions to dominate stable operation along summer period. Dealing with solar energy is concerned with sun availability during summer and winter periods. Table 3.13 illustrates the specifications and design limits that considered for different MED configurations under winter operating conditions.

Table 3.13: Specifications of MED desalination plant (all configurations) under winter operating conditions for 100m<sup>3</sup>/day capacity.

<b>Design point:</b>	<b>MED-(BF, FF, FFH, PF)</b>
Ambient temperature, °C	20
Seawater temperature, °C	25
Brine blow down temperature, °C	40
Top steam temperature (TST), °C	Depends on each technique
Sea water salinity, ppm	42,000
Brine blow down salinity, ppm	70,000
Condenser effectiveness	0.8
Condenser inner tube diameter, m	0.039
Condenser outer tube diameter, m	0.04
Number of effects	16
Number of feed heaters (in case of MED-FFH)	15
Effect inner tube diameter, m	0.0295



Effect outer tube diameter, m	0.03
Productivity, m <sup>3</sup> /day	100
Brine mass flow rate, kg/s	calculated
Distillate profile mass flow rate, kg/s	calculated
Feed mass flow rate, kg/s	calculated
Cooling water mass flow rate, kg/s	calculated
Steam mass flow rate, kg/s	calculated
Vapor temperature through the effects, °C	calculated
Brine temperature through the effects, °C	calculated
Effects area, m <sup>2</sup>	calculated
Feed heaters area, m <sup>2</sup>	calculated
Condenser area, m <sup>2</sup>	calculated
Gain ratio	calculated

### 3.3.2 Solar power cycle configurations

Operating conditions (TBT) of MED allow the use of Parabolic Trough Collector (PTC) in solar power plants. Conventional PTC uses heat transfer oil as heat transfer fluid and the hot oil is stored in an insulated tank. In solar PTC application to desalination, the heated oil could be sent to a boiler, which would generate the steam required by a conventional MED plant. In this work, boiler unit with heat transfer oil is used in the analysis. The storage element isn't investigated in this work. There are two methods of combining solar thermal power cycle with MED plants. The first is direct contact of PTC field to the first MED effect, and the second is utilizing solar Rankine cycle for desalination and electricity production by mean of using the exhausted steam from the turbine to operate the first effect.

#### *a. Solar desalination with MED (SDMED)*

Figure (3.12) shows a schematic diagram of the process units for the first technique. This technique consists of a pump unit to overcome the pressure losses, solar collector field (PTC-LS-3 type [54]) for thermal power delivering, boiler heat exchanger for vapor release and MED with 16 effects. The organic HTO across the PTC would transfer its thermal power to the fluid (water) across the boiler heat exchanger unit.

The generated steam would raise the preheated seawater brine to the desired temperature (TBT). The rest of the working fluid (water) would be condensed again to the boiler heat exchanger unit. In this part and based on previous studies [61], HTO is selected as a working fluid for PTC. Table 3.15 shows and summarize the design points for this technique. The specifications and design parameters for this technique are pin pointed as follows:

- Direct normal irradiance under winter operating conditions is assumed for Egypt-Suez Gulf region (latitude: 30° N; longitude: 32.55° E)). It is estimated by reference [40] that the daily average global radiation in a typical day in winter would be in the range of 21~22MJ/m<sup>2</sup>. To dominate long operation along the day light (11 hrs), the solar radiation would be estimated and fixed at 503W/m<sup>2</sup> (21.4MJ/m<sup>2</sup>≈503.7W/m<sup>2</sup>). For all day operation (24 hrs), the daily average is estimated as 252W/m<sup>2</sup>. Figure (3.13) shows the variations of solar radiation on the specified location in 21 of January. Also, Table 3.14 illustrates some of the data results of the solar model according to the location of operation. Designing the solar field based on lower values of solar radiation such as winter conditions give the allowance to collect huge amount of solar radiation based on larger expected area. Although the PTC operates at 850W/m<sup>2</sup> but this value could cause a very need to storage element (extra costs) during winter or may also not be able to operate the

plant based on lower operation area. However, under summer conditions it will be expected that there is an excessive energy due to large field area and it might be handled through bypassing some loops in the solar field for maintenance operation.

- The distillate product is fixed at  $100\text{m}^3/\text{day}$  ( $1.157\text{kg/s}$ ), and the inlet seawater feed temperature stream is fixed at  $25^\circ\text{C}$  with a salinity about  $42,000\text{ppm}$ . The outlet brine stream temperature is adjusted as  $40^\circ\text{C}$  and the number of effects is fixed at 16 effects.
- According to pinch technology and the design operating temperature for the recommended working fluid, the outlet collector temperature would be fixed at  $350^\circ\text{C}$  and the boiler heat exchanger evaporator temperature will be adjusted at  $75^\circ\text{C}$  putting in mind the 1<sup>st</sup> effect effectiveness and higher gain ratio.
- The efficiency of the positive displacement pump unit is about 75%.
- PTC configuration and design specifications are adjusted according to LS-3 type [61].

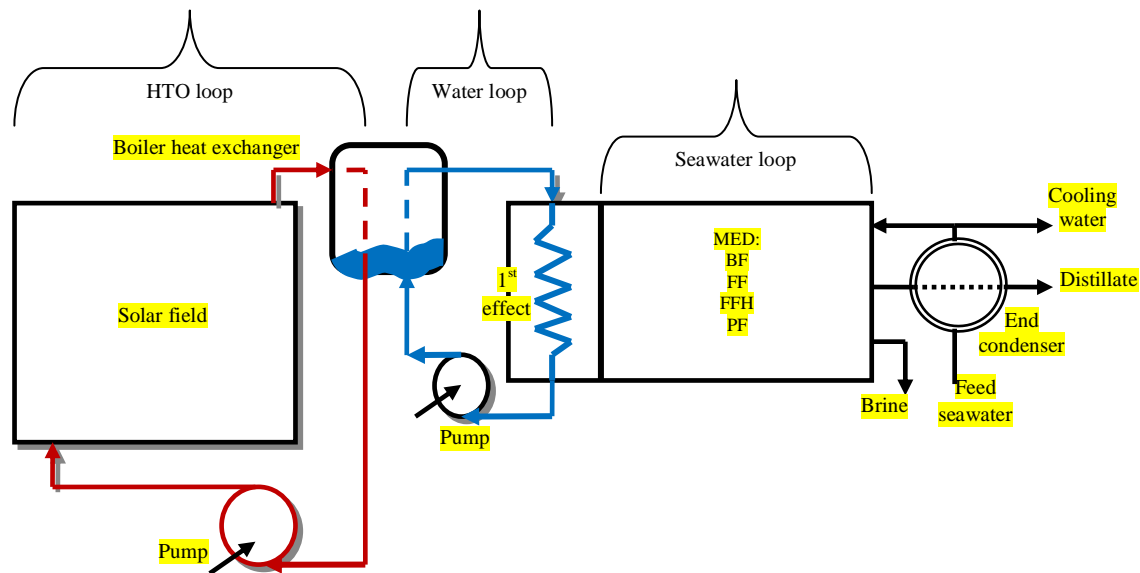


Figure (3.12) A schematic diagram of solar MED units for desalination:  
Solar field, Boiler heat exchanger, Pump, MED.

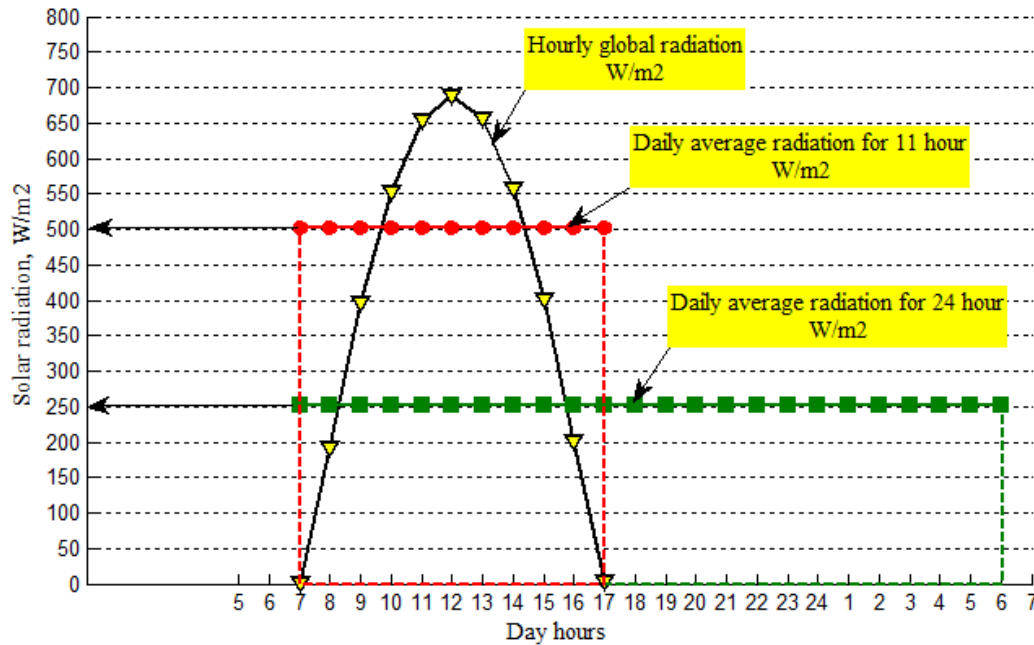


Figure (3.13) Solar radiation data results based on hourly, daily average (11 hrs), and daily average (24 hrs) variations.

Table 3.14: Data results for solar radiation model based on the specified location of operation.

Parameter:	Data results
Location	Suez Gulf region
longitude	longitude: 32.55° E
latitude	latitude: 30° N
Equation of time, min	-11.25
Day hours	10.37
Declination-angle	-20.138
Daily average solar radiation, MJ/m <sup>2</sup>	21.76
Monthly average of daily total radiation, MJ/m <sup>2</sup>	15.623
Extraterrestrial intensity, W/m <sup>2</sup>	1409.19
Sun temperature, K	5833.11
Sun rise time	6.814
Sun set time	17.19
Julian day	21 of January

#### *b. Power & Solar desalination with MED (PSDMED)*

This technique consists of two pumps for circulation and pressure drops, solar collector field (PTC), boiler heat exchanger, turbine expander unit, recuperator for regeneration and de-superheating, and MED with 16 effects. This technique is similar to the previous however; turbine and recuperator units are added to this one for electricity and regeneration. Moreover, the first effect would operate as a brine heater for MED and a condenser unit for the Rankine cycle. Figure (3.14) shows a schematic diagram of the process units for the second technique. Table 3.15 shows and summarize the design points for this technique. The specifications and design parameters for this technique are pin pointed as follows:

- Solar radiation and ambient temperature would be fixed at the same as the previous technique (252W/m<sup>2</sup> & 20°C).

- The distillate product is fixed at 100m<sup>3</sup>/day, and the inlet seawater feed temperature stream is fixed at 25°C with a salinity about 42,000ppm. The outlet brine stream temperature is adjusted as 40°C and the number of effects is fixed as 16 effects. The brine blow down salinity is assumed as 70,000ppm.
- Due to the MED operating conditions (TBT) and boiler heat exchanger effectiveness, the collector outlet temperature is maintained at 350°C (HTO) to dominate a saturated vapor (Toluene) that enters the turbine unit first stage in the range of 200°C. The outlet turbine conditions would be maintained at 85°C (saturated temperature) putting in consideration the recuperator unit effectiveness and the top steam temperature (TST °C).
- The efficiency of turbine, generator, recuperator and pump units is fixed at 85%, 95%, 80% and 75% respectively.
- PTC configuration and design specifications are adjusted according to LS-3 type [54].

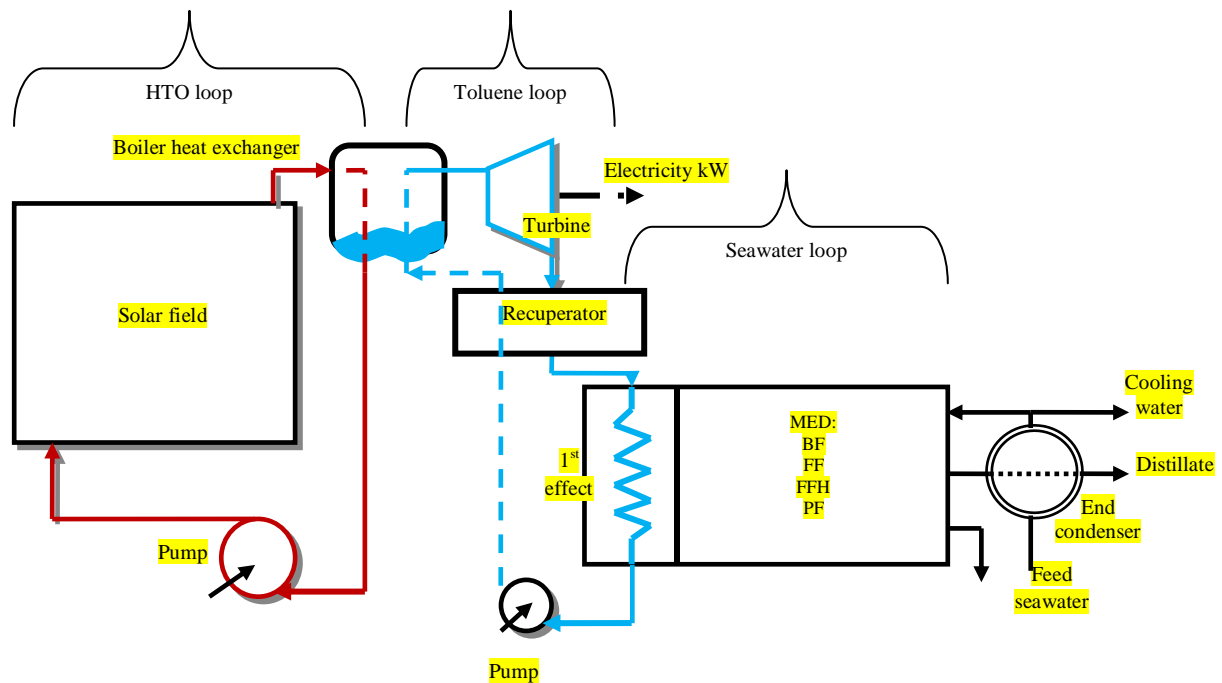


Figure (3.14) A schematic diagram of solar MED components for desalination and power generation: Solar field, Boiler heat exchanger, Pump, Turbine, Recuperator, MED.

Table 3.15: Design points considered for MED according to the 1<sup>st</sup> and the 2<sup>nd</sup> techniques.

Design point:	1 <sup>st</sup> technique (SDMED)	2 <sup>nd</sup> technique (PSDMED)
$G_b$ , $W/m^2$	252 (winter)	252 (winter)
$T_{amb}$ , $^{\circ}C$	20	20
$T_{co}$ , $^{\circ}C$	350	350
$\eta_b$ , %	---	85
$\eta_g$ , %	---	95
$\eta_p$ , %	75	75
Seawater condenser effectiveness	0.8	0.8
Recuperator effectiveness	0.8	0.8
Boiler heat exchanger effectiveness	0.8	0.8
Boiler inner tube diameter, m	0.0127	0.0127
Boiler outer tube diameter, m	0.0129	0.0129
$T_{sea}$ , $^{\circ}C$	25	25
$T_{steam}$ from boiler, $^{\circ}C$	75	200
$T_b$ , $^{\circ}C$	40	40
Feed salinity, ppm	42000	42000
Brine blow down salinity, ppm	70000	70000
No. of effects	16	16
Product mass flow rate, kg/s	1.157	1.157
Solar field mass flow rate per loop, kg/s	1	1
Plant life time, year	20	20
Power generation cost, \$/kWh	0.06	0.06

### 3.3.3 Results of SDMED & PSDMED techniques

#### a. Results of SDMED

As indicated earlier, this technique is established to desalinate seawater regardless the method of power consumption and/or production. Therefore; the system is mainly contains solar collector field (PTC LS-3), boiler heat exchanger (BHX), pump, and MED desalination plant. Turbine unit is not present in this technique. HTO (hot saturated liquid) is maintained through the PTC collector, however; pure water (dry saturated steam) is maintained between BHX and the first effect of MED process.

Generally, it is so clear from Table 3.16 that MED-PF considered very promising against the remaining configurations. MED-FFH comes next and followed by MED-BF. MED-FF configuration considered not applicable due the results obtained. Also results show that MED-BF cannot compete against MED-PF and MED-FFH due to many aspects such as the salinity gradients in the first effect.

The salinity gradients in the first effect considered very high and would affect on the tubes and the effect status generally (in this work, the salinity concentration of blow downstream from the first effect would be around 69 to 70g/kg). MED-FF consumes large power trying to increase the feed temperature stream that comes from the condenser unit to the desired TBT (from 36 $^{\circ}C$  up to 73 $^{\circ}C$ ). And that's explained larger area needed per effect and lower gain ratio.

Therefore; MED-BF, FF is eliminated from the comparison (based on this techniques results) due to lower gain ratio, larger solar collector area, larger effects area, and larger total water price. MED-PF noticed durable and reliable against MED-FFH by achieving lower solar collector area needed (1096 vs. 1005m<sup>2</sup>) meaning by this lowering control and maintenance issues. For both configurations (MED-PF, FFH), the plant under the specified operating conditions (100m<sup>3</sup>/day) harvest about one solar PTC

(LS-3 type) with one loop. However, MED-PF achieves lower Reynolds number due to lower mass flow rate across the solar field (about 0.372kg/s). Therefore; MED-PF gives lower exergy destruction rate per solar collector against MED-FF (159 vs. 173.5 kW) due to the less in area needed. Also the same behavior is obvious for all cycle's units. Although the total effects heat transfer area for MED-PF considered higher vs. MED-FFH but by adding the calculated heat transfer area of the feed heaters (about 53m<sup>2</sup>) it becomes 835m<sup>2</sup> vs. 853m<sup>2</sup> giving an advantage to MED-PF configuration.

The Gain Ratio (GR) for MED-PF noticed higher than MED-FFH (15.2 vs. 13.93) due to the minimum rate of steam needed (0.076 vs. 0.083kg/s). Total water price (TWP \$/m<sup>3</sup>) is around 5.7 and 5.4\$/m<sup>3</sup> with a little bit advantage to the MED-PF configuration against MED-FFH. Moreover, thermo-economic unit product cost (\$/GJ) considered lower to MED-PF configuration against MED-FFH.

Related to this solar operation technique, MED-PF configuration considered the most reliable one among the other configurations based on many terms such as total water price, areas, mass flow rates, exergy destruction rates for each unit, and gain ratio and so on. However; reducing the number of effects gives an advantage to MED-FFH configuration against the MED-PF.

Therefore; it depends on the designers' decision about the reliable operating conditions, areas, and cost. However; increasing the number of effects gives an advantage to the desalination plant by reducing the TWP and increasing the GR. Figure (3.15) shows that by increasing the number of effects, the GR will increase. It is obvious from Figure (3.15) that MED-PF and MED-FFH exhibits larger GR against MED-BF and MED-FF respectively. Moreover; dealing with effects number less than 8~10 effects, MED-FFH is dominated however; going further than 10 effects MED-PF reveals more reliable and dependable.

Table 3.16: Data results for 1<sup>st</sup> technique operated by Water and HTO fluids.

<b>Parameter:</b>	<b>MED-BF</b>	<b>MED-FF</b>	<b>MED-FFH</b>	<b>MED-PF</b>
<b><u>Solar Collector field:</u></b>				
High pressure, bar	5.5	5.5	5.5	5.5
Total solar field area, m <sup>2</sup>	1545	3408	1096	1005
Solar field flow rate, kg/s	0.572	1.262	0.406	0.372
Solar field R <sub>e</sub> number	1.1×10 <sup>4</sup>	2.75×10 <sup>4</sup>	1.073×10 <sup>4</sup>	7980
No. of collectors (LS-3)/No. of loops	2/1	6/1	1/1	1/1
Solar field width, m	11	27	10.5	8
Solar collector thermal efficiency, %	69.7	69.7	69.7	69.7
Solar collector thermal power, kW	271	598	192.5	176.5
Exergy destruction rate, kW	244.5	540	173.5	159
Exergy inlet rate, kW	370.2	816.3	262.6	240.7
Cost stream to BHX, \$/GJ	3.837	3.677	3.911	3.931
<b><u>Boiler heat exchanger unit:</u></b>				
Vapor pressure, bar	0.485	0.485	0.485	0.485
Area, m <sup>2</sup>	0.575	1.268	0.408	0.374
Outlet HTO temperature, °C	130	130	130	130
Steam mass flow rate, kg/s	0.1171	0.2583	0.083	0.076
Exergy destruction rate, kW	82.5	182	58.5	53.6
Cost stream to MED, \$/GJ	5.65×10 <sup>-3</sup>	4.82×10 <sup>-3</sup>	6.05×10 <sup>-3</sup>	6.16×10 <sup>-3</sup>
Cost stream to pump, \$/GJ	3.837	3.677	3.911	3.931
<b><u>HTO pump unit:</u></b>				
Power, kW	0.428	0.95	0.304	0.278
Mass flow rate, kg/s	0.572	1.262	0.406	0.372
Exergy destruction rate, kW	0.212	0.4764	0.1507	0.138
Cost stream to PTC, \$/GJ	4.289	4.058	4.406	4.437
<b><u>MED section (16 effects):</u></b>				
M <sub>db</sub> kg/s	1.157	1.157	1.157	1.157
M <sub>p</sub> kg/s	2.894	2.894	2.894	2.894
M <sub>cw</sub> kg/s	0.702	0.702	0.702	0.702

$M_s$ , kg/s	0.1171	0.2583	0.083	0.076
$T_f$ , °C	36.38	36.38	36.38	36.38
$T_d$ , °C	27.85	27.85	27.85	27.85
TBT, °C	73.53	73.53	73.53	73.53
TVT, °C	72.76	72.76	72.76	72.76
TFT, °C	36.38	36.38	69.92	36.38
Condenser area, m <sup>2</sup>	13	13	13	13
Total effects area, m <sup>2</sup>	1135.4	2486	800	835
Total feed heaters area, m <sup>2</sup>	---	---	53	---
GR	9.88	4.48	13.93	15.2
Exergy destruction rate, kW	5136	5168	5135	5134
Cost stream to BHX, \$/GJ	$5.65 \times 10^{-3}$	$4.82 \times 10^{-3}$	$6.05 \times 10^{-3}$	$6.16 \times 10^{-3}$
Product cost stream, \$/GJ	1.756	1.82	1.73	1.72
<b>Performance &amp; cost:</b>				
Specific thermal power consumption, kWh/m <sup>3</sup>	65.2	143.8	46.25	42.4
Total operating & maintenance cost, \$/h	10.5	12.75	9.94	9.8
Total plant cost, \$/y	$2.345 \times 10^5$	$4.226 \times 10^5$	$1.88 \times 10^5$	$1.79 \times 10^5$
Total water price, \$/m <sup>3</sup>	7.139	12.87	5.75	5.47

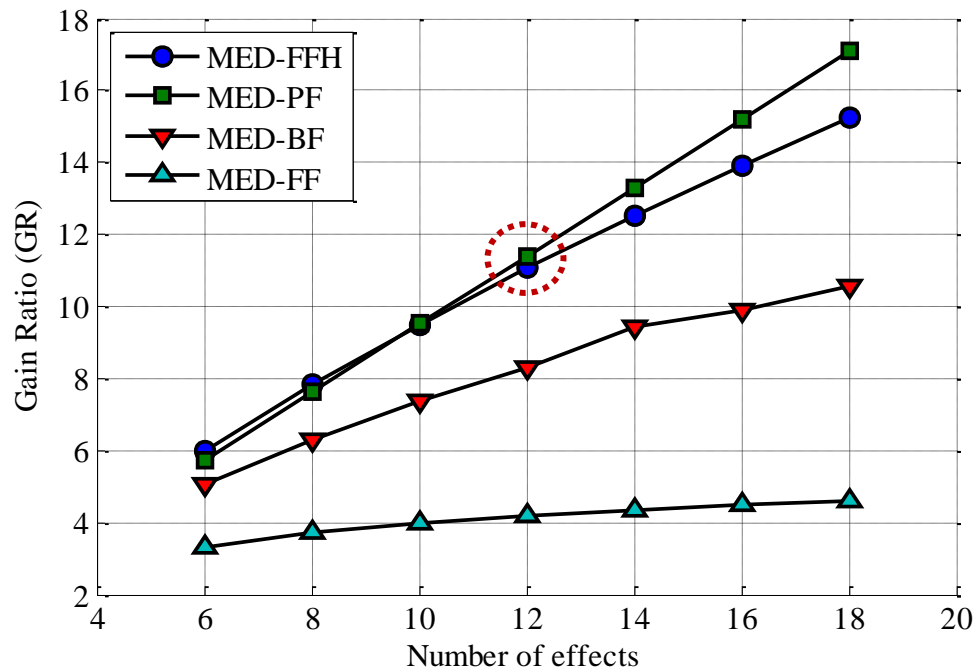


Figure (3.15) The GR variations for different MED configurations due to the variations of effect numbers at 100m<sup>3</sup>/day based on SDMED technique.

#### b. Results of PSDMED technique

In this technique; power is generated via turbine unit beside seawater desalination. Therefore; the system is mainly contains solar collector field (PTC LS-3), boiler heat exchanger (BHX), turbine, recuperator for regeneration, pump, and MED desalination plant. HTO (saturated liquid) is maintained through the PTC collector, however; Toluene organic fluid (dry saturated steam) is maintained between the organic Rankine cycle (ORC) and the first effect of MED process. Generally, it is so clear form Table 3.17 that MED-PF shows very promising against the remaining configurations. MED-FFH comes

next and followed by MED-BF. MED-FF considered not applicable due the poor results obtained based on energy, exergy, and thermo-economic terms. Also MED-BF can't compete against MED-PF and MED-FFH due to many reasons such as presented in the previous subsection. MED-FF consumes large power trying to increase the feed temperature stream that comes from the end condenser unit to the desired TBT (from 36°C up to 88°C). And that's explained larger area needed per effect and lower gain ratio. For the reasons that presented in the previous technique, MED-BF, and MED-FF are eliminated from the comparison. MED-PF is considered reliable against MED-FFH by achieving lower solar collector area needed (about 2.8% less area) meaning by this lowering control and maintenance issues. For both configurations (MED-PF, FFH), the plant under the specified operating conditions (100m<sup>3</sup>/day) harvest about two solar PTC (LS-3 type) with one loop.

Although the total effects area for MED-PF is considered higher vs. MED-FFH but by adding the calculated area of the feed heaters (about 68m<sup>2</sup>) it becomes 548m<sup>2</sup> vs. 505m<sup>2</sup> giving an advantage to MED-PF configuration. The Gain Ratio (GR) for MED-PF is higher than MED-FFH (2.45 vs. 2.38) due to the minimum rate of steam needed (0.472 vs. 0.486kg/s). Total water price (TWP \$/m<sup>3</sup>) is around 5\$/m<sup>3</sup> for both configurations with an advantage to the MED-PF configuration against MED-FFH. Moreover; thermo-economic unit product cost (\$/GJ) considered the same for both. Related to this solar operation technique, MED-PF configuration is the most reliable one among the other configurations based on many terms such as total water price, areas, mass flow rates, exergy destruction rates for each unit, and gain ratio and so on.

Table 3.17: Data results for 2<sup>nd</sup> technique operated by Toluene and HTO fluids.

<b>Parameter:</b>	<b>MED-BF</b>	<b>MED-FF</b>	<b>MED-FFH</b>	<b>MED-PF</b>
<b><u>Solar Collector field:</u></b>				
High pressure, bar	5.5	5.5	5.5	5.5
Total solar field area, m <sup>2</sup>	2855	5762	1393	1353
Solar field flow rate, kg/s	1.157	2.334	0.564	0.548
Solar field R <sub>e</sub> number	3.28×10 <sup>4</sup>	6.56×10 <sup>4</sup>	1.608×10 <sup>4</sup>	1.608×10 <sup>4</sup>
No. of collectors (LS-3)/No. of loops	5/1	10/1	2/1	2/1
Solar field width, m	25	50	12	12
Solar collector thermal efficiency, %	69.7	69.7	69.7	69.7
Solar collector thermal power, kW	501.4	1012	244	237
Exergy destruction rate, kW	445.7	900	217	211
Exergy inlet rate, kW	684	1380	333.6	324
Cost stream to BHX, \$/GJ	3.593	3.454	3.75	3.75
<b><u>Boiler heat exchanger unit:</u></b>				
Vapor pressure, bar	7.5	7.5	7.5	7.5
Area, m <sup>2</sup>	1524	3.07	0.74	0.722
Outlet HTO temperature, °C	151.5	151.5	151.5	151.5
Steam mass flow rate, kg/s	0.9972	2.012	0.4864	0.472
Exergy destruction rate, kW	62	125	30.26	29
Cost stream to turbine, \$/GJ	0.1026	0.076	0.1417	0.1435
Cost stream to pump, \$/GJ	3.593	3.454	3.75	3.75
<b><u>Turbine unit:</u></b>				
Power developed, kW	120	241	58.2	56.76
Outlet temperature, °C	111.2	111.2	111.2	111.2
Exergy destruction rate, kW	40.24	82	20	19.07
Cost of power, \$/GJ	3.794	3.17	4.565	4.59
Cost stream to recuperator, \$/GJ	0.1026	0.076	0.1417	0.1435
<b><u>Recuperator unit:</u></b>				
Power rejected, kW	32	64.2	15.5	15
Area, m <sup>2</sup>	1	2	0.46	0.45
TST, °C	90.67	90.67	90.67	90.67



<i>Preheated stream temperature, °C</i>	101.9	101.9	101.9	101.9
<i>Cost stream to BHX, \$/GJ</i>	2.517	1.845	3.493	3.54
<i>Cost stream to MED, \$/GJ</i>	0.1026	0.076	0.1417	0.1435
<b><u>Rankine pump unit:</u></b>				
<i>Power, kW</i>	1.162	2.346	0.566	0.55
<i>Mass flow rate, kg/s</i>	0.9972	2.012	0.4864	0.4727
<i>Exergy destruction rate, kW</i>	0.844	1.7	0.411	0.4
<i>Cost stream to recuperator, \$/GJ</i>	38.57	28.3	53.73	54.46
<b><u>HTO pump unit:</u></b>				
<i>Power, kW</i>	0.428	1.898	0.43	0.417
<i>Mass flow rate, kg/s</i>	0.572	2.334	0.564	0.548
<i>Exergy destruction rate, kW</i>	0.212	1.148	0.258	0.251
<i>Cost stream to PTC, \$/GJ</i>	4.289	3.601	4.046	4.056
<b><u>MED section (16 effects):</u></b>				
<i>M<sub>db</sub>, kg/s</i>	1.157	1.157	1.157	1.157
<i>M<sub>f</sub>, kg/s</i>	2.894	2.894	2.894	2.894
<i>M<sub>cw</sub>, kg/s</i>	0.6733	0.6733	0.6733	0.6733
<i>M<sub>s</sub>, kg/s</i>	0.9972	2.012	0.4864	0.4727
<i>T<sub>f</sub>, °C</i>	36.38	36.38	36.38	36.38
<i>T<sub>db</sub>, °C</i>	27.85	27.85	27.85	27.85
<i>TBT, °C</i>	88.23	88.23	88.23	88.23
<i>TVT, °C</i>	87.46	87.46	87.46	87.46
<i>TFT, °C</i>	36.38	36.38	84.61	36.38
<i>Condenser area, m<sup>2</sup></i>	12.93	12.93	12.93	12.93
<i>Total effects area, m<sup>2</sup></i>	987	1983	480	505
<i>Total feed heaters area, m<sup>2</sup></i>	---	---	68.7	---
<i>GR</i>	1.16	0.58	2.38	2.45
<i>Exergy destruction rate, kW</i>	5076	5089	5072	5072
<i>Cost stream to BHX, \$/GJ</i>	0.1026	0.0759	0.1417	0.1435
<i>Product cost stream, \$/GJ</i>	1.749	1.799	1.72	1.72
<b><u>Performance &amp; cost:</u></b>				
<i>Specific thermal power consumption, kWh/m<sup>3</sup></i>	71.13	143.5	43.7	33.7
<i>Total operating &amp; maintenance cost, \$/h</i>	13.4	17.64	11.1	11
<i>Total plant cost, \$/y</i>	2.638×10 <sup>5</sup>	4.517×10 <sup>5</sup>	1.686×10 <sup>5</sup>	1.66×10 <sup>5</sup>
<i>Total water price, \$/m<sup>3</sup></i>	8.031	13.75	5.132	5.057

### *c. General comparisons: Case study*

It is clear from the previous analysis that MED-PF configuration is reliable. However, MED-FFH is dominated when less number of effects is operated (normally 8~12 effects). It is very important now to decide which technique thermo-economically attractive. Consider an example of solar energy to operate MED-PF plant with a capacity of 5000m<sup>3</sup>/day with 8 effects, and the top steam temperature is maintained at 73°C (see reference [36]). The example specification is pointed as following:

- Sea water temperature 27°C.
- Salt concentration in feed, 45 g/kg.
- Required Distillate 5000m<sup>3</sup>/day.
- Brine temperature at the last effect, 40°C.
- Salt concentration at the reject stream, 70 g/kg.

For SDMED technique, the plant consumes about 1.009×10<sup>5</sup>m<sup>2</sup> solar collectors with 37kg/s mass flow rate through the field, and the circulation pump consumes about 30kWe. The gain ratio is about 7.56 with evaporators total heat transfer area about 17425m<sup>2</sup> of MED-PF effects. The product TWP is in the range of 1.645\$/m<sup>3</sup> with specific power consumption about 2.179kWh/m<sup>3</sup>. For PSDMED technique, the plant harvest about 1.32×10<sup>5</sup>m<sup>2</sup> solar collectors with 50.83kg/s mass flow rate through the field, and the

circulation pump consumes about 164.3kWe. The Turbine unit would supply about 5.381MWe to serve the plant facilities and the rest might supply to the community grid. The gain ratio is about 1.26 with evaporators total heat transfer area about 15061m<sup>2</sup> of MED-PF effects. The product TWP is in the range of 1.845\$/m<sup>3</sup> with specific power consumption (SPC) about 2.676kWh/m<sup>3</sup>. The GR considered very low (1.257) in this technique. That's because the effect of latent heat of vaporization of the toluene which is considered very low compared against the water. Table 3.18 shows the data comparison between the proposed techniques based on 5000m<sup>3</sup>/d parallel feed configuration.

Table 3.18: Data results for both techniques based on 5000m<sup>3</sup>/d.

	1 <sup>st</sup> technique: SDMED-PF	2 <sup>nd</sup> technique: PSDMED-PF
$A_{cob}$ , m <sup>2</sup>	1.009×10 <sup>5</sup>	1.32×10 <sup>5</sup>
$SPC$ , kWh/m <sup>3</sup>	2.17	2.67
$GR$	7.56	3
$TWP$ , \$/m <sup>3</sup>	1.645	1.845
$C_d$ , \$/GJ	0.4878	0.4117
Total exergy destruction, MW	155.7	157.8
Overall exergy efficiency, %	31.82	33.1
Turbine power, MW	--	5.381
$M_s$ , kg/s	7.65	46.05
$A_{effects}$ , m <sup>2</sup>	17425	15061

It is noticed that PSDMED gives higher values against the SDMED technique comparing based on TWP (\$/m<sup>3</sup>), solar field area and total exergy destruction rate. However; it considered attractive based on the results of effects area, exergy efficiency, and the developed power by the organic turbine. This is referring to the cost of power developed by the turbine unit to serve the auxiliaries (pumps, fans, other facilities...) through the plant. Solar collector area might be drop by 48% under summer operating conditions. There are an amount of 64,230m<sup>2</sup> might be out of service for maintenance and cleaning operations during the summer time. The effect of evaporators' numbers ( $N_{eff}$ ) considered a vital tool to judge the plant performance. Figure (3.16) shows the effect of evaporators' numbers on SDMED technique. The results are obtained based on SDMED case study (5000m<sup>3</sup>/d). It is pin pointed from Figure (3.16-a) that increasing  $N_{eff}$  would decrease the SPC kWh/m<sup>3</sup>. That is referring to the effect of total feed flow rate and cooling water flow rate according to the increase of  $N_{eff}$ . Reducing the mass flow rates would decrease the required pumping power. Steam temperature has no significant effect on the SPC however; increasing the steam temperature would little bit decrease the SPC. Thermo-economic product cost (\$/GJ) is also decreased by the increasing of the  $N_{eff}$  (Figure (3.16-b)). Also the gain ratio (GR) is increased as a direct effect of  $N_{eff}$ . For  $N_{eff}$  around 10, the GR would become 9. However, the opposite behavior is significantly happened for evaporators' area. Also, solar field area is gradually decreased by the increase of  $N_{eff}$ . Physically that's happened due to the decrease of steam mass flow rate across the heat exchanger unit. Figure (3.17) shows the effect of daily productivity on the system daily productivity. It is shown from the figure that by increasing the productivity, the thermo-economic product cost would decrease. That's referring to the effect of GR of the system and the effect of product exergy stream. Increasing the product exergy will decrease the thermo-economic cost. Figure (3.18) shows the effect of the productivity on the developed power by the turbine unit in PSDMED technique. It is become clear that the developed power by the turbine is increased due to the demanded increase in the steam mass flow rate by the first effect of the MED. The increasing in the demanded steam would increase the ORC mass flow rate thence increasing the power from the turbine unit. The advantage of this technique (PSDMED) is that the powered developed may serve the auxiliaries in the cycle and the rest of power is considered a gain to the main electricity grid.

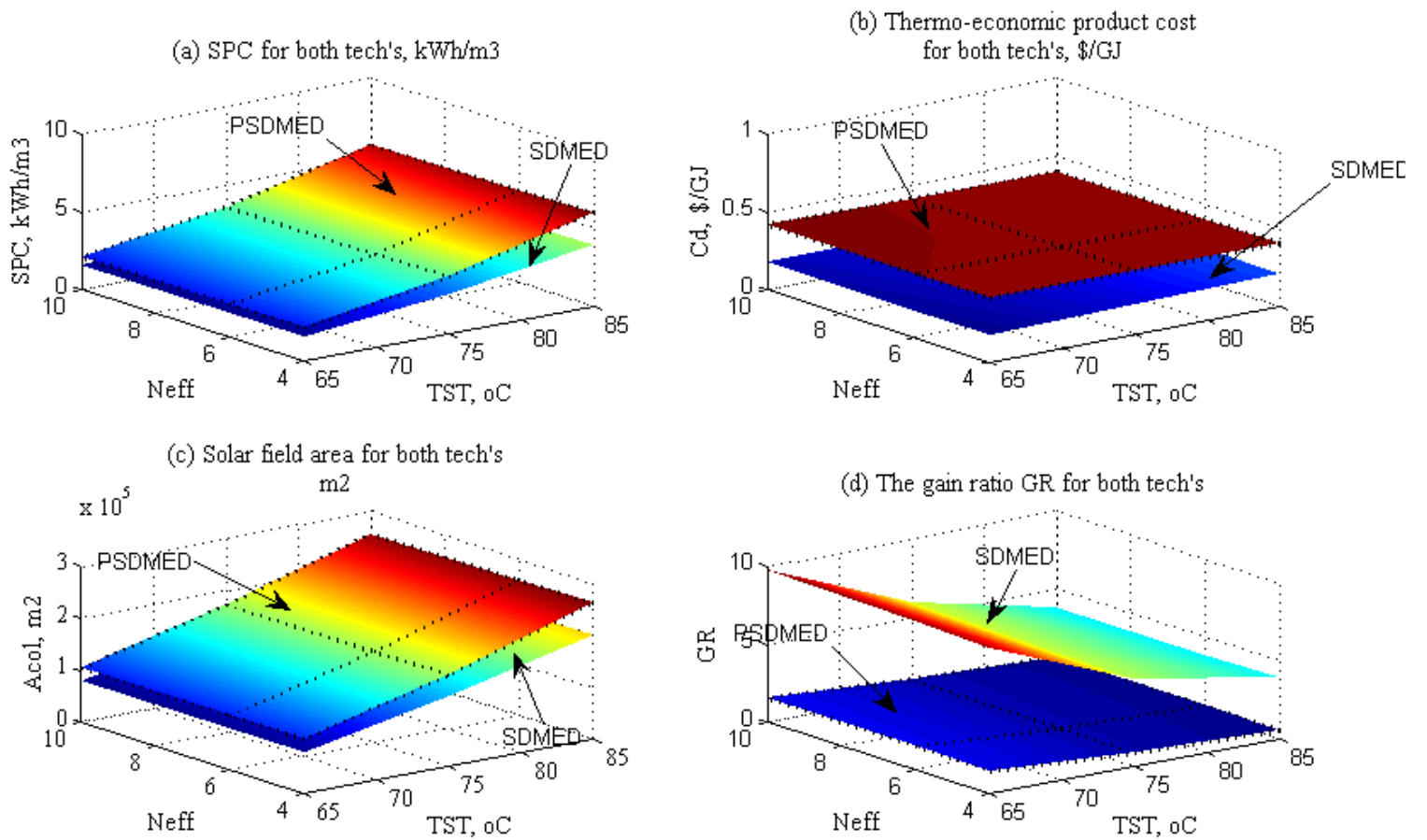


Figure (3.16) Effect of evaporators number and steam temperature on based on both techniques: (a) SPC, kWh/m<sup>3</sup>, (b) Thermo-economic product cost, \$/GJ, (c) Solar field area, m<sup>2</sup>, (d) Gain ratio.

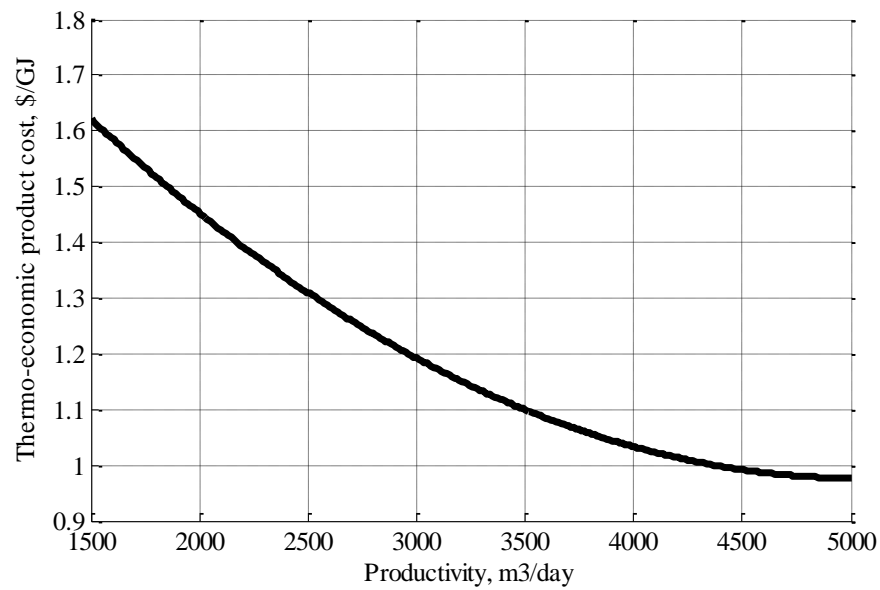


Figure (3.17) Effect of daily productivity ( $\text{m}^3/\text{d}$ ) on thermo-economic product cost (\$/GJ) for SDMED-PF case study.

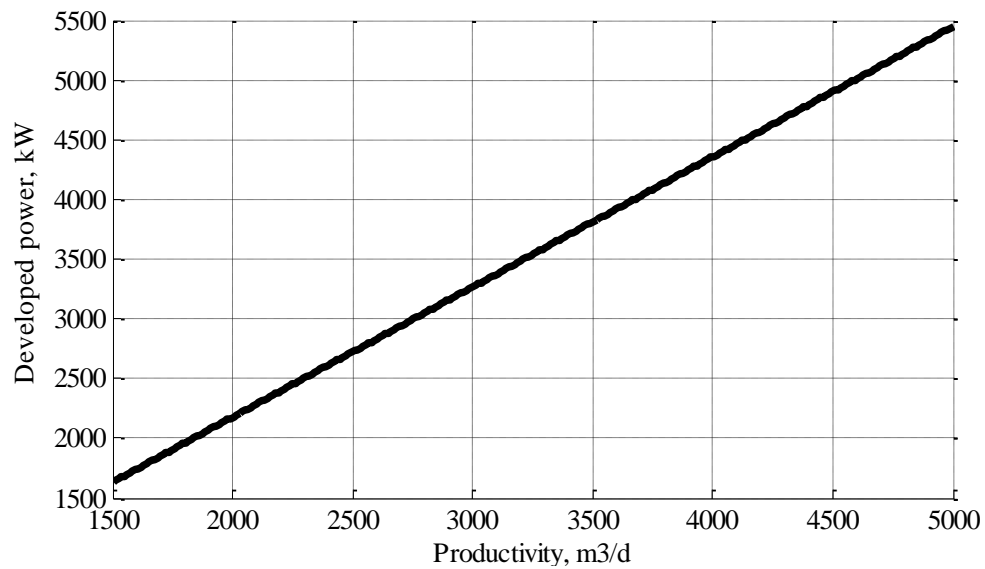


Figure (3.18) Effect of daily productivity ( $\text{m}^3/\text{d}$ ) on the developed power by the turbine unit based on PSDMED-PF technique.

### 3.4 Solar Thermal Organic Cycles Assisted Multi Effect Distillation-Vapor Compression (MED-VC) Desalination Processes

Solar energy can positively operate and power MED-VC desalination processes according to many reasons such as; low top brine temperature (TBT), low top steam temperature (TST), high gain ratio, and lower specific power consumption comparing against multi-stage flash and/or reverse osmosis desalination types. According to vapor compression type (mechanical or thermal), the combination technique with concentrated solar power plant (CSP) would be determined from technique to another. The following sub-sections explain the process techniques and the promise of coupling CSP plants with MED-VC desalination process.

#### 3.4.1 Solar SMED-PF-TVC: 1<sup>st</sup> technique

Firstly, multi-effect distillation parallel feed configuration (MED-PF) is recommended by the authors to be operated with vapor compression type. In the parallel feed (MED-PF) arrangement, the feed leaving the condenser is divided and distributed almost equally to each effect. Darwish et al. [45] and Dessouky et al. [43] both gave more details about MED feed arrangement.

The efficiency of the MED process is enhanced by compressing the vapor from the last effect in order to increase its temperature to drive the first evaporation effect. The Performance Ratio (PR) of a MED process can be significantly increased by coupling a thermal vapor compression TVC unit. The compressor acts as a steam ejector and requires motive steam at a pressure of 3–20bar.

Vapor is removed from one of the multi-effect (ME) evaporators at about 0.1bar and is compressed to about 0.25bar [63]. Operating conditions (TBT) of MED-PF-TVC allow the use of parabolic trough collector (PTC) in solar power plants. In solar PTC application to desalination, the heated oil could be sent to a boiler heat exchanger (BHX), which would generate the necessary steam by a conventional MED-TVC plant.

This technique consists of pump unit to overcome the pressure losses, solar collector field (PTC-LS-3 type [54]) for thermal power, BHX for vapor release and MED-PF-TVC type with 5 effects. The organic HTO across the PTC would transfer its thermal power to the fluid (water) across the BHX unit. The generated motive steam is used to compress part of the vapor generated in the last effect by the steam ejector.

The expanded motive steam and the recompressed vapor leaving the steam ejector are directed to and condensed in the first effect. Part of the condensate returns to the boiler, and the other part join the potable water product. The vapor formed in the first effect by boiling is directed to the second effect where it acts as a heat source [64]. Figure (3.19) shows a schematic diagram of the process units for the 1<sup>st</sup> technique. Table 3.18 shows the design points and specifications for the 1<sup>st</sup> technique. The environmental conditions are selected based on Suez Gulf site: latitude angle =30° N, and longitude =32.55° E.

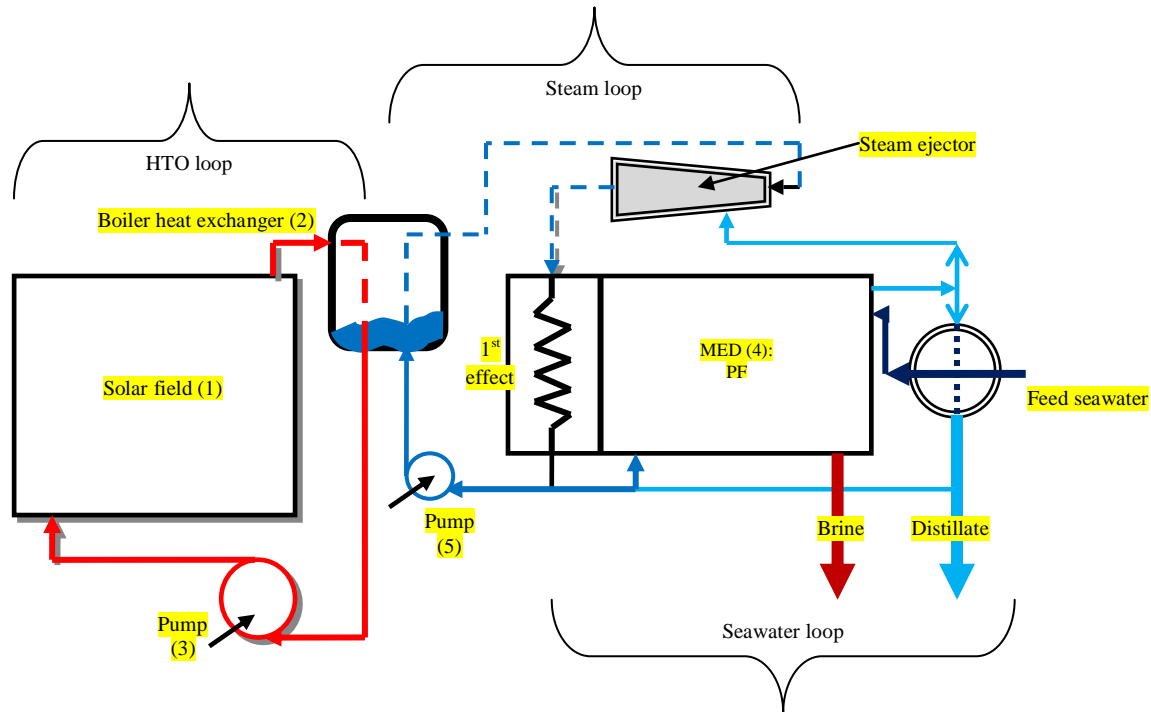


Figure (3.19) A schematic diagram of solar MED-PF-TVC components: (1) Solar field, (2) Boiler heat exchanger, (3) HTO pump, (4) MED-PF-TVC, (5) Water pump.

### 3.4.2 Solar SMED-PF-MVC: 2<sup>nd</sup> technique

The multi-effect distillation–mechanical vapor compression process (MED–MVC) is one of the attractive techniques for remote and small population areas. The MED–MVC is compact and confined. The system is driven by electric power; therefore, it is suitable for remote population areas. The MED–MVC can also be driven mechanically by diesel engine. Another advantage of the MED–MVC system is the absence of the down condenser and the cooling water requirements. The MED–MVC system is a viable alternative to the reverse osmosis (RO) systems. The barrier to achieving this potential is the absence of a specially designed steam compressor of a capacity comparable to that of the multi-stage flash (MSF) unit capacity [65]. The MED–MVC system has specific power consumption similar to the RO system, which may vary between 6–8 kWh/m<sup>3</sup>. However, the MVC system reliability and its plant factor are highly superior to the RO system with value close to 90%. Moreover, the system has much simpler pretreatment system and limited operational problems related to fouling and scaling [43]. During the last two decades, the compressor capacity is increased from values below 500 m<sup>3</sup>/d to higher values of 1000 m<sup>3</sup>/d. This allowed for design of three effects MVC units capable of producing 3000 m<sup>3</sup>/d. However, more recently, the compressor capacity is increased to a higher value of 5000 m<sup>3</sup>/d, which gives a production capacity of 15000 m<sup>3</sup>/d for a three-effect units [43]. It should be noted that the multi effect units has the same power rating as the single unit and the increase in its capacity is approximately proportional to the number of effects. To reduce the specific power consumption (SPC), the MVC unit is added to the MED–PF with 16 effects. To operate such technique, solar organic Rankine cycle (S-ORC) is dominated to develop the suitable power for vapor compressor. The process cycle consists of two pumps for circulation and pressure drops, solar collector field (PTC), boiler heat exchanger, turbine expander unit, recuperator for regeneration, and MED–PF with 16 effects. The end condenser is removed

Table 3.19: Design points for SMED-PF-VC according to the 1st and the 2<sup>nd</sup> techniques.

76

Product mass flow rate, kg/s	52.6	52.6
Plant life time, year	20	20
Power generation cost, \$/kWh	0.06	0.06
Working fluids	HTO-Water-Seawater	HTO-Toluene-Seawater

### 3.4.3 Results of SMED-PF-TVC technique

The obtained results about this technicality SMED-PF-TVC to producing what equates 4545m<sup>3</sup>/d exhibition through the next Table 3.20 was complete here. The results indicated that the complete area for the solar station around 9.476×10<sup>4</sup>m<sup>2</sup> with total mass flow rate across the solar station reached at 33.76kg/s. That consumption performed for what about 170 modules of solar PTC heaters distributed on 8 rows. According for the solar area requested the total thermal power collected is about 1.664×10<sup>4</sup>kW with total exergy inlet 2.27×10<sup>4</sup>kW and exergy destruction rate with 1.51×10<sup>4</sup>kW.

The cost stream from the solar field to the boiler heat exchanger (BHX) unit reached at 3.345 \$/GJ. Based on the quantitative motive steam designating and which informs 2500kPa, the informed square area of the thermal BHX unit is around 57m<sup>2</sup>, and the degree heat of the steam according for the pressing is around 225°C. The mass flow rate of the motive steam is about 6.545kg/s.

Based on the energy requested, and the meant solar field area, the informed power of the recirculation organic pump is around 122kW. For MED-PF-TVC part (five effects), the assigned productivity (52.6kg/s) exhibits about 168kg/s as a total feed seawater. The cooling water feed loss from the end condenser is about 10.16kg/s, however, the feed water mass flow rate to the effects is 157.8kg/s. The cooling feed water (10.16kg/s) is noticed very low according to many aspects such as increasing the number of evaporators, decreasing the compression ratio, and increasing the end condenser effectiveness.

For parallel feed configuration, the feed mass flow rate per each effect considered equivalent about 31.56kg/s per effect. The motive steam mass flow rate is 6.545kg/s and entrained about 4.988kg/s with an entrained ratio with a value of 1.312. The steam temperature reaches 60.33°C with 1<sup>st</sup> effect top brine temperature (TBT) about 58.47°C with 1<sup>st</sup> effect top vapor temperature (TVT) about 57.47°C. This temperature loss is founded due to the effect of boiling point elevation (BPE). The end condenser area is 532m<sup>2</sup> with total heat transfer area for the evaporators about 11024.61m<sup>2</sup>. The Specific Power Consumption (SPC) for such technique is obtained less than 2 kWh/m<sup>3</sup> with total water price in the range of 1.3\$/m<sup>3</sup>. Also the gain ratio is obtained in the range of 7.8~8 based on only 5 effects.

The effect of steam ejector is significantly high on the gain ratio according to the compression ratio (CR) and the motive steam pressure. It is evident that without steam ejector at the same number of effects (Neff=5) the gain ratio would become in the range of 3.5~4.

However, adding the steam ejector unit increased the gain ratio up to 8. Figures (3.21-3.22) show the effect of CR and number of evaporators (Neff) on SPC, thermo-economic product cost, solar field area, and total exergy destruction rate.

Figure (3.21-a) shows that by increasing the CR the SPC would increase, however, the evaporators number increasing would decrease the SPC. Therefore, it is recommended to keep the CR to minimum values related to the desalination plant specifications. In this work, the CR is fixed at value equal to 2 with Neff=5.

Also Figure (3.21-b) shows the same behavior for thermo-economic product cost. The minimum value of thermo-economic product cost (0.25\$/GJ) is obtained at CR=2 and Neff=5. Also, Figure (3.22-a, b) shows that minimum solar field area, and total exergy destruction rate that could be obtained at minimum CR and Neff.



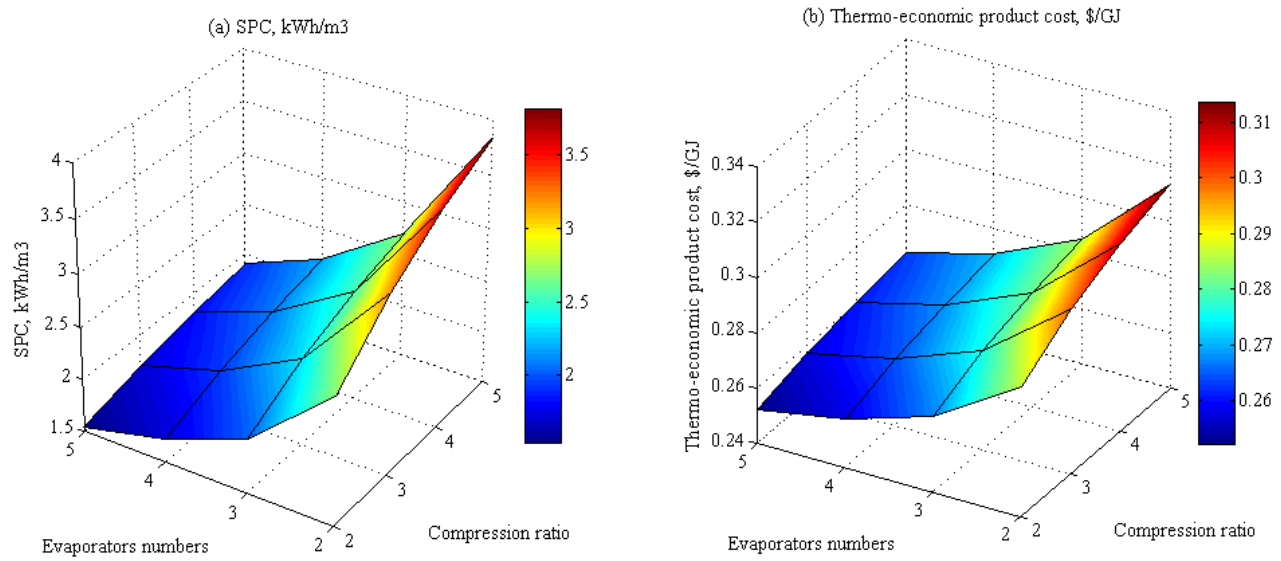


Figure (3.21) Effect of CR and number of evaporators on both: (a) SPC, kWh/m<sup>3</sup>, and (b) Thermo-economic product cost, \$/GJ.

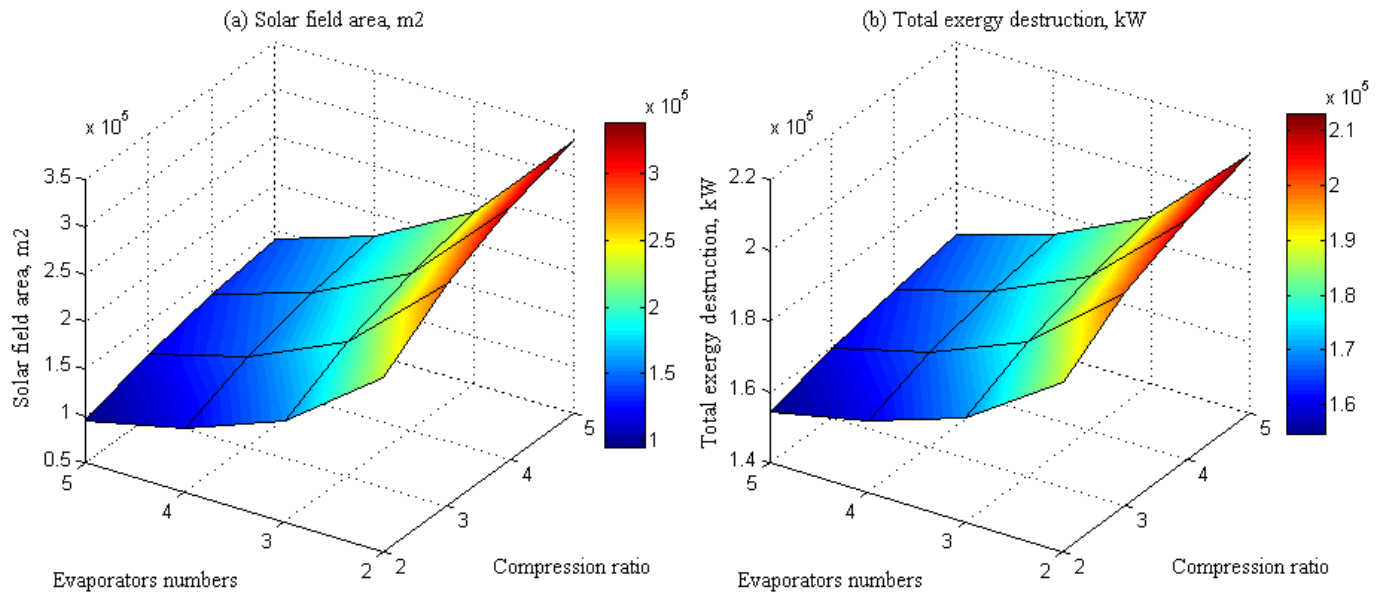


Figure (3.22) Effect of CR and number of evaporators on both: (a) Solar field area, m<sup>2</sup>, and (b) Total exergy destruction rate, kW.

Table 3.20: Data results for SMED-PF-TVC operated by Water and HTO fluids.

<b><u>Parameter:</u></b>	<b><u>SMED-PF-TVC</u></b>
<b><u>Solar Collector field:</u></b>	
High pressure, bar	5.5
Total solar field area, m <sup>2</sup>	9.476×10 <sup>4</sup>
Solar field flow rate, kg/s	33.76
Solar field R <sub>e</sub> number	1×10 <sup>5</sup>
No. of collectors (LS-3)/No. of loops	170/8
Solar field width, m	113
Solar collector thermal efficiency, %	69.7
Exergy destruction rate, kW	1.51×10 <sup>4</sup>
Exergy inlet rate, kW	2.27×10 <sup>4</sup>
Cost stream to BHX, \$/GJ	3.345
<b><u>Boiler heat exchanger unit:</u></b>	
Motive steam pressure, kPa	2500
Area, m <sup>2</sup>	57
Outlet HTO temperature, °C	118.3
Motive steam temperature, °C	225.7
Motive steam mass flow rate, kg/s	6.545
Exergy destruction rate, kW	1320
Cost stream to MED, \$/GJ	0.00153
Cost stream to pump, \$/GJ	3.345
<b><u>HTO pump unit:</u></b>	
Power, kW	122
Mass flow rate, kg/s	33.76
Exergy destruction rate, kW	80
Cost stream to PTC, \$/GJ	4.744
<b><u>MED-PF-TVC section (5 effects):</u></b>	
Productivity, M <sub>d</sub> , kg/s	52.6
Total feed seawater M <sub>f</sub> , kg/s	168
Cooling flow rate M <sub>co</sub> , kg/s	10.16
Feed water to evaporators from end condenser, M <sub>fb</sub> , kg/s	157.8
Motive steam M <sub>ms</sub> , kg/s	6.545
Entrained vapor, M <sub>ev</sub> , kg/s	4.988
Total steam mass flow rate M <sub>st</sub> , kg/s	11.53
Entrained vapor ratio	1.312
Compressed vapor pressure, kPa	20.25
Steam temperature T <sub>s</sub> , °C	60.33
Pre-heated feed temperature T <sub>p</sub> , °C	41.81
Distillate temperature from end condenser T <sub>d</sub> , °C	29.2
1 <sup>st</sup> effect brine temperature TBT, °C	58.47
1 <sup>st</sup> effect vapor temperature TVT, °C	57.47
1 <sup>st</sup> effect distillate temperature TDT, °C	57.42
1 <sup>st</sup> /n <sup>th</sup> effect pressure, kPa	17.68/10.12
End condenser area, m <sup>2</sup>	532.8
Total effects area, m <sup>2</sup>	11024.61
GR	8.037
Exergy destruction rate, kW	2.693×10 <sup>5</sup>
Cost stream to BHX, \$/GJ	0.00153
Product cost stream, \$/GJ	0.2522
<b><u>Performance &amp; cost:</u></b>	
Specific power consumption SPC, kWh/m <sup>3</sup>	1.58~2
Total Water Price TWP, \$/m <sup>3</sup>	1.323

#### 3.4.4 Results of SMED-PF-MVC technique

Results obtained for this technique are illustrated in Table 3.21. It is clear that the demanded productivity would harvest about  $1.437 \times 10^4 \text{ m}^2$  of solar field with about 5.8kg/s mass flow rate across the solar collector's loops. Therefore, the solar field contains 25 collectors divided by one loop. Then, the field width should figure as 75m length. Less in total solar field area means less in total exergy destruction rate which become 2243kW through the solar field.

The power demanded from the desalination plant via vapor compressor is developed by the ORC turbine. Based on the specified design operating conditions for this technique, the BHX area is  $14 \text{ m}^2$ , with mass flow rate across the ORC about 4.1kg/s. The developed power by the turbine unit is about 765kW and that considered very low related to the total plant productivity ( $4545 \text{ m}^3/\text{d}$ ).

Recuperator and ORC condenser exhibits areas such 5 and  $56 \text{ m}^2$  respectively. The ORC pump consumes about 21kWe however, the solar field recirculation pump consumes about 6kWe. For MED-PF-MVC section, the total productivity 52.6kg/s needs about 157.8kg/s of feed seawater.

In this technique the end condenser unit is eliminated. Therefore, the feed water per each effect become 9.86kg/s based on  $N_{\text{eff}}=16$  effect. The steam mass flow rate is maintained at 3.52kg/s and the 1<sup>st</sup> effect TBT is maintained at  $59^\circ\text{C}$ . The compression ratio (CR) reached at 1.94~2 with total evaporators area about  $9.261 \times 10^5 \text{ m}^2$ .

The total evaporator's area considered too large because of the large number of evaporators ( $N_{\text{eff}}=16$ ). Increasing the  $N_{\text{eff}}$  would increase the gain ratio ( $\text{GR}=15$ ). But it is significantly for this technique that the SPC is about  $4 \text{ kWh/m}^3$  with thermo-economic product cost with a value of 0.3\$/GJ. The effect of steam temperature and  $N_{\text{eff}}$  on SPC and thermo-economic product cost is explained in Figure (3.23-a, b).

It is clear that by reducing the steam temperature (80 down to  $60^\circ\text{C}$ ); at the same time increasing the  $N_{\text{eff}}$  (up to 16 effects) the SPC and thermo-economic product cost are decreasing gradually. The same behavior is obtained for Figure (3.24-a, b) related to solar field area and total exergy destruction rate. Minimum solar field area and total exergy destruction rate are obtained at minimum values of steam temperature ( $60^\circ\text{C}$ ) and maximum values of  $N_{\text{eff}}$  (16 effects).

However, increasing the  $N_{\text{eff}}$  would increase the CR. But that effect is significantly low compared with the effect of steam temperature. Steam temperature has a great influence on the CR against  $N_{\text{eff}}$ . However,  $N_{\text{eff}}$  has a great influence on the GR compared against the steam temperature (see Figure (3.25-a, b)).

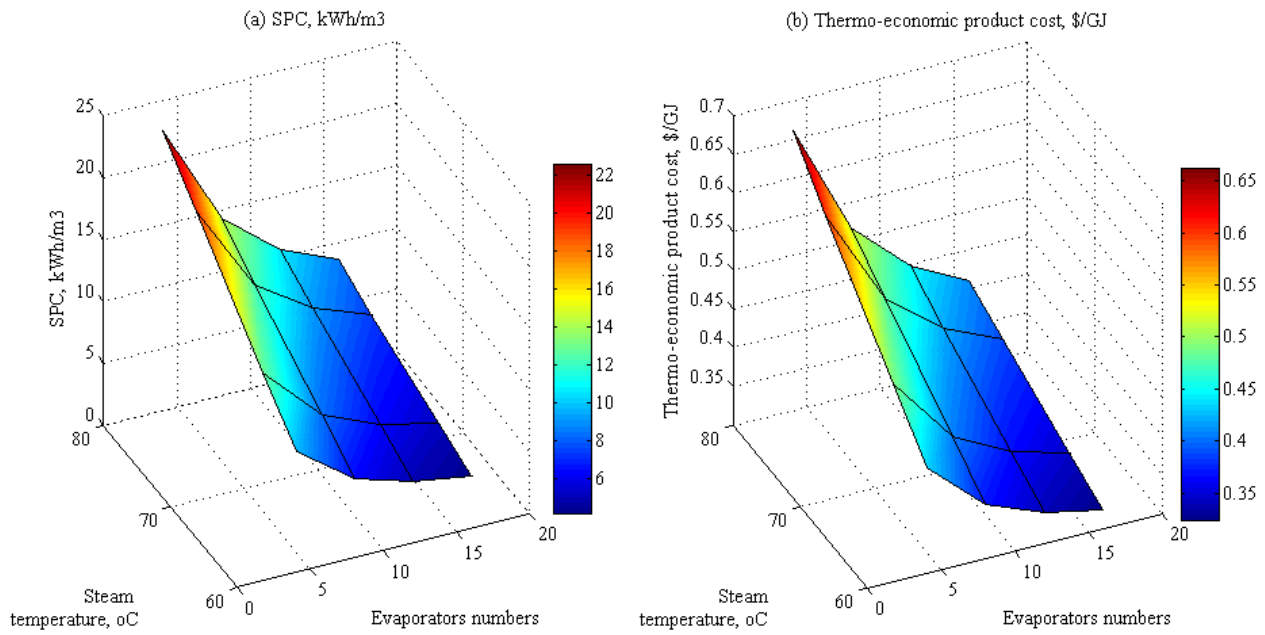


Figure (3.23) Effect of Neff and steam temperature on both: (a) SPC, kWh/m<sup>3</sup>, and (b) Thermo-economic product cost, \$/GJ.

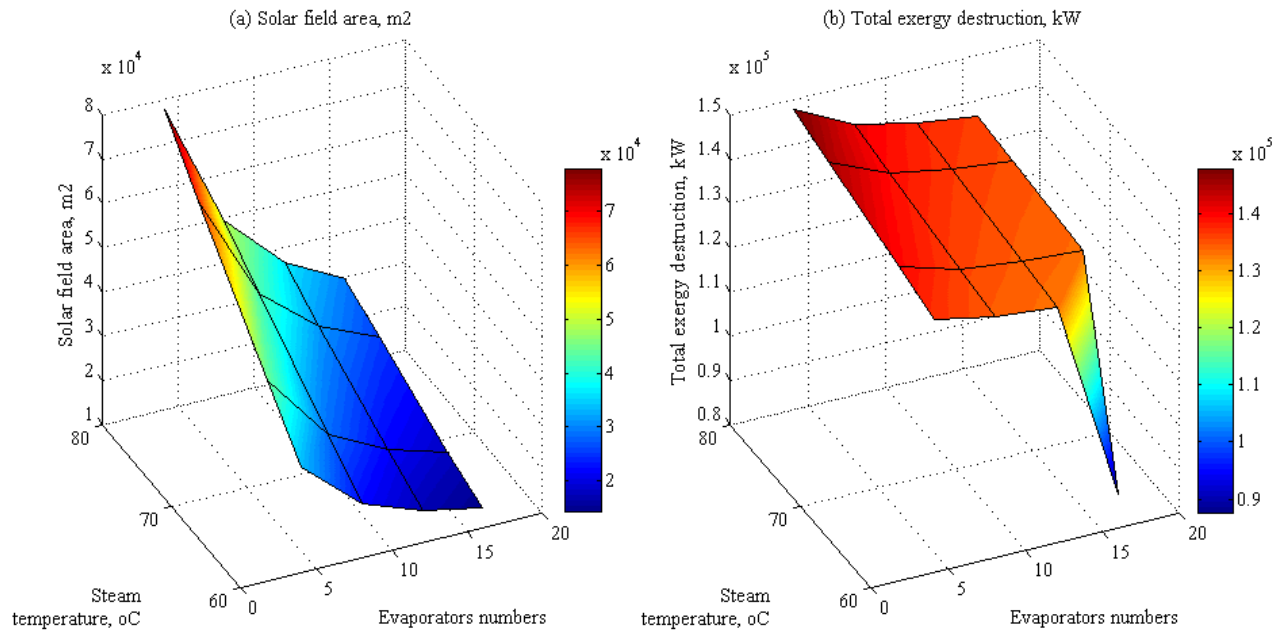


Figure (3.24) Effect of Neff and steam temperature on both: (a) Solar field area, m<sup>2</sup>, and (b) Total exergy destruction rate, kW.

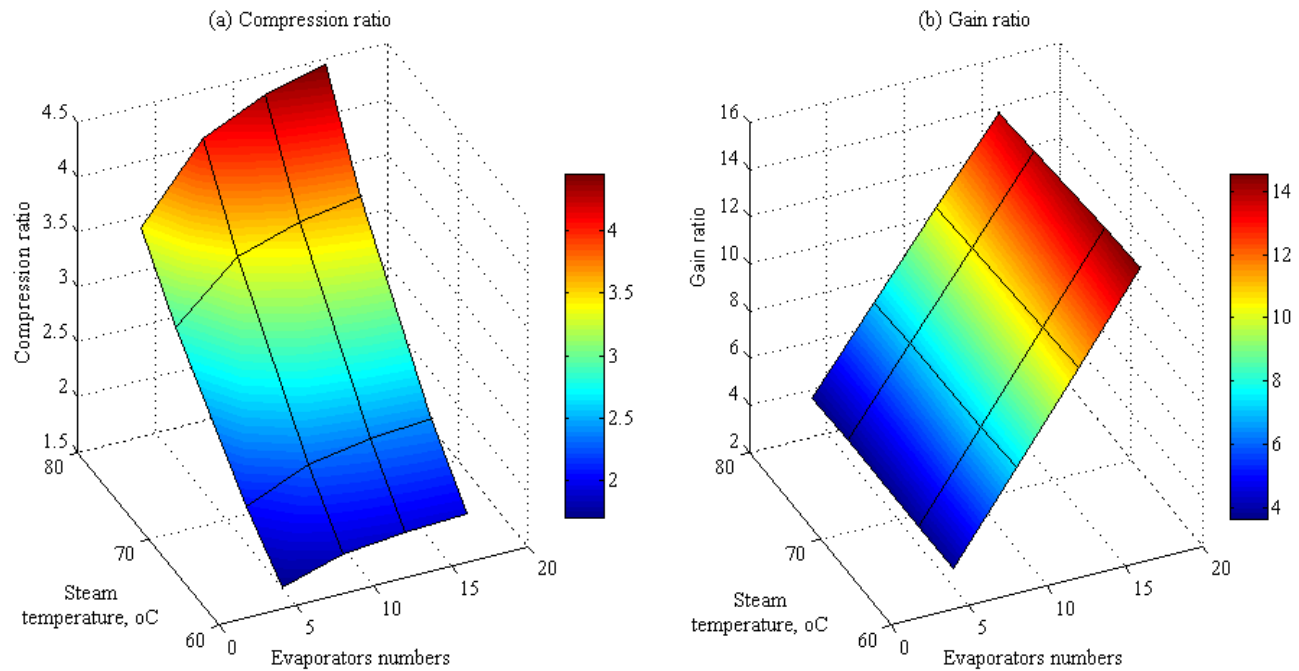


Figure (3.25) Effect of Neff and steam temperature on both: (a) CR, and (b) GR.

Table 3.21: Data results for SMED-PF-MVC operated by Toluene and HTO fluids.

<u>Parameter:</u>	<u>SMED-PF-MVC</u>
<b><u>Solar Collector field:</u></b>	
High pressure, bar	5.5
Total solar field area, m <sup>2</sup>	1.437×10 <sup>4</sup>
Solar field flow rate, kg/s	5.815
Solar field R <sub>e</sub> number	9.835×10 <sup>4</sup>
No. of collectors (LS-3)/No. of loops	25/1
Solar field width, m	75
Solar collector thermal efficiency, %	69.7
Exergy destruction rate, kW	2243
Exergy inlet rate, kW	3442
Cost stream to BHX, \$/GJ	3.319
<b><u>Boiler heat exchanger (BHX) unit:</u></b>	
Vapor pressure, bar	32.75
Area, m <sup>2</sup>	14
Outlet HTO temperature, °C	151.2
Outlet steam temperature to the Turbine, °C	300
Steam mass flow rate, kg/s	4.103
Exergy destruction rate, kW	167
Cost stream to turbine, \$/GJ	4.018
Cost stream to pump, \$/GJ	3.319
<b><u>Turbine unit:</u></b>	
Total power developed, kW	764.53
Exhaust temperature, °C	138.8
Exergy destruction rate, kW	147
Cost of power, \$/GJ	6.39
Cost stream to recuperator, \$/GJ	4.018

<b><u>Recuperator unit:</u></b>	
Power rejected, kW	485
Area, m <sup>2</sup>	5
Outlet stream temperature to the condenser, °C	58.1
Outlet stream temperature to the BHX, °C	101.5
Cost stream to BHX, \$/GJ	9.663
Cost stream to condenser, \$/GJ	4.018
<b><u>Condenser unit:</u></b>	
Power rejected, kW	1784
Area, m <sup>2</sup>	56
Cost stream to MED-MVC, \$/GJ	0.0267
Cost stream to pump, \$/GJ	4.018
<b><u>Rankine pump unit:</u></b>	
Power, kW	21
Mass flow rate, kg/s	4.103
Exergy destruction rate, kW	19.5
Cost stream to recuperator, \$/GJ	5.498
Outlet temperature stream to recuperator, °C	38
<b><u>HTO pump unit:</u></b>	
Power, kW	6
Mass flow rate, kg/s	5.815
Exergy destruction rate, kW	3.665
Cost stream to PTC, \$/GJ	3.523
<b><u>MED-PF-MVC section (16 effects):</u></b>	
Productivity $M_d$ , kg/s	52.6
Total feed mass flow rate $M_f$ , kg/s	157.8
Steam mass flow rate $M_s$ , kg/s	3.525
Pre-heated feed temperature $T_f$ , °C	28
Steam temperature TST, °C	60
1 <sup>st</sup> effect brine temperature TBT, °C	59.91
1 <sup>st</sup> effect vapor temperature TVT, °C	59.13
1 <sup>st</sup> effect distillate temperature TDT, °C	58.88
Vapor compressor power, kW	471.2
Compression ratio	1.939
Total effects area, m <sup>2</sup>	9.261×10 <sup>5</sup>
GR	15
Exergy destruction rate, kW	1.322×10 <sup>5</sup>
Product cost stream, \$/GJ	0.3183
<b><u>Performance &amp; cost:</u></b>	
Specific power consumption SPC, kWh/m <sup>3</sup>	4.18
Total water price, \$/m <sup>3</sup>	0.94

### 3.4.5 General comparison: Case study

To distinguish between these two techniques, it is important to united most of the operating conditions to give clear and real aspects about the best technique. Therefore, the design operating conditions for both techniques are considered as following:

- Seawater temperature =25°C.
- Neff=4 effects.
- Compression Ratio CR=2.
- Steam temperature=60°C.
- Blow down brine temperature=46.8°C.

- Productivity=4545m<sup>3</sup>/d.
- Seawater salinity=46000ppm.
- Blow down salinity=69000ppm.
- Motive steam in case of MED-PF-TVC=25bar.
- Outlet collector temperature=350°C.

Table 3.22 shows the obtained results for both techniques based on the united design operating conditions. It is obvious from the table that the 1<sup>st</sup> technique gives remarkable results against the 2<sup>nd</sup>. Except the solar field area, all performance parameters reveals that SMED-PF-TVC considered attractive based on GR, SPC, thermo-economic product cost ( $C_d$ ), total water price ( $TWP$ ), and even the area of each effect. Although the 1<sup>st</sup> technique consumes larger area than the 2<sup>nd</sup> but the cost of pumping units, turbine and the vapor compressor has a great influence on the total water price and the thermo-economic product cost, hence the SPC. Also the steam mass flow rate for the 1<sup>st</sup> technique is less by 40% than the 2<sup>nd</sup> technique casing an increase in GR for the 1<sup>st</sup>. Adding steam ejector unit improves the cycle performances even with less numbers of evaporators. The steam ejector unit would optimize the MED section by reducing the number of effects meaning by this reducing the surface area of the effect resulting lower costs. Moreover; it increases the gain ratio of the MED section in order to reduce the thermal load on the boiler heat exchanger unit.

Reducing the thermal load would reduce the total area demanded by the solar field i.e. reducing the costs. The SPC, kWh/m<sup>3</sup> is noticed attractive for MED-TVC against MED-MVC (2.44 Vs 9.68kWh/m<sup>3</sup>) because of using more pumps in the MED-MVC in addition using of the mechanical compressor itself. Figure (3.26) shows the effect of daily productivity on the thermo-economic product cost. The figure reveals that increasing the daily productivity would totally decrease the thermo-economic product cost. That's due to the effect of increasing the exergy rate of the product stream. Furthermore; the figure shows that MED-TVC technique gives lower and remarkable results against the MED-MVC as shown on the curve. Figure (3.27) shows the effect of daily productivity on the developed power for both techniques. The figure curves reveal that the thermal power by MED-TVC is massive compared with the electric power from the turbine unit of MED-MVC technique. It is become possible to decrease the thermal power from the boiler unit by reducing the motive steam pressure. Thence the thermal load that demanded by the solar field would decrease.

Table 3.22: Data results for both techniques based on 4545m<sup>3</sup>/d.

	1 <sup>st</sup> technique: SMED-PF-TVC				2 <sup>nd</sup> technique: SMED-PF-MVC			
$A_{cob}$ , m <sup>2</sup>	117908.9				33181.5			
SPC, kWh/m <sup>3</sup>	2.44				9.68			
GR	6.44				3.82			
TWP, \$/m <sup>3</sup>	1.57				2.17			
$C_d$ , \$/GJ	0.2578				0.4265			
$M_b$ , kg/s Profile	26.23	26.27	26.32	26.37	26.23	26.27	26.32	26.37
$M_s$ , kg/s Profile	8.15				13.74			
$M_b$ , kg/s Profile	39.45 (for each effect)				39.45 (for each effect)			
$T_b$ , °C Profile	57.53	53.95	50.37	46.8	57.28	53.79	50.29	46.8
$T_v$ , °C Profile	56.74	53.17	49.59	46.01	56.5	53	49.51	46.01
$T_d$ , °C Profile	56.7	53.12	49.56	46	56.17	52.56	48.93	45.31
$P$ , kPa Profile	17.09	14.41	12.1	10.12	16.68	14.02	11.73	9.76
$S_b$ , kg/kg Profile	0.06918	0.06906	0.068936	0.06881	0.06918	0.06906	0.06893	0.0688
$A_{effects}$ , m <sup>2</sup> Profile	4995.76	5002.41	5011.95	5017.05	5008.45	5015.65	5025.3	5037.7
Note: shaded cells gives nearly the same results.								

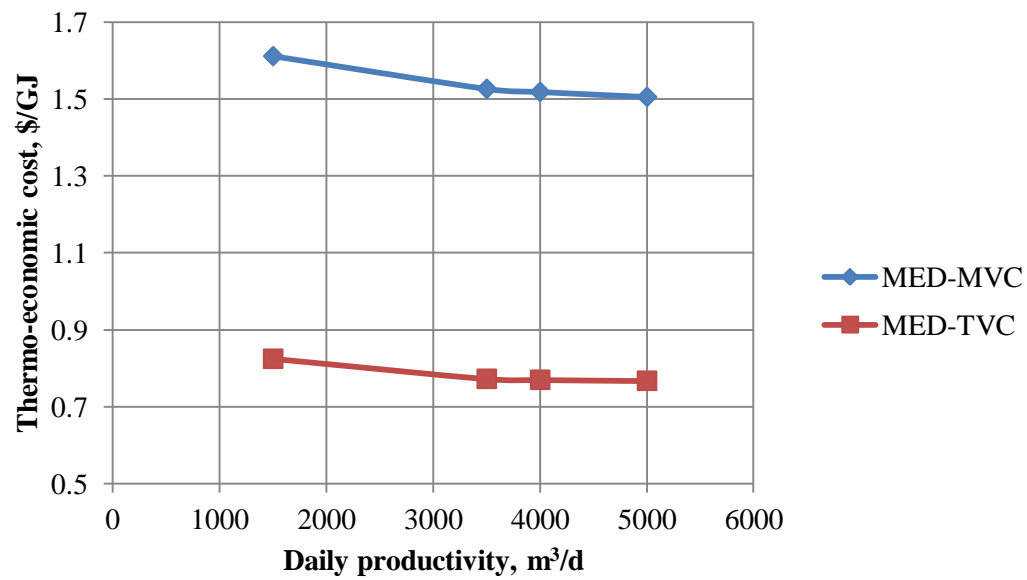


Figure (3.26) The effect of daily productivity ( $\text{m}^3/\text{d}$ ) on thermo-economic product cost for both techniques (MED-MVC & MED-TVC).

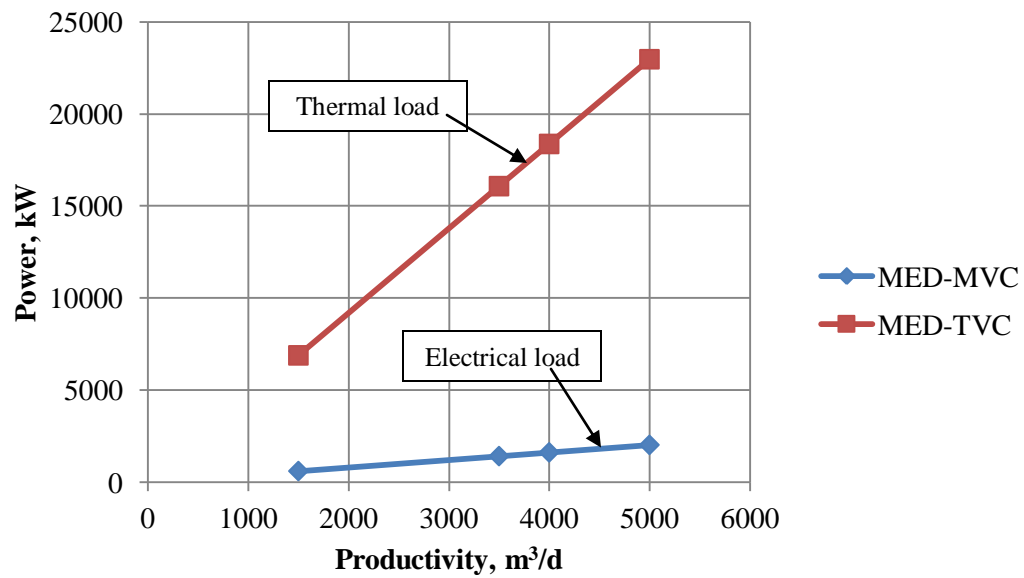


Figure (3.27) Effect of daily productivity ( $\text{m}^3/\text{d}$ ) on the developed power for both techniques (MED-MVC & MED-TVC).



### 3.5 Solar Thermal Organic Cycles Assisted Multi Stage Flash (MSF) Desalination Process

Multi-Stage Flash (MSF) evaporation process is currently the workhorse of the desalination industry with a market share close to 60% of the total world production capacity [66]. MSF process has also a possibility for use with solar power. Operation temperatures of multi-stage flash distillation systems allow the use of different solar collectors in solar powered plants [67]. A solar MSF desalination system was tested in Kuwait with a capacity of a 10m<sup>3</sup>/d [68]. This system consists of a 220 m<sup>2</sup> parabolic trough collector, and a 12-stage MSF desalination block. The thermal storage system was used to level off the variation of thermal energy supply and allowed the production of fresh water to continue during periods of low radiation and nighttime. The output of the system is reported to be over ten times the output of solar stills for the same solar collection area (about 40kg/m<sup>2</sup>). Sharaf et al [69, 70] examined a small unit for water desalination by solar energy and flash evaporation process. The system was built to produce an amount of 20kg of distillate water during the day light by the using a solar flat plate collector (FPC). Lourdes-Garcia [67] concluded that the use of solar energy could compete with a conventional energy supply in MSF distillation processes in some climatic conditions. Results obtained in Lourdes-Garcia [67] work were useful in competitiveness evaluations of solar against the conventional energies in MSF plants. Several medium capacity plants for MSF desalination using solar energy have recently been implemented.

It is clear from literatures that the possibility of utilizing solar energy with different types of distillation processes such as MSF already exists. However, such techniques didn't imply solar organic power cycle and the productivity is noticed not exceeded over 500m<sup>3</sup>/day. Moreover, thermo-economic approach is not implemented for such processes. In this part, investigation analysis is introduced about powering MSF-BR configuration with a capacity of 5000m<sup>3</sup>/day by using solar power cycles. Table 3.23 shows the specifications that considered in this study related to Eoun Mousa MSF desalination plant. Two different techniques are studied in this work: The 1<sup>st</sup> technique is to utilize the solar power by using the PTC concentrator to deliver a sufficient thermal power via heat exchanger boiler to power on the MSF-BR directly through the brine heater. And the 2<sup>nd</sup> technique is to utilize the rest of exhaust power from solar organic Rankine cycle (SORC) turbine to drive the MSF-BR brine heater. Both techniques used Therminol-VP1 [62] heat transfer oil (HTO) for indirect vapor generation via heat exchanger boiler. The 1<sup>st</sup> technique can't produce electric power (only fresh water); however the 2<sup>nd</sup> technique can produce electric power and fresh water. Solar Desalination Systems (SDS) software package is used to design and model the process units of the proposed techniques. Solar radiation under winter operating conditions is assumed for Egypt-Suez Gulf region (latitude: 30° N; longitude: 32.55° E)).

Table 3.23: Specifications of Eoun Mousa [36] MSF desalination plant (5000m<sup>3</sup>/day).

Design point:	Value:
Productivity, m <sup>3</sup> /day	5000
Top brine temperature, °C	110
Brine blow down temperature, °C	40
Top steam temperature, °C	113
Seawater temperature, °C	20 (winter condition)
Feed seawater splitter ratio	0.482
Seawater salinity concentration, ppm	48,620
Brine blow down concentration, ppm	70,900
Number of stages	20(17/3)

### 3.5.1 The 1<sup>st</sup> technique: SDMSF-BR

This technique consists of pump unit to overcome the pressure losses, solar collector field (PTC-LS-3 type [54]), BHX unit for vapor release and brine-heater (BH) unit for thermal power transfer and MSF-BR with 20 stages. Seawater inlet feed stream would be preheated across the MSF condenser tube banks till reach the inlet point stream to the brine heater.

At the same time, the organic HTO across the PTC would transfer its thermal power to the fluid (water) via BHX unit. The generated steam would raise the preheated seawater brine to the desired top temperature (TBT). The rest of the working fluid (water) would be condensed again to the BHX unit. Figure (3.28) shows a schematic diagram of the process units for the 1<sup>st</sup> technique. Based on previous studies [39], Therminol-Vp1 HTO is selected for PTC. Table 3.24 shows and summarize the design points for this 1<sup>st</sup> technique.

### 3.5.2 The 2<sup>nd</sup> technique (PSDMSF)

This technique consists of pumps for circulation and pressure drops, solar collector field (PTC), BHX unit, turbine expander unit, BH unit, and MSF-BR with 20 stages. Figure (3.29) shows a schematic diagram of the process units for the 2<sup>nd</sup> technique. Table 3.24 shows and summarize the design points for this 2<sup>nd</sup> technique.

Table 3.24: Design points for MSF-BR according to the 1<sup>st</sup> and the 2<sup>nd</sup> techniques.

Design point:	1 <sup>st</sup> technique (SDMSF)	2 <sup>nd</sup> technique (PSDMSF)
$G_b, W/m^2$	252 (winter)	252 (winter)
$T_{amb}, ^\circ C$	25	25
$T_{co}, ^\circ C$	350	350
$\eta_b, \%$	---	85
$\eta_g, \%$	---	95
$\eta_p, \%$	75	75
$T_{sea}, ^\circ C$	20	20
$TBT, ^\circ C$	110	110
$T_b, ^\circ C$	40	40
Feed salinity, ppm	48620	48620
No. of stages	40 (37/3)	40 (37/3)
Product mass flow rate, kg/s	57.7	57.7
Make up splitter ratio	0.482	0.482
Plant life time, year	20	20
Power generation cost, \$/kWh	0.06	0.06

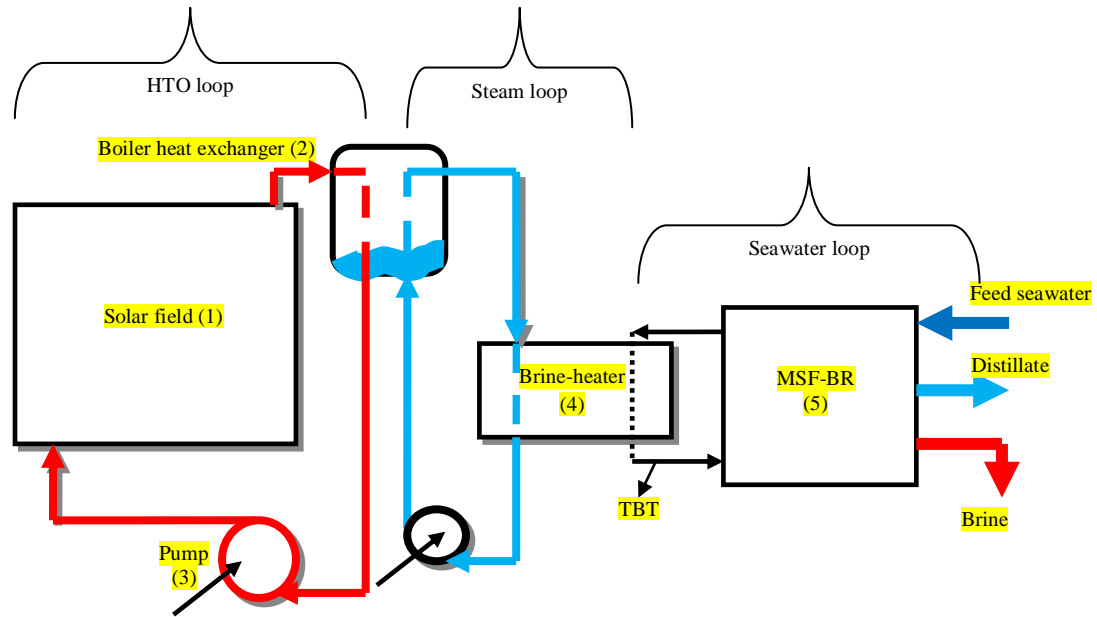


Figure (3.28) A schematic diagram of solar MSF-BR components: (1) Solar field, (2) Boiler heat exchanger, (3) Pump, (4) Brine heater, (5) MSF-BR.

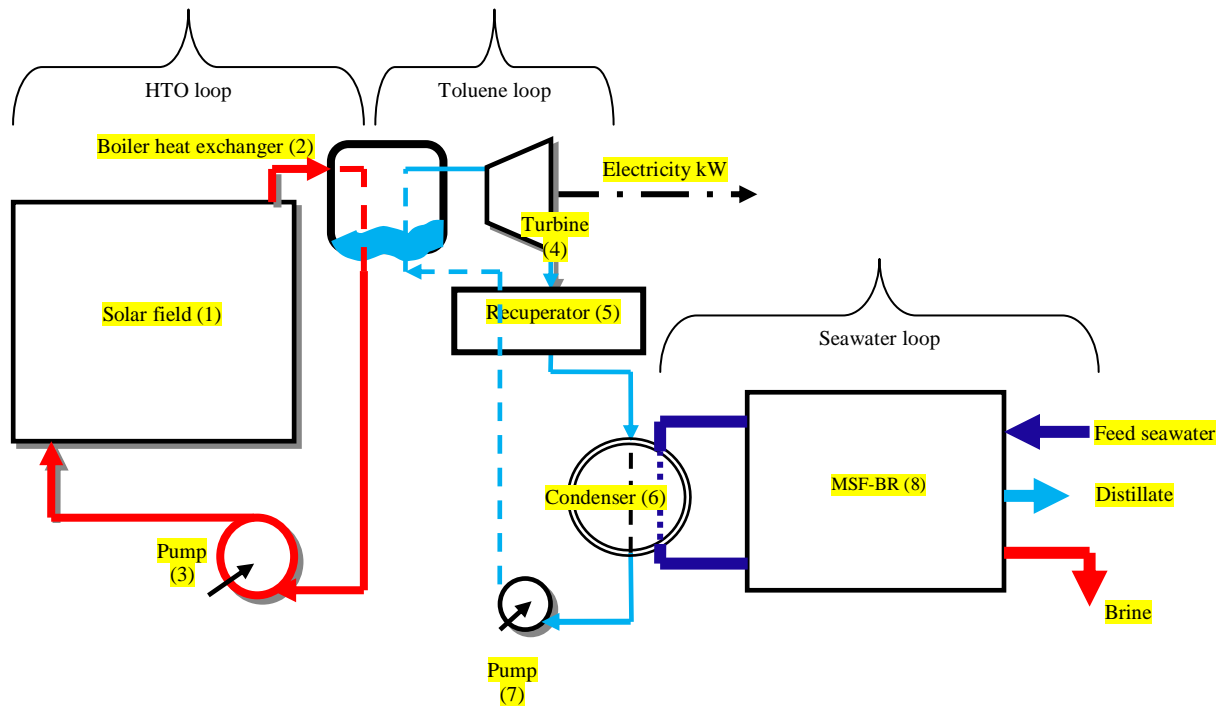


Figure (3.29) A schematic diagram of solar MSF-BR components: (1) Solar field, (2) Boiler heat exchanger, (3) HTO Pump, (4) Turbine, (5) Recuperator, (6) Condenser, (7) Pump (8) MSF-BR.

### 3.5.3 The Techniques Comparison Results

Under the above specifications, and related to the analysis (exergy and thermo-economic) that been performed in the Appendix. Figure (3.30) shows the results obtained for the two proposed techniques (1<sup>st</sup> and 2<sup>nd</sup> techniques). The comparison is performed based on SPC, kWh/m<sup>3</sup>, thermo-economic product cost, \$/GJ, total solar field area  $A_{col}$ , m<sup>2</sup>, and the gain ratio (GR).

The effect of TBT and Nstg is quite clear related to the results obtained. For the SPC, increasing the TBT would decrease the SPC for both techniques. However, the first technique gives significant results considered lower against the second. Also increasing the Nstg would decrease the SPC but the great effect on the SPC is caused by the TBT against the Nstg.

The same effect is caused by the TBT and the Nstg on the cp, \$/GJ. By increasing the TBT and the Nstg, the cp would significantly decrease. However, the first technique would result lower value against the second one. The existence of turbine unit would increase the outlet exergy rate however, it would increase the hourly costs causing an increase in the product cost in \$/GJ.

Increasing the TBT would exceed the solar field area. However, increasing the Nstg would decrease the solar field area. Solar field area is considered a vital parameter to judge the system performance. In most cases, land area could be limited, therefore; lower solar field area is favorable. To achieve minimum solar field area related to the first technique, the TBT should be operated at 90°C and Nstg=40 stages.

Related to the second technique, increasing the TBT would decrease the solar field area. This is quite dominant by the ORC effect. To achieve minimum solar field area related to the second technique, TBT would be maintained at 120°C with the operation of Nstg.

The gain ratio is a very important parameter to judge the system performance. Nstg is the main parameter that would affect on the GR. For both techniques, increasing the Nstg would increase the GR. However; the first technique significantly achieves higher favorable results than the second. This is because the effect of latent heat of vaporization related to water (in the 1<sup>st</sup> technique) and toluene (in the 2<sup>nd</sup> technique).

The values of 120°C and 40 are assigned for the TBT and Nstg respectively. The results related to these new assumptions are illustrated in Table 3.25. Solar collector field area considered very important parameter in this comparison according to its direct effect on both of cost and thermo-economic results. PTC collector is chosen here based on LS-3 system where the module width is 5.67m, length 100m, glass envelope diameter 0.1m, and inlet tube absorber diameter 0.0655m.

For field design especially with large capacities it is recommended to ensure that Reynolds number between  $1 \sim 9 \times 10^4$ . In case of 1<sup>st</sup> technique, the field area is about 61680m<sup>2</sup> with cycle flow rate about 24.45kg/s leading to 110 collectors for 8 loops and Reynolds number about  $9.45 \times 10^4$ . This exhibits a field width with 76m.

The 2<sup>nd</sup> technique gives larger area compared with the 1<sup>st</sup> due higher operating temperatures. Moreover; the existence of turbine unit needs high and sufficient collector temperature. Because of increasing the outlet collector temperature will permit to increase the evaporator temperature too.

The 2<sup>nd</sup> technique consumes about 93050m<sup>2</sup>, with cycle mass flow rate about 43.2kg/s, the field width is about 50m with total 18 loops design, and Reynolds number equal  $9.2 \times 10^4$  with 167 collectors. In case of the 2<sup>nd</sup> technique, larger solar field area will be absolutely available under summer condition and that will cause an excessive thermal power for the organic turbine.

Therefore; nearly about 51% of winter field area would be out of service during summer conditions for maintenance operations. However; in the 1<sup>st</sup> technique, there is no need for this operation because there is no turbine unit in this technique. 1<sup>st</sup> technique has an advantage based on evaporation

pressure through the absorber tube (2.2bar) against the 2<sup>nd</sup> technique (32bar). Because higher values may cause severe stresses on the absorber tube.

The gain ratio for the 1<sup>st</sup> technique is massively greater than the 2<sup>nd</sup> technique (11~12 vs. 1~2). And that because, the 2<sup>nd</sup> technique achieves higher mass flow rate due to higher outlet operating conditions of the collector. Exergy analysis considered not far in values for both techniques with an advantage for the 2<sup>nd</sup> based on overall exergy efficiency and exergy inlet to the cycle. This because, the exergy inlet is directly affected by the solar field and larger solar field area surly goes to the 2<sup>nd</sup> technique. At the same time larger area gives larger exergy destruction and larger exergy income to the system.

Therefore, exergy efficiency is a useful tool to judge the system performance. However, hourly operating & maintenance parameter (\$/h) is noticed larger in the 2<sup>nd</sup> technique instead of the 1<sup>st</sup> due to two reasons; the existence of turbine unit and the effect of solar field area. That was clear and obvious in total plant cost for both techniques (see Table 3.25). Specific total water price considered little bit lower for 1<sup>st</sup> technique instead of the 2<sup>nd</sup> due to the largest solar field area exhibited by the 2<sup>nd</sup> technique.

Also the thermo-economic unit product cost considered the same (ranged between 1~1.1 and \$/GJ) however; there is a little bit advantage to the 2<sup>nd</sup> technique due the cost of power that developed from the turbine work (4MW).

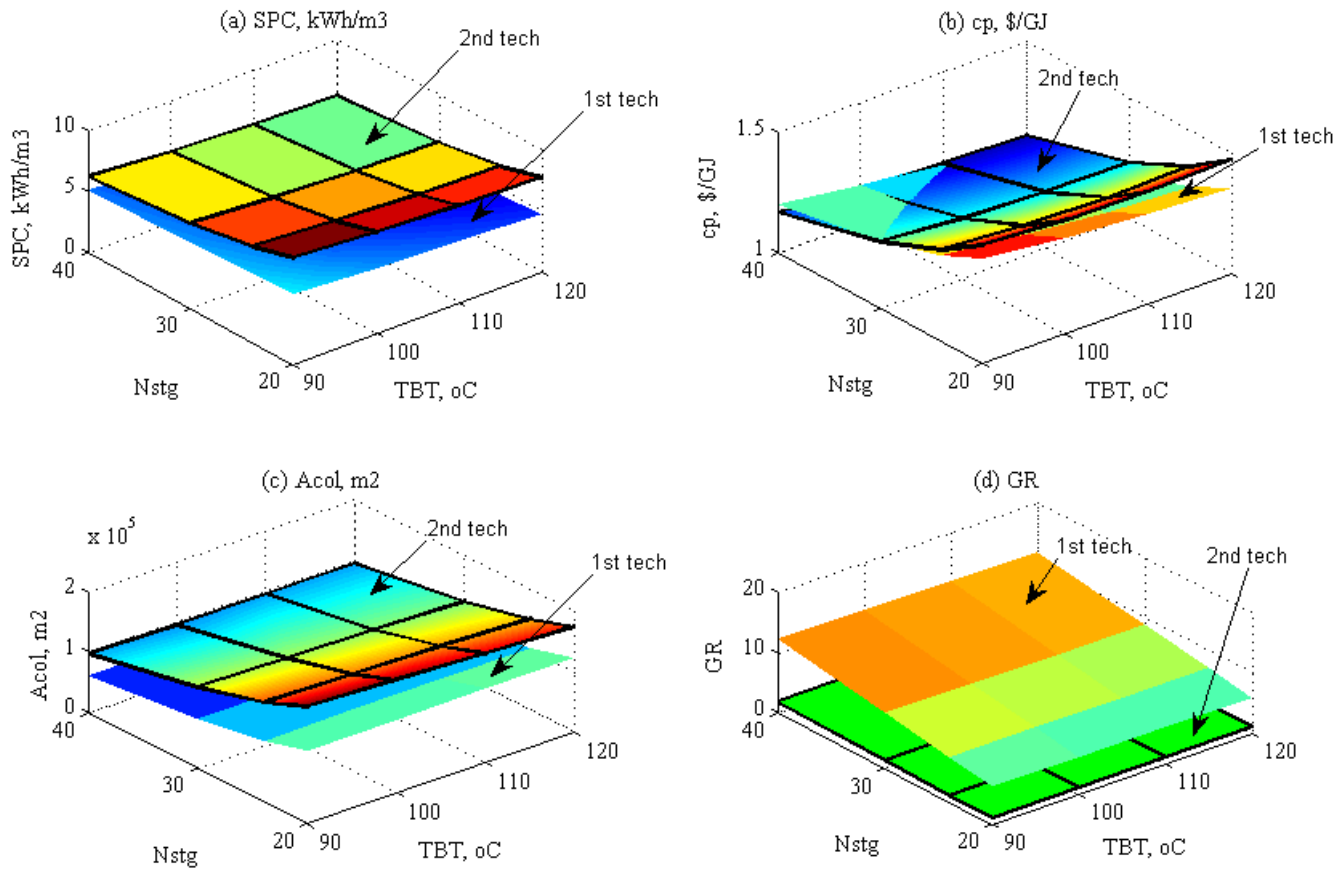


Figure (3.30) Effect of TBT and Nstg on: (a) SPC, kWh/m<sup>3</sup>, (b) cp, \$/GJ, (c) A<sub>col</sub>, m<sup>2</sup>, (d) GR.

Table 3.25: Data results for 1<sup>st</sup> and 2<sup>nd</sup> techniques operated by Water and Toluene fluids.

<b>Parameter:</b>	<b>SDMSF (Water)</b>	<b>PSDMSF (Toluene)</b>
Evaporation pressure, bar	2.25	32.75
Total solar field area, m <sup>2</sup>	61680	93050
Solar field flow rate, kg/s	24.45	43.2
Solar field $R_e$ number	$9.45 \times 10^4$	$9.24 \times 10^4$
No. of collectors (LS-3)/No. of loops	110/8	167/18
Solar field width, m	76	50
Solar collector thermal efficiency, %	69.7	69.7
Boiler HEX area, m <sup>2</sup>	35	91.5
Outlet HTO temperature, °C	145	178
Boiler HEX mass flow rate, kg/s	24.45	43.2
Brine heater effectiveness, %	66.6	30
Brine heater area, m <sup>2</sup>	436	492
Organic cycle mass flow rate, kg/s	4.96	29.46
GR	11.67	1.96
Turbine power, MW	--	4.407
Total exergy destruction, MW	414.28	421
Total exergy efficiency, %	14.67	14.46
Total operating & maintenance cost, \$/h	270	320
Total water price, \$/m <sup>3</sup>	1.436	1.7
Thermo-economic unit product cost, \$/GJ	1.103	1.1
SPC, kWh/m <sup>3</sup>	4.09	5

It is become clear from the related comparison that only desalination without power generation constitutes lower (means favorable) in the following:

- **Solar collector field** area (almost half) meaning by this decreasing maintenance issues and increasing the possibility to control the solar field.
- **Pumping power** requirements leading to less electricity demands and it could be recovered by diesel engine or adding some panels of Photo Voltaic (PV) collectors.
- **Exergy destruction** rate and this is a very important term in the comparison because increasing the rate of irreversibility will cause a significant decrease in total exergy efficiency. Although, turbine unit would increase the exergetic efficiency of the power technique but its destruction rate is also in the scope.
- **Total plant cost** which is noticed lower however; there is not a large deviation. This deviation might be larger while comparing based on larger capacities (up to 5000~10000m<sup>3</sup>/day).

Increasing the power generation from the turbine unit is combined with the increasing of desalinating plant capacity. The example of MSF-BR with a capacity of 30,000m<sup>3</sup>/day would harvest about 6,12604m<sup>2</sup> of solar field area and generating about 45MWe with overall exergy efficiency about 13.5%. This is indicated with larger irreversibility and hard work of control and maintenance issues. Therefore; solar large capacities operation demand more economical considerations putting in minds the existence of energy storage and/or energy backup system.

Figure (3.31) shows the effect of daily productivity on the thermo-economic product cost. It is clear from the figure that the thermo-economic product cost is decreased by the increasing of the plant productivity. The product exergy stream is considered the main cause of this increase. The exergy rate of the product stream is considered a gain to overall system performance. Thence; it would cause a decrease in the overall system product cost. Also, the effect of productivity (m<sup>3</sup>/d) on the rated power is clarified in Figure (3.32). Increasing the productivity would increase the power rate and this may serve to develop the excess power to the public grid.

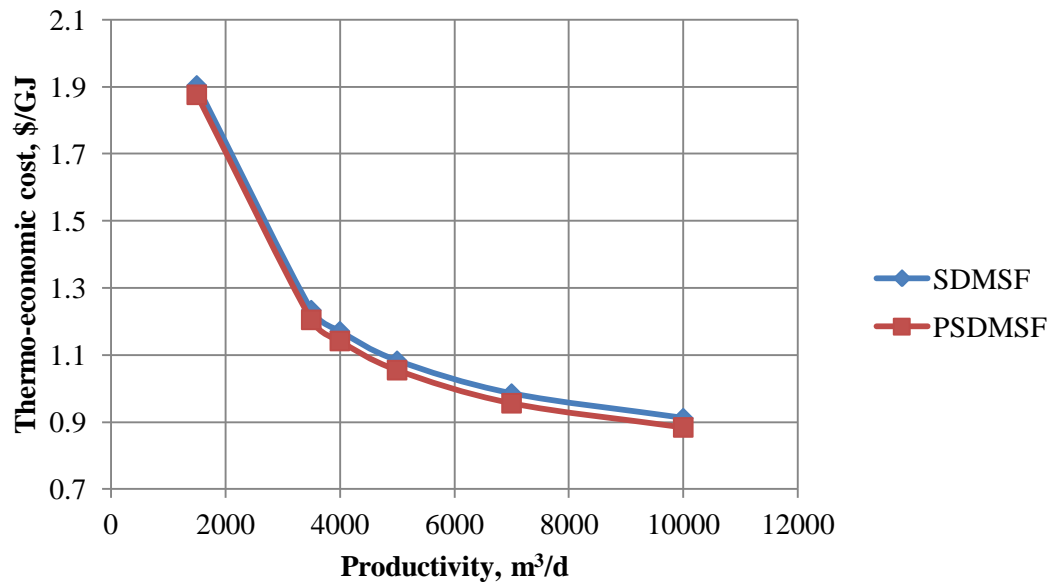


Figure (3.31) The daily productivity effect on the thermo-economic product cost for both techniques (SDMSF & PSDMSF).

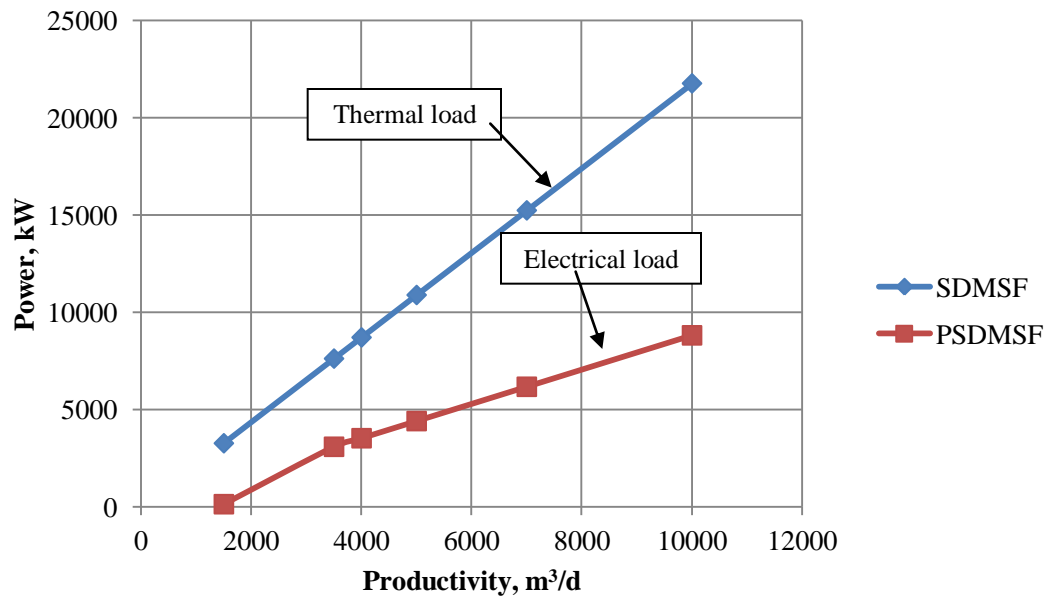


Figure (3.32) The effect of productivity on the developed power for both techniques (SDMSF & PSDMSF).

# Chapter 4: Comparison of Different Types of Solar Desalination Processes: Results & Discussions

## 4.1 Process Configurations

To reduce the negative impacts from the conventional desalination plants, solar energy considered an alternative solution to reduce the negatives from desalination processes to the environment. To combine desalination processes with solar energy, there are many aspects should be taken in consideration such as:

- **The location of operation:** It is very important to allocate solar desalination plants in the Sunbelt area and near the saline water source (sea or well). In this study, solar radiation under winter operating conditions is considered based on the site data of Suez Gulf region- Egypt (latitude: 30° N; longitude: 32.55° E)).
- **The amount of water production:** It is very important to decide the amount of fresh water production (small-medium-large capacities) based on the remote area need.
- **The size area of the site:** Size area of the site considered a vital parameter to decide the type of solar desalination plant.
- **The type of the technology:** There are many techniques of combining the solar energy and desalination processes such as direct vapor generation, indirect vapor generation, and combination with organic Rankine cycle.
- **The production cost:** It is very important to decide the price of the fresh water production based on the region of the sink (local and/or tourism sectors).

In this part, two case studies are performed to compare and elect the most reliable solar desalination technique. The study is performed based on two different methods. The first method is to compare the techniques based on individual operating conditions for each technique. And the second method is to compare based on uniform operating conditions for all techniques. The aim of this work may be concluded into these points:

- Solar desalination processes are compared based on uniform and different operating conditions putting in consideration the design limits of each process.
- Electing the most reliable technique based on the aspects that mentioned above (productivity, solar field area, total water price, and location of operation).
- The terms of comparison are solar field area  $\text{m}^2$ , productivity  $\text{m}^3/\text{day}$ , specific power consumption  $\text{kWh}/\text{m}^3$ , total exergy destruction rate MW, thermo-economic product cost  $\$/\text{GJ}$ , specific solar field area  $\text{m}^2/(\text{m}^3/\text{day})$ , and hourly costs  $\$/\text{h}$ .

The techniques of combining solar power (organic) cycles with desalination processes are wide and vary. In this work, two different techniques of combining solar power cycle with desalination technologies are utilized.

The first is via mechanical power developed by solar organic Rankine cycle (SORC) and the second is by thermal power transferred via boiler heat exchanger (BHX) unit between the solar field and the desalination process. The first method usually performed for RO and MED-MVC technologies. The second method is performed for thermal types of desalination processes such as MED, MED-TVC, and MSF.



#### 4.1.1 Solar organic Rankine cycle for RO and MED-MVC processes

Solar organic Rankine cycle (SORC) often contains: Solar parabolic trough collector (PTC), boiler heat exchanger unit (BHX), circulation pump, turbine, generator, recuperator, and condenser/pre-heater unit. In this technique, solar organic Rankine cycle (SORC) is utilized to develop the sufficient power to operate the high pressure pump (HPP) in the RO and the vapor compressor in the MED-MVC. Heat transfer oil (HTO) is used through the solar PTC field [54] to transfer the collected thermal power via BHX unit to any process heat. Thence, HTO would transfer the thermal power to the organic oil (Toluene) passes through the Rankine cycle. The generated power from the organic turbine would power on the high pressure pump for the RO process and/or the mechanical vapor compressor for the MED-MVC process. Also the pre-heated seawater from the Rankine cycle condenser unit goes directly to the RO process and/or the first effect of the MED-MVC process. RO with pressure exchanger unit configuration (RO-PEX) and MED parallel feed configuration (MED-PF) are confirmed in this study. Figure (4.1) shows schematic a diagram of the SORC powered on the RO-PEX and MED-MVC processes.

#### 4.1.2 Solar thermal organic cycle for MED, MED-TVC and MSF-BR processes

In this technique, solar thermal power from the solar field is directly transferred to the BHX unit. Thence, the thermal power would be transferred to the steam cycle to power on the thermal desalination process. Such cycles often contain solar PTC collector with HTO which is directly fed towards the BHX unit for thermal power transmission, and pump unit for circulation and to overcome pressure losses, and the desalination process for fresh water production. Such configurations needn't any turbine however it would consume larger thermal power compared against the previous technique. Moreover, it also consumes electricity for distillate, brine, seawater pumps and other facilities. Brine heater unit is added in case of multi stage flash brine recycle configuration (MSF-BR). Multi effect distillation with parallel feed configuration is considered for MED and MED-TVC. Figure (4.2) shows a schematic diagram of the solar thermal power cycle assisted MED-PF, MED-TVC, and MSF-BR desalination processes.

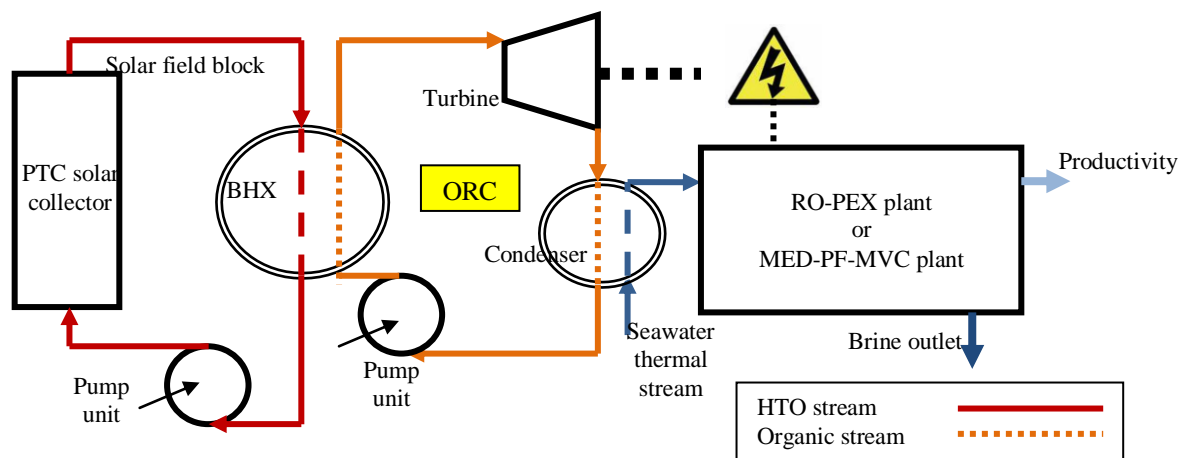


Figure (4.1) A schematic diagram of SORC assisted RO-PEX and MED-PF-MVC desalination processes.

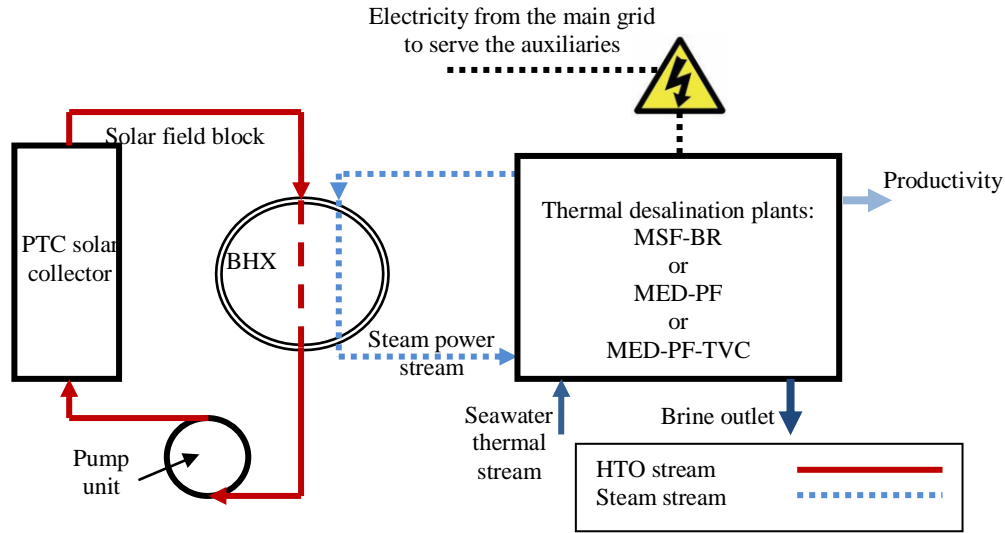


Figure (4.2) A schematic diagram of solar thermal power cycle assisted thermal desalination processes (MSF-BR, MED-PF, MED-PF-TVC).

## 4.2 Comparison Methodology

Desalination processes are different types, different configurations and different techniques. Moreover, each type has its own operating conditions (productivity, salinity range, temperature, etc). Therefore, in this section the comparisons are performed based on two main methods. The first is performed based on individual operating condition for each type, and the second is performed based on uniform operating conditions to give a clear judge about the most reliable technique.

### 4.2.1 Individual operating conditions

In this subsection, the proposed configurations are compared based on different operating conditions (salinities, productivities, etc) and different design limits (number of stages or effects, temperature drop, etc). For solar assisted RO (S-RO), it is required to desalinate and produce a total capacity of 3500m<sup>3</sup>/day (Sharm El-Shiekh desalination plant [36]). The number of pressure vessels is 42 and the element number is about 7 elements per each vessel. The element area is about 35.3m<sup>2</sup> and the feed seawater salinity is 45,000ppm. Solar assisted MED-MVC (S-MED-MVC) is performed based on a capacity of 1500m<sup>3</sup>/day [71]. Parallel feed configuration is maintained for the use in MED process. The number of effects isn't exceeded above two effects and the compression ratio of the compressor is in the range of 1.35. For solar MED (S-MED), solar thermal power plant is utilized to target a capacity of 4545m<sup>3</sup>/day [51]. The heating steam temperature is in the range of 70-73°C and the blow down brine salinity is about 69,000ppm. The number of effects is maintained at four effects. For solar assisted MED-TVC (S-MED-TVC), a capacity of 4545m<sup>3</sup>/day is targeted [72]. The top steam temperature (TST) is in the range of 60°C for only four effects. The motive steam pressure is about 2500kPa and the ejector compression ratio is about 2.165. A productivity of 32728m<sup>3</sup>/day is produced by solar thermal power assisted MSF-BR type (S-MSF-BR) [43]. The top brine temperature (TBT) isn't exceeded above 106°C and the total number of stages is about 24 stages. Tables 4.1-4.6 illustrate the specifications of all introduced techniques according to different operating conditions.

Table 4.1: Specifications and design input data based on S-RO-PEX (1<sup>st</sup> method).

<b>Parameter:</b>	<b>S-RO-PEX</b>
Solar collector type/working fluid	PTC-LS-3 [54]/Therminol-VP1 [62]
Developed power type/working fluid	ORC/Toluene [47]
Solar radiation, W/m <sup>2</sup>	252 (winter)
Ambient temperature, °C	30
Top solar collector temperature, °C	350
Inlet turbine condition/Condensation condition, °C	300/35
Seawater temperature, °C/Seawater salinity, ppm	20/45,000
Turbine, Generator, Pumps efficiency, %	85%, 95%, 75%
Recuperator effectiveness, %	80
Productivity, m <sup>3</sup> /day	3500
Recovery ratio, %	30
PEX, HPP, BP efficiencies, %	96%, 80%, 80%
Number of elements/Number of pressure vessels	7/42
Area of the element, m <sup>2</sup>	35.3
Fouling factor	0.85
Load factor	0.9
Membrane life time/Plant life time, year	5/20

Table 4.2: Specifications and design input data based on S-MED-MVC (1<sup>st</sup> method).

<b>Parameter:</b>	<b>S-MED-MVC</b>
Solar collector type/working fluid	PTC-LS-3 [54]/Therminol-VP1 [62]
Developed power type/working fluid	ORC/Toluene [47]
Solar radiation, W/m <sup>2</sup>	252 (winter)
Ambient temperature, °C	30
Top solar collector temperature, °C	350
Inlet turbine condition/Condensation condition, °C	300/35
Seawater temperature, °C	21
Seawater salinity/Brine blow-down salinity, ppm	42,000/70,000
Turbine, Generator, Pumps efficiency, %	85%, 95%, 75%
Recuperator effectiveness, %	80
Productivity, m <sup>3</sup> /day	1500
Top vapor temperature, °C	65
Compression ratio	1.35
Compressor efficiency, %	75
Adiabatic index	1.32
Number of MED effects, #	2
Effects temperature drop, °C	5
Feed, brine, distillate pumps efficiencies, %	75%, 75%, 75%
Load factor	0.9
Plant life time, year	20

Table 4.3: Specifications and design input data based on S-MED (1<sup>st</sup> method).

<b>Parameter:</b>	<b>S-MED</b>
Solar collector type/working fluid	PTC-LS-3 [54]/Therminol-VP1 [62]
Developed power type/working fluid	Indirect vapor generation/steam
Solar radiation, W/m <sup>2</sup>	252 (winter)
Ambient temperature, °C	30
Top solar collector temperature, °C	350
Top steam temperature, °C	73
Brine blow down temperature, °C	36
Seawater temperature, °C	28
Seawater salinity/Brine blow-down salinity, ppm	46,000/69,000
Pump efficiency, %	75
Productivity, m <sup>3</sup> /day	4545
Number of MED effects, #	4 parallel feed configuration
Effects temperature drop, °C	9.3
End condenser effectiveness, %	59
Feed, brine, distillate pumps efficiencies, %	75%, 75%, 75%
Load factor	0.9
Plant life time, year	20

Table 4.4: Specifications and design input data based on S-MED-TVC (1<sup>st</sup> method).

<b>Parameter:</b>	<b>S-MED-TVC</b>
Solar collector type/working fluid	PTC-LS-3 [54]/Therminol-VP1 [62]
Developed power type/working fluid	Indirect vapor generation/steam
Solar radiation, W/m <sup>2</sup>	252 (winter)
Ambient temperature, °C	30
Top solar collector temperature, °C	350
Top steam temperature, °C	62
Brine blow down temperature, °C	46.8
Seawater temperature, °C	30
Seawater salinity/Brine blow-down salinity, ppm	46,000/69,000
Steam ejector compression ratio, CR	2.165
Motive steam pressure, kPa	2500
Expansion ratio, ER	250
Pump efficiency, %	75
Productivity, m <sup>3</sup> /day	4545
Number of MED effects, #	4 parallel feed configuration
Effects temperature drop, °C	4
End condenser effectiveness, %	66
Feed, brine, distillate pumps efficiencies, %	75%, 75%, 75%
Load factor	0.9
Plant life time, year	20

Table 4.5: Specifications and design input data based on S-MSF-BR (1<sup>st</sup> method).

<b>Parameter:</b>	<b>S-MSF-BR</b>
Solar collector type/working fluid	PTC-LS-3 [54]/Therminol-VP1 [62]
Developed power type/working fluid	Indirect vapor generation/steam
Solar radiation, W/m <sup>2</sup>	252 (winter)
Ambient temperature, °C	30
Top solar collector temperature, °C	350
Top steam temperature, °C	116
Top brine temperature, °C	106
Brine blow down temperature, °C	40.2
Seawater temperature, °C	25
Seawater salinity/Brine blow-down salinity, ppm	42,000/70,000
Cooling water splitter ratio	0.5082
Chamber load, kg/s.m	180
Vapor velocity, m/s	12
Pump efficiency, %	75
Productivity, m <sup>3</sup> /day	32728
Number of MSF-BR stages, #	24 (21/3)
Stages temperature drop, °C	2.8
Feed, brine, distillate pumps efficiencies, %	75%, 75%, 75%
Load factor	0.9
Plant life time, year	20

#### 4.2.2 Uniform operating conditions

In this method, all the operating conditions are uniformly confirmed. Productivity, salinity, solar radiation, and efficiencies are maintained at the same values. This method is very important because it gives a clear decision about the most effective technique. However, sometimes it becomes non realistic because it takes the designer to assign non real data for some techniques. Table 4.6 demonstrates the specifying parameters for the proposed types of solar desalination processes.

Table 4.6: Specifications of solar assisted thermal and mechanical desalination processes (2<sup>nd</sup> method).

<b>Parameter:</b>	<b>Solar-RO, MVC, MED, TVC, MSF</b>
Solar collector type/working fluid	PTC-LS-3 [54]/Therminol-VP1 [62]
Developed power type/working fluid	ORC/Toluene [47]
Solar radiation, W/m <sup>2</sup>	252 (winter)
Ambient temperature, °C	30
Capacity, m <sup>3</sup> /day	5000
Top solar collector temperature, °C	350
Top steam temperature, °C	60
Inlet turbine condition/Condensation condition, °C	300/35
Seawater temperature, °C/Seawater salinity, ppm	25/45,000
Brine blow-down temperature, °C/Blow-down salinity, ppm	40/65500
Power cost, \$/kJ	1.6×10 <sup>-5</sup>
Condenser's efficiency, %	80
Pumps efficiency, %	75
Turbine, generator efficiencies, %	85, 95
Plant life time, year	20
Load factor	0.9
Fouling factor	0.85
Interest rate, %	5

## 4.3 Results and Discussions

Results are run out from SDS software package [39] based on the earlier two methods related to some indicators putting in mind the design limits and the feasibility of the systems. The indicators are listed as:

- Solar field area ( $A_{col}$ ),  $m^2$  and Specific solar field area (SSA),  $m^2/(m^3/day)$ .
- Specific power consumption (SPC),  $kWh/m^3$ .
- Thermo-economic product cost ( $c_p$ ),  $$/GJ$ .
- Total exergy destruction rate ( $I_{total}$ ), MW.
- Total water price (TWP),  $$/m^3$ .
- Gain ratio ( $GR = M_{distillate}/M_{steam}$ ).
- Area of desalination unit,  $m^2$ .
- Operating hours cost,  $$/h$ .

### 4.3.1 Results of the 1<sup>st</sup> method

The main criteria of this method that the investor/sponsor would be able to judge and elect the process based on the above indicators regardless different specifications or design limits. The investor that would like to construct or design a solar assisted desalination plant would judge the process based on the above indicators regardless the differences in the specifications. Suppose that the investor wants to elect the technology regardless the specifications. As shown from Table 4.7 that S-RO exhibits lower solar field area meaning by this it is highly recommended to be operated in small remote areas (tourist sector). Also it achieves lower results related to TWP,  $I_{total}$ , SPC, operation costs and SSA. However, the thermo-economic product cost is in the range of 65~72\$/GJ and this is recorded highly comparing against the remaining processes. Also it is noticed that the desalination processes that operated by SORC (S-RO, S-MED-MVC) normally give high thermo-economic product cost comparing with the thermal ones such as S-MSF-BR, TVC, and MED. That's because the existence of organic turbine which cause an increase in the thermo-economic product cost due to its operating cost and the cost of power produced. It is clear now that the investor would elect the S-RO technique however there are many limitations should be pinpointed:

- Use of Toluene is risky because it is flammable and toxic and has a negative impact on the environment.
- Noise from the ORC operation related to the turbine existence.
- Hazards.
- Limited capacity within the range of 100-5000  $m^3/day$ .

Therefore; Photovoltaic powered desalination may be useful on order to eliminate such tackles. However; photovoltaic has its limitations regarding to the thermal operation of desalination systems. For larger capacities, MED and MSF are dominant and reliable however; the irreversibility would become massive and the solar field area becomes larger than S-RO case. As it shown from Table 5.7 that S-MSF-BR consumes the largest area with a SSA about 20  $m^2/(m^3/day)$ . Also the operating hours cost reached about 1900\$/h against 90\$/h in the S-RO operation. But the TWP for S-MSF-BR still in the acceptance range depending on the type of consumption sector. For thermal desalination types (only MED, MED-TVC, MSF-BR), MSF and MED-TVC are attractive according to the lower values of GR, TWP, and thermo-economic product cost. MED is less in construction (area of desalination sector is about 6420  $m^2$ ) however; it would take the investor to sell the fresh production in the range of 2.8-3  $$/m^3$ . Therefore, it depends on investor or the designer to elect the best technique according to the sector of

consumption. Also, it is clear that S-MSF-BR and S-MED-TVC would be operated for industrial or local sectors. S-RO would be constructed for tourist sector. Generally S-RO and S-MED-TVC gives attractive results regardless the target of operation or the type of consumption sink.

Table 4.7: Data results for all solar desalination processes based on different operating conditions method.

Parameters	SRO	SMED-MVC	SMED	SMED-TVC	SMSF-BR	Election
<i>Prod m<sup>3</sup>/day</i>	3500	1500	4545	4545	32728	SMSF-BR
<i>Accl m<sup>2</sup></i>	7359	12450	186113	123666	638011	SRO
<i>SPC kWh/m<sup>3</sup></i>	2.8	11	7.23	3	7.847	SRO
<i>cp \$/GJ</i>	72	2.186	1.712	1.09	1.07	SMSF-BR
<i>I<sub>total</sub> MW</i>	2.8	35.5	178.6	163	2018	SRO
<i>TWP \$/m<sup>3</sup></i>	0.616	2.968	2.854	1.944	1.548	SRO
<i>GR</i>	19.11	1.92	3.7	6.11	7.14	SRO
<i>SSA m<sup>2</sup>/(m<sup>3</sup>/d)</i>	2.113	8.3	41	27.2	19.5	SRO
<i>No of units</i>	nv=42 ne=7	Neff=2	Neff=4	Neff=4	Nstg=24	NAN
<i>dT drop oC</i>	nan	5	9.3	4	2.8	SMSF-BR
<i>Area des unit m<sup>2</sup></i>	10437	3378	6420	14238	81153	SRO
<i>Operating cost \$/h</i>	90	167	486	331	1900	SRO

#### 4.3.2 Results of the 2<sup>nd</sup> method

It is clear from the previous method that the comparison couldn't give a clear or a final decision to elect the most reliable technique because there are a different design limits and productivity range. In this method, all operating conditions (temperature drop, salinity, feed temperature...) are uniformed to give a clear decision about the most reliable process regardless the sector of operation. The investor has to inspect the following scenarios:

- Productivity (5000m<sup>3</sup>/day):** Suppose that the investor is concerned about the productivity regardless the other indicators or terms.
- Same solar field area:** The investor has a limited area of operation.
- Same TWP \$/m<sup>3</sup> (0.5<TWP<1):** The investor care about the price of the production regardless any other terms such as area or productivity.

In this scenario (Table 4.8), the RO productivity (5000m<sup>3</sup>/day) is assigned for all techniques. To ensure a uniform case especially for thermal desalination techniques, the temperature drop between effects or stages remains constant and has a range of 3.4°C to 3.45°C. It is found that S-RO gives the lower solar area followed by S-MED-MVC. That's explained by the operation of SORC which causes a significant decrease in the solar field regardless the other aspects. However, the operation of S-MED-MVC would consume much power based on the vapor compressor. Among all thermal processes, S-RO gives enviable results based on total exergy destruction, SSA, TWP, and operating hour costs. Solar field considered a key factor of increasing or decreasing the TWP, *I<sub>total</sub>*, and operating costs. Less solar field area means, lower results in these parameter specially the *I<sub>total</sub>*. For thermal processes, S-MED-TVC significantly attractive and gives first-rate results based on SSA, TWP, *I<sub>total</sub>*, and achieves higher GR. It is obvious from Table 4.8 that at the same productivity S-RO comes as first order. Moreover, the operation of SORC might be reducing the solar field area. Generally, S-MED-TVC is elected next after the S-RO technique and elected first while comparing against the thermal desalination processes. Table

4.9 shows the data results obtained due to the limited solar field scenario. In this scenario, solar field of  $10,754\text{m}^2$  is assigned for the comparison. This specified value ( $10,754\text{m}^2$ ) is resulted by the operation of S-RO technique at productivity of  $5000\text{m}^3/\text{day}$ . For the same specified solar field area by the investor, S-RO would produce  $5000\text{m}^3/\text{day}$  however; the remaining techniques would produce less moreover; the TWP would be greater than the S-RO case. S-MED-MVC comes next after S-RO based on the production ( $1334\text{m}^3/\text{day}$ ) however; the SPC considered the uppermost between all processes related to the vapor compressor operation. But it achieves attractive results according to SSA, TWP, operating costs, and thermo-economic product cost. S-MSF-BR gives the highest TWP ( $6.48\$/\text{m}^3$ ) among the remaining techniques. Also, it gives the highest value of total exergy destruction rate ( $I_{total}=46\text{MW}$ ). However, it considered the less in desalination area condenser meaning by this less of complication. According to the solar field scenario, S-RO and S-MED-MVC might be achieving attractive and significant results. The remaining techniques might be favorable for larger capacities.

Table 4.8: Data results for solar desalination processes based on the same productivity.

Parameters	SRO	SMED-MVC	SMED	SMED-TVC	SMSF-BR	Election
Acol m2	10754	40252	132367	102374	115732	SRO
SPC kWh/m3	2.844	10.72	2.64	2.06	5.4	SMED-TVC
cp \$/GJ	66	1.312	1.088	0.9147	1.35	SMED-TVC
Itotal MW	4.137	168.42	191	183	496	SRO
TWP \$/m3	0.5728	1.714	1.887	1.55	2.006	SRO
GR	18.78	5.68	5.82	8.166	6.26	SRO
SSA m2/(m3/d)	2.151	8.05	26.47	20.47	23.15	SRO
No of units	nv=50 ne=8	Neff=6	Neff=6	Neff=6	Nstg=21	NAN
dT drop oC	nan	3.45	3.45	3.45	3.4	NAN
Area des unit m2	14120	22393	21801	18795	10105	SMSF-BR
Operating cost \$/h	120	321	354	290	376	SRO

Table 4.9: Data results for solar desalination processes based on same solar field area.

Parameters	SRO	SMED-MVC	SMED	SMED-TVC	SMSF-BR	Election
Md m3/day	5000	1334	405.2	522.3	461.5	SRO
SPC kWh/m3	2.844	10.67	2.134	1.57	4.71	SMED-TVC
cp \$/GJ	66	1.436	4.264	3.312	4.788	SMED-MVC
Itotal MW	4.137	45	15.5	19.11	46	SRO
TWP \$/m3	0.5728	1.889	6.377	4.933	6.486	SRO
GR	18.78	5.68	5.82	8.166	6.26	SRO
SSA m2/(m3/d)	2.151	8.06	26.6	20.6	23.31	SRO
No of units	nv=50 ne=8	Neff=6	Neff=6	Neff=6	Nstg=21	NAN
dT drop oC	nan	3.45	3.45	3.45	3.4	NAN
Area des unit m2	14120	5975	1766	1963	935	SMSF-BR
Operating cost \$/h	120	94.5	97	96.6	118	SMSF-BR



Table 4.10 illustrates the data results for all process techniques based on the same TWP (0.5-1\$/m<sup>3</sup>). For such operation, it is quite difficult to uniform all processes under the same TWP because each technique has its design limits that control the operating costs. In this scenario, the investor should be concerned about the total water prices of production regardless any other aspects. The TWP is a very important term because it concludes the costs of all process units. It is clear from Table 4.10 that S-RO gives the minimum values of solar field area and operating costs.

However, thermal desalinating technologies are quite attractive based on the remaining parameters such as productivity, and thermo-economic product cost. This scenario demands special designs for thermal processes as noticed in number of effects and stages. Moreover, it becomes very complicated referring to the increase in desalination area condenser. Surely it would give a massive production with lower TWP however; it costs time and materials. Therefore; S-RO still dominant based on solar field area and operating costs regardless the productivity.

Table 4.10: Data results for solar desalination processes based on the same TWP.

Parameters	SRO	SMED-MVC	SMED	SMED-TVC	SMSF-BR	Election
<i>Md m3/day</i>	5000	5000	25000	25000	45000	<b>SMSF-BR</b>
<i>SPC kWh/m3</i>	2.844	5.386	1.488	2.8	5.47	<b>SMED</b>
<i>cp \$/GJ</i>	66	0.7	0.489	0.64	0.81	<b>SMED</b>
<i>Itotal MW</i>	4.137	164	850	885	4321	<b>SRO</b>
<i>Acol m2</i>	10754	20300	221513	378842	429390	<b>SRO</b>
<i>GR</i>	18.78	14.8	17.34	10.84	14.8	<b>SRO</b>
<i>SSA m2/(m3/d)</i>	2.151	4.06	8.861	15.15	9.54	<b>SRO</b>
<i>No of units</i>	nv=50 ne=8	Neff=16	Neff=18	Neff=8	Nstg=50	<b>NAN</b>
<i>dT drop oC</i>	nan	1.3	1.15	2.59	1.4	<b>SMED-MVC</b>
<i>Area des unit m2</i>	14120	114095	744817	125704	284323	<b>SRO</b>
<i>Operating cost \$/h</i>	120	161	650	965	1584	<b>SRO</b>
<i>TWP \$/m3</i>	0.57	0.86	0.69	1	0.9	<b>SRO</b>

Based on the analysis performed in this chapter, the following pinpoints can be drawn:

- The results of the individual method reveal that S-RO is quite attractive according to lower TWP, lower SSA, lower SPC, and lower exergy destruction rate.
- The uniform method is performed according to three different scenarios such as the same productivity, the same solar field area, and the same TWP.
- For all scenarios S-RO gives attractive results compared against the other techniques. Also it is noticed that SORC could reduce the solar field area.
- S-MED-TVC gives attractive results while comparing with thermal desalination processes.
- The second technique has an advantage concluded in developing power but depending on the amount of distillate product and the outlet collector/boiler operating conditions.
- Generally, S-RO and S-MED-TVC are attractive mainly related to the solar field area and TWP. However, the remaining processes could produce a massive fresh water quantity regardless the SPC or the solar field area.
- Solar thermal power is considered site and load specific. It is very important to decide the location of operation and the load. Also, it is very important to enhance and optimize the desalination system first before coupling with solar section.

#### 4.3.3 CSP Vs PV Assisted RO: Case Study

In this part, it becomes very important to compare between CSP and PV for the assistance of RO membrane desalination. As mentioned earlier, CSP powered ORC for the operation of RO-PEX gives attractive results against the remaining thermal operations. Seawater desalination system that combines with reverse osmosis (RO) powered by photovoltaic (PV) against CSP-RO to deliver 100 m<sup>3</sup>/day of sweet water is investigated. Silicon cells are chosen for the PV array and the polyamide thin-film composite seawater Film-tech membranes are selected for the RO system. The software SDS is adopted to study the influences of the feed pressure on the performance of the system. Technical description of the proposed system is presented in Table 4.11.

Table 4.11: Specifications and input data for PV-RO and CSP-RO systems (100m<sup>3</sup>/day).

RO system	
Productivity, m <sup>3</sup> /day	100
Feed salinity, ppm	43500
Element area, m <sup>2</sup>	30
Fouling factor	0.85
Recovery ratio, %	20
High pressure pump efficiency, %	75
Pressure vessels/elements	3/7
PV system [73]	
Number of cells in series	8
Area of the cells, m <sup>2</sup>	0.427
Maximum power rating, W	44.06
Rated voltage, V	16.5
Rated current, A	2.67
CSP-ORC system	
Top ORC temperature, °C	300
Bottom ORC temperature, °C	35
ORC turbine efficiency, %	85
Solar field type/working fluid	PTC-LS3/Therminol-VP1 HTO
Solar radiation, W/m <sup>2</sup>	650

For solar PV powered RO, the system contains the following:

- PV panels for power generation.
- Inverter unit for the conversion of DC to AC.
- Batteries.
- RO section (intake pretreatment unit, filter, motor, high pressure pump, RO membranes, and accumulation tank).

For solar ORC powered RO, the system contains the following:

- PTC field (LS-3 type) with Threminol-VP1 heat transfer oil.
- Organic circulations pump with 75% efficiency.
- BHX unit with thermal effectiveness about 80%.
- Organic turbine (85% efficiency) with toluene organic fluid.
- Recuperator unit for heat regeneration and condenser unit for heat rejection with effectiveness about 80%.

Figure (4.3) shows a schematic diagram of the PV-RO system. Figure (4.1) is introduced earlier for solar ORC-RO system (CSP-RO). Results of the considered systems are illustrated in Table 4.12.

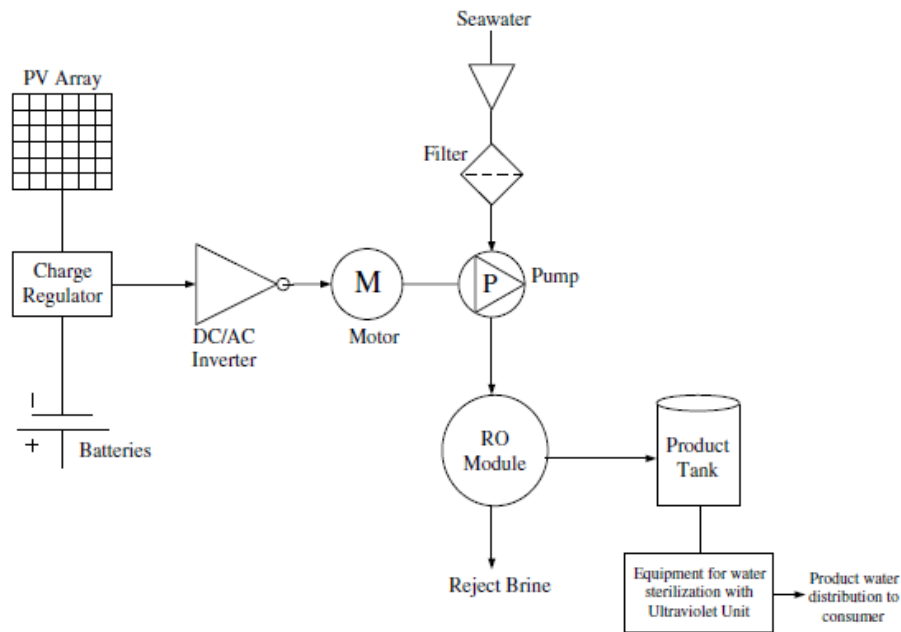


Figure (4.3) A schematic diagram of solar PV powered RO system for 100m<sup>3</sup>/day [73].

It is obvious from Table 4.12 that CSP-RO system gives attractive results according to the design and cost analysis. From the side of solar field area, CSP-RO achieved about 241m<sup>2</sup> against 430~440m<sup>2</sup> for the PV-RO system. Less area means less in controlling and maintenance issues. High solar area for PV system is referring to lower efficiency of the PV modules (10%) compared with thermal one (73%). However; the simplicity to assemble PV-RO system is remarkable against the CSP field. The total water price (TWP, \$/m<sup>3</sup>) is an effective term to judge the system applicability. It is clear that TWP of the PV-RO system is a double value of the CSP-RO system. That's because the high price of the PV panels. Reducing the capital costs of the PV panels may reduce the TWP.

Thence it can compete with the thermal technologies. The possible way to reduce the TWP is to increase the rate of technology construction by constructing many of PV-RO systems with higher productivities for larger remote areas. It may be noted that PV powered RO system is suitable for areas that have no access to water network and the local electric grid. A major advantage of the proposed system is that it allows the membrane operation at constant pressure although batteries increase maintenance requirements and also can cause environmental problems. The disadvantage of the system is the sensitivity of the membranes to fouling by precipitation of sparingly soluble salts and to damage by oxidized compounds in the feed water.

Table 4.12: Data results for both systems (CSP Vs PV) combined with RO desalination unit.

Parameter	CSP-RO	PV-RO [73]
Operating pressure, bar	46.16	47
Product salinity, ppm	530	500
Power, kW	35	35.4
SPC, kWh/m <sup>3</sup>	8.3	8.8
Solar field area, m <sup>2</sup>	241	410
Solar collector efficiency, %	73	9.9~10
TWP, \$/m <sup>3</sup>	4.32	8.5

# Chapter 5: Conclusion, Recommendations and Future Work

## 5.1 Conclusion

The SDS software program is developed for design and simulation of different types and configurations of conventional and solar desalination processes. The desalination plant components such as heat exchangers, flash chambers, evaporators, pumps, steam ejectors, compressors, reverse osmosis membranes, pipes, etc., are modeled and stored as blocks in SimuLink visual library. The library enables the user to construct different desalination techniques and configurations by clicking the mouse over the required units (blocks). The interface aids plant designers, operators and other users to perform different calculations such as energy, exergy, and thermo-economics. In addition, the package enables the designers to perform different modifications of an existing plant or to develop the conceptual design of new configurations. Some operating desalination plants are simulated by the present package to show its reliability and flexibility. The developed SDS package has some features concluded in:

- Easy model construction.
- Easy to convert the designed code to be self executable and work under different computer languages (Visual basic, Visual C, Visual C++, and Visual Fortran).
- The model allows users easily change to the plant variables and different operating conditions with ultimate stream allowance.

Related to the developed SDS package, different analyses for different solar desalination processes are performed based on solar radiation data for Suez Gulf region- Egypt (latitude: 30° N; longitude: 32.55° E)). For RO desalination plant, a case study is presented by operating Sharm El-Shiekh reverse osmosis desalination plant (capacity of 145.8m<sup>3</sup>/h) with solar organic Rankine cycle. The analyses are performed according to different types of operating conditions (saturation and superheat). The investigations are performed based on energy, exergy, and cost analyses. The results of Butane, Hexane, and Toluene are compared with the conventional working fluid (Water). Based on the analysis performed in this work, the following conclusions can be drawn:

- Water and Toluene are suitable for both operations. However, Water needs expansion wet turbine for dryness fraction ranged between 0.7 and 0.95 for both operations. Moreover, the evaporation high pressure (85.9 bar) considered not safe for the collector design requirements. Solar dish may be used for such type of operation however; it isn't considered in this work. Between all units, solar collector field exhibits the largest effect on the cycle specific cost, minimum exergy destruction, and overall exergy efficiency.
- Recuperator configuration with higher values of recuperator effectiveness ( $\epsilon_{rec}=0.8$ ) gives a superior results based on total solar field area, Rankine efficiency, exergy destruction, and specific total cost. Basic configuration comes next and followed by OFH+REC configuration. Therefore, recuperator unit has a massive effect on the cycle performance and it is recommended to be added in the cycle for both operations (saturation and superheat).
- Different configurations of reverse osmosis energy recovery units powered by solar organic Rankine cycle have been performed using the exergy and thermo-economic analysis. The numerical results reveal that by the presence of PEX recovery unit, the needed solar collector field area to generate a sufficient power will not exceed about 1887m<sup>2</sup> with a percentage of decreasing in the range of 65% against the basic configuration and PWT comes next with a percentage of 43.5%. These results show that PWT comes next after PEX configuration which is considered more economical than either stand alone.

Also, suggestions are pinpointed to combine between solar filed (PTC solar collectors) and different configurations of MED (BF, FF, FFH, and PF) desalination plant (capacity of 100m<sup>3</sup>/day). The cycle is compared with the proposed techniques according to the terms of energy, exergy, cost and thermo-economic analysis. Based on the analysis performed in this work, the following conclusions can be draw:

- Technical limitations for MED concluded in increasing number of effects up to 16~20 stages and lowering the TBT in the range of 70~75°C. This may increase the gain ratio moreover; its effect on total water price is still not noticed. Also, increasing the effects number would reduce the SPC kWh/m<sup>3</sup>, the thermo-economic product cost \$/GJ, condenser area m<sup>2</sup>, and seawater feed mass flow rate.
- Both MED-FFH and MED-PF gives attractive results. However; MED-PF considered most efficient when the number of effects is increased up to 16~18 effects. The use of feed heaters enhances the GR, but adds more complexity, capital cost, and pumping energy.
- Toluene gives attractive results however, to develop much power (example of 11MWe), it is recommended to increase outlet collector temperature to 300°C at the same time increasing the demanded fresh water productivity up to 20,000m<sup>3</sup>/day. Also; the designer should put in consideration the controlling issues of the large area of the solar field.

The design of MED-PF-VC has the advantage of using a low-temperature heat source (steam or hot water) when it operates at low TBT, and this can give much lower equivalent work or available consumed energy than MSF units. Suggestions are pinpointed to combine between solar filed (PTC solar collectors) and different techniques of MED-PF-VC (TVC and MVC) desalination plant (capacity of 4545m<sup>3</sup>/day). Based on the analysis performed in this work, the following conclusions can be draw:

- Decreasing the compression ratio down to a specified limit (CR=2) may increase the cycle performance and would decrease the SPC kWh/m<sup>3</sup>.
- Increasing the steam temperature will increase the SPC kWh/m<sup>3</sup> and the CR.
- SMED-PF-TVC gives attractive results compared against SMED-PF-MVC technique. It achieves lower SPC, steam flow rate, total water price and thermo-economic product cost compared with SMED-PF-MVC technique.
- The existence of steam ejector unit may reduce the need of more evaporators to increase the GR.

MSF-BR distillation process is powered by solar thermal power instead of fossil fuel, however the techniques studied in this field are still will not developed well. Based on the analysis performed in this work, the following conclusions can be drawn:

- Technical limitations for MSF-BR concluded in increasing number of stages up to 40 stages and lowering the TBT in the range of 90~120°C. This may increase the gain ratio moreover; its effect on total water price is still not noticed.
- Toluene gives attractive results however, the second technique is favorable due to the obtained data for exergy efficiency, and thermo-economic unit product cost. Toluene achieves minimum collection area required to operate and power MSF-BR leading by this minimum exergy destruction, and minimum operating and maintenance cost requirements.
- To develop much power (example of 45MWe), it is recommended to increase outlet collector temperature to 350°C at the same time increasing the demanded fresh water productivity up to 30,000m<sup>3</sup>/day. However; the designer should put in consideration the control issues of the large area of the solar field.

- Power and desalination technique is favorable against the stand alone desalination based on high exergy efficiency, low exergy destruction. However; stand alone technique is favorable due to lower solar field area and total water price.

As a final result, a comparison involving the considered techniques of solar assisted desalination processes is performed. Solar thermal power by PTC technology is utilized as indirect vapor generation with organic Rankine cycle for RO and MED-MVC desalination processes. Indirect vapor generation without turbine unit is used for MED, MED-TVC, and MSF-BR processes. Based on the analysis performed in this work, the following conclusions can be drawn:

- The comparison is performed based on two main methods. The first is to compare based on individual design limits for each type. The other is to compare based on uniform parameters.
- The results of the individual method reveal that Solar-RO is quite attractive according to lower TWP, lower SSA, lower SPC, and lower exergy destruction rate.
- For all scenarios Solar-RO gives attractive results compared against the other techniques. Also it is noticed that SORC could reduce the solar field area.
- Solar-MED-TVC gives attractive results while comparing with thermal desalination processes.
- The second technique has an advantage concluded in developing power but depending on the amount of distillate product and the outlet collector/boiler operating conditions.
- Generally, Solar-RO and Solar-MED-TVC are attractive mainly related to the solar field area and TWP. However, the remaining processes could produce a massive fresh water quantity regardless the SPC or the solar field area.

## 5.2 Recommendations

The following recommendations are pin pointed as following:

- For solar ORC, Butane, Hexane, and Toluene working fluids are considered for FPC, CPC, and PTC respectively.
- RO-PEX configuration is considered a power saver technique according to thermo-economic results.
- MED-PF-TVC gives attractive results against the remaining thermal desalination processes especially against MED-PF-MVC.
- Generally, solar powered RO-PEX is the most reliable desalination process according to thermo-economic data results putting in mind the salinity range and the total productivity with the side of MSF-BR.

## 5.3 The Future Work

The future work can be summarized as follows:

- Adding the Photovoltaic-desalination library to the SDS software.
- Using the developed SDS package to analyze hybrid desalination processes.
- Design and simulation of solar combined gas turbine and solar Stirling cycles.
- Adding a library of other renewable such as Wind, Geothermal.

# The Appendix

## Appendix-A

### A. Working fluids: thermo physical properties

#### A.1 Water thermo physical properties

##### A.1.1 Density kg/m<sup>3</sup>

The equation is applicable in the temperature range of 10 to 180°C and for salinity from 0 to 160 g/kg.

$$\rho = 0.5 \times a_o + a_1 \times Y + a_2 \times (2 \times Y^2 - 1) + a_3 \times (4 \times Y^3 - 3 \times Y)$$

Where:

$$a_o = 2.016110 + 0.115313 \times \sigma + 0.000326 \times (2 \times \sigma^2 - 1)$$

$$a_1 = -0.0541 + 0.01571 \times \sigma - 0.000423 \times (2 \times \sigma^2 - 1)$$

$$a_2 = -0.006124 + 0.00174 \times \sigma - 0.000009 \times (2 \times \sigma^2 - 1)$$

$$a_3 = 0.000346 + 0.000087 \times \sigma - 0.000053 \times (2 \times \sigma^2 - 1)$$

$$Y = \frac{2t - 200}{160}$$

$$\sigma = \frac{2X - 150}{150}$$

##### A.1.2 Dynamic viscosity

The Validity range of this correlation is 10-150 °C and 0-130 g/kg salt concentration.

$$\mu = \mu_w \times \mu_R$$

$\mu_w$ : Viscosity of pure water.

$\mu_R$ : Relative viscosity and =1 for pure water & > 1 for salt solution.

$$\ln \mu_w = -3.79418 + \frac{604.129}{139.18 + t}$$

t: Temperature in °C.

$$\mu_R = 1 + a_1 \times X + a_2 \times X^2$$

Where,

$$a_1 = 1.474 \times 10^{-3} + 1.5 \times 10^{-5} \times t - 3.927 \times 10^{-8} \times t^2$$

$$a_2 = 1.0734 \times 10^{-5} + 8.5 \times 10^{-8} \times t - 2.23 \times 10^{-10} \times t^2$$

##### A.1.3 Boiling point elevation

This equation is valid for X (salt concentration) from 20 to 160 g/kg for t (temperature) from 20 to 180°C.

$$BPR = (B + C \times X) \times X$$

Where:

$$10^3 \times B = 6.71 + 6.43 \times 10^{-2} \times t + 9.74 \times 10^{-5} \times t^2$$

$$10^5 \times C = 2.38 + 9.59 \times 10^{-3} \times t + 9.42 \times 10^{-5} \times t^2$$

#### A.1.4 Specific heat capacity kJ/kg°C

$$C_p = A + B \times t + C \times t^2 + D \times t^3$$

Where:

$$A = 4206.8 - 6.6197 \times X + 1.2288 \times 10^{-2} \times X^2$$

$$B = -1.1262 + 5.4178 \times 10^{-2} \times X - 2.2719 \times 10^{-4} \times X^2$$

$$C = 1.2026 \times 10^{-2} - 5.3566 \times 10^{-4} \times X + 1.8906 \times 10^{-6} \times X^2$$

$$D = 6.8774 \times 10^{-7} + 1.517 \times 10^{-6} \times X - 4.4268 \times 10^{-9} \times X^2$$

X is the salinity ratio in kg/kg

#### A.1.5 Thermal conductivity W/m°C

$$k = A + B \times t + C \times t^2$$

$$A = 576.6 - 34.64 \times CA + 7.286 \times CA^2$$

$$B = 10^{-3} \times (1526 + 466.2 \times CA - 226.8 \times CA^2 + 28.67 \times CA^3)$$

$$C = -10^{-5} \times (581 + 2055 \times CA - 991.6 \times CA^2 + 146.4 \times CA^3)$$

And,

$$CA = \frac{28.17 \times X}{1000 - X}$$

#### A.1.6 Latent heat of vaporization kJ/kg

$$L = 2501.897149 - 2.407064037 \times T + 1.192217 \times 10^{-3} \times T^2 - 1.5863 \times 10^{-5} \times T^3$$

#### A.1.7 Saturation pressure bar

$$P_{sat} = 872.3 \times \exp^{-(T-585.5/169.5)^2} + 39.07 \times \exp^{-(T-342.4/124.4)^2}$$

#### A.1.8 Specific enthalpy of dry saturated vapor kJ/kg

$$h_v = -3.078e - 18 \times T^9 + 4.762e - 15 \times T^8 - 3.076e - 12 \times T^7 + 1.074e - 9 \times T^6 - 2.193e - 7 \times T^5 + 2.646e - 5 \times T^4 - 0.001824 \times T^3 + 0.06417 \times T^2 + 0.894 \times T + 2504$$

#### A.1.9 Specific enthalpy of saturated liquid kJ/kg

$$h_l = -0.033635409 + 4.207557011 \times T - 6.200339 \times 10^{-4} \times T^2 + 4.459374 \times 10^{-6} \times T^3$$

#### A.1.10 Specific entropy of saturated liquid kJ/kg°C

$$s_l = -0.00057846 + 0.015297489 \times T - 2.63129 \times 10^{-5} \times T^2 + 4.11959 \times 10^{-8} \times T^3$$



#### A.1.11 Specific entropy of saturated vapor kJ/kg°C

$$s_v = -4.697e - 21 \times T^9 + 7.274e - 18 \times T^8 - 4.706e - 15 \times T^7 + 1.648e - 12 \times T^6 - 3.39e - 10 \times T^5 + 4.2e - 8 \times T^4 - 3.27e - 6 \times T^3 + 0.0002231 \times T^2 - 0.02823 \times T + 9.16$$

### A.2 Toluene thermo physical properties

#### A.2.1 Density for liquid and vapor phases kg/m<sup>3</sup>

$$\rho_{tl} = -7.981^{-19} \times T^9 + 7.002^{-16} \times T^8 - 2.087^{-13} \times T^7 + 1.821^{-11} \times T^6 + 1.971^{-9} \times T^5 - 3.474^{-7} \times T^4 - 3.29^{-6} \times T^3 + 0.001316 \times T^2 - 0.9326 \times T + 884.5$$

$$\rho_{tv} = 7.873^{15} \times \exp^{-((Tco-868.2)/97.11)^2} + 1898 \times \exp^{-((Tco-666.7)/219.2)^2}$$

#### A.2.2 Dynamic viscosity for liquid and vapor phases kg/m<sup>3</sup>

Toluene physical properties for liquid and vapor phases are obtained from the following correlations;

$$\mu_{tl} = 10^{-6} \times (3.262729 \times 10^{-5} \times T^3 + 5.14015 \times 10^{-2} \times T^2 - 27.89675 \times T + 5.305598 \times 10^3)$$

$$\mu_{tv} = 10^{-6} \times (6.338982 \times 10^{-8} \times T^4 - 1.602562 \times 10^{-4} \times T^3 + 1.519286 \times 10^{-1} \times T^2 - 63.99838 \times T + 1.011961 \times 10^4)$$

#### A.2.3 Specific enthalpy of dry saturated vapor kJ/kg

$$h_v = 2.323e - 019 \times T^9 + 2.638e - 16 \times T^8 - 7.835e - 14 \times T^7 + 6.784e - 12 \times T^6 + 7.627e - 10 \times T^5 - 1.392e - 7 \times T^4 - 1.443e - 6 \times T^3 + 0.002331 \times T^2 + 1.019 \times T + 490.4$$

#### A.2.4 Specific enthalpy of saturated liquid kJ/kg

$$h_l = -3.023e - 19 \times T^9 - 2.041e - 16 \times T^8 + 6.098e - 14 \times T^7 - 5.372e - 12 \times T^6 - 5.526e - 10 \times T^5 + 9.276e - 8 \times T^4 + 2.962e - 6 \times T^3 + 0.001018 \times T^2 + 1.628 \times T + 63.19$$

#### A.2.5 Specific entropy of saturated vapor kJ/kg°C

$$s_v = -6.571e - 16 \times T^6 - 7.761e - 14 \times T^5 + 2.712e - 10 \times T^4 - 1.128e - 7 \times T^3 + 2.61e - 5 \times T^2 - 0.001973 \times T + 1.813$$

#### 1.2.6 Specific entropy of saturated liquid kJ/kg°C

$$s_l = 1.038 \times \exp^{(0.002218 \times T)} - 0.7889 \times \exp^{(-0.004717 \times T)}$$

#### A.2.7 Saturation pressure bar

$$P_{sat} = 7.025e - 22 \times T^9 - 4.53e - 19 \times T^8 + 1.187e - 16 \times T^7 - 2.775e - 14 \times T^6 + 6.104e - 12 \times T^5 + 2.474e - 9 \times T^4 + 2.434e - 7 \times T^3 + 1.429e - 5 \times T^2 + 0.0005795 \times T + 0.009935$$

### A.3 **Therminol-VP1** heat transfer oil thermo physical properties

#### A.3.1 Specific heat capacity kJ/kg°C

$$C_p = -0.6622 \times \exp^{(0.001186 \times T)} + 2.178 \times \exp^{(0.0007637 \times T)}$$

#### A.3.2 Pressure bar

$$P = 1.059e - 9 \times T^4 - 3.412e - 7 \times T^3 + 3.867e - 5 \times T^2 - 0.001491 \times T + 0.01249$$

#### A.3.3 Specific enthalpy kJ/kg

$$h = 0.00137 \times T^2 + 1.5 \times T - 18.46$$

#### A.3.4 Specific entropy kJ/kg°C

$$s = 1.038 \times \exp^{(0.002218 \times T)} - 0.7889 \times \exp^{(-0.004717 \times T)}$$

For further information about the related working fluids (Hexane and Butane, please visit the following links:

- [www.therminol.com](http://www.therminol.com)
- <http://webbook.nist.gov/chemistry/>

## Appendix-B

### B. Solar desalination units: Processes Mathematical models

The demanded power from desalination plants (block) permit the use of medium size of power source from solar field in case of direct vapor generation technique. Therefore, solar desalination plants (SDP) often contains the following:

- Low and/or medium temperature solar collectors (FPC, CPC, PTC).
- Solar field recirculation pumps.
- Control valves, sensors, flow meters, tanks, regulators, ...
- Organic Rankine cycle (turbine, condenser, heat exchanger, recuperator ...) in case of producing electricity for mechanical parts.
- Desalination blocks (thermal, membrane and/or mechanical) depending on the technique and the supplying method.

The application of solar energy to produce fresh water is receiving increased interest due to the need for solving the water shortage problems in various areas of the world at the same time as conventional energy sources used for obtaining water in different scenarios become depleted. Over the past few decades, the reverse osmosis (RO) process of seawater desalination has gained much popularity. RO is a membrane process, and was developed in direct competition with distillation processes. Its main feature is that it requires no thermal energy but, rather, mechanical energy in the form of a high pressure pump. Solar thermal energy coupled to a power cycle by using direct mechanical power can also be employed. Solar troughs and linear Fresnel can concentrate the sunlight by about **70–100 times**. Typical operating temperatures are in the range of **350–450°C**. Plants of 200MW rated power and more can be built by this technology.

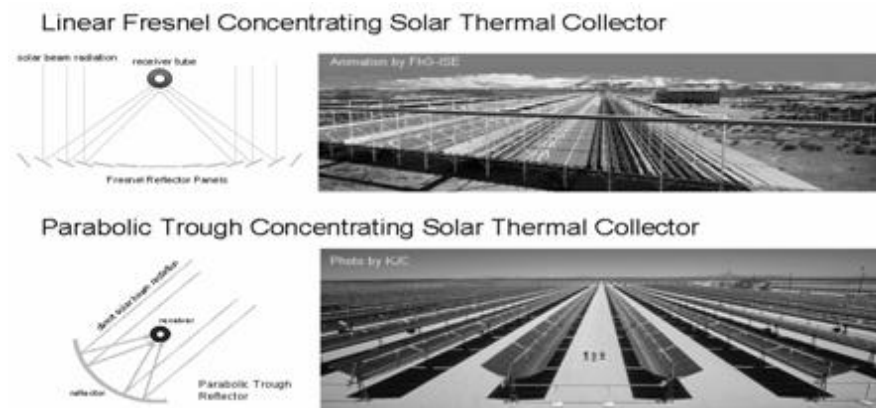


Figure (1) Linear and Parabolic troughs for solar concentrated thermal power.

The CSP technologies have some features:

- Concentrating solar power plants can generate electricity which can be used for membrane desalination.
- CSP plants can be used for combined heat and power.
- Thermal desalination methods like multi effect distillation (MED) or multi stage flash (MSF) can be powered by CSP, either directly or in co-generation with electricity.

- CSP reduces emissions of local pollutants and considerably contribute to global climate protection.

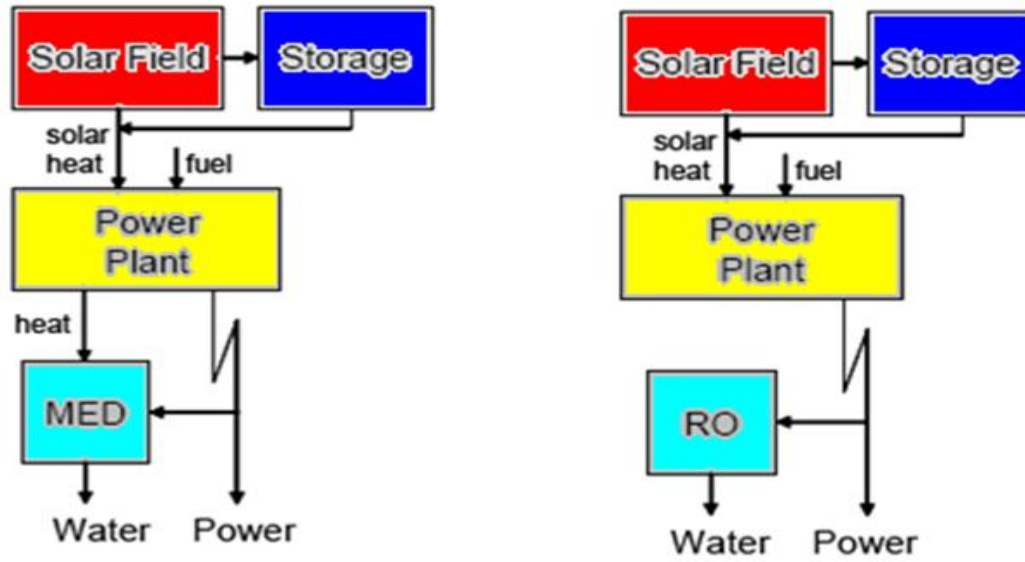


Figure (2) CSP's technology implementation for different types of thermal desalination plants.

In this part, it is very important to highlight on the different mathematical models for different processes of solar desalination plants. Solar radiation model, different types of solar collectors, different types of energy units, different types of desalination plants are pinpointed and mathematically analyzed based on approaches such as energy, exergy, thermo-economic, and cost.

### B.1 Mathematical approaches

The mathematical approaches that used in the analysis for solar desalination plants are basically preformed according to 1<sup>st</sup> and 2<sup>nd</sup> laws of thermodynamics. For any system goes under steady state, the mass, energy, and entropy balances equations under steady state condition should be developed as following;

$$\begin{aligned}\sum \dot{m}_{in} - \sum \dot{m}_{out} &= 0, kg/s \\ \sum \dot{e}_{in} - \sum \dot{e}_{out} &= 0, kJ/kg \\ \sum \dot{s}_{in} - \sum \dot{s}_{out} &= 0, kJ/kg \cdot ^\circ C\end{aligned}$$

Unlike energy, which is conserved in any process according to the first law of thermodynamics, exergy is destroyed due to irreversibility taking place in any process, which manifests itself in entropy creation or entropy increase. The general form of the availability is defined by the following equation;

$$A_2 - A_1 = A_q + A_w + A_{fi} - A_{fo} - I$$

Where  $A_2 - A_1 = 0$  is the non-flow availability change in steady state condition,  $A_q = \sum_j (1 - T_{amb}/T_j) Q_j$  is the availability transfer due to the heat transfer between the control volume and its surroundings,  $A_w = -W_{cv} + P_o(V_2 - V_1)$  is equal to the negative value of the work produced by the control volume

but in most cases the control volume has a constant volume, therefore  $A_w$  can be further simplified. And  $I = T_{amb} \times S_{gen}$  is the availability destruction in the process. The flow availability expressed as  $A_{fi,o} = \sum_{i,o} \dot{m}_{i,o} a_{fi,o}$ . So the general form in steady state condition would become;

$$0 = A_q + A_w + A_{fi} - A_{fo} - I$$

Thermo-economic is the branch of engineering that combines exergy analysis and economic principles to provide the system designer or operator with information not available through conventional energy analysis and economic evaluations but crucial to the design and operation of a cost effective system. In a conventional economic analysis, a cost balance is usually formulated for the overall system operating at steady state as following;

$$\sum_{out} \dot{C} = \sum_{in} \dot{C} + Z^{IC\&OM}$$

Where  $\dot{C}$  the cost rate according to inlet and outlet streams, and  $Z^{IC\&OM}$  is the capital investment and operating & maintenance costs. In exergy costing a cost is associated with each exergy stream. Thus, for inlet and outlet streams of matter with associated rates of exergy transfer  $E_{i,o}$ , power  $W$ , and the exergy transfer rate associated with heat transfer  $E_q$  it can write as following;

$$\dot{C}_{i,o} = c_{i,o} \dot{E}_{i,o}$$

$$\dot{C}_w = c_w \dot{W}$$

$$\dot{C}_q = c_q \dot{E}_q$$

Where  $c_{i,o,w,q}$  denote average costs per unit of exergy in \$/kJ for inlet (i), outlet (o), power (w), and energy (q) respectively.

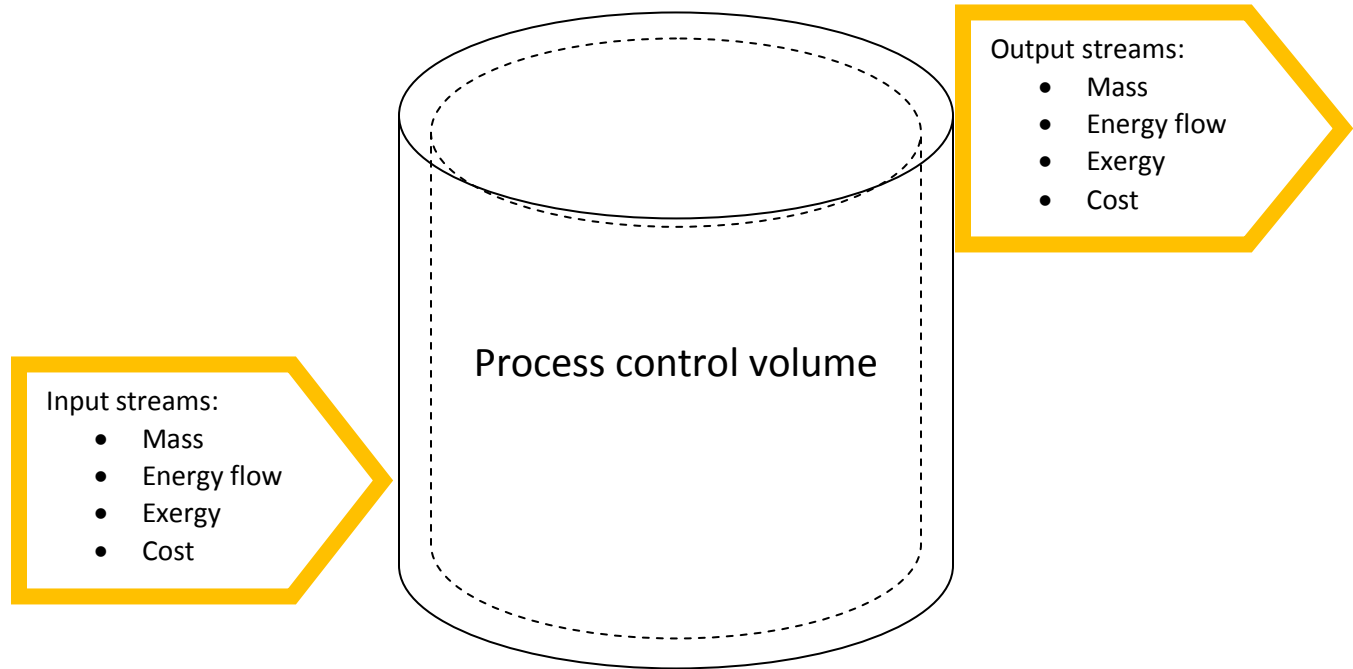


Figure (3) Assumptions of flow streams across any process.

### B.1.1 Solar collectors

The collector is the heart of any solar energy system. The performance of such solar energy systems is largely dependent on the portion of solar insolation that is transferred to the fluid, which also depends on the working temperatures of this fluid. The useful portion of the insolation is a function of the design of the collector, its tilt and its orientation. It is also function of the design fluid temperatures and environmental parameters of the location such as air temperature, wind velocity, and insolation.

The solar collector instantaneous efficiency can be determined from its characteristic curve using the solar irradiance, mean collector and ambient temperatures. The curve used for FPC, evacuated tube, and CPC are expressed by Eq. (1) and the parameters given in Table 1. The corresponding efficiency equation for the medium-high temperatures parabolic trough collectors (PTC) is given by Eq. (2).

$$\eta_{col} = \eta_o - a_1 \left( \frac{T_{co} - T_{amb}}{G_b} \right) - a_2 \left( \frac{T_{co} - T_{amb}}{G_b} \right)^2 G_b \dots (1)$$

$$\eta_{col} = \eta_o - a_{11}(T_{co} - T_{amb}) - a_{21} \left( \frac{T_{co} - T_{amb}}{G_b} \right) - a_{31} \left( \frac{T_{co} - T_{amb}}{G_b} \right)^2 \dots (2)$$

Table 1: Efficiency parameters for different types of solar collectors [48].

Solar collector	$a_1$ W/m <sup>2</sup>	$a_2$ W/m <sup>2</sup>	$a_{11}$ W/m <sup>2</sup>	$a_{21}$ W/m <sup>2</sup>	$a_{31}$ W/m <sup>2</sup>	$\eta_o$	Operating temp, °C
FPC	2.9	0.0108	--	--		0.768	80-100
CPC	0.59	0.0019	--	--		0.665	120-170
PTC	--	--	$4.5 \times 10^{-6}$	0.039	$3 \times 10^{-4}$	0.75	>170-400

The collector total area is estimated based on the collector energy balance equation as a function of collector efficiencies as;

$$A_{col} = \frac{Q_u}{\eta_{col}} G_b, m^2$$

Where  $Q_u$  is the collector useful thermal power and ( $G_b$ ) is the global solar flux over the collector area, and  $A_{col}$  is the collector total area. The collector useful energy equation may exist according to the following relation;

$$Q_u = \dot{m}_{col} \times \Delta H \text{ Where } \Delta H \text{ is the enthalpy difference across the collector in kJ/kg.}$$

The exergy destruction across the solar collector is presented as following;

$$I_{collector} = A_{col} \times G_b \times \left( 1 - \frac{T_{amb}}{T_{sun}} \right) + \dot{m}_{col} [h_i - h_o - T_{amb}(s_i - s_o)]_{col}$$

Where  $h$  represent the specific enthalpy, and  $s$  represents the specific entropy. Thermo-economic analysis for solar collector to any unit is presented as following;

$$C_{col-\dots} = C_{q=0} + C_{\dots-col} + Z_{col}^{IC\&OM}$$

And the product cost rate in \$/kJ from solar collector field to any other unit (...);

$$c_{col-\dots} = \frac{c_{\dots-col} E_{\dots-col} + Z_{col}^{IC\&OM}}{E_{col-\dots}}$$

Where  $E$  is the exergy rate in kW.

### B.1.2 Pump unit

Pump work  $W_p$  in kW is calculated as:

$$W_p = \frac{\dot{m} \times \Delta P}{\rho \times \eta_p}, kW$$

Where  $\Delta P$  pressure difference between the condenser low pressure and the turbine high is pressure, and  $\rho$  is the density of the working fluid, and  $\eta_p$  is pump efficiency.

The pump outlet enthalpy is obtained via the following relation:

$$h_{out} = \frac{W_p}{\dot{m}} + h_{in}, kJ/kg$$

By knowing the environmental conditions ( $T_{amb}$ ), the exergy destruction rate could be obtained from the following relation:

$$I_p = \dot{m}_p [h_{in} - h_{out} - T_{amb} \times (s_i - s_o)] + W_p, kW$$

And thermo-economically;

$$C_{p-...} = C_w + C_{...-p} + Z_p^{IC\&OM}$$

So; the unit product cost for the pump becomes;

$$c_{p-...} = \frac{c_w E_w + c_{...-p} E_{...-p} + Z_p^{IC\&OM}}{E_{p-...}}$$

Where, subscripts ( $w, p$ ) denotes for power in kW and pump.

### B.1.3 Turbine unit

For models based on design approach, it is very important to find out the mass flow rate through the turbine by the knowing some parameters such as turbine efficiency, generator efficiency, and the developed power by the turbine. The outlet enthalpy of the turbine kJ/kg;

$$h_{out} = h_{in} - \eta_t \times (h_{in} - h_{out_s}), kJ/kg$$

Where  $\eta_t$  is the turbine efficiency and the subscript ( $s, t$ ) tends to isentropic state and turbine. The cycle flow rate kg/s is presented as following;

$$\dot{m}_t = \frac{W_t}{\eta_t \times \eta_{g \times} (h_{in} - h_{out_s})}, kg/s$$

Where  $\eta_g$  is the generator efficiency.

Based on exergy analysis, the exergy destruction rate in kW is developed based on the following relation:

$$I_t = \dot{m}_t [h_{in} - h_{out} - T_{amb} \times (s_i - s_o)] - W_t, kW$$

Steam turbine would maintain one auxiliary equation for two streams outlet (power stream  $c_w$ , and exhaust stream to any followed unit). For this, the unit product power for steam turbine can be represented as follows;

$$c_w = \frac{C_{...-t} (E_{...-st} - E_{t-...}) + Z_t^{IC\&OM}}{E_w}, c_{...-st} = c_{t-...}$$

$$C_{t-...} + C_{w-...} = C_{...-t} + Z_t^{IC\&OM}$$

### B.1.4 Heat exchanger units

Heat exchanger units include condensers, boiler heat exchangers, recuperators, and so on. For such units, it is recommended (based on design model) to assign the unit effectiveness ( $\epsilon_{cond}$ ). The following relations govern such units according to energy, exergy, and thermo-economic approaches.

Condenser heat rejection kW:

$$Q_{cond} = \dot{m}_{hot} \times \Delta h_{hot} = \dot{m}_{cold} \times \Delta h_{cold}, kW$$

$$\epsilon_{cond} = \frac{\Delta T_{cold}}{T_{hot_{max}} - T_{cold_{min}}}$$

Based on exergy analysis, the exergy destruction rate in kW is developed based on the following relation:

$$I_{cond} = m_{hot}[h_{in} - h_{out} - T_{amb} \times (s_i - s_o)] + m_{cold}[h_{in} - h_{out} - T_{amb} \times (s_i - s_o)], kW$$

Thermo-economically, recuperator example is demonstrated as following:

$$C_{rec-...1} + C_{rec-...2} = C_{...1-rec} + C_{...2-rec} + Z_{rec}^{IC\&OM}$$

$$C_{...1-rec} = C_{rec-...1}$$

$$C_{...2-rec} = C_{rec-...1}$$

Where subscripts ...1 denotes hot side stream from unit (1) and ...2 denotes cold side stream from unit (2).

### B.1.5 Reverse osmosis desalination unit

Reverse osmosis (RO) is a filtration method that removes many types of large molecules and ions from solutions by applying pressure to the solution when it is on one side of a selective membrane. The result is that the solute is retained on the pressurized side of the membrane and the pure solvent is allowed to pass to the other side. To be "selective," this membrane should not allow large molecules or ions through the pores (holes), but should allow smaller components of the solution (such as the solvent) to pass freely. Reverse osmosis is most commonly known for its use in drinking water purification from seawater, removing the salt and other substances from the water molecules. This is the reverse of the normal osmosis process, in which the solvent naturally moves from an area of low solute concentration, through a membrane, to an area of high solute concentration. The movement of a pure solvent to equalize solute concentrations on each side of a membrane generates a pressure and this is the "osmotic pressure." Applying an external pressure to reverse the natural flow of pure solvent, thus, is reverse osmosis. The process is similar to membrane filtration. However, there are key differences between reverse osmosis and filtration.

The predominant removal mechanism in membrane filtration is straining, or size exclusion, so the process can theoretically achieve perfect exclusion of particles regardless of operational parameters such as influent pressure and concentration. Reverse osmosis, however involves a diffusive mechanism so that separation efficiency is dependent on solute concentration, pressure and water flux rate. Formally, reverse osmosis is the process of forcing a solvent from a region of high solute concentration through a semipermeable membrane to a region of low solute concentration by applying a pressure in excess of the osmotic pressure. The membranes used for reverse osmosis have a dense barrier layer in the polymer matrix where most separation occurs. In most cases, the membrane is designed to allow only water to pass through this dense layer, while preventing the passage of solutes (such as salt ions). This process requires that a high pressure be exerted on the high concentration side of the membrane, usually 2–17 bar (30–250 psi) for fresh and brackish water, and 40–70 bar (600–1000 psi) for seawater, which has around 24 bar (350 psi) natural osmotic pressure that must be overcome. This process is best known for its use in desalination (removing the salt from sea water to get fresh water), but since the early 1970s it has also been used to purify fresh water for medical, industrial, and domestic applications. Figure (4) shows a schematic photograph of the RO process.



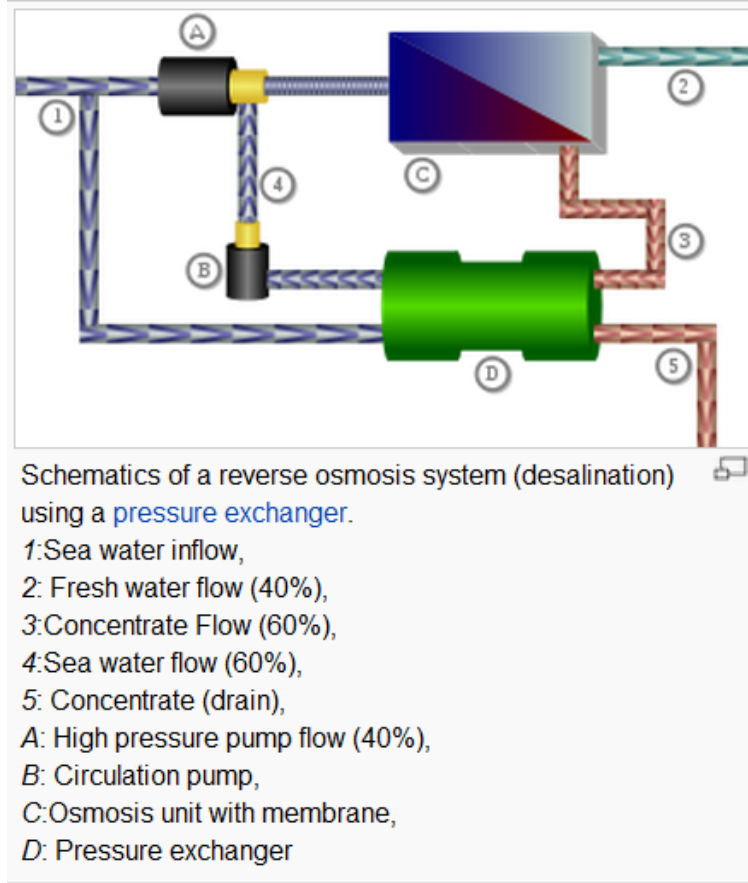


Figure (4) Schematic diagram of RO-PEX process.

The mathematical model for the proposed RO unit is written as follows [43]:

The feed flow rate  $M_f$  based on recovery ratio  $RR$  and distillate flow rate  $M_d$  is:

$$M_f = \frac{M_d}{RR}$$

The distillate product salt concentration  $X_d$ ;

$$X_d = X_f \times (1 - SR)$$

Where;  $X_f$  is the feed flow rate salt concentration, and  $SR$  is the salt rejection percentage; and the rejected brine is found from;

$$M_b = M_f - M_d$$

The rejected salt concentration  $\text{kg/m}^3$  is estimated by;

$$X_b = \frac{M_f \times X_f - M_d \times X_d}{M_b}$$

The average salt concentration  $\text{kg/m}^3$  is estimated as;

$$X_{av} = \frac{M_f \times X_f + M_b \times X_b}{M_f + M_b}$$

The temperature correction factor  $TCF$  is found by the relation below;

$$TCF = \exp \left( 2700 \times \left( \frac{1}{273 + t} - \frac{1}{298} \right) \right) \quad [43]$$

The membrane water permeability  $k_w$ ;

$$k_w = 6.84 \times 10^{-8} \times (18.6865 - (0.177 \times X_b)) / (t + 273))$$

The salt permeability  $k_s$  is;

$$k_s = FF \times TCF \times 4.72 \times 10^{-7} \times (0.06201 - (5.31 \times 10^{-5} \times (t + 273)))$$

Where FF is the membrane fouling factor. The calculations of osmotic pressure for feed side, brine side, and distillate product side are found as follows;

$$\Pi_f = 75.84 \times X_f$$

$$\Pi_b = 75.84 \times X_b$$

$$\Pi_d = 75.84 \times X_d$$

The average osmotic pressure on the feed side;

$$\Pi_{av} = 0.5 \times (\Pi_f + \Pi_b)$$

The net osmotic pressure across the membrane;

$$\Delta\Pi = \Pi_{av} - \Pi_d$$

The net pressure difference across the membrane;

$$\Delta P = \left( \frac{M_d}{3600 \times TCF \times FF \times A_e \times n_e \times n_v \times k_w} \right) + \Delta\Pi$$

Where  $A_e$  is the element area in  $m^2$ ,  $n_e$  is number of membrane elements, and  $n_v$  is the number of pressure vessels. The required high pressure pump power input in kW to the RO is estimated as;

$$HPP_{power} = \frac{1000 \times M_f \times \Delta P}{3600 \times \rho_f \times \eta_p}$$

Where  $\rho_f$  is the feed flow rate density, and  $\eta_p$  is the driving pump mechanical efficiency. The specific power consumption in  $kWh/m^3$  is estimated as;

$$SPC = \frac{HPP_{power}}{M_d}$$

Based on exergy balance for RO section;

$$I_{RO} = W_{HPP} - m_b \times (h_f - h_b) + m_p \times (h_f - h_p), kW$$

Where  $h_f$ ,  $h_b$ , and  $h_p$  is calculated based on seawater specific heat capacity, salinity  $X$ , and feed seawater temperature for each stream where;

$$h_{f,p,b} = h_o + (A \times T + B/2 \times T^2 + C/3 \times T^3 + D/4 \times T^4), \text{ Where; } h_o = 9.6296 \times X - 0.4312402 \times X^2$$

And;

$$A = 4206.8 - 6.6197 \times X + 1.2288 \times 10^{-2} \times X^2$$

$$B = -1.1262 + 5.4178 \times 10^{-2} \times X - 2.2719 \times 10^{-4} \times X^2$$

$$C = 1.2026 - 5.3566 \times 10^{-4} \times X + 1.8906 \times 10^{-6} \times X^2$$

$$D = 6.8774 \times 10^{-7} + 1.517 \times 10^{-6} \times X - 4.4268 \times 10^{-9} \times X^2$$

Thermo-economic balance for the RO section;

$$C_p + C_{brine} = C_{feed} + Z_{RO}^{IC\&OM}$$

For Pelton wheel recovery turbine (PWT);

$$C_{w-HPP} + C_{brine-blowdown} = C_{brine-RO-PWT} + Z_{PWT}^{IC\&OM}$$

For pressure exchanger unit (PEX);

$$C_{feed-RO} + C_{brine-blowdown} = C_{feed} + C_{brine-RO-PEX} + Z_{PEX}^{IC\&OM}$$

By solving the above equations together, the following equation could maintain the overall thermo-economic balance of the system.

$$C_{brine-blowdown} + C_{product} = C_{cw-cond} + C_{q-col} + C_{w-pump} + Z_{total}^{IC\&OM}$$

Present results of Sharm El-Shiekh desalination plant for SDS Vs ROSA6.1 and Mabrouk [36].

Variable	SDS	ROSA6.1	VDS	Units
<i>SPC</i>	7.68	7.76	7.76	kWh/m <sup>3</sup>
<i>HP</i>	1131	1131.42	1130	kW
<i>Mf</i>	485.9	458.9	486	m <sup>3</sup> /h
<i>Mb</i>	340.1	340.15	340.23	m <sup>3</sup> /h
<i>Xb</i>	64180	62005	66670	ppm
<i>Xd</i>	250	283.83	200	ppm
<i>SR</i>	0.9944	--	0.9927	--
<i>ΔP</i>	6850	6670	6700	kPa

Based on thermo-economic fundamentals as presented in the appendix; the thermo-economic balance equations for each component in the combined processes (ORC/RO) should be presented as following;

For Rankine cycle pump unit;

$$C_{pump-rec} = C_w + C_{cond-pump} + Z_{pump}^{IC\&OM}$$

For solar collector; the relation should become;

$$C_{col-st} = C_q + C_{rec-col} + Z_{col}^{IC\&OM}$$

And for steam turbine unit;

$$C_{st-rec} + C_{w-HPP} = C_{col-st} + Z_{st}^{IC\&OM}$$

For recuperator unit, the relation becomes as following;

$$C_{rec-cond} + C_{rec-col} = C_{st-rec} + C_{pump-rec} + Z_{rec}^{IC\&OM}$$

For condenser unit;

$$C_{cond-pump} + C_{cond-HPP} = C_{cw} + C_{rec-cond} + Z_{cond}^{IC\&OM}$$

For high pressure pump of RO unit;

$$C_{HPP} = C_{cond-HPP} + C_{w-st} + Z_{HPP}^{IC\&OM}$$

For RO module;

$$C_p + C_{brine} = C_{feed} + Z_{RO}^{IC\&OM}$$

For Pelton wheel recovery turbine;

$$C_{w-HPP} + C_{brine-blowdown} = C_{brine-RO-PWT} + Z_{PWT}^{IC\&OM}$$

For pressure exchanger unit;

$$C_{feed-RO} + C_{brine-blowdown} = C_{feed} + C_{brine-RO-PEX} + Z_{PEX}^{IC\&OM}$$

By solving the above equations together, the following equation could maintain the overall thermo-economic balance of the system.

$$C_{brine-blowdown} + C_{product} = C_{cw-cond} + C_{q-col} + C_{w-pump} + Z_{total}^{IC\&OM}$$

Where

$$Z_{total}^{IC\&OM} = Z_{pump}^{IC\&OM} + Z_{col}^{IC\&OM} + Z_{st}^{IC\&OM} + Z_{rec}^{IC\&OM} + \dots \\ Z_{cond}^{IC\&OM} + Z_{HPP}^{IC\&OM} + Z_{PEX,PWT}^{IC\&OM}$$

Assuming that for any flow from the environment, external valuation of the unit exergo-economic cost is performed. In this work, this involves seawater, and solar radiation (free) and external consumption. Also, for any flow without later usefulness (losses), zero unit exergo-economic cost is assigned and this involves brine blow down. Therefore, the overall equation will become as follows;

$$C_p = C_{w-pump} + Z_{total}^{IC\&OM} \\ c_p = \frac{C_{cw} + C_{w-pump} + Z_{total}^{IC\&OM}}{E_p} \text{ \$/GJ}$$

Where  $E_p$  is the exergy of the product stream from RO desalination plant.

### B.1.6 Multi stage flash (MSF-BR) desalination unit

Multi-stage flash distillation (MSF) is a water desalination process that distills sea water by flashing a portion of the water into steam in multiple stages of what are essentially countercurrent heat exchangers. The plant has a series of spaces called stages, each containing a heat exchanger and a condensate collector. The sequence has a cold end and a hot end while intermediate stages have intermediate temperatures. The stages have different pressures corresponding to the boiling points of water at the stage temperatures. After the hot end there is a container called the brine heater. When the plant is operating in steady state, feed water at the cold inlet temperature flows, or is pumped, through the heat exchangers in the stages and warms up. When it reaches the brine heater it already has nearly the maximum temperature. In the heater, an amount of additional heat is added. After the heater, the water flows through valves back into the stages which have ever lower pressure and temperature. As it flows back through the stages the water is now called brine, to distinguish it from the inlet water. In each stage, as the brine enters, its temperature is above the boiling point at the pressure of the stage, and a small fraction of the brine water boils ("flashes") to steam thereby reducing the temperature until equilibrium is reached.

The equilibrium is stable, because if at some point more vapor forms, the pressure increases and that reduces evaporation and increases condensation. In the final stage the brine and the condensate has a temperature near the inlet temperature. Then the brine and condensate are pumped out from the low pressure in the stage to the ambient pressure. The brine and condensate still carry a small amount of heat that is lost from the system when they are discharged. The heat that was added in the heater makes up for this loss. The heat added in the brine heater usually comes in the form of hot steam from an industrial process co-located with the desalination plant. The steam is allowed to condense against tubes carrying the brine (similar to the stages). The energy that makes possible the evaporation is all present in the brine as it leaves the heater. The reason for letting the evaporation happen in multiple stages rather than a single stage at the lowest pressure and temperature, is that in a single stage, the feed water would only warm to an intermediate temperature between the inlet temperature and the heater, while much of the steam would not condense and the stage would not maintain the lowest pressure and temperature. Figure (5) shows a schematic diagram of MSF desalination process.

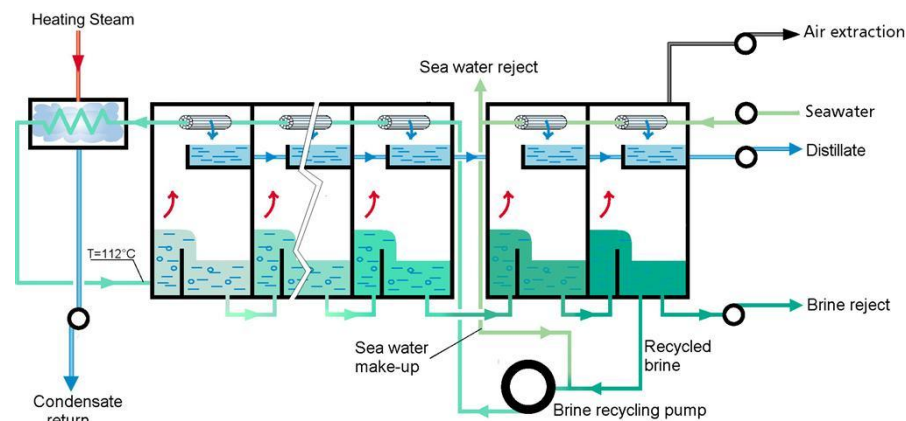


Figure (5) Schematic diagram of MSF brine recycle process.

The mathematical model based on design approach is presented as following [43]:

For known distillate product, feed stream to the mixer unit is obtained:

$$M_f = (S_b / (S_b - S_f)) \times M_d$$

Total needed feed ( $M_{ft}$ ) based on 1<sup>st</sup> splitter ratio:

$$M_{ft} = M_f / SPL1$$

Therefore the rest of feed loss:

$$M_{fl} = M_{ft} - M_f$$

The brine blow-down loss:

$$M_b = M_f - M_d$$

Stage temp drop based on top brine temperature (TBT), last stage brine temperature ( $T_n$ ) and number of stages ( $N$ ):

$$T_{stg} = TBT - T_n / N$$

The recycle brine flow rate  $M_r$  and latent heat  $L$  is then calculated:

$$Y = (C_p \times T_{stg}) / L$$

$$M_r = M_d / (1 - (1 - Y)^N)$$

Then the salinity of the recycle stream is calculated  $S_r$ :

$$S_r = \frac{(S_f \times M_f + (M_r - M_d) \times S_b - M_b \times S_b)}{M_r}$$

The outlet temperature of the distillate product  $T_d$  could be calculated based on brine blow down temperature  $T_n$ , non equilibrium allowance  $NEA$ , and boiling point ratio  $BPR$ .

$$T_d = T_n - NEA - BPR$$

The non-equilibrium allowance  $NEA$  and  $BPR$  are calculated by the following equations;

$$NEA = A + B \times T_n + C \times T_n^2 + D \times T_n^3$$

Where  $A=2.556$ ,  $B=-0.203 \times 10^{-1}$ ,  $C = -0.129 \times 10^{-1}$  and  $D = 0.1123 \times 10^{-5}$

$$BPR = (B + C \times S) \times S$$

Where  $S$  is the stream salinity and,

$$10^3 \times B = 6.71 + 6.43 \times 10^{-2} \times T_n + 9.74 \times 10^{-5} \times T_n^2$$

$$10^5 \times C = 2.38 + 9.59 \times 10^{-3} \times T_n + 9.42 \times 10^{-5} \times T_n^2$$

For the heat recovery and rejection sections, the overall heat transfer coefficient based on vapor temperature  $T_v$ :

$$U = 1.7194 + 3.2063E - 3 \times T_v + 1.5971E - 5 \times T_v^2 - 1.9918E - 7 \times T_v^3$$

The exergy destruction balance across the MSF plant can be introduced as following;

$$I = W_p + E_{bo} + E_{fi} - E_{fo} - E_d, kW$$

Where,  $W_p$  is the total pumping power required,  $E$  is the exergy rate, and subscripts ( $bo$ ,  $fi$ ,  $fo$ ) denotes to TBT, inlet feed, and outlet feed streams respectively. Thermo-economically, the balanced equations should be presented as follows;

$$C_d + C_{brine} + C_{condi} = C_{condo} + C_{fi} + Z_{msf}^{IC\&OM}$$

Where  $C_d$  is the distillate product cost \$/h,  $C_{brine}$  is the brine blow down cost and is specified as zero cost, and  $C_{fi}$ . The unit specific cost of inlet seawater feed stream to the MSF condenser is considered the same as outlet preheated stream entered the condenser/brine-heater unit ( $c_{cwi-cond}=C_{fi}$ ). So the relation would become as follows;

$$c_d = \frac{C_{condo} E_{condo} - c_{fi} \Delta E_f + Z_{msf}^{IC\&OM}}{E_d}$$

### B.1.7 Multi effect distillation desalination unit

Multiple-effect distillation (MED) is a distillation process often used for sea water desalination. It consists of multiple stages or "effects". In each stage the feed water is heated by steam in tubes. Some of the water evaporates, and this steam flows into the tubes of the next stage, heating and evaporating more water. Each stage essentially reuses the energy from the previous stage. The tubes can be submerged in the feed water, but more typically the feed water is sprayed on the top of a bank of horizontal tubes, and then drips from tube to tube until it is collected at the bottom of the stage. The plant can be seen as a sequence of closed spaces separated by tube walls, with a heat source in one end and a heat sink in the other end. Each space consists of two communicating subspaces, the exterior of the tubes of stage  $n$  and the interior of the tubes in stage  $n+1$ . Each space has a lower temperature and pressure than the previous space, and the tube walls have intermediate temperatures between the temperatures of the fluids on each side. Figure (6) shows a schematic diagram of the MED process. There are some features of such kind of desalination process.

- Low energy consumption (less than  $1.0 \text{ kWh/m}^3$ ) compared to other thermal processes.
- Operates at low temperature ( $< 70^\circ\text{C}$ ) and at low concentration ( $< 1.5$ ) to avoid corrosion and scaling.
- Does not need pre-treatment of sea water and tolerates variations in sea water conditions.
- Highly reliable and simple to operate.
- Low maintenance cost.
- 24 hour a day continuous operation with minimum supervision.
- Can be adapted to any heat source including hot water or waste heat from power generation or industrial processes.

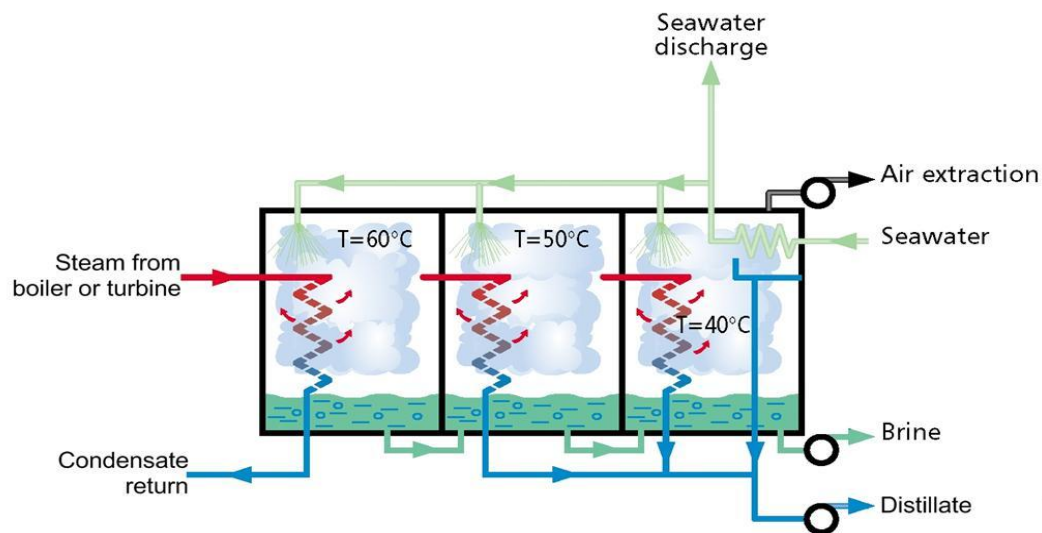


Figure (6) Schematic diagram of multi effect distillation process.

The analysis introduced in MED section, is presented based on single effect evaporation module. The first method used to desalt seawater in large quantities was the single effect desalting system consisting of an evaporator-condenser combination (Fig. 7). Single effect evaporation (SEE) has limited industrial

applications. The system is used in marine vessels and this because the system has thermal performance ratio less than one, i.e.; the amount of water produced is less than the amount of heating steam used to operate the system. The main components of the unit are the evaporator and the feed pre-heater condenser. The evaporator consist of an evaporator\condenser heat exchanger tubes, a vapor space, un-evacuated water pool, a line for removal of non condensable gases, a water distribution system, and a mist eliminator. A heat source (steam  $S$ ) heats the incoming feed  $F$  to the evaporator from its entering feed temperature  $T_f$  to its boiling temperature  $T_b$ , and evaporates part of it equal to  $D$ . The vapor  $D$  is directed to the condenser where it condenses and heats the cooling water  $M_{sea}$  from seawater temperature  $T_{sea}$  to the feed temperature  $T_f$ . Part of  $M_{sea}$  leaving the condenser is used as feed  $F$  while the balance  $B (=M_{sea}-F)$  is called brine blow-down and is rejected back to the sea. In the condenser of a single-effect desalting system, a small portion of the latent heat given off by condensing the vapor  $D$  is utilized to heat the feed-water  $F$ , while the balance  $D \times L = F \times C_p \times (T_f - T_{sea})$  is rejected back to sea. The mathematical model for this type is illustrated as following:

Energy balance for the condenser unit based on the specified effectiveness  $\varepsilon$ :

$$T_f = \varepsilon \times (T_v - T_{sea}) + T_{sea}$$

where  $T_v$  is the vapor temperature;

The distillate temperature is obtained from the same equation:

$$T_d = T_v - (\varepsilon \times (T_v - T_{sea}))$$

Mass and material balances;

$$M_f = M_d \times S_b / (S_b - S_f)$$

$$M_b = M_d \times S_f / (S_b - S_f)$$

And steam flow rate  $M_s$  could be obtained from the following relation;

$M_s = M_d / PR$  where  $PR$  is the performance ratio which is also obtained as following;

$$PR = \frac{L(T_s)}{L(T_v) + C_p(T_{av}, S_f) \times (T_v - T_f) \times \frac{S_b}{(S_b - S_f)} + \frac{S_f}{S_b - S_f} \times C_p(T_{av}, S_f) BPE(T_b, S_b)}$$

Where,  $BPE$  is the boiling point elevation as a function of brine temperature and salinity percent;

Cooling water blow down from the condenser unit is obtained from the following energy balance relation;

$$M_{cw} = \frac{M_d \times L(T_v)}{C_p(T_{av}, S_f) \times (T_f - T_{sea})} - M_f$$

Where the  $T_{av}$  is the average temperature for the feed seawater across the condenser unit ( $T_{av} = \frac{T_f + T_{sea}}{2}$ )

Therefore; the total mass flow rate is then calculated;

$$M_{ft} = M_{cw} + M_f$$

Heat Transfer areas for condenser and evaporator units ( $A_c, A_e$ ) are obtained based on logarithmic mean temperature  $LMT$ , latent heat  $L$  and overall heat transfer coefficient  $U$ ;

For condenser unit;

$$LMT_c = \frac{(T_f - T_{sea})}{\log \frac{(T_v - T_{sea})}{(T_v - T_f)}}$$

$$A_c = \frac{M_d \times L(T_v)}{U_c(T_v) \times LMT_c}$$

$$A_e = \frac{M_d \times \frac{S_b}{(S_b - S_f)} \times C_p(T_b, S_b) \times (T_b - T_f) + M_d \times L(T_v)}{U_e(T_s - T_b)}$$

Thermo-physical properties and overall heat transfer coefficient are calculated from the following correlations:

- Boiling point elevation:

$$BPE = 0.0825431 + 0.0001883 \times T + 0.00000402 \times T^2 \times S - 0.0007625 + 0.0000902 \times T - 0.00000052 \times T^2 \times S^2 + 0.0001522 - 0.000003 \times T - 0.00000003 \times T^2 \times S^3$$

- Specific heat capacity:

$$\begin{aligned} a &= 4206.8 - 6.6197 \times S + 1.2288 \times 10^{-2} \times S^2 \\ b &= -1.1262 + 5.4178 \times 10^{-2} \times S - 2.2719 \times 10^{-4} \times S^2 \\ c &= 1.2026 \times 10^{-2} - 5.3566 \times 10^{-4} \times S + 1.8906 \times 10^{-6} \times S^2 \\ d &= 6.8774 \times 10^{-7} + 1.517 \times 10^{-6} \times S - 4.4268 \times 10^{-9} \times S^2 \\ Cp &= a + b \times T + c \times T^2 + d \times T^3 \end{aligned}$$

- Latent heat of vaporization:

$$L = 2501.897149 - 2.407064037 \times T + 1.192217 \times 10^{-3} \times T^2 - 1.5863 \times 10^{-5} \times T^3$$

- The overall heat transfer coefficients for evaporator and end condenser units:

$$\begin{aligned} Ue &= 1.9695 + 1.2057 \times 10^{-2} \times T - 8.5989 \times 10^{-5} \times T^2 + 2.5651 \times 10^{-7} \times T^3 \\ Uc &= 1.7194 + 3.2063 \times 10^{-3} \times T + 1.5971 \times 10^{-5} \times T^2 - 1.9918 \times 10^{-7} \times T^3 \end{aligned}$$

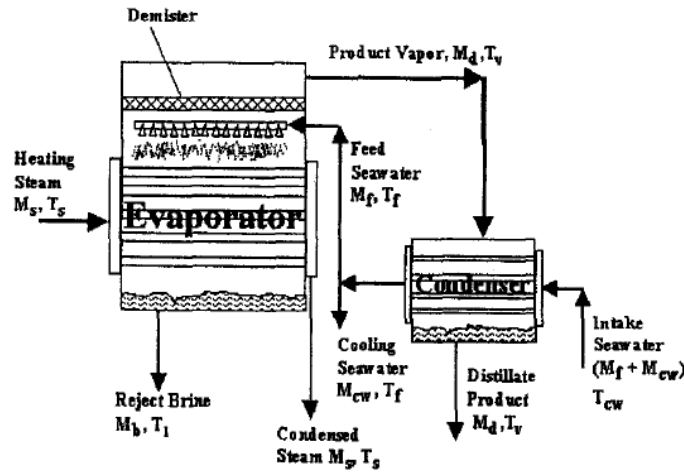


Figure (7) Schematic display of Single Effect Evaporation (SEE) process.

The exergy destruction rate is calculated based on the overall exergy balance equation:

$$I = W_{fp} + W_{bp} + W_{dp} + E_{si} - E_{so} + E_f + E_d, kW$$

Where,  $W$  and  $E$  represent the pumping power and exergy streams. And subscripts ( $fp$ ,  $bp$ ,  $dp$ ,  $s$ ) denotes the feed pump, brine pump, distillate pump and steam respectively. Thermo-economically, the MED process streams can be presented as follows;

$$C_d + C_{brine} + C_{steam-p} = C_{steam-med} + C_{fi} + Z_{med}^{IC\&OM}$$

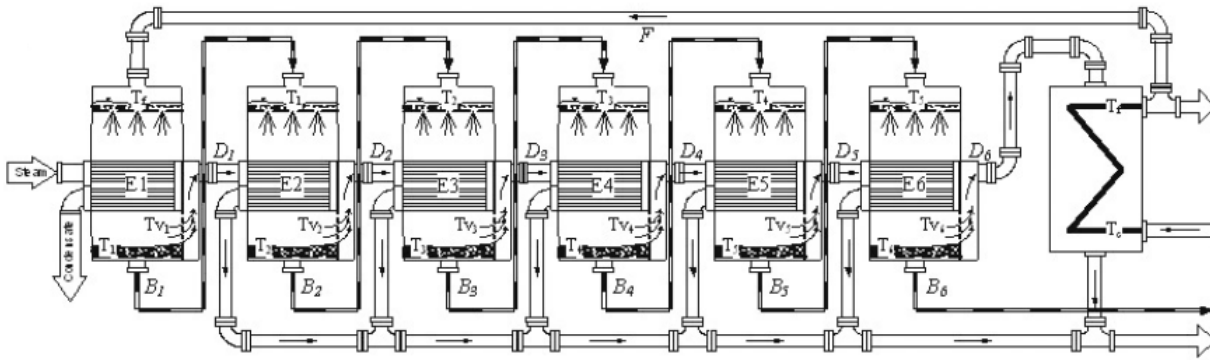
Where  $C_d$  is the distillate product cost \$/h,  $C_{brine}$  is the brine blow down cost and is specified as zero cost, and  $C_{fi}$ . So the relation for thermo-economic distillate cost would become as follows;

$$C_d = \frac{C_{fi} Ex_{fi} + C_{steam-med} \Delta Ex_{steam} + Z_{med}^{IC\&OM}}{Ex_d}$$

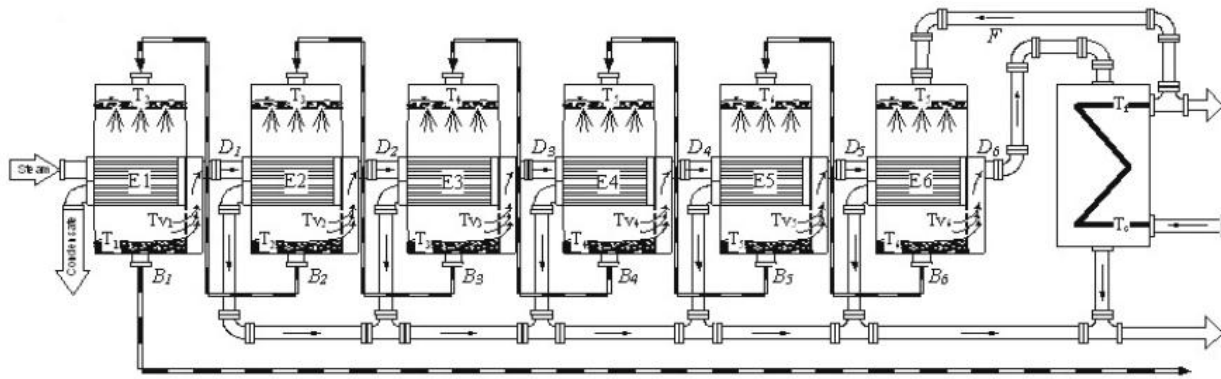
Figures below show schematic diagrams of different MED configurations.



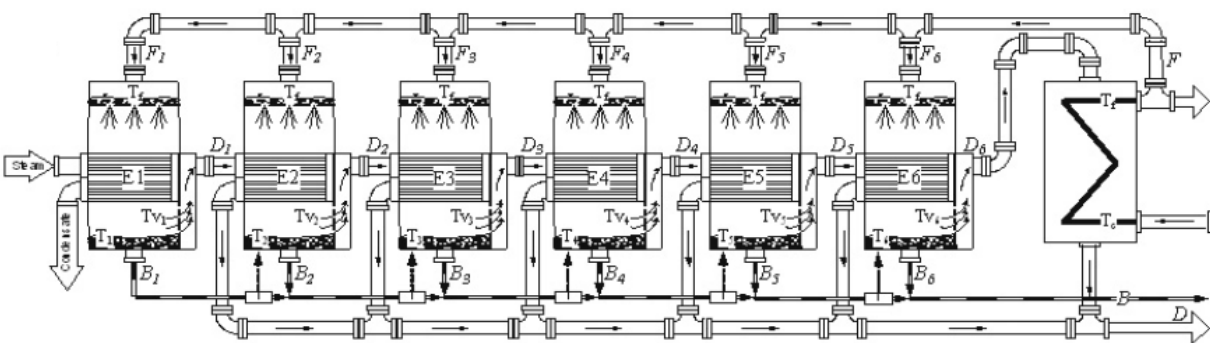
*B.1.7-a MED forward feed configuration*



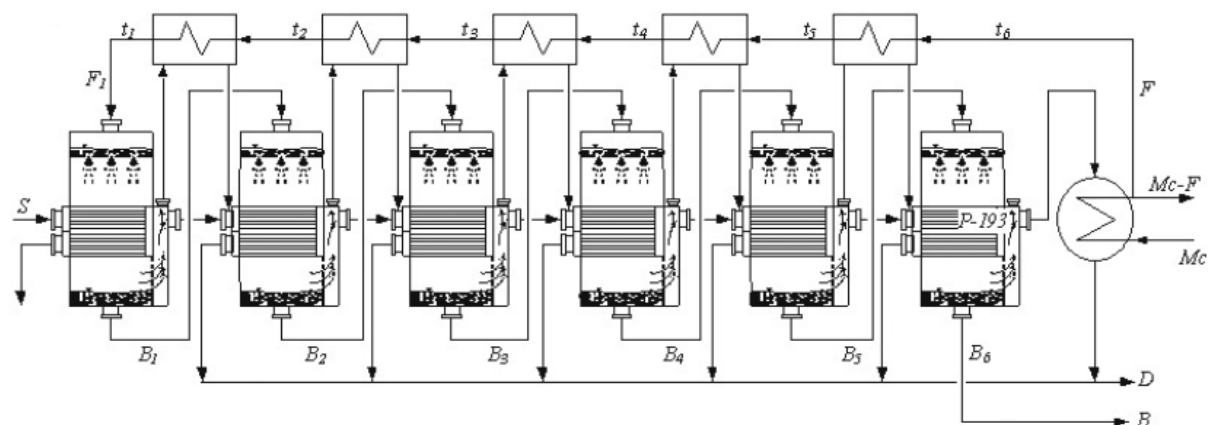
*B.1.7-b MED backward feed configuration*



*B.1.7-c MED parallel feed configuration*



#### B.1.7-d MED forward feed configuration with feed water heaters



### B.1.1.8 Multi effect distillation thermal vapor compression desalination unit

The MED-TVC evaporator is basically an MED evaporator fitted with a *thermo-compressor*. The purpose of the thermo-compression of the vapor is to take advantage of the pressure of the available steam, when this pressure is sufficient (i.e. above 2 bar abs), to enhance the units' performance. The incoming steam, called motive steam, is fed into the thermo-compressor through a sonic nozzle. Its expansion will allow low pressure steam from a cell of the evaporator to be sucked out. Both steams will be mixed in the thermo-compressor body. The mixture is then compressed to the pressure of the first bundle through a shock wave. The latent heat of the sucked vapor is thus recycled in the evaporator and is again available for desalination, leading to energy savings. The performance of a thermo-compressor is expressed by the mass of sucked steam (in kg) per kg of motive steam. Figure (8) shows a schematic diagram of multi effect distillation-thermal vapor compression process.

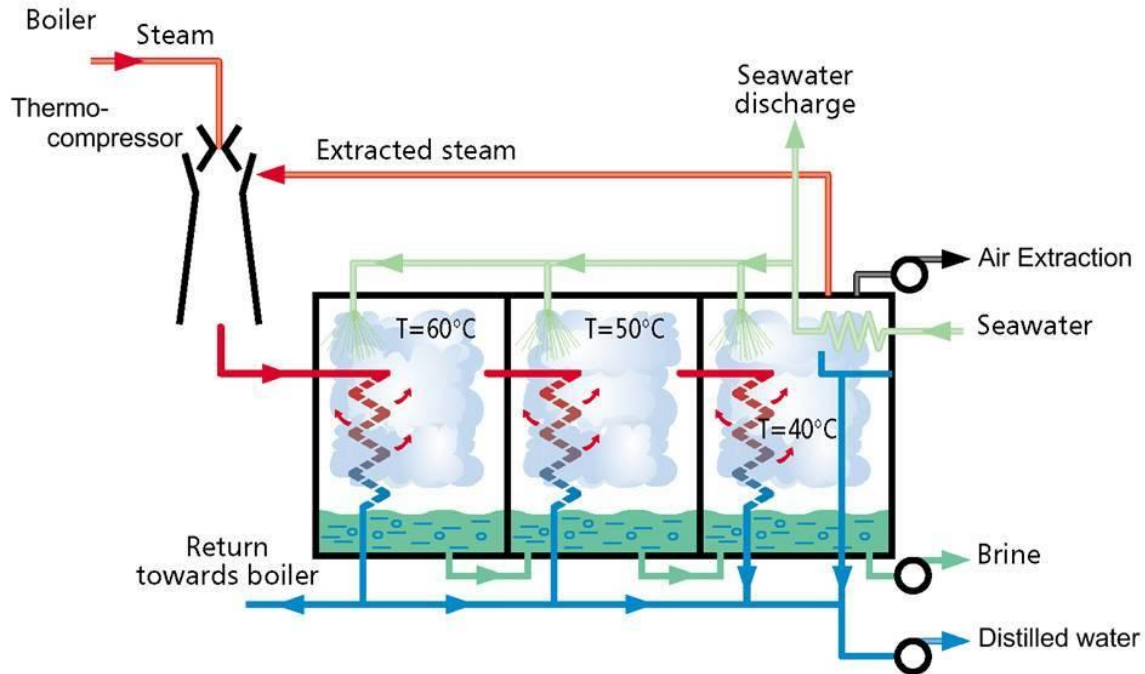


Figure (8) A schematic diagram of multi effect distillation thermal vapor compression process.

The most important and critical step in modeling the TVC desalination system is the evaluation of the performance of the steam jet ejector. The main data required from analyzing the steam jet ejector is the determination of the mass of motive steam required per unit mass of the entrained vapor ( $R_a$ ), given the pressure of the motive steam ( $P_{ms}$ ), discharge pressure ( $P_d$ ) and the suction pressure or entrained vapor pressure ( $P_{ev}$ ). There are a limited number of methods available in the literature to analysis the steam jet ejector. However, these methods require tedious and lengthy calculation procedures. Additionally, most of these methods are based on using many correction factors that depend heavily on the detail design of the ejector. Dessouky, [43], developed the following relationships to evaluate the performance of the steam jet ejector. The mathematical model of MED-TVC parallel feed configuration with feed water heaters is introduced as follows:

Last effect vapor temperature is function of blow down brine temperature:

$$T_v = T_b - BPE$$

And the temperature drop between effects is then obtained based on the number of effects:

$$\Delta T = (T_s - T_v)/N_{eff}$$

Where,  $T_s$  is the steam temperature,  $T_v$  is the vapor temperature.

Brine flow temperature profile is then obtained:

$$T_{bn} = T_b + (N_{eff} - 1)\Delta T$$

The corresponding saturation vapor pressure  $P_v$  kPa is obtained as follows:

$$P_v = -1.335e - 17 \times T_v^9 + 1.328e - 14 \times T_v^8 - 5.605e - 12 \times T_v^7 + 1.3e - 9 \times T_v^6 - 1.786e - 7 \times T_v^5 + 1.585e - 5 \times T_v^4 - 0.0007782 \times T_v^3 + 0.02466 \times T_v^2 - 0.2679 \times T_v + 1.739$$

The pressure drop in the demister in kPa/m (based on backing density  $\rho$ , vapor velocity  $V$ , wire diameter  $d$ , length of packing  $L_p$ ) is evaluated from the correlation below:

$$P_p = 3.88178 \times (\rho_p^{0.375798}) \times (V_v^{0.81317}) \times (d_w^{-1.56114147}) \times (L_p/1000)$$

The vapor pressure past the demister in kPa is then calculated:

$$P_{ev} = P_v - P_p$$

For mass balance and material the distillate profile is calculated according to 1<sup>st</sup> effect productivity as a function of latent heat and number of effects:

$$D_1 = \frac{D_t}{L(T_{v1}) \times \sum 1/L(T_{v1:n})}$$

Then the distillate profile can be calculated:

$$D_{1:n} = \frac{D_1 \times L(T_{v1})}{L(T_{v1:n})}$$

Brine and salt balances could be calculated:

$$M_b = D_t(S_f/(S_b - S_f))$$

The motive steam mass flow rate that entered the steam ejector is then calculated from the energy balance across the 1<sup>st</sup> effect:

$$M_{ms} = \frac{(M_f \times C_p(T_f, S_f) \times (T_b - T_f) + D_1 \times L(T_{v1}))}{L(T_s) \times (1 + \frac{1}{Ra})}$$

The amount of entrained vapor mass flow rate  $M_{ev}$  is then calculated from the entrainment ratio ( $Ra$ ):

$$M_{ev} = M_{ms}/Ra$$

The total steam mass flow rate to evaporator:

$$M_{st} = M_{ev} + M_{ms}$$

The system performance parameters are calculated as follows:

$$PR = D_t/M_{ms}$$

Heat Transfer areas H.T.A for the evaporator is calculated based on the evaporator thermal load  $Q_e$ :

$$Q_e = (M_{ms} + M_{ev}) \times L(T_s)$$

$$A_e = \frac{Q_e}{U_e(T_b) \times (\Delta T - BPE(T_b))}$$

Where,  $BPE$  is the boiling point elevation as a function of last effect brine temperature ( $T_b$ ).

Heat transfer area for feed heaters  $A_{fh}$  is calculated based on LMT:

$$A_{fh} = \frac{M_f \times C_p(\Delta t, S_f) \times \Delta t}{U_e(\Delta t) \times LMT_{fh}}$$

The steam ejector mathematical model is obtained based on the following model:

The pressure of compressed vapor kPa  $P_s$  is function of vapor pressure and compression ratio (Cr) and the entrained vapor from effect number  $n$ :

$$P_s = Cr \times P_{ev}$$

The high velocity at Nozzle exit ( $V_{ne}$ ) can be calculated based on enthalpy difference ( $h_{si} - h_{so}$ ) across the ejector nozzle:

$$V_{ne} = \sqrt{(2000 \times (h_{si} - h_{so}))}$$

The entrainment ratio is obtained as following by calculating temperature and pressure correction factors:

$$PCF = 3 \times 10^{-7} \times P_{ms}^2 - 0.0009 \times P_{ms} + 1.6101$$

Where,  $P_{ms}$  is the motive steam pressure in kPa, and  $T_v$  is the vapor temperature from effect number  $n$ .

$$TCF = 2 \times 10^{-8} \times T_v^2 - 0.0006 \times T_v + 1.0047 [43]$$

$$Ra = 0.296 \times \frac{P_s^{1.19}}{P_{ev}^{1.04}} \times \left(\frac{P_{ms}}{P_{ev}}\right)^{0.015} \times \left(\frac{PCF}{TCF}\right)$$

The expansion ratio:

$$Er = \frac{P_{ms}}{P_{ev}}$$

The nozzle cross section area ( $A_1$ ) based on the nozzle diameter  $D_n$ :

$$A_1 = \frac{\pi D_n^2}{4}$$

The area ratios ( $A_1/A_3$  &  $A_2/A_1$ ) and the areas ( $A_3$  &  $A_2$ ) of the nozzle outlet and the diffuser are then calculated:

$$\frac{A_1}{A_3} = 0.34 \times P_s^{1.19} \times P_{ms}^{-1.12} \times Ra^{-0.16}$$

$$\frac{A_2}{A_1} = 1.04 \times P_s^{-0.83} \times P_{ms}^{0.86} \times Ra^{-0.12}$$

Nozzle outlet area  $m^2$ :

$$A_3 = \frac{A_1}{\frac{A_1}{A_3}}$$

Diffuser area  $m^2$ :

$$A_2 = A_1 \times \frac{A_2}{A_1}$$

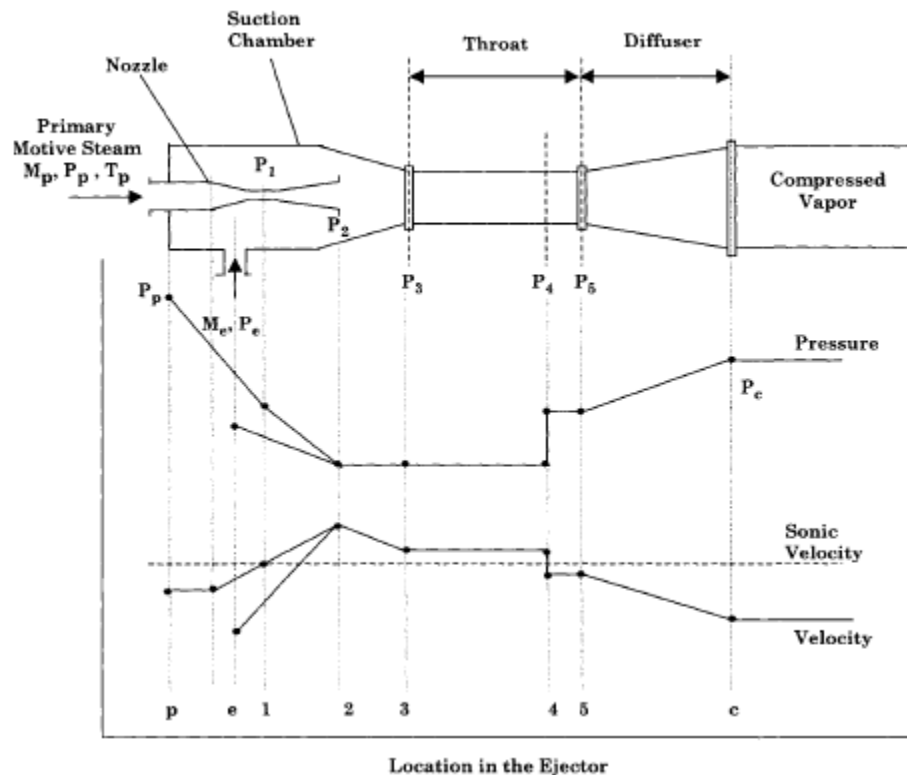


Figure (9) Pressure and velocity profiles inside the steam jet ejector.

#### B.1.9 Multi effect distillation mechanical vapor compression desalination unit

Mechanical vapor-compression desalination process (MVC) is the most attractive and valuable among different single stage desalination processes. The MVC system is compact, confined, and does not require external heating source, which is opposite to thermal, absorption, or adsorption vapor compression. The system is driven by electric power; therefore, it is suitable for remote population areas with access to power grid lines. Another advantage of the MVC system is the absence of the down condenser and the cooling water requirements. This is because the compressor operates on the entire vapor formed within the system. Other advantages of the system include:

- Moderate investment cost.
- Proven industrial reliability to long lifetime operation.
- Simple seawater intake and pretreatment.
- The system adopts the horizontal falling film tube configuration, which allows for high heat transfer coefficient.
- The low temperature operation,  $60^{\circ}\text{C}$ , allows for reduced scaling and heat losses and minimum requirement of thermal insulation.
- The system is modular type and it is simple to enlarge production volume by adopting additional modules.
- High product purity.
- Simple system adjustment to load variations, through temperature manipulation.

- Provide low power to water ratio without reducing the fuel utilization potential.

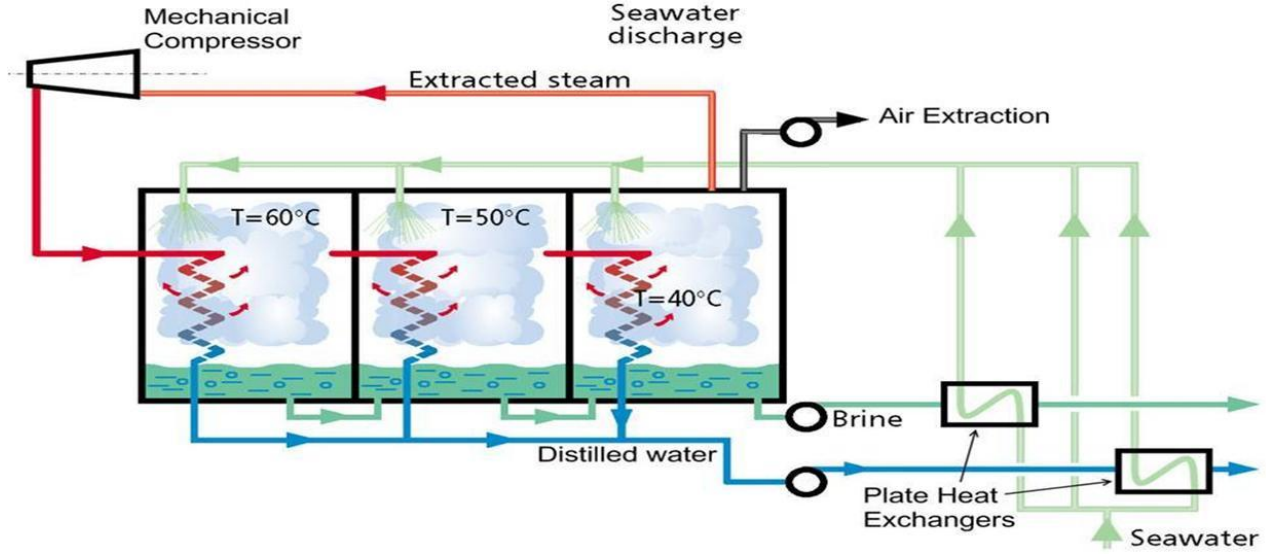


Figure (10) A schematic diagram of multi effect distillation mechanical vapor compression process.

The mathematical model of MED part considered the same as that presented in MED-TVC. Therefore, the model is pinpointed on the mechanical vapor compressor unit. The specific volume of inlet vapor at brine temperature is obtained as follows:

$$v_{comp_i} = 163.3453 - 8.04142 \times T + 0.17102 \times T^2 - 1.87812 \times 10^{-3} \times T^3 + 1.03842 \times 10^{-5} \times T^4 - 2.28215 \times 10^{-8} \times T^5$$

The compression ratio:

$$Cr = \frac{P_{comp_o}}{P_{comp_i}}$$

The compressor horse power needed:

$$W_{comp} = M_s \times \frac{\gamma}{\eta_{comp} \times (\gamma - 1)} \times (P_{comp_i} \times v_{comp_i}) \times \left( \frac{P_{comp_o}}{P_{comp_i}} \right)^{\left( \frac{\gamma-1}{\gamma} \right)}$$

Where,  $M_s$  is the steam mass flow rate in kg/s,  $\gamma$  is the isentropic index, and  $P_{comp}$  is the pressure in kPa.

## Appendix-C

### C. Cost Correlations for Desalination Processes

#### C.1 Reverse Osmosis (RO) [56]

Direct capital costs DCC can be calculated based on the following steps:

Cost of seawater and intake pump ( $CC_{swip}$ ) pretreatment  $\$/m^3/day$ ,

$$CC_{swip} = 996 \times M_f^{0.8} [56]$$

Cost of high pressure pump ( $CC_{hpp}$ ) \$,

$$CC_{hpp} = 393000 + 10710 \times \Delta P_f [56]$$

Premeator price \$,

$$P_p = 1000$$

Pressure vessel price \$,

$$PV_p = 1000$$

Number of premeators  $N_p$  as a function of elements ( $n_e$ ) and pressure vessels ( $n_v$ ),

$$N_p = n_e \times n_v$$

Elements capital costs (membrane + pressure vessels),

$$CC_e = Fe \times P_p \times N_p + Fe \times PV_p \times n_v$$

Where,  $Fe=1$  as a corrective factor,

The equipment capital cost is then calculated as follows:

$$CC_{equip} = CC_{swip} + CC_{hpp} + CC_e$$

And the site cost is calculated from the following correlation:

$$CC_{site} = 10\% \times CC_{equip} [56]$$

Then the direct capital cost is calculated:

$$DCC = CC_{equip} + CC_{site}$$

Indirect capital costs (ICC), total capital costs (TCC), annualized capital costs, and operating & maintenance cost are then calculated as presented in the following table. Where, ACC is the annual capital cost  $\$/year$ ,  $A_f$  is the annualized factor  $1/y$ .

$OC_{power}$ : operating cost of annual power  $\$/kWh$

$OC_{labor}$ : annual labor cost  $\$/m^3$

$OC_{mnce}$ : annual maintenance cost  $\$/m^3$

$OC_{chmcal}$ : annual chemical cost  $\$/m^3$

$OC_{insurce}$ : annual insurance cost

$OC_{mbrane}$ : annual operating cost of membranes



$OC_t = OC_{power} + OC_{labor} + OC_{mtnce} + OC_{chmcal} + OC_{insurce} + OC_{mbrne}$ : *operating cost \$/year*  
*Zro: The hourly costs for the RO \$/hr*

*ICC and O&M costs for RO desalination plant [56].*

<i>DCC, \$</i>	<i>ICC, \$</i>	<i>TCC, \$</i>	<i>ACC, \$/year</i>	<i>O&amp;M, \$/year</i>	<i>Z<sup>IC&amp;OM</sup>, \$/h</i>
$CC_{swip} = 996 \times M_f^{0.8}$	$ICC = 27\% \times$	$TCC = ICC +$	$ACC = TCC \times$	$OC_{power} = LF \times 0.06 \times SPC \times M_d$	$Z^{IC\&OM} =$
$CC_{hpp} = 393000 + 10710 \times \Delta P_f$	<i>DCC</i>	<i>DCC</i>	<i>A<sub>f</sub></i>	$OC_{labor} = LF \times 0.01 \times M_d$	$(ACC + OC_{ro})$
$CC_e = Fe \times P_p \times N_p + Fe \times PV_p \times n_v$				$OC_{chm} = LF \times 0.04 \times M_d$	<i>/8760</i>
$CC_{equip} = CC_{swip} + CC_{hpp} + CC_e$				$OC_{insur} = 0.005 \times TCC \times A_f$	
$CC_{site} = 10\% \times CC_{equip}$				$OC_{memb} = P_p \times N_p / LT_m$	
$DCC = CC_{equip} + CC_{site}$				$OC_{ro} = OC_{power} + OC_{labor} +$	
				$OC_{chm} + OC_{insur} + OC_{memb}$	

## C.2 Multi Effect Distillation (MED)

For MED process, the following table summarizes the cost consideration that considered in this study.

Cost parameters for MED desalination plant [43].

Parameter:	Correlation:
Interest rate, %	5
Plant life time, y	20
Amortization factor, 1/y	$A_f = \frac{i \cdot (1+i)^{LTp}}{(1+i)^{LTp} - 1}$
Direct capital costs, \$	$DCC = 9 \times 10^5$
Annual fixed charges, \$/y	$AFC = A_f \times DCC$
Annual heating steam costs, \$/y	$AHSC = \frac{SHC \times L_s \times LF \times M_d \times 365}{1000 \times PR}, SHC = \frac{1.466\$}{Mkj}$
Annual electric power cost, \$/y	$AEPC = SEC \times SPC \times LF \times M_d \times 365, SEC = 0.06\$/kWh$
Annual chemical cost, \$/y	$ACC = SCC \times LF \times M_d \times 365, SCC = 0.025\$/m^3$
Annual labor cost, \$/y	$ALC = SLC \times LF \times M_d \times 365, SLC = 0.1\$/m^3$
Total annual cost, \$/y	$TAC_{MED} = AFC + AHSC + AEPC + ACC + ALC$
Operating and maintenance costs, \$	$OMC_{MED} = 0.02 \times DCC$
Hourly operating & maintenance costs in \$/h	$Z_{MED}^{IC\&OM} = \frac{OMC_{MED} \times A_f + AFC}{8760}$
The total plant costs, \$/y	$TPC = TCC_{col} + TCC_{bhx} + TCC_{rec} + TCC_p + TCC_t + TAC_{MED}$
Total water price \$/m <sup>3</sup>	$TWP = TPC / (D_p \times 365 \times LF)$

For the operation of vapor compressor with MED, the following correlation calculates the compressor costs based on compression ratio (CR), compressor efficiency, steam mass flow rate  $M_s$ , and operating hours (OH).

$$IC_{comp} = 7364 \times M_s \times CR \times \left( \frac{\eta_{comp}}{1-\eta_{comp}} \right)^{0.7}, \text{ Indirect capital cost [43]}$$

$$TCC_{comp} = IC_{comp} \times A_f, \text{ Total capital costs}$$

$$Z_{comp} = TCC_{comp} / (OH \times 365), \text{ Hourly costs}$$

The hourly cost for the steam ejector is calculated based on the following correlation,

$$Z_{steam\ ejector} = 1000 \times 16.14 \times 0.989 \times \left( M_{vapor} \times \left( \frac{T_i}{P_i} \right)^{0.05} \right) \times P_e^{-0.75}, \$/h [43]$$

### C.3 Multi Stage Flash (MSF)

For this part, investment and operating & maintenance costs analyses are performed for each component, solar field, steam turbine, condenser, and pump units. For that purpose; the amortization factor is estimated based on the following relation [43];

$$A_f = \frac{i \cdot (1+i)^{LT_p}}{(1+i)^{LT_p} - 1}$$

Where  $i$  is the interest rate and set as 5%,  $LT_p$  is the plant lifetime and set as 20 years. For this MSF part, cost analyses are estimated based on direct capital costs ( $DCC$ ), indirect capital costs ( $ICC$ ), and the total capital costs ( $TCC$ ). For MSF desalination plant, the annual fixed charges in \$/y may be represented by [43] as following;

$$AFC = A_f \times (DCC + IDCC)$$

And  $IDCC$  is the indirect capital costs and equal to  $0.4 \times DCC$  [43]. The operating and maintenance costs are presented in \$ as following;

$$OMC = 0.02 \times (DCC + IDCC)$$

And the annual chemical cost is obtained in \$/y as;

$$ACC = SCC \times LF \times D_p \times 365$$

Where,  $SCC$  is the specific chemical costs ( $0.025\$/m^3$  [43]), and  $LF$  is the plant load factor and is fixed about 0.9, and  $D_p$  is the distillate product. The annual labor costs in \$/y is given as following;

$$ALC = SLC \times LF \times D_p \times 365$$

Where,  $SLC$  is the specific labor costs ( $0.1\$/m^3$ ). The total annual costs in \$/y for MSF is calculated according to the following,

$$TAC_{msf} = AFC + ACC + ALC + (OMC \times A_f)$$

And the unit product cost in \$ is found as;

$$UPC_{msf} = TAC_{msf} / (D_p \times 365 \times LF)$$

The operating and maintenance cost in \$/h for MSF ( $Z_{msf}^{IC\&OM}$ ) is found to be as following;

$$Z_{msf}^{IC\&OM} = (OMC \times A_f + AFC) / 8760$$

Then the total water price \$/m<sup>3</sup> should be found as;

$$TWP = TPC / (D_p \times 365 \times LF)$$

## Appendix-D

### D. SDS Software Package

SDS software models, simulates, and analyzes solar desalination systems. It enables user to pose a question about a system, model the system, and see what happens. With SDS, user can easily build models from scratch, or modify existing models to meet your needs. It becomes very easy to solve real problems in a variety of industries, including:

- Concentrated Solar Plants (CSP)
- Different types and configurations of desalination processes
- Different techniques of solar desalination systems
- Different thermal units
- Different analysis

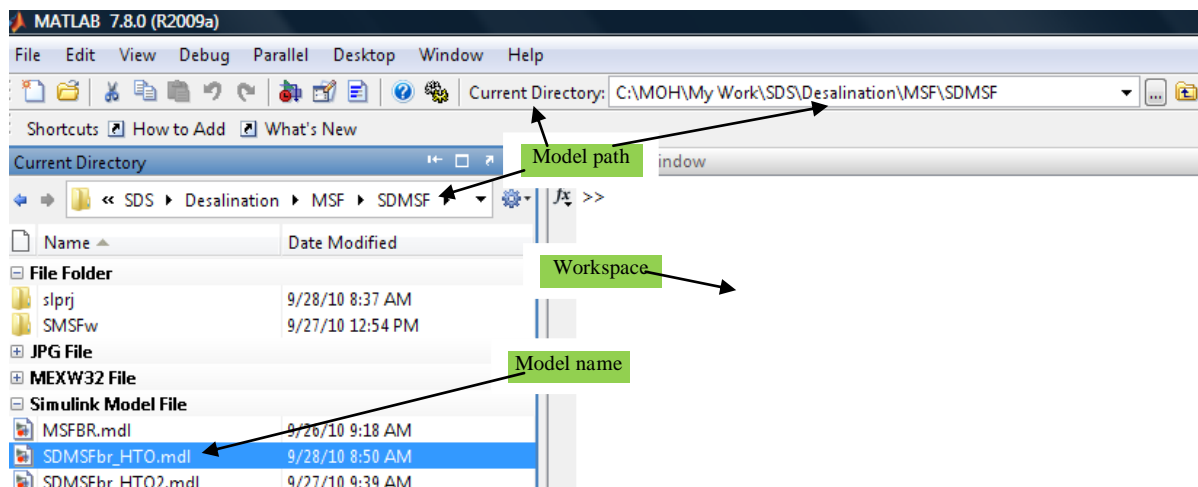
SDS provides a graphical user interface (GUI) for building models as block diagrams, allowing user to draw models as you would with pencil and paper. Also, it includes a comprehensive block library of sinks, sources, linear and nonlinear components, and connectors. If these blocks do not meet your needs, however, user can also create his own blocks (units). The interactive graphical environment simplifies the modeling process, eliminating the need to formulate differential and difference equations in a language or program.

SDS software is tightly integrated with the MATLAB environment. It requires MATLAB to run, depending on it to define and evaluate model and block parameters. It can also utilize many MATLAB features. For example, Simulink can use the MATLAB environment to:

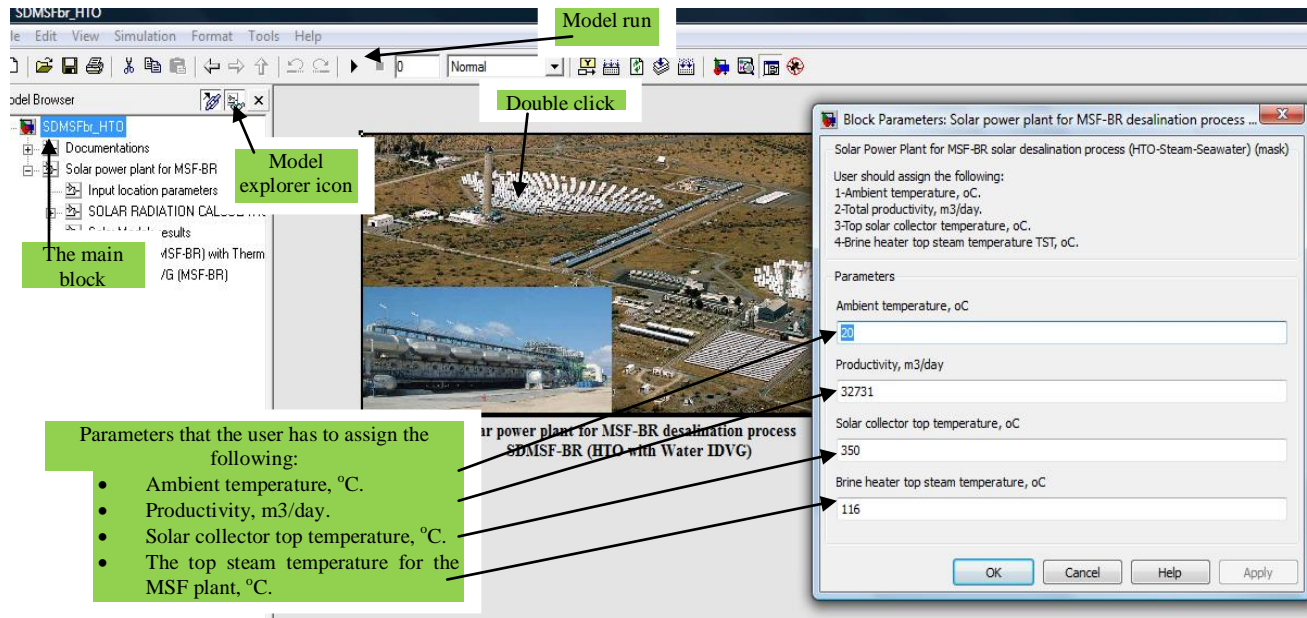
- Define model inputs.
- Store model outputs for analysis and visualization.
- Perform functions within a model, through integrated calls to MATLAB operators and functions.

#### D.1 Multi-Stage Flash Brine Recycle (MSF-BR) Model: Case Study

To run the solar combined with MSF-BR desalination model, user has to log into the SDS path then double clicking on the file name of the model (SDMSFbr\_HTO.mdl).



To assign the plant productivity  $\text{m}^3/\text{day}$ , ambient temperature  $^{\circ}\text{C}$  and solar radiation data, user has to click on the model explorer icon then double clicking on the main block. The block parameters menu will open and the user can easily assign the main input data. Also it is very easy to assign the data of the location such as longitude, latitude, and the day number of the year.



In the sub menu, user can easily find out the units and the sub-units that represent the proposed process. In the following figure, the process units are PTC solar field, boiler heat exchanger unit, pump, brine heater, and MSF-BR desalination plant. By double clicking on the blocks, user can easily specify the operating conditions and the permitted design consideration for each unit individually. User also has the ability to use the capabilities of the MatLab/SimuLink that included in the software tools. The tools are concluded in to the following items:

- ✓ Users can easily copying the units and duplicate and pasting them.
- ✓ User can delete the unwanted units.
- ✓ User can take copies to clipboard with high permeation to edit and reform.
- ✓ Also printing the models and their sub models is easily available.
- ✓ User can redo his work for instant accident such as removing or deleting any parameter or unit.
- ✓ User can drive out his results through different ways such as “mat” files, matlab “workspace”, or/and display block.
- ✓ Also, it is become easy for the user to handle the “mat” to an “excel sheet” or construct a new figure.

Consider an example of MSF-BR desalination plant with a capacity of  **$32728\text{m}^3/\text{day}$** . The input parameters and specifications are illustrated in the following table. The process validity of MSF-BR example is examined with Dessouky (Fundamental of salt water desalination, Book) and also illustrated in Table below. The data results show a good agreement for the developed program (SDS) with Dessouky [50] results.

32728m<sup>3</sup>/day MSF-BR

Top brine temperature (TBT), °C

106

Brine blow down temperature, °C

40.2

Feed seawater temperature, °C

25

Cooling water splitter ratio

0.5082

Sea water salinity, ppm

42000

Brine blow down salinity, ppm

70000

No. of stages

24 (21/3)

Chamber Load, kg/s.m

180

Vapor velocity, m/s

12

Weir coefficient

0.5

Design point results:

Dessouky [43]

SDS

Total feed, kg/s

1861

1862

Distillate flow rate, kg/s

378.8

378.8

Make up, kg/s

947

947

Brine recycle flow rate, kg/s

3384

3384

Brine blow-down flow rate, kg/s

568.2

568.2

Steam mass flow rate, kg/s

52.52

53.04

Top vapor temperature, °C

101.2

101.98

Top feed temperature, °C

97.75

97.78

Recycle blow down temperature, °C

48.25

48.42

Vapor temperature at last stage, °C

—

38.2

Recycle stream salinity, ppm

62170

62163

Stage length, m

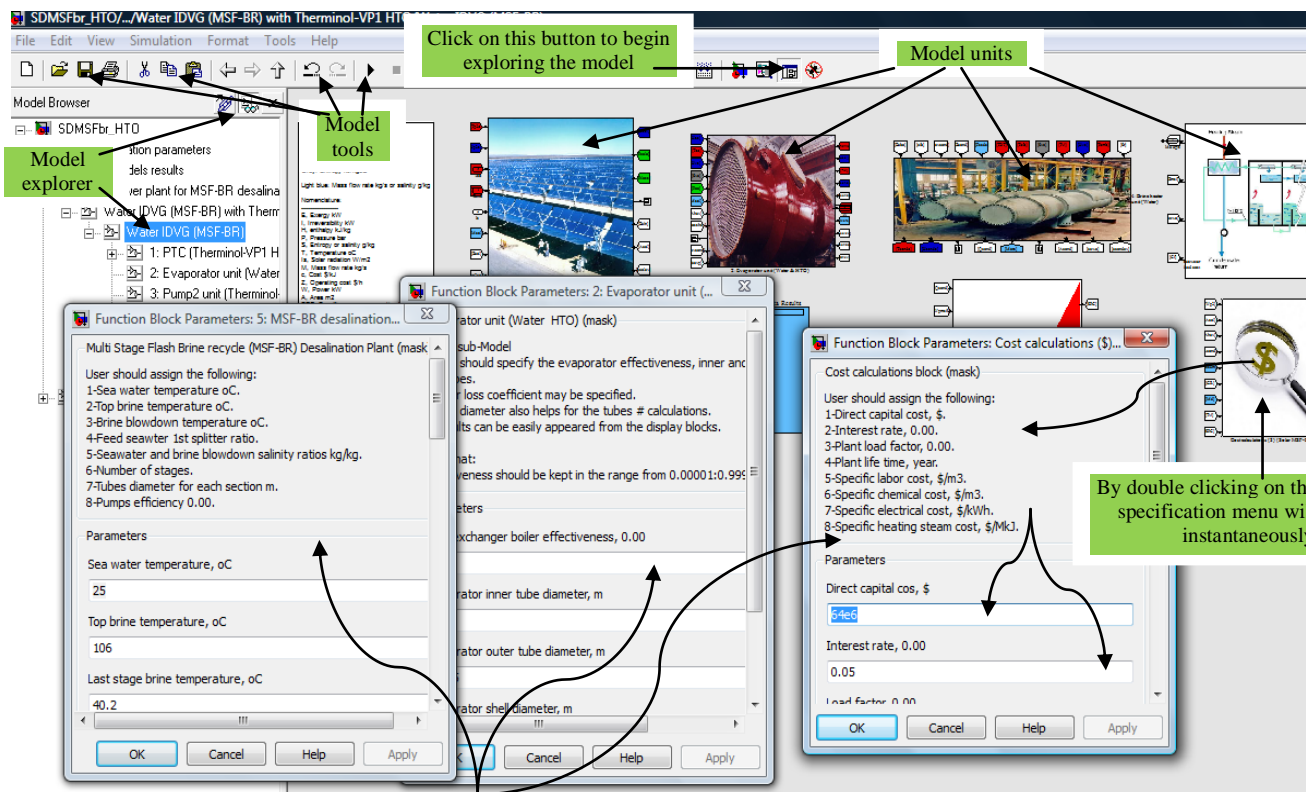
2.56

2.58

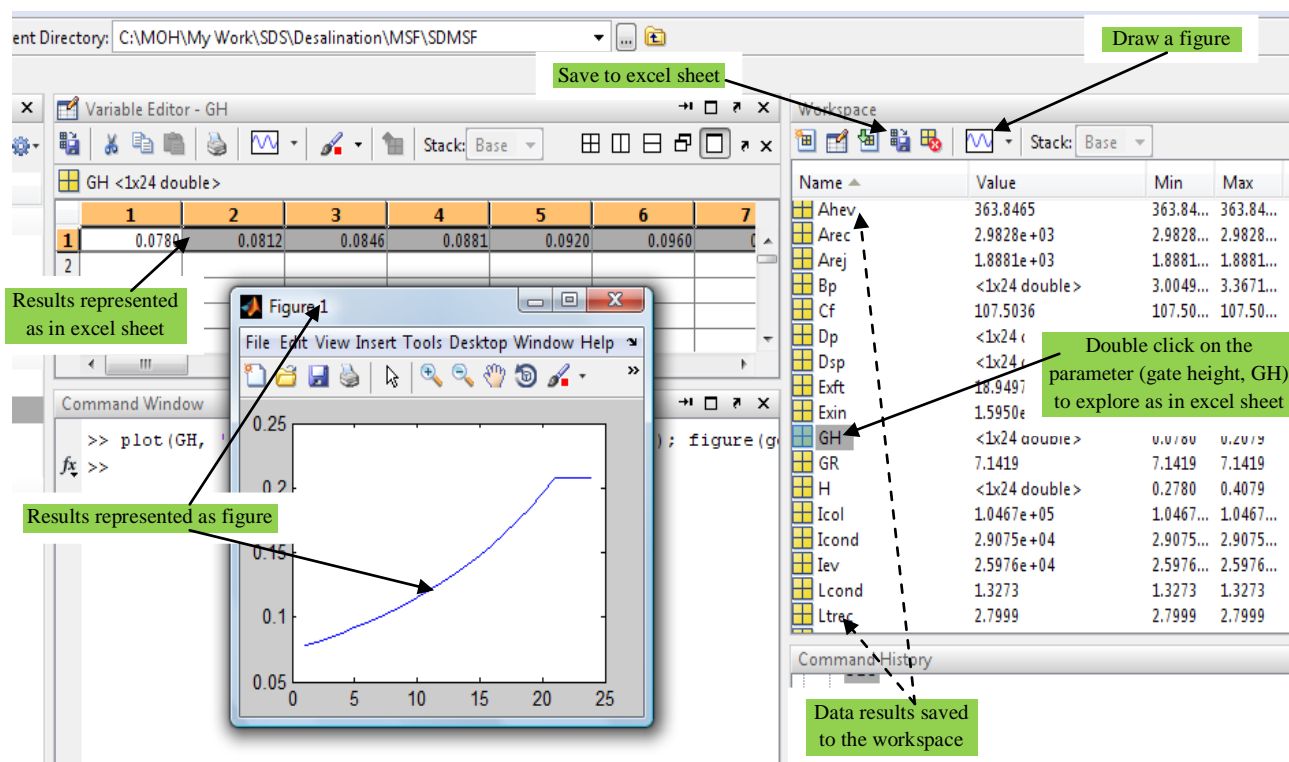
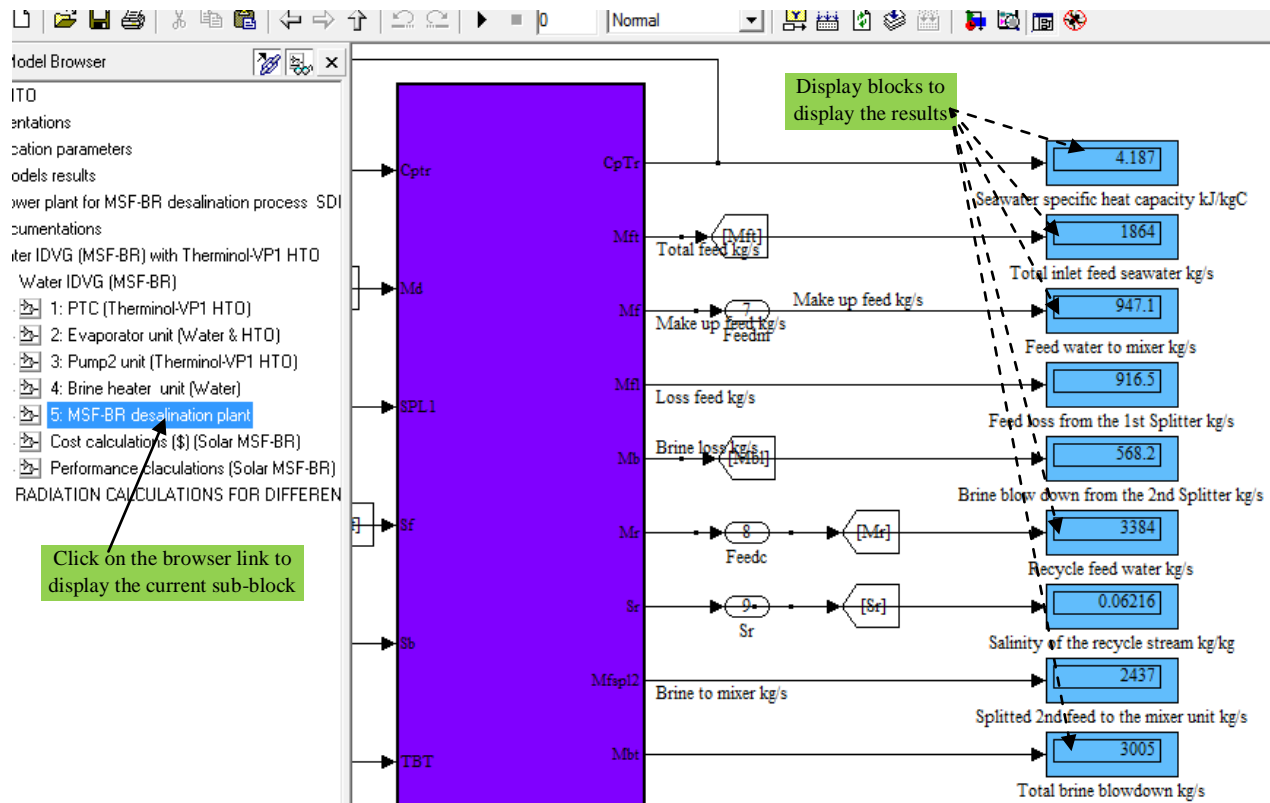
Performance ratio

7.21

7.14



Specification blocks related to each unit





## D.2 Solar Radiation model

Solar radiation model is a very effective tool to specify the solar energy over the location of operation. The model code is presented as following [40]:

The declination angle throughout the year is defined as following:

$$d = 23.45 \sin \left[ \frac{360}{365} (284 + n) \right]$$

Where  $n$  is the day of the year. The value of  $n$  for any day of the month  $d$  can be determined easily with the aid of the table below.

Month	$n$ for the Day of the Month, $D$	Month	$n$ for the Day of the Month, $D$
January	$D$	July	$181 + D$
February	$31 + D$	August	$212 + D$
March	$59 + D$	September	$243 + D$
April	$90 + D$	October	$273 + D$
May	$120 + D$	November	$304 + D$
June	$151 + D$	December	$334 + D$

The hour angle  $h$  is calculated from the following expression:

$$h = 15(LST - 12)$$

Where LST = Local Solar Time [hr].

The following equations are presented to calculate these angles:

$$\cos \theta_H = \cos l \cosh \cos d + \sin l \sin d$$

$$\text{Since } \beta = 90 - \theta_H,$$

$$\sin \beta = \cos l \cosh \cos d + \sin l \sin d$$

The relation gives the sun's azimuth,  $\phi$ :

$$\cos \phi = \frac{1}{\cos \beta} (\cos d \sin l \cos h - \sin d \cos l)$$

A summary of the sign convention is:

$l$ : north latitudes are positive, south latitudes are negative

$d$ : the declination is positive when the sun's rays are north of the equator, i.e. for the summer period in the northern hemisphere, March 22 to September 22 approximately, and negative when the sun's rays are south of the equator.

$h$ : the hour angle is negative before solar noon and positive after solar noon.

$\phi$ : the sun's azimuth angle is negative east of south and positive west of south.

The solar models for the estimation of the total insolation on horizontal surfaces:



### ASHREA correlations:

$$It1 = (G_{bn} \times \cos(z)) + G_d$$

$$G_{bn} = A \exp(-B / \cos(z))$$

$$G_d = C \times G_{bn}$$

$$\cos(z) = \sin\phi \sin(d) + \cos\phi \cos(d) \cos(h)$$

Where,

$A$  is the apparent solar irradiance at air mass zero,  $B$  is the atmosphere extinction coefficient, and  $C$  is the diffuse radiation factor and  $z$  is the zenith angle. The following table shows the coefficients for average clear day solar radiation calculations.

	A		B	C	Declination, deg	Equation of Time, hr
	Btu hr · ft <sup>2</sup>	W m <sup>2</sup>	Dimensionless Ratios			
January	390	1230	0.142	0.058	−20.0	−0.19
February	385	1215	0.144	0.060	−10.8	−0.23
March	376	1186	0.156	0.071	0.0	−0.13
April	360	1136	0.180	0.097	11.6	0.02
May	350	1104	0.196	0.121	20.0	0.06
June	345	1088	0.205	0.134	23.45	−0.02
July	344	1085	0.207	0.136	20.6	−0.10
August	351	1107	0.201	0.122	12.3	−0.04
September	365	1151	0.177	0.092	0	0.13
October	378	1192	0.160	0.073	−10.5	0.26
November	387	1221	0.149	0.063	−19.8	0.23
December	391	1233	0.142	0.057	−23.45	0.03

### HOTTEL MODEL:

Unlike ASHREA model, which gives an estimate for both direct and diffuse radiation, the present model is capable of estimating the direct irradiation only. The direct beam irradiation on horizontal surface is given as following:

$$G = G_o(a_0 + a_1 e^{-k/\cos(z)})$$

Where;

$$G_o = 1353 \times (1 + 0.033 \cos(\frac{360n}{365})) \cos(z)$$

For tropical climate type:

$$\begin{aligned} a_0 &= 0.4237 - 0.00821(6-A)^2 \\ a_1 &= 0.5055 + 0.00595(6.5-A)^2 \\ k &= 0.2711 + 0.01858(2.5-A)^2 \end{aligned}$$

Where  $A$  is the sea level parameter.

## References

- [1] Ali M. El-Nashar, The economic feasibility of small solar MED seawater desalination plants for remote arid areas, *Desalination* 134 (2001) 173–186.
- [2] Fath H. desalination technology: The role of Egypt in the region. Fifth International Water Technology Conference, Alexandria, Egypt (2000).
- [3] Hisham M. El-Kady, F. El-Shibini. Desalination in Egypt and the future application in supplementary irrigation, *Desalination* 136 (2001) 63–72.
- [4] Azza Hafez, Samir El-Manharawy “Economics of seawater RO desalination in the Red Sea region, Egypt. Part 1. A case study”, *Desalination* 153 (2002) 335–347.
- [5] <http://www.oksolar.com/abctech/solar-radiation.htm>.
- [6] Hazim Mohameed Qiblawey, Fawzi Banat. Solar thermal desalination technologies. *Desalination*. 220 (2008) 633–644.
- [7] Mohamed A. Eltawil, Zhao Zhengming, Liqiang Yuan. A review of renewable energy technologies integrated with desalination systems. *Renewable and Sustainable Energy Reviews* 13 (2009) 2245–2262.
- [8] Soteris A. Kalogirou, Solar thermal collectors and applications, *Progress in Energy and Combustion Science* 30 (2004) 231–295.
- [9] Moh’d S. Abu-Jabal, I. Kamiya, Y. Narasaki, Proving test for a solar- powered desalination system in Gaza–Palestine, *Desalination* 137 (2001) 1–6.
- [10] Kyritsis S. Proceedings of the Mediterranean Conference on Renewable Energy Sources for Water Production. European Commission, EURORED Network, CRES, EDS, Santorini, Greece; 10–12 June, 1996. p. 265–70.
- [11] Valverde Muela V. Planta Desaladora con Energía Solar de Arinaga (Las Palmas de Gran Canaria). Departamento de Investigacion Nuevas Fuentes. Centro de Estudios de la Energía; April, 1982.
- [12] Palma F. Seminar on new technologies for the use of renewable energies in water desalination, Athens, 1991. Commission of the European Communities, DG XVII for Energy, CRES (Centre for Renewable Energy Sources) 1991.
- [13] Manjares R, Galvan M. Solar multistage flash evaporation (SMSF) as a solar energy application on desalination processes. Description of one demonstration project. *Desalination* 1979;31(1–3):545–54.
- [14] Delyannis EE. Status of solar assisted desalination: a review, *Desalination* 1987; 67:3–19.
- [15] Hanafi A. Design and performance of solar MSF desalination system. *Desalination* 1991; 82 (1–3): 165–74.
- [16] Banat F, Jwaied N. Economic evaluation of desalination by small-scale autonomous solar-powered membrane distillation units. *Desalination* 2008; 220:566–73.
- [18] A. Lamei, P. van der Zaag, E. von Münch, Basic cost equations to estimate unit production costs for RO desalination and long-distance piping to supply water to tourism-dominated arid coastal regions of Egypt, *Desalination* 225 (2008) 1–12.
- [19] Patrick Hearps, Dylan McConnell. Renewable Energy Technology Cost Review. Melbourne Energy Institute, Technical Paper Series (2011). [www.energy.unimelb.edu.au](http://www.energy.unimelb.edu.au).
- [20] Veera Gnaneswar Gude a, Nagamany Nirmalakhandan b, Shuguang Deng. Renewable and sustainable approaches for desalination. *Renewable and Sustainable Energy Reviews* 14 (2010) 2641–2654.
- [21] T.S. Saitoh and A. Hoshi, Proposed solar Rankine cycle system with phase change steam accumulator and CPC solar collector. IECEC2002, paper no. 20150.

- [22] Vahab Hassani, Henry W. Price, Modular trough power plants, Proceedings of Solar Forum 2001, Solar Energy: The Power to Choose, APRIL 21-25, 2001, Washington, DC.
- [23] Andrew C. McMahan, Design & optimization of organic rankine cycle solar-thermal power plants, university of wisconsin-madison 2006.
- [24] Lourdes García-Rodríguez, Julián Blanco-Gálvez, Solar-heated Rankine cycles for water and electricity production: POWERSOL project, Desalination 212 (2007) 311–318.
- [25] D. Manolakos, G. Papadakis, S. Kyritsis, K. Bouzianas, Experimental evaluation of an autonomous low-temperature solar Rankine cycle system for reverse osmosis desalination, Desalination 203 (2007) 366–374.
- [26] Rong Zhang, Hiroshi Yamaguchi, Katsumi Fujima, Masatoshi Enomoto and Noboru Sawada, A Feasibility Study of CO<sub>2</sub>-Based Rankine Cycle Powered by Solar Energy, JSME International Journal, Series B, Vol.48, No.3, 2005.
- [27] A. S. Nafey, Simulation of solar heating systems—an overview, Renewable and Sustainable Energy Reviews 9 (2005) 576–591.
- [28] O.A. Hamed and S. Aly, Simulation and design of MSF desalination process. Desalination, 80 (1991) 1–14.
- [29] S. Ithara and L.I. Stiel, The optimal design of multistage flash evaporators by dynamic programming, Desalination, 4 (1968) 248–257.
- [30] H. Sonnenschein, A modular optimizing calculation method of power station energy balance and plant efficiency. J. Eng. Power, 104 (1982) 255.
- [31] E. Perz, A computer method for thermal power cycle calculation. Trans. ASME, 113 (1991) 184–189.
- [32] Mahmoud Bourouis, Luc Pibouleau, Pascal Floquet, Serge Domenech, Darwish M. K. Al-Gobaisi, Simulation and data validation of multi stage flash desalination plants, Desalination, 115 (1998) 1–14.
- [33] N. Woudstra and M. Verschoor, CYCLE-TEMPO, Delft University of Technology, 1995.
- [34] P. Schausberger, G. Rheina-Wolbeck, A. Friedl, M. Harasek and E.W. Perz, Enhancement of an object-oriented power plant simulator by seawater desalination topics. Desalination, 156 (2003) 335–360.
- [35] J. Uche, L. Serra, L. Alberto, A. Valero, J. Turrigano and C. Torres, Software for the analysis of water and energy systems. Desalination, 156 (2003) 367–378.
- [36] A.A. Mabrouk et. al, A new visual package for design and simulation of desalination processes. Desalination 194 (2006) 281–296.
- [37] Adrian Gambier, Essameddin Badreddin, Dynamic modelling of MSF plants for automatic control and simulation purposes: a survey. Desalination 166 (2004) 191–204.
- [38] William J. Palm, SIMULINK, Introduction to MATLAB7 for Engineers, Version 7, 2005.
- [39] M.A. Sharaf et. al, A New Visual Library for Design and Simulation of Solar Desalination Systems (SDS), Desalination Journal, 2010.
- [40] Moustafa M. Elsayed, Ibrahim S. Taha, Jaffar A. Sabbagh, Design of solar thermal systems, Scientific publishing center King Abdulaziz University, Jeddah, 57-61 (1994).
- [41] Agustín M. Delgado-Torres et. al, Solar-powered Rankine cycles for fresh water production, Desalination 212 (2007) 319–327.
- [42] www.dow.com.
- [43] Hisham T. El-Dessouky, Hisham M. Ettouney, Fundamental of salt water desalination, Kuwait University, Elsevier 2002 (book).

- [44] M.A. Darwish, Hassan K. Abdulrahim, Feed water arrangements in a multi-effect desalting system, *Desalination* 228 (2008) 30–54.
- [45] M.A. Darwish, Faisal Al-Juwayhel, Hassan K. Abdulrahim, Multi-effect boiling systems from an energy viewpoint, *Desalination* 194 (2006) 22–39.
- [46] Mark Wilf, Craig Bartels, Optimization of seawater RO systems design, *Desalination* 173 (2005) 1–12.
- [54-47] M.A. Sharaf et. al, Combined Solar Organic Rankine Cycle with Reverse Osmosis Desalination Process: Energy, Exergy, and Cost Evaluations, *Renewable energy* 2010.
- [48] Joan Carles Bruno, Jesu's Lo'pez-Villada, Eduardo Letelier, Modeling and optimization of solar organic Rankine cycle engines for reverse osmosis desalination, *Applied Thermal Engineering* 28 (2008) 2212–2226.
- [49] Agustín M. Delgado-Torres, Lourdes García-Rodríguez, Preliminary assessment of solar organic Rankine cycles for driving a desalination system, *Desalination* 216 (2007) 252–75.
- [50] Donghong Wei, Xuesheng Lu, Zhen Lu, Jianming Gu, Performance analysis and optimization of organic Rankine cycle (ORC) for waste heat recovery, *Energy Conversion and Management* 48 (2007) 1113–1119.
- [51] Pedro J. Mago, Louay M. Chamra, Kalyan Srinivasan, Chandramohan Somayaji, An examination of regenerative organic Rankine cycles using dry fluids, Received 18 October 2006; accepted 25 June 2007.
- [52] Agustín M. Delgado-Torres, Lourdes García-Rodríguez, Vicente J. Romero-Ternero, Preliminary design of a solar thermal-powered seawater reverse osmosis system, *Desalination* 216 (2007) 292–305.
- [53] Agustín M. Delgado-Torres, Lourdes García-Rodríguez, Status of solar thermal-driven reverse osmosis desalination, *Desalination* 216 (2007) 242–251.
- [54] Agustín M. Delgado-Torres, Lourdes García-Rodríguez, Comparison of solar technologies for driving a desalination system by means of an organic Rankine cycle, *Desalination* 216 (2007) 276–291.
- [55] Voros N. G, Kiranoudis C. T, Maroulis Z. B, “ Solar energy exploitation for reverse osmosis desalination plants”, *Desalination* 115 (1998) 83–101.
- [56] Malek A, Hawlader MN, Ho JC. Design and economics of RO seawater desalination. *Desalination*, 105 (1996) 245–261.
- [57] Peter Geisler, Wolfgang Krumm, Thomas Peters, Optimization of the energy demand of reverse osmosis with a pressure-exchange system, *Desalination* 125 (1999) 167–172.
- [58] Ian B. Cameron, Rodney B. Clemente, SWRO with ERI's PX Pressure Exchanger device: a global survey, *Desalination* 221 (2008) 136–142.
- [59] Bernhard M, Zarza E. Advanced MED solar desalination plants: Configurations, costs, future-seven years of experience at the Plataforma Solar de Almeria (Spain), *Desalination* 108 (1996) 51-58.
- [60] Ophir A, Lokiec F. Advanced MED process for most economical sea water desalination. *Desalination* 182 (2005) 187–198.
- [61] M. A. Sharaf et. Al. Exergy and thermo-economic analyses of a combined solar organic cycle with multi effect distillation (MED) desalination process. *Desalination* 272 (2011) 135–147.
- [62] [www.therminol.com](http://www.therminol.com).
- [63] Diego-César Alarcón-Padilla, Lourdes García-Rodríguez. Application of absorption heat pumps to multi-effect distillation: a case study of solar desalination. *Desalination* 212 (2007) 294–302.

- [64] M.A. Sharaf, A.S. Nafey, Lourdes García-Rodríguez. Thermo-economic analysis of solar thermal power cycles assisted MED-VC (multi effect distillation-vapor compression) desalination processes. *Energy* 36 (2011) 2753-2764.
- [65] El-Sayed YM. Thermo-economics of some options of large mechanical vapor-compression units. *Desalination*, 125 (1999) 251–257.
- [66] Hisham T. El-Dessouky, Hisham M. Ettouney, Yousef Al-Roumi, Multi-stage flash desalination: present and future outlook, *Chemical Engineering Journal*, 73 (1999) 173-190.
- [67] Lourdes Garcia-Rodriguez, Carlos Gómez-Camacho. Conditions for economical benefits of the use of solar energy in multi-stage flash distillation. *Desalination* 125 (1999) 133-138.
- [68] S.M.A. Mustafa, D.I. Jarrar and H.I. Mansy, *Solar Energy*, 35 (1985) 333.
- [69] M.A. Sharaf et. al, Theoretical and experimental study of a small unit for solar desalination using flashing process, *Energy Conversion and Management* 48 (2007) 528–538.
- [70] M.A. Sharaf et. al, Enhancement of solar water distillation process by surfactant additives, *Desalination* 220 (2008) 514–523.
- [71] Nafey AS, Fath H, Mabrouk A. Thermoeconomic design of a multi-effect evaporation mechanical vapor compression (MEE–MVC) desalination process. *Desalination* 230 (2008) 1–15.
- [72] Najem M, Darwish MA, F.A. Youssef. Thermovapor compression desalters: energy and availability-Analysis of single- and multi-effect systems. *Desalination* 110 (1997) 223-238.
- [73] P. Gandhidasan, Sultan A. Al-Mojel. Effect of feed pressure on the performance of the photovoltaic powered reverse osmosis seawater desalination system. *Renewable Energy* 34 (2009) 2824–2830.

## تصميم و ماثلة أنظمة التحلية بالطاقة الشمسية

### ملخص الرسالة

إن الأرقام المتعلقة بالمياه العذبة في العالم تدعو للقلق. فهي لا تمثل أكثر من 3% فقط من مجمل المياه الموجودة في كوكبنا الأرضي، كما أن ما يزيد عن 77.6% من هذه النسبة هي على هيئة جليد، و حوالي 21.8% هي مياه جوفية، والكمية المتبقية بعد ذلك والتي لا تتجاوز 0.6% هي المسؤولة عن تلبية احتياجات أكثر من ستة مليارات من البشر في كل ما يتعلق بالنشاط الزراعي والصناعي وسائر الاحتياجات اليومية. أما عن المياه في الوطن العربي فبالرغم من أنه يضم عشر مساحة اليابسة فإنه يصنف على أنه من المناطق الفقيرة في مصادر المياه العذبة، إذ لا يحتوى إلا على أقل من 1% فقط من كل الجريان السطحي للمياه، وحوالي 2% من إجمالي الأمطار في العالم.

إن فقر الوطن العربي فيما يتعلق بمصادر المياه انعكس على التأمين المائي للفرد والذي يجب أن لا يقل عن ألف متر مكعب سنوياً وفقاً للمعدل العالمي. حيث وصل متوسط حصة الإنسان العربي في جل البلاد العربية إلى ما يقارب خمسمائة متر مكعب في العام، في حين أن أعداد الدول العربية الواقعة تحت خط الفقر المائي (أقل من ألف متر مكعب للفرد سنوياً) بلغت حوالي 19 دولة منها 14 دولة تعاني شحاً حقيقياً في المياه إذ لا تكفي المياه سد الاحتياجات الأساسية لمواطنيها. ومن هنا تنبع أهمية الإلتفات إلى قضية المياه، ووضع السياسات المتعلقة باستخدامها وترشيدها وزيادة كمياتها.

لذلك تعتبر تحلية المياه أحد أهم مصادر الحصول على المياه ولكنها في ذات الوقت تستهلك طاقة كبيرة. وعلى النقيض من مشكلة المياه، فإن الوطن العربي و خاصة مصر يقع في النطاقات العالمية لمعدلات الإشعاع الشمسي إن لم يكن أعلاها حيث تتسم ظروفها المناخية بوفرة الأشعة الشمسية طوال العام وزيادة معدلاتها عن معدلات الأشعة الساقطة على الدول التي تقع في نفس دوائر العرض. كما أن ارتفاع معدلات الإشعاع طوال العام بمصر يسمح باستخدامه في شتى المجالات وبالأخص تحويله لطاقة كهربائية يمكن لها أن تضع مصر في مصاف الدول المنتجة والمصدرة للطاقة الكهربائية.

لذلك، فإن استخدام الطاقة الشمسية في تكنولوجيا تحلية المياه يعتبر من الطرق العملية و المستحدثة والتي باتت ذات أولوية في الوقت الراهن لحل مشكلة المياه في ظل الارتفاع المتطرد في أسعار الطاقة التقليدي بصفة عامه و الوقود الأحفوري بصفة خاصة. ولذلك، أُعتبرت طرق التحلية باستخدام الطاقة الشمسية من الطرق التي زاد الأهتمام بتطويرها في العقود الأخيرة. و بصفة عامة، تعتبر تقنيات التحلية الشائعة الاستخدام مثل الوميض متعدد المراحل، التقطير متعدد التأثير، ضغط البخار و الضغط الأسموزي العكسي من التقنيات ذات الإنتاجية العالية للمياه المحلاة (100-50,000 م<sup>3</sup>/اليوم).

ولحساب تكلفة المتر المكعب المنتج من الطاقة الشمسية، تعرض الرسالة برنامج حاسوبي متطور تم بناءه لتصميم ومحاكاة أنظمة التحلية بالطاقة الشمسية. وبنى البرنامج ليساعد مصممي المحطات الشمسية الحرارية على تكوين التركيبات المختلفة لعمليات التحلية وكذلك تنفيذ مختلف العمليات الحسابية مثل حسابات إيزان الطاقة، الأكسيري و التكلفة الاقتصادية من خلال واجهة تمكن المستخدم من بناء و تكوين المحطة المطلوبة خاصة المحطات الشمسية، وكذلك إدخال و إخراج البيانات الخاصة بطريقة سهلة و ميسرة. كما يساعد البرنامج أيضاً على إجراء أية تعديلات في المحطة الأصلية وإقتراح نموذج جديد من شأنه توفير الطاقة والوصول بالمحطة إلى أعلى إنتاجية و كفاءة ممكنة و بأقل تكلفة. وقد تم تمثيل و محاكاة مكونات محطات التحلية بالطاقة الشمسية مثل المبادلات الحرارية، حجرات التبخير الفجائي، المجمعات الشمسية، المضخات، المبخرات، الضواغط البخارية، محطات التناضح العكسي،... إلخ.

وقد تم تحويل المكونات والوحدات الى بلوكات BLOCKS و تخزينها في مكتبة البرامج حيث يقوم المستخدم بإنشاء مختلف التركيبات باضغط علي زر الفأرة ومن ثم إدخال البيانات الى الوحدة المستهدفة. وقد تم استخدام البرنامج في دراسة أداء محطات التحلية بالطاقة الشمسية مثل التبخير الوميضي، والتبخير متعدد التأثير، والضغط الحراري للبخر، والضغط الميكانيكي للبخر، والتناضح العكسي. وأيضا تم دراسة وتحليل عدد كبير من الموائع العضوية والتي تستخدم في محطات الطاقة الشمسية مع إمكانية تغيير التقنية المستخدمة مثل التوليد المباشر والتوليد الغير المباشر. كما عرضت الرسالة كيفية اداء وعمل البرنامج وطريقة تشغيله مع بيان بعض النتائج كإجراء مثالي.

وقد تناولت الرسالة عدة إقتراحات لتحسين الأداء وخفض التكلفة. وكان من أهم الأقتراحات إختيار الطولوين في تشغيل المحطات التي تعمل طبقا لدورة الرانكين باستخدام الطاقة الشمسية. كما تم إختيار واعتماد تقنية التناضح العكسي باستخدام المبادل الضغطي و إعتداد التبخير الحراري المتوازي كحل بديل عن التبخير الضغطي مع إمكانية زيادة الوحدات الي 16 وحدة. و بصفة عامة، وجد أن محطات التناضح العكسي هي الأنسب من ناحية توفير الطاقة و إمكانية التشغيل مع الطاقة الشمسية علي الرغم من أن الإنتاجية متوسطة (100-10000 متر مكعب يوميا) مقارنة بتكنولوجيا التبخيرالوميضي متعدد المراحل. وعلي الرغم من أن التبخير الوميضي المتعدد المراحل يعطي أعلى إنتاجية إلا أنه يستهلك طاقة حرارية كبيرة وبالتالي يستهلك مساحة أكبر لموقع التشغيل الشمسي. وقد بينت النتائج إنخفاض تكلفة المتر المكعب في تقنية التناضح العكسي عنها في باقي التقنيات مع وجود إمكانية في إنخفاض مساحة التشغيل وهو الأمر المستهدف خاصة في تكنولوجيا الطاقة الشمسية.

## صفحة الموافقة

### تصميم و مماثلة أنظمة التحلية بالطاقة الشمسية

رسالة مقدمة من

محمد عبد الوهاب شرف الدين

ماجستير الهندسة الميكانيكية-جامعة قناة السويس-2007

للحصول علي درجة دكتوراه

في

الفلسفه في هندسة الطاقة

### تمت الموافقة من لجنة الحكم و المناقشة

1	أ.د. منصور عوض محمد أستاذ بقسم الطاقة الشمسية المركز القومي للبحوث القاهرة
2	أ.د. محمد رضا عبد القادر أستاذ بقسم القوي الميكانيكية كلية الهندسة جامعة بورسعيد
3	أ.د. محمد عبد الفتاح الزكي أستاذ بقسم هندسة الفلزات كلية البترول و التعدين بالسويس جامعة قناة السويس
4	د. سيد عثمان الحلبي أستاذ مساعد و رئيس قسم العلوم الهندسية كلية البترول و التعدين بالسويس جامعة قناة السويس



## لجنة الإشراف

### تصميم و مماثلة أنظمة التحلية بالطاقة الشمسية

رسالة مقدمة من

محمد عبد الوهاب شرف الدين  
ماجستير الهندسة الميكانيكية-جامعة قناة السويس-2007

للحصول علي درجة دكتوراه  
في  
الفلسفه في هندسة الطاقة

### تحت إشراف

1	أ.د. محمد عبد الفتاح الزكي أستاذ بقسم هندسة الفلزات والمواد-كلية هندسة البترول والتعدين-جامعة قناة السويس
2	د. سيد عثمان الحلبي أستاذ مساعد و رئيس قسم العلوم الهندسية-كلية البترول و التعدين بالسويس -جامعة قناة السويس
3	د. لورديس جارسيا رودريجز أستاذ مساعد بقسم هندسة الطاقة-جامعة سيفيليا-أسبانيا



جامعة قناة السويس  
كلية هندسة البترول والتعدين-السويس  
قسم العلوم الهندسية

## تصميم ومماثلة أنظمة التحليه بالطاقه الشمسيه

رسالة مقدمة من

محمد عبد الوهاب شرف الدين

مدرس مساعد-قسم العلوم الهندسيه-كلية هندسة البترول والتعدين  
ماجستير الهندسة الميكانيكية-جامعة قناة السويس-2007

للحصول علي درجة

دكتوراه الفلسفه في هندسة الطاقه

من

قسم العلوم الهندسيه-كلية هندسة البترول والتعدين  
جامعة قناة السويس